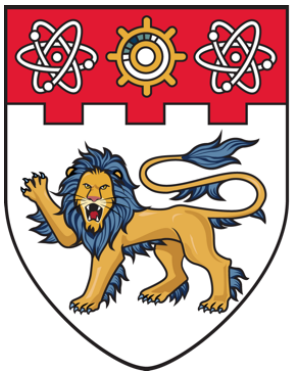

NANYANG TECHNOLOGICAL UNIVERSITY
SINGAPORE

HYDROPHOSPHINATION AS A VALUABLE TOOL TO CHIRAL DIPHOSPHINES AND THEIR DERIVATIVES

TEO HONG XIANG RONALD

SCHOOL OF PHYSICAL AND MATHEMATICAL SCIENCES

2021

HYDROPHOSPHINATION AS A VALUABLE TOOL TO CHIRAL DIPHOSPHINES AND THEIR DERIVATIVES

TEO HONG XIANG RONALD

SCHOOL OF PHYSICAL AND MATHEMATICAL SCIENCES

A thesis submitted to the Nanyang Technological University in partial fulfilment of the requirement for the degree of Doctor of Philosophy

2021

Statement of Originality

I hereby certify that the work embodied in this thesis is the result of original research done by me except where otherwise stated in this thesis. The thesis work has not been submitted for a degree or professional qualification to any other university or institution. I declare that this thesis is written by myself and is free of plagiarism and of sufficient grammatical clarity to be examined. I confirm that the investigations were conducted in accord with the ethics policies and integrity standards of Nanyang Technological University and that the research data are presented honestly and without prejudice.

05/08/2021

Date

Teo Hong Xiang Ronald

Supervisor Declaration Statement

I have reviewed the content and presentation style of this thesis and declare it of sufficient grammatical clarity to be examined. To the best of my knowledge, the thesis is free of plagiarism and the research and writing are those of the candidate's except as acknowledged in the Author Attribution Statement. I confirm that the investigations were conducted in accord with the ethics policies and integrity standards of Nanyang Technological University and that the research data are presented honestly and without prejudice.

5-8-2021
Date

Sumod A. Pullarkat

5/8/2021
Date

Leung Pak-Hing

Authorship Attribution Statement

This thesis contains material from two papers, either published or submitted in the following peer-reviewed journals where I was the first author.

Chapters 2 is published as Teo, R. H. X.; Chen, H. J.; Li, Y.; Pullarkat, S. A.; Leung, P.-H., Asymmetric Catalytic 1,2-Dihydrophosphination of Secondary 1,2-Diphosphines – Direct Access to Free *P**- and *P**,*C**-Diphosphines. *Adv. Synth. Catal.* **2020,** *362* (12), 2373-2378. DOI: 10.1002/adsc.202000131.

The contributions of the co-authors are as follows:

- Dr Li, Y. collected and resolved the X-ray crystallographic data,
- Dr. Pullarkat, S. A. revised the manuscript draft and assisted in idea generation,
- Prof. Leung, P.-H. revised the manuscript draft and assisted in idea generation,
- Dr. Chen, H. J. assisted in reactions, purifications and revision of manuscript draft,
- I designed the study, performed the experiments, collected the Nuclear Magnetic Resonance (^{1}H, ^{13}C and ^{31}P{^{1}H}), High Resolution Mass Spectroscopy, High Performance Liquid Chromatography optical rotation data, and
- I prepared the manuscript draft and Supporting information.

Chapters 3 is published as Teo, R. H. X.; Lee, J. X. T.; Tan, W. R.; Shum, W. Q.; Li, Y.; Pullarkat, S. A.; Tan, N. S.; and Leung, P.-H., Catalytic Asymmetric Hydrophosphination as a Valuable Tool to Access DiHydrophosphinated Curcumin and its Derivatives. *Organometallics*, **2021**, *40* (20), 3454-3461. DOI: 10.1021/acs.organomet.1c00466

The contributions of the co-authors are as follows:

- Dr Li, Y, collected and resolved the X-ray crystallographic data,
- Dr. Pullarkat, S. A. revised the manuscript draft and assisted in idea generation,
- Prof. Tan, N. S. and Prof. Leung, P.-H. revised the manuscript draft and assisted in idea generation,
- Lee, J. X. T. conducted the biological testing on the cancer cell lines,
- Tan, W. R. conducted the biological testing on the cancer cell lines,
- Shum, W. Q. assisted in reactions, purifications and revision of manuscript draft,
- I designed the study, performed the experiments, collected the Nuclear Magnetic Resonance (^{1}H, ^{13}C and ^{31}P{^{1}H}), High Resolution Mass Spectroscopy, High Performance Liquid Chromatography optical rotation data, and
- I prepared the manuscript draft and Supporting Information.

05/08/2021

Date

Teo Hong Xiang Ronald

Abstract

Chiral diphosphine ligands are a ubiquitous class of privileged ligand which finds extensive application in transition metal catalysis and biochemistry. This thesis explores the development of a new methodology of accessing *P*-chiral diphosphine ligands with high to excellent enantioselectivities and moderate diastereoselectivities. Next, the synthesis of *C*-chiral diphosphines from naturally occurring curcumin and derivatives was attempted and the cytotoxicity of the diphosphine metal complexes was evaluated and compared against cisplatin and curcumin in the MKN74 and MCF7 cancer cell-lines. Lastly, the challenges associated with the generation of chiral phosphine-phosphino-chalcogenide and their complexes were discussed in detail and an example of the catalytic property of the phosphine-phosphino-chalcogenide metal complexes was illustrated.

Acknowledgements

I would like to thank the Division of Chemistry and Biological Chemistry, School of Physical and Mathematical Sciences and Nanyang Technological University, for supporting my research as well as the award of the prestigious Nanyang President's Graduate Scholarship.

I am grateful to my main supervisor, Prof. Leung Pak-Hing, who has been a great mentor in my academic journey. The freedom he has given me to explore science and the advice and assistance rendered whenever I encountered setbacks have made my postgraduate journey an enjoyable one. Besides academic guidance, the advice he offered regarding administrative matters, teaching and people management have also been greatly useful.

I would like to extend my appreciation to my co-supervisor, Dr. Sumod A. Pullarkat, who has been a steady source of support and guidance since I first joined this group seven years ago. He has always been there whenever I needed guidance and advice. His willingness to accept me as his URECA student seven years ago has facilitated my learning journey as a researcher and I have since gained many valuable knowledge and experiences along the way.

I would like to thank my Thesis Advisory Committee Members. Prof. Leong Weng Kee has given me numerous precious advice, ideas and directions for my projects. Prof. Tan Nguan Soon has kindly provided me advice on my projects and assisted me in our collaborated project.

I would also like to thank Jeannie and Wei Ren from Lee Kong Chian School of Medicine for their contributions towards the biological applications of the functionalized curcumin complexes on cancer cells.

Special mention goes to Jeremy for his patience, encouragement, and support. He has taught me essential laboratory skills and consistently helped me whenever I needed help even after leaving NTU.

My lab mates and friends, Jeffery, Shafiq, Ce Qing, Jia Sheng, Po Kai and Wee Shan, have been my constant support. The late nights spent together in lab, meals we had, trips embarked together and jokes we made have made my postgraduate journey an enjoyable and memorable one. My student, Wen Qian, has also been of a great help during the last lap in my postgraduate journey. I am fortunate to have her as my student to support me in the completion of my two final projects.

I am also appreciative of the staff in the Central Facilities Lab – Ai Hua, Ee Ling, Dr. Li Yongxin, Joan, and Wen Wei, for their assistance in TA duties, administrative matters, and technical support.

I am grateful to my life partner who supported me in her own ways when I was occupied and stressed over projects and writings. Her patience and support have indeed been indispensable.

Last but not least, I am extremely grateful to and appreciative of my family for their unconditional support and encouragement over the years. Without them, I might not have been who I am today.

Table of Contents

Nomenclature

The nomenclature used throughout the thesis conforms to the format adopted by Chemical Abstracts (Chemical Abstracts, 13th Collective Index, Index Guide, 1992-1996).

X-ray Structural Data

The single crystal X-ray analyses were kindly performed by Dr. Li. Yongxin at the Nanyang Technological University (Division of Chemistry and Biological Chemistry). Full structural data (listings of crystal and refinement data, bond distances/angles, and thermal parameters) are available from Prof. Leung Pak-Hing upon request.

Abbreviations and Symbols

AcOEt	ethyl acetate
Ar	aryl group
BDMC	bisdemethoxycurcumin
BINAP	2,2′-bis(diphenylphosphino)-1,1′-binaphthyl
Bn	benzyl
Bp	boiling point
br	broad
calcd.	calculated
$CDCl_3$	chloroform-d1
$CHCl_3$	chloroform
conc.	concentrated
Cur	curcumin
d	doublet (NMR)

DBTA	dibenzoyl-tartaric acid
DCM	dichloromethane
dec.	decomposed
de	diastereomeric excess
DIOP	2,3-*O*-isopropylidene-2,3-dihydroxy-1,4-bis(diphenylphosphino)butane
DIPAMP	1,2-bis((2-methoxyphenyl)phenylphosphino)ethane
dm	decimetre(s)
DMC	demethoxycurcumin
DMF	*N*,*N*-dimethylformamide
ee	enantiomeric excess
equiv.	equivalence
ESI-MS	electrospray ionization mass spectrometry
Et	ethyl
g	gram(s)
h	hour(s)
^{i}Pr	isopropyl
Hz	hertz
m	multiplet (NMR)
Me	methyl
min	minute(s)
mL	millilitre(s)
mmol	millimole(s)
Mp	melting point
Naph	naphthalene
NMR	nuclear magnetic resonance

Ph	phenyl
ppm	parts per million
Pr	propyl
R	rectus (Latin right absolute configuration)
rac	racemic
rt	room temperature
S	sinister (Latin left absolute configuration)
s	singlet (NMR)
t	triplet (NMR)
t	time
T	temperature
^{t}Bu	*tert*-butyl
THF	tetrahydrofuran
TMEDA	tetramethylethylenediamine
δ	NMR chemical shift in ppm
°	degree (angles)
Å	angstrom(s)
°C	degree Celsius
$[\alpha]_D$	specific rotation measured at sodium D line (589 nm)

Summary

In chapter I, an overview of chiral phosphines and diphosphines ligands is given. Recent developments pertaining to the syntheses of chiral monophosphines, along with their limitations, and applications of chiral monophosphines and diphosphines will be discussed. In addition, the research gap will be introduced and the aims of this thesis will be stated.

In chapter II, an efficient catalytic protocol to access *P*-chiral diphosphines will be introduced. The viability of catalytic asymmetric hydrophosphination to synthesize *P*-chiral diphosphines from *rac*-diphosphines will be studied and discussed in greater details.

In chapter III, the modification of curcuminoids with secondary phosphines *via* asymmetric hydrophosphination reactions will be introduced. The complexes of these modified curcumins efficacies as anti-cancer drugs are evaluated using MKN74 and MCF7 cell-lines.

In chapter IV, the syntheses and study of phosphine-(phosphino chalcogenide) complexes, and details pertaining to the failure of asymmetric hydrophosphination as a viable synthetic tool will be introduced. In addition, synthesis of enaminones using the developed phosphine-(phosphino sulfide) complex will be discussed.

In chapter V, the conclusions of this thesis will be given and future work will be mentioned briefly.

Chapter I

Introduction

1.1 Chirality

Chirality, known since the 18th century, has played a vital role in many aspects in living organisms and in the sciences. It was first observed by Louis Pasteur, in 1848, in his study on two different crystals of sodium ammonium tartrate that were non-superimposable optically. These crystals could be categorized into right and left hemihedral facets in which individual non-identical compound either rotated a plane of polarized light to the right (dextrorotatory) or to the left (levorotatory).[1] The ever-present phenomenon of chirality in plants and animals due to the numerous homochiral compounds *i.e*. proteins, amino acids, carbohydrates, enzymes, *etc*, demonstrated the prevalence of this concept.[2] For instance, the basic execution of genetic control in animals requires the encoding of information between proteins and genes of specific shapes. As such, isotacticity of amino acids is required because both the D- and L- amino acids will give rise to two different three-dimensional spatial structures.[3] In another example, the incident of the highly controversial racemic thalidomide drug in the 1950s caused thousands of birth defects in infants born to women who had been prescribed the drug as a remedy for morning sickness. This was due to the presence of the malignant (*S*)-enantiomeric form of thalidomide that was responsible for its teratogenicity.[4] To date, the concept of chirality found in many areas such as pharmaceuticals, fragrances and other fine chemicals, has exemplified the importance of the different intrinsic chemical, biological and physical properties of the different stereoisomers.

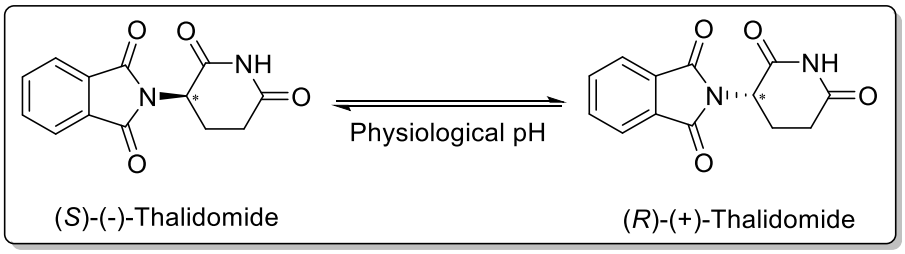

Figure 1. Racemization of Thalidomide drug.

1.1.1 Types of Chirality

There exist different types of chirality, namely point chirality, planar chirality, axial chirality and helical chirality.

Point chirality, or central chirality, can be described as a central atom being covalently bonded to four different substituents, that gives rise to nonplanar, non-superimposable mirror images. The absolute configuration (*R*/*S* sequence) can be determined using the Cahn-Ingold-Prelog (CIP) rules.[5]

Planar chirality exists in molecules due to a 'potential' plane of symmetry if not for the fact that one or more substituents are being positioned out of the plane, but perpendicular to the 'potential' plane of symmetry, destroying the plane of symmetry. One method to define the absolute configuration was suggested by Schlögl.[6]

Axial chirality exists in a molecule where four substituents are positioned about a chiral axis. The restricted rotation about a bond gives rise to two non-superimposable stereoisomers.

Lastly, helical chirality is exhibited in molecules which twist like a corkscrew. This chirality governs the formation of many biological and artificial supramolecular assemblies. In non-rigid molecules, like DNA, helical conformation can be a result of specific directional non-covalent interactions between functional groups.[7] In rigid molecules, energetically favoured

helical conformation can be adopted due to the presence of steric interactions in the non-helical conformation.[8]

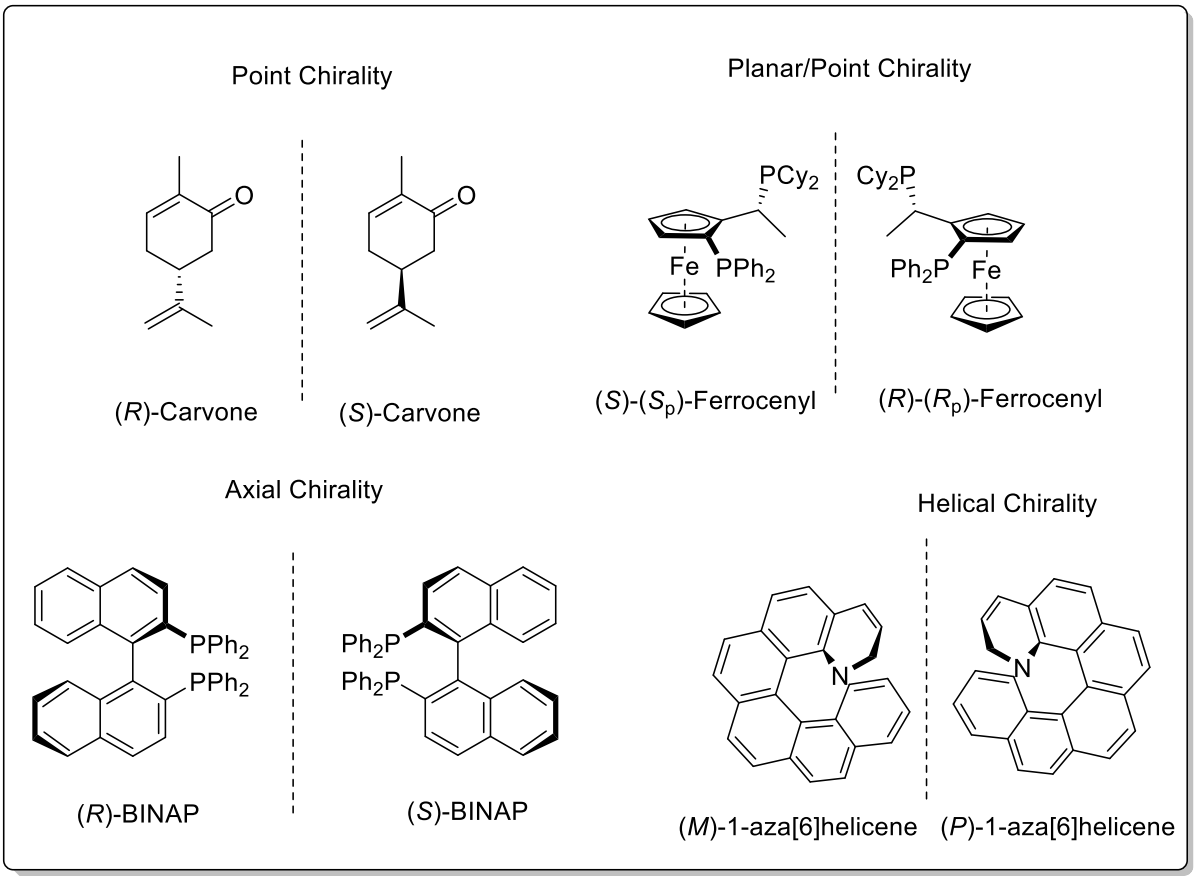

Figure 2. Examples of molecules exhibiting different modes of chirality.

1.2 Chiral Phosphines

The studies on chirality since the 1800s have played a huge role in the development of many areas in chemistry including the discovery of chiral phosphines.

Phosphines, defined as compounds containing a phosphorus atom bonded to carbon or hydrogen atoms, have always been indispensable in chemistry since their discovery. The high inversion barrier exhibited by most phosphorus centers allows phosphorus-containing compounds to be excellent candidates for the generation of chiral center(s). In contrast to amines which have inherently low inversion barrier of about 5-10 kcal/mol,[9] most phosphines

have stable stereogenic centers about the phosphorus atom with inversion barrier greater than 30 kcal/mol.[9a, b, e, 10] For inversion *via* the pyramidal transition state to occur, the geometry of the center atom has to change from trigonal pyramidal to trigonal planar in which the lone pair of electrons on phosphorus resides in a non-bonding *p* orbital.[9a]

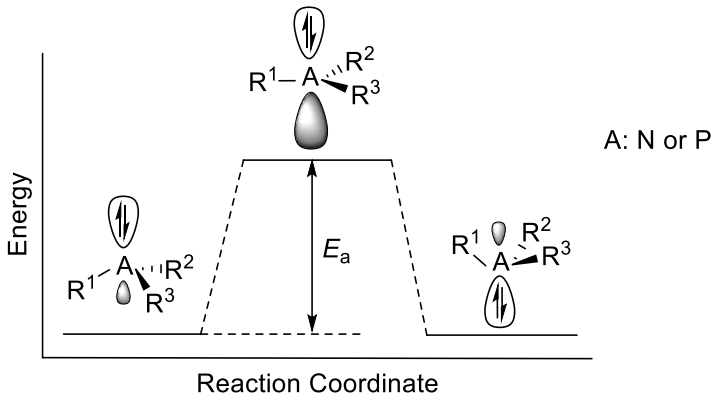

Figure 3. General reaction profile of the pyramidal inversion of amines and phosphines.

To compare the inversion barrier of phosphines and amines, the difference in energy of highest occupied molecular orbital (HOMO) of both the pyramidal and planar structures were calculated by Montgomery.[9a] In general, the energy provided at room temperature was found to be insufficient to cause most phosphines to undergo pyramidal inversion, but sufficient to cause most amines to readily undergo inversion.

Since the first reported optically active phosphine in 1961 by Horner *et al.*,[11] chiral phosphines have garnered popularity due to their potential in metal-assisted and organocatalytic asymmetric reactions. In the same year, the newly discovered optically pure phosphines were used as ligands in asymmetric hydrogenation reactions by both Horner *et al.*[12] and Knowles *et al.*[13] These encouraging discoveries by both teams, coupled with the high performance of the chiral phosphines, spurred the development of a myriad of chiral phosphines and contributed to the rapid development of asymmetricity and many other asymmetric applications in research and industries.[14] During the developmental period of

optically pure phosphine ligands, many research groups were motivated by the excellent results these ligands could generate and these groups devoted their efforts to design and create many additional novel privileged chiral phosphines.[15] The significance of these compounds were acknowledged with the Nobel Prize being awarded to works contributed by Noyori *et al.*[16] and Knowles *et al.*[17]

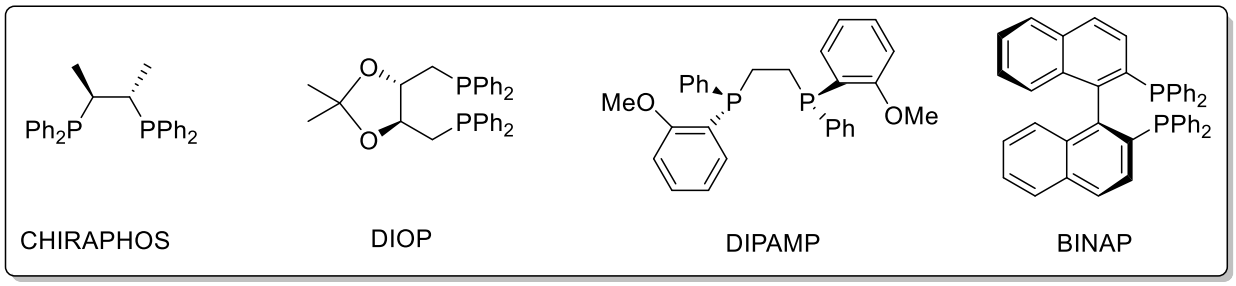

Figure 4. Examples of chiral phosphines.

Structural variation of the phosphine motifs to generate novel efficient chiral ligands based upon the type of reaction can allow chemists to control the reactivity and selectivity of the catalysts for use in different asymmetric applications. The electronic properties of phosphines can be tuned by varying the substituents on the phosphorus atom. The presence of electron-donating substituents around the phosphorus center will destabilize the HOMO (highest occupied molecular orbital) of the phosphine. As a result, the electron density of the phosphorus atom is increased, making it more nucleophilic. On the other hand, when there are electron-withdrawing substituents on the phosphorus, the σ^* orbital (lowest unoccupied molecular orbital, LUMO) will be lowered. As a result, the phosphine more electrophilic. The quantification of the electronic properties of the phosphines can be done using the Tolman Electronic Parameter, devised by Tolman in 1970.[18] This technique makes use of the ability of the bound carbonyl ligand to accept back-donated electrons from the phosphine into the π^* molecular orbital of the carbonyl ligand. When a phosphine ligand is bonded to the same metal center as a carbonyl ligand in a complex, the electron density of the phosphine being donated

into the metal center will cause π back-donation from the metal into the π^* molecular orbital of the carbonyl. This back-donation will weaken the C≡O bond and the resulting weakened bond can be observed using infrared spectroscopy (IR) given that wavenumber is directly proportional force constant. Specifically, the amount of electron density available for back-donation from the metal *d*-orbital to the π^* molecular orbital of C≡O is dependent on the types of substituent present around the phosphorus atom in the phosphine ligand. The presence of electron-donating substituents will lead to greater electron density being donated into the metal *d*-orbital and consequently, there will be greater back-donation from the metal *d*-orbital into the π^* molecular orbital of the carbonyl, resulting in a much weaker C≡O bond. On the contrary, the presence of electron-withdrawing substituents will result in less significant back-donating effect due to stronger π back-donation into the σ^* molecular orbital of the phosphine.

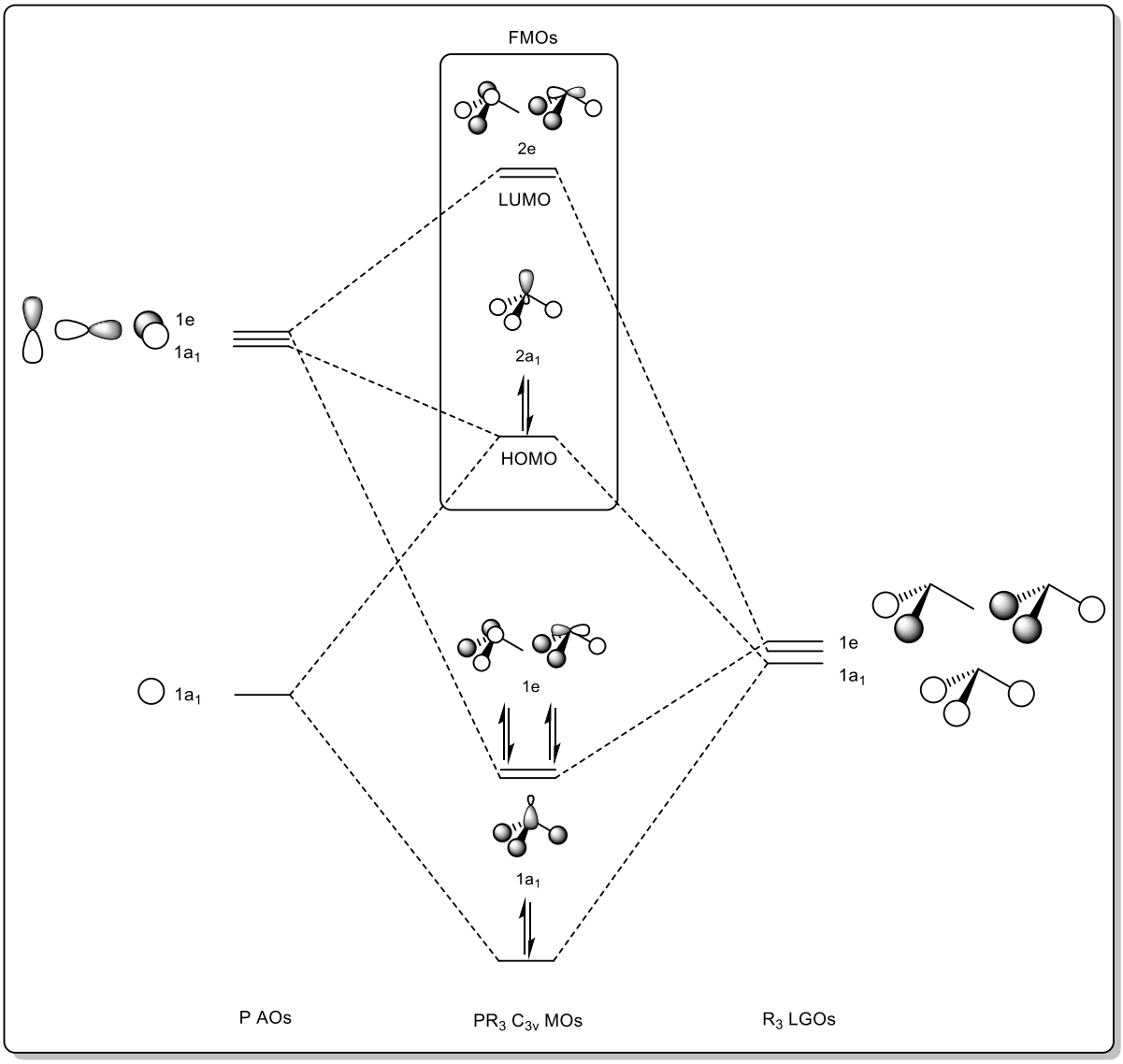

Figure 5. Molecular orbital diagram of PR_3.

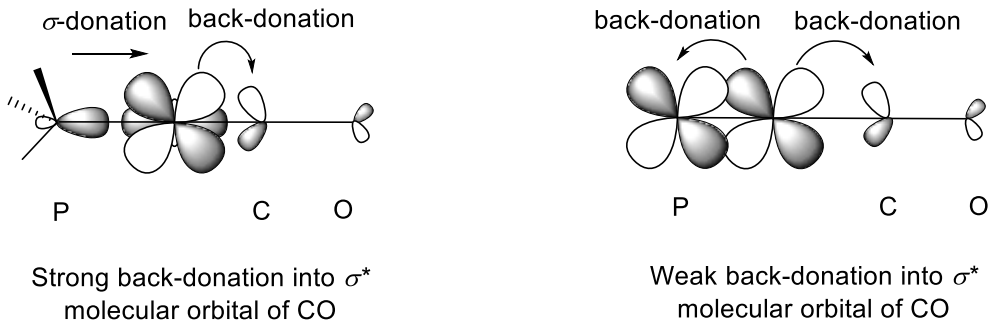

Figure 6. Orbital interactions between phosphorus, metal and carbon monoxide.

Another parameter - the Tolman cone angle - has been instrumental in determining the steric properties of phosphine ligand.[19] The cone angle of the phosphine (θ) was determined using the space-filling calotte (CPK) molecular model of these phosphines. θ is the apex angle of a cylindrical cone drawn, with center being 2.28 Å away from the center of phosphorus and just touching the *Van der Waals* radii of the peripheral atoms. Cone angle of bidentate phosphines is dependent on the bite angle.[20] The cone angle of the individual phosphorus atom is determined by the angle between the bisector of the P–M–P bite angle and the line extended from the center, 2.28 Å away from the center of the phosphorus, to when it just touches the *Van der Waal*s radii of the outermost atoms.

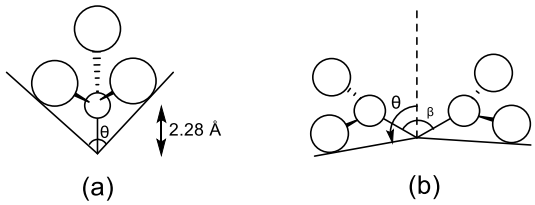

Figure 7. (a) Cone angle of phosphines. (b) Bite angle of diphosphines.

1.2.1 Classification of Optically Active Phosphines

Optically active phosphines can exhibit various modes of chirality. In addition to having point chirality at the phosphorus center, chirality can also stem from other units in the compound to afford axial or planar chirality, or even from chiral substituents along the carbon backbone of the organic fragment.

Given that discovery of chiral phosphines has been diversified, these optically pure phosphines could be categorized into monophosphines, diphosphines and polyphosphines, and can be further subcategorized into their different modes of chirality.

1) *P*-Stereogenic Monophosphines

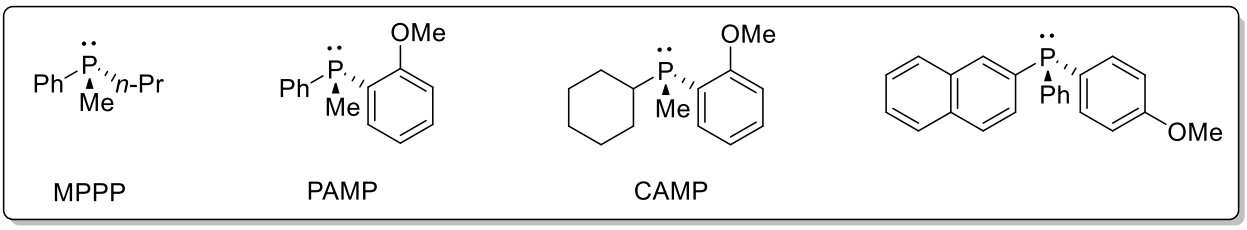

2) *P*-Stereogenic Diphosphines

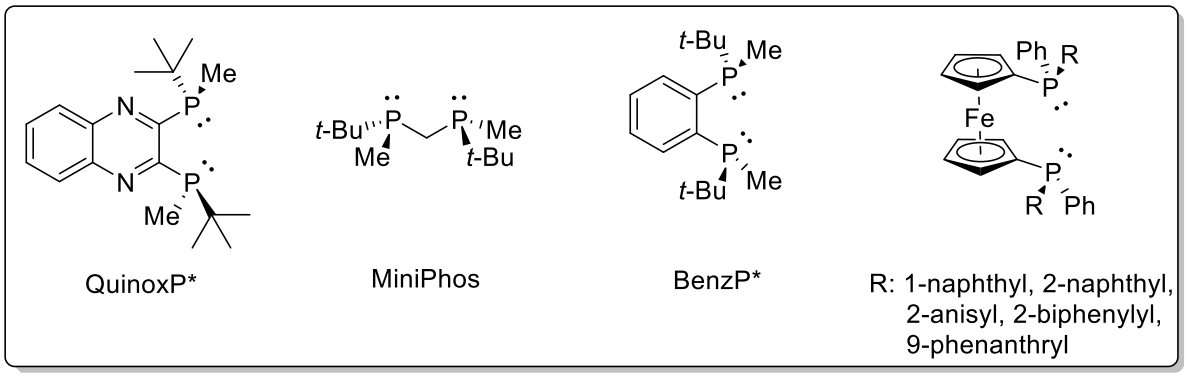

3) *C*-Stereogenic Monophosphines

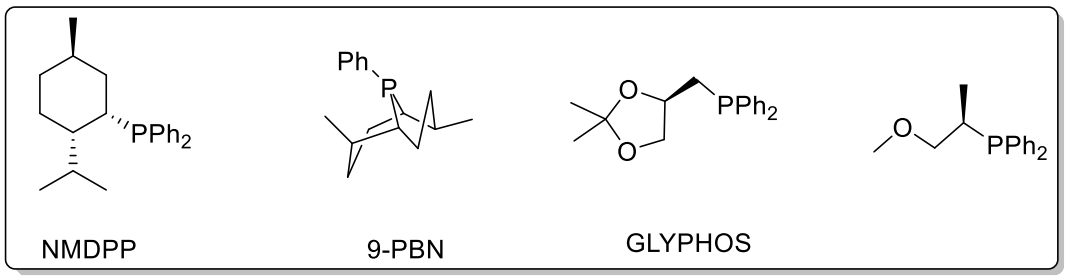

4) *C*-Stereogenic Diphosphines

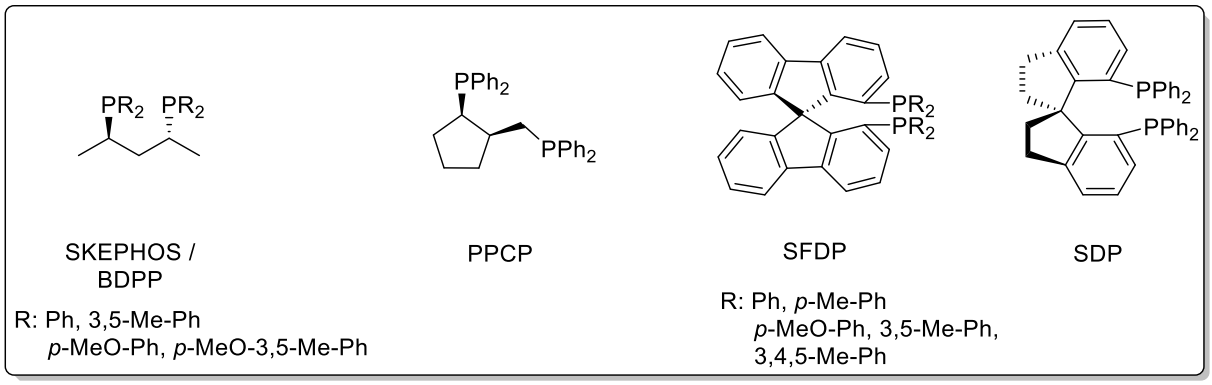

5) Phosphines with Axial and Planar Chirality

Since the 1990s, there has been many reports on asymmetric catalytic reactions mediated by axially chiral diphosphines, with the most commonly utilized diphosphine being BINAP. Thereafter, many variants of modified BINAP ligands have been synthesized to improve the enantioselectivity of the ligands in asymmetric catalytic reactions. Among the altered ligands, modifications of the aryl groups on the phosphorus atom and structural changes to the atropoisomeric biaryls were the most commonly found methods of functionalization in literatures.

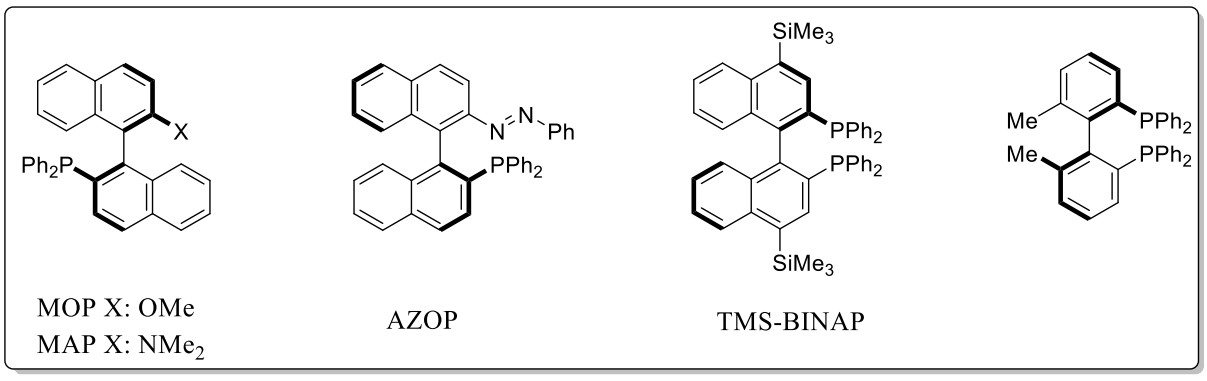

The most common backbone of planar chiral phosphines is based on ferrocene. This scaffold is easily tunable electronically and sterically by simple derivatizations. These ligands can be combined with and without other forms of chiral elements. Displayed below are

selected examples of planar chiral mono- and diphosphines.

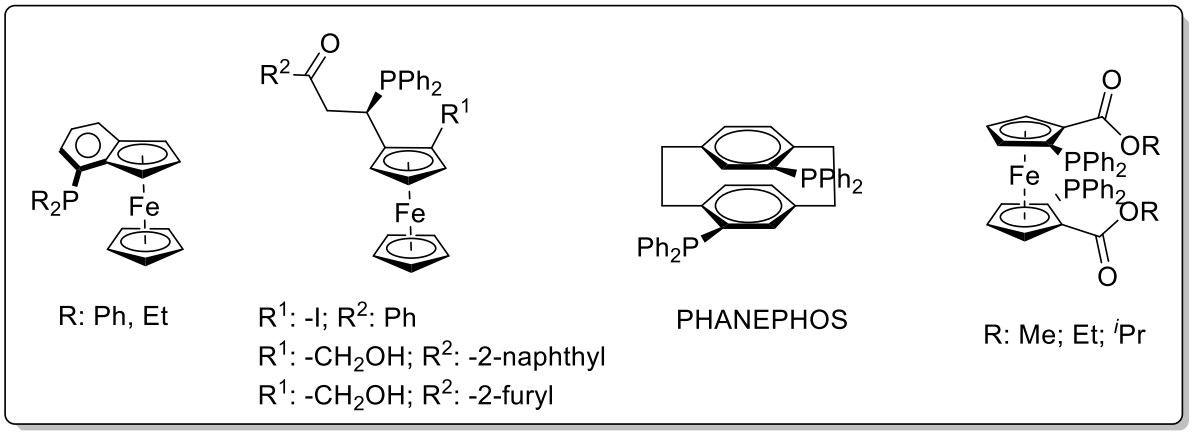

1.3 Synthetic Methodologies of Optically Active Phosphines

Given the diverse applications of optically active phosphines, it is not surprising that research groups around the world have devoted many years to developing various methodologies to create useful and novel chiral phosphines. Phosphines, in general, are air sensitive and are susceptible to oxidation. This oxidative nature of phosphines makes handling and storage cumbersome and challenging. Many researchers choose to handle and store these compounds in their more stable form by paralyzing the lone pair of electrons on the phosphorus atoms. This can be done by converting the phosphines to phosphine oxides, boranes and sulfides, *etc*. However, deprotection of these phosphine derivatives to return the free phosphines could have an adverse effect on the yield and optical activity of the desired phosphine.[21]

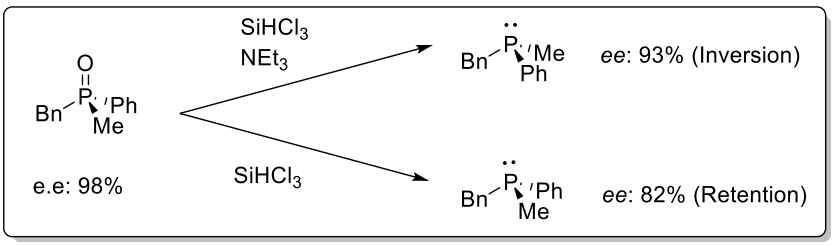

Scheme 1. Reduction of chiral phosphine oxide with silanes.

Besides the classical protection-deprotection methodology used to afford optically active phosphine moieties, a plethora of synthetic pathways has been devised. The pathways can be classified into syntheses *via* a) the chiral pool, b) chiral auxiliaries, and c) asymmetric reactions. Due to the large number of literature available for the various methodologies, only selected examples will be discussed.

1.3.1 Chiral Pool

Chiral pool synthesis utilizes cheap, natural, and readily available chiral compounds, such as amino acids, carbohydrates and lactic acids. These chiral compounds can be converted to the desirable chiral products without the need to induce chirality during the synthesis. One such example is the synthesis of DIOP, the first chelating diphosphine being reported. Tartaric acid was used in this straightforward four-step reaction. This backbone provides a scaffold that connects the two phosphine groups in close proximity to the stereogenic carbon centers, and the chirality on the two carbon centers can be retained throughout the process from the protection of the diol group with acetone to the nucleophilic substitution of the tosylates by sodium diphenylphosphide.[15a, b]

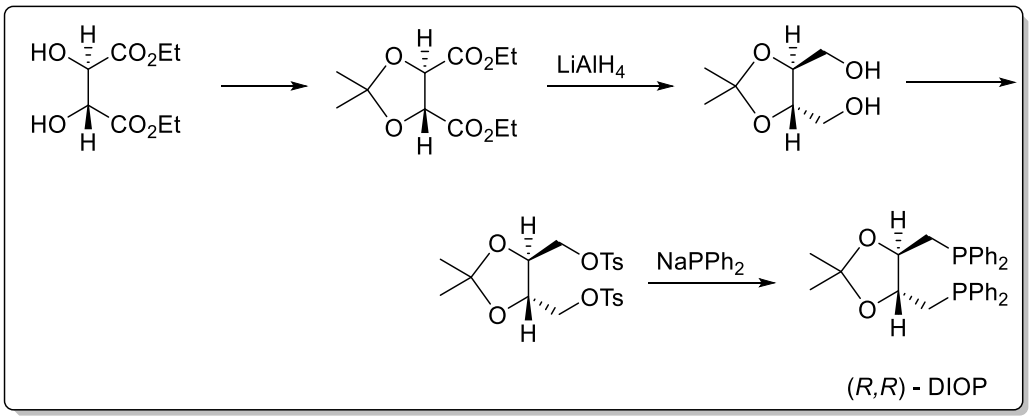

Scheme 2. Four-step process to synthesize optically pure DIOP.

The successful invention of DIOP brought forth a few concepts about C_2-symmetric diphosphine ligands. Enlightened by this pioneering work, the early research on phosphorus bidentate ligands yielded a number of chiral ligands with well-defined chiral backbone from optically active natural products as starting materials. Some of these ligands include, but are not limited to, CHIROPHOS,[22] the first member of the 1,2-diphosphine family, CYCPHOS,[23] PROPHOS[24] and PHENPHOS.[25] The C_1-symmetric diphosphines were synthesized using a very similar protocol as that of CHIROPHOS, using other naturally occurring analogues such as: (*S*)-mandelic acid, (*S*)-lactic acid, and (*S*)-hexahydromandelic acid.

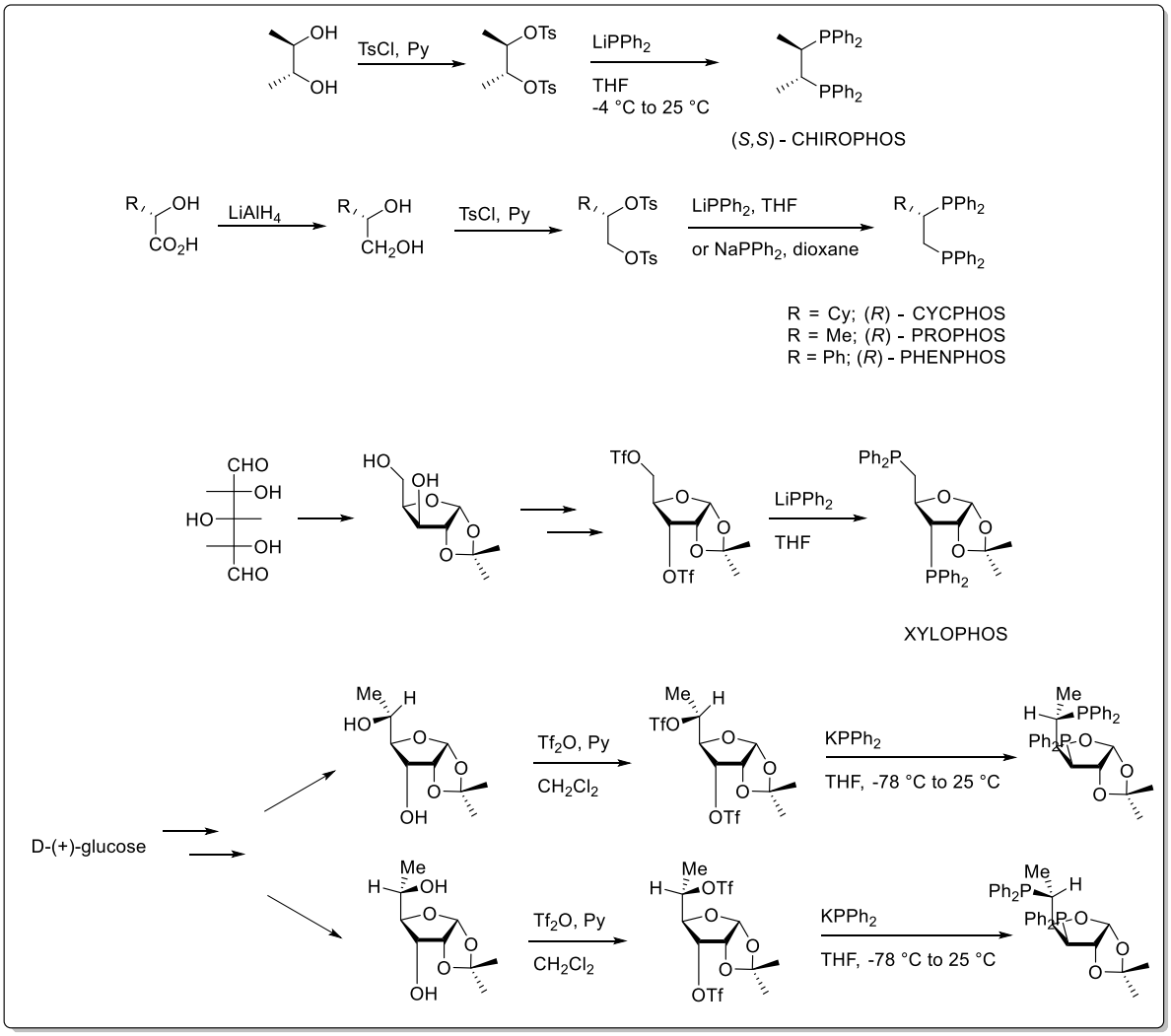

Scheme 3. Synthesis of C_1- and C_2-symmetric 1,2-diphosphine ligands from chiral pool.

Certain natural products that bear chiral centers in their backbone skeleton, such as carbohydrates and their derivatives, are also good candidates for chiral phosphines synthesis. One example is the synthesis of XYLOPHOS from the readily available D-(+)-xylose.[26] From D-(+)-glucose, Diéguez *et al*. were able to produce two different diphosphines with a simple introduction of an additional stereogenic center into the backbone.[27] Despite being an excellent chiral backbone for building enantiopure phosphines, carbohydrates having the D-(+)-configuration are often the only readily available enantiomers.

Chiral pool synthesis was also used in the early development of *P*-chiral diphosphines. One such example was reported by King *et al.* whose group employed the widely available (–)-menthol for the synthesis of *P*-chirogenic diphosphines by converting the natural product to (–)-menthyl chloride and (+)-neomenthyl chloride.[25] These chlorides were subsequently used in the reaction with the sodium salt of phenylphosphide to give the respective chiral monophosphines. The generation of the following *P*-chiral diphosphines was accomplished by the reaction between monophosphines and vinylphosphines.

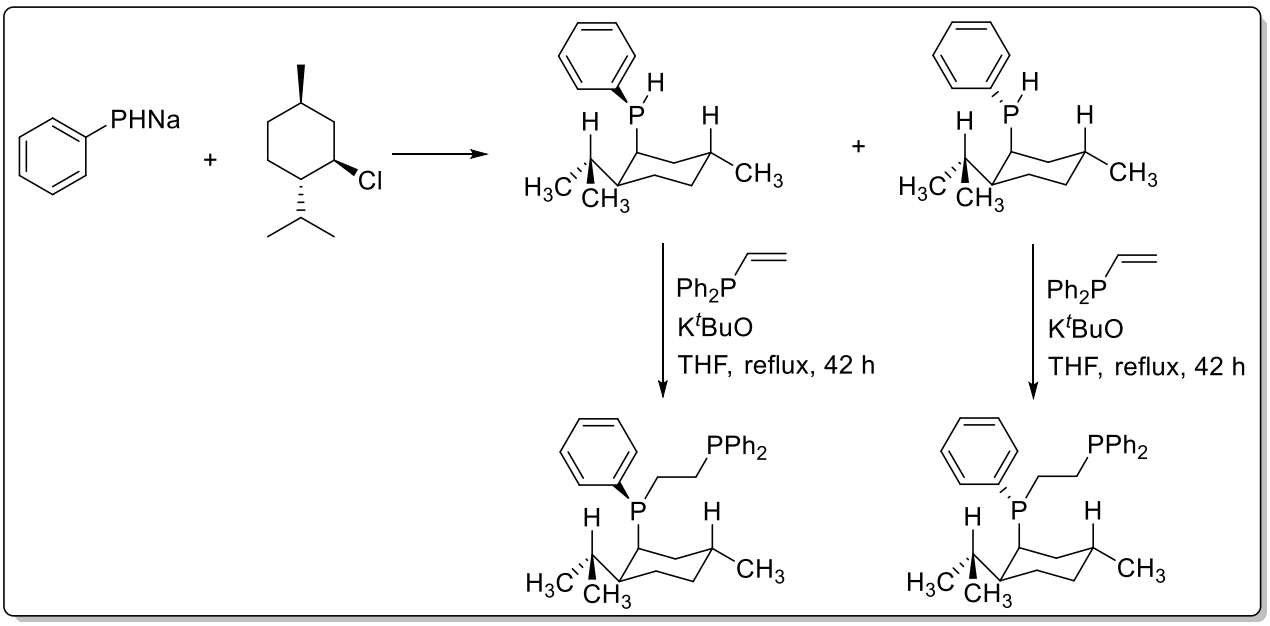

Scheme 4. Chiral pool synthesis of *P*-chiral-diphosphines reported by King *et al*.

However, due to the finite number of naturally occurring chiral compounds, the diversity of such compounds is limited. In addition, the occurrence of only a single hand form in nature makes the other hand form limited in availability and expensive in production.

1.3.2 Optical Resolution/Chiral Auxiliary

With the ever-increasing demand and popularity of optically active phosphines both in the industries and in science, optical resolution and chiral auxiliary methods provide simple yet easily accessible methods to these phosphines. In general, the optical resolution and chiral auxiliary methodologies as means to generate chiral phosphines have seen much improvement over the years.[28] These methodologies rely on the fact that diastereomers have different physical properties in order to obtain enantioenriched products from a racemic mixture. Derivatization of the racemic mixture with an optically pure reactant will yield two diastereomeric products and these diastereomers can be separated either through column chromatography or through crystallization. An additional step to remove the derivative is needed to obtain the desired chiral compound. In certain cases, kinetic resolution could be used in which the rates of reaction between the optically pure derivative and the two enantiomers of the compound are significantly different. In such cases, it is likely that only one enantiomer reacts with the chiral derivative while the other enantiomer remains unreactive.

Early chiral phosphines synthesized using the chiral auxiliary method were CAMP and DIPAMP, from an optically active secondary alcohol, (–)-menthol obtained from peppermint oil. This multistep procedure involved the formation of menthyl ester diastereomers that can be separated using physical means. The *S* isomer was further reacted with a Grignard reagent, PhMgCl, to install a phenyl group and form the common intermediate **1**, before eventually affording both CAMP and DIPAMP.[17, 29]

C$_2$-symmetrical atropoisomeric BINAP was also developed by Noyori using a chiral palladacycle, an efficient resolving agent having coordination sites on the palladium(II) metal center for coordination with the enantiomers to form diastereomers. The diastereomers formed were subjected to fractional recrystallization, before undergoing a reduction to remove the chiral auxiliary.[15f] Noyori further improved this process by using (+)-camphorsulfonic acid and DBTA as the resolving agent.[30]

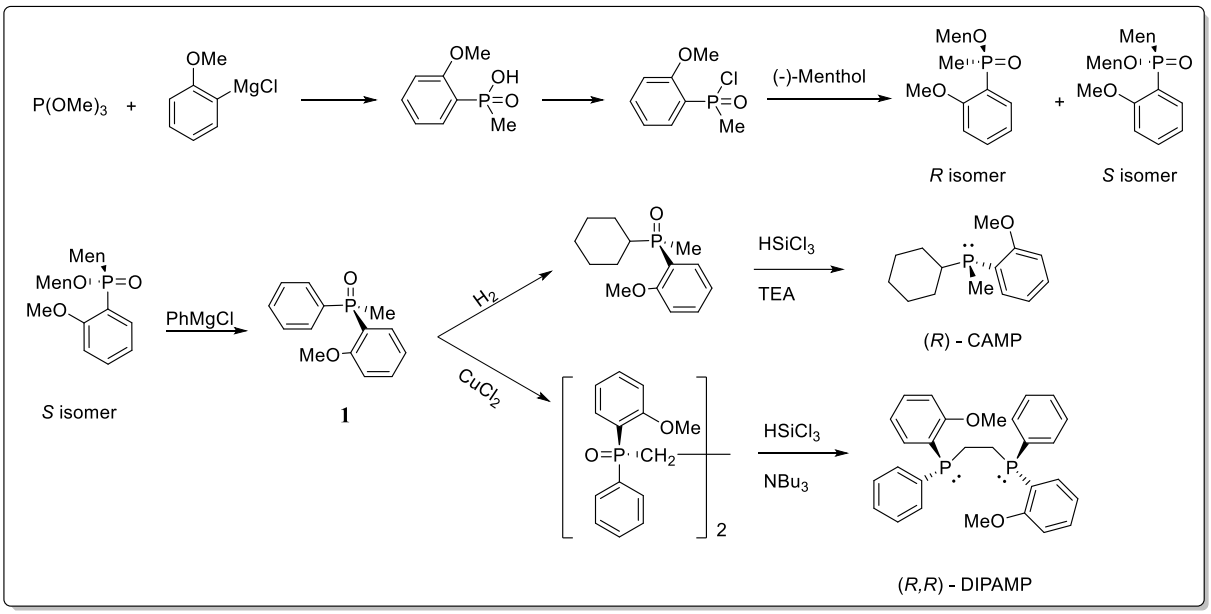

Scheme 5. Synthetic pathway to synthesize CAMP and DIPAMP using (–)-Menthol.

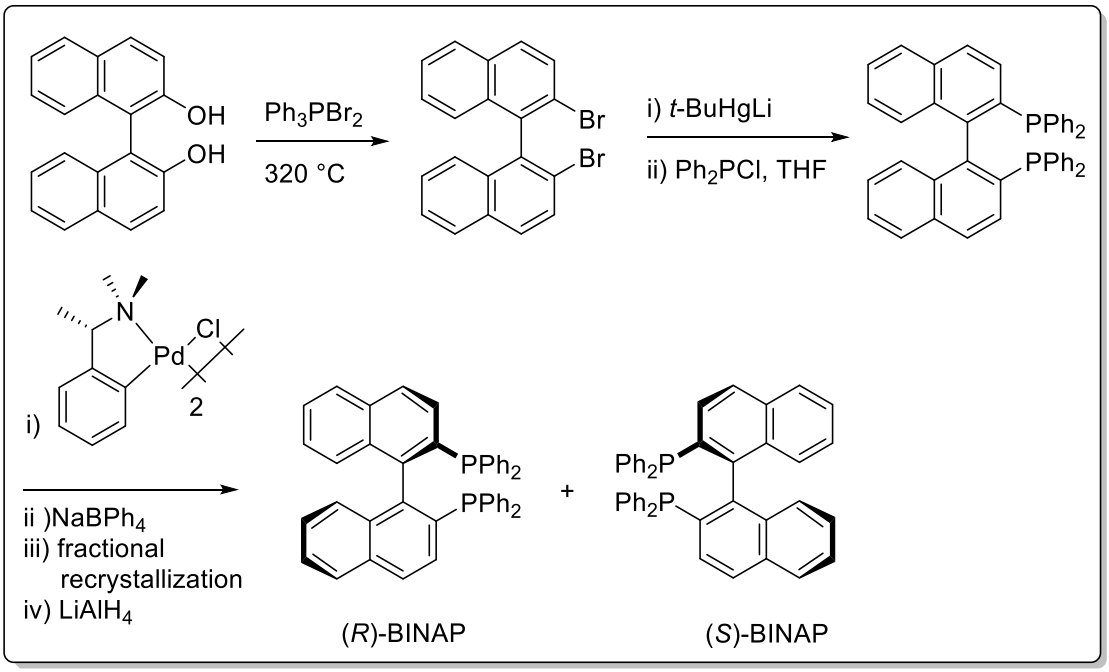

Scheme 6. Using palladacycle resolving agent to obtain enantiopure BINAP.

In addition, optically pure organic acids, such as (–)-2,3-dibenzoyl-L-tartaric acid ((–)-DBTA) and (+)-2,3-dibenzoyl-D-tartaric acid ((+)-DBTA), are also commonly utilized as optical resolution reagents. The established chiral phosphine, NORPHOS, was synthesized *via* the Diels-Alder reaction, with the separation of the enantiomers done using (–)-DBTA as the resolving agent, followed by the reduction of the oxides with trichlorosilane to allow the preparation of both NORPHOS enantiomers.[31]

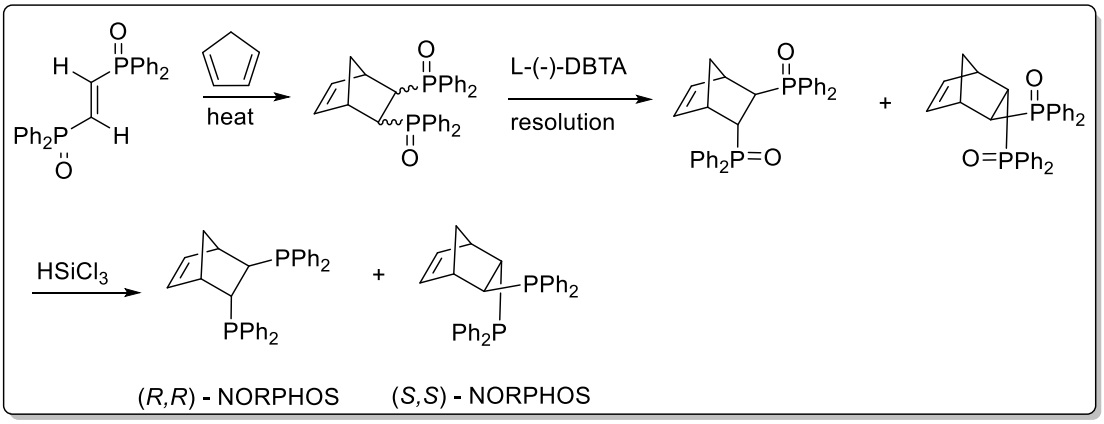

Scheme 7. Synthesis of NORPHOS *via* Diels-Alder reaction with optical resolution.

Besides being used to produce *C*-chiral diphosphines, DBTA could also be used to form C_2-symmetric planar and *C*,*P*-stereogenic diphosphines. Merck's chemists applied this technique with the other hand form of the organic tartaric acid to generate chiral PHANEPHOS. The diastereomers formed with (+)-DBTA had different solubility in chloroform at room temperature and thermal crystallization method was used to separate the two distinct diastereomers.[32] Zhang and co-worker were able to obtain optically pure four-stereogenic centers diphosphine, DuanPhos, from the use of either (+)-DBTA or (–)-DBTA.[33]

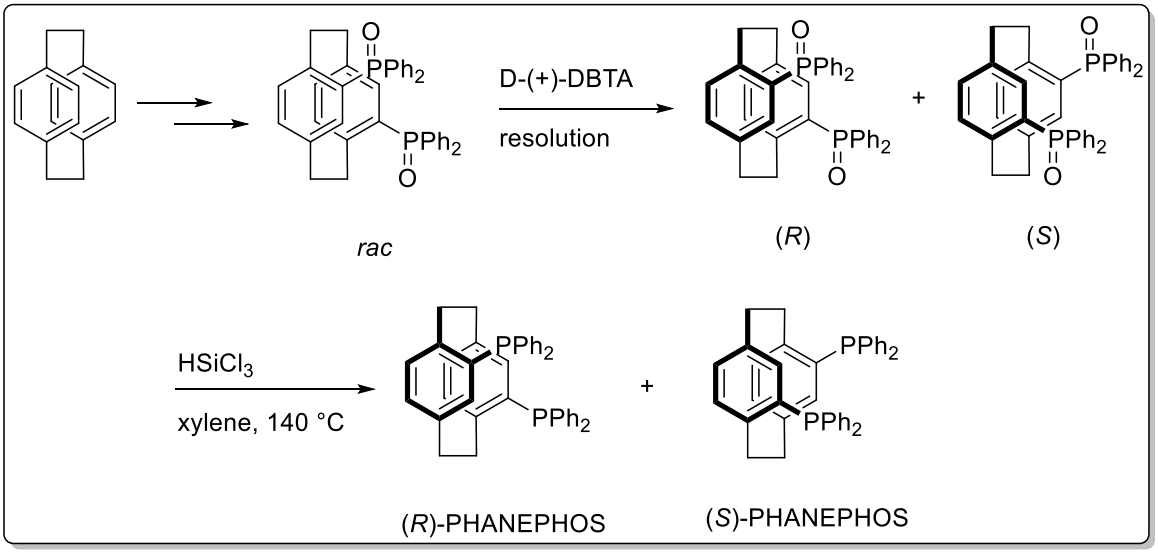

Scheme 8. Synthesis of PHANEPHOS using optically pure DBTA.

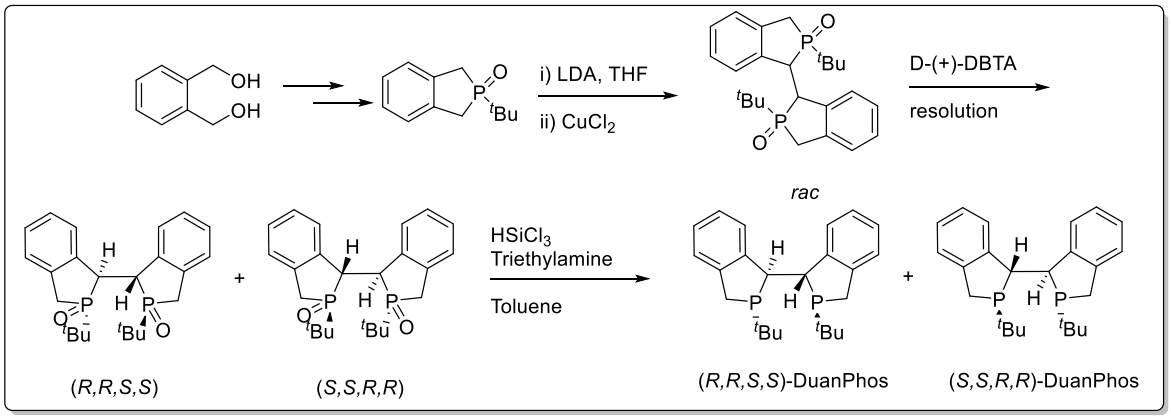

Scheme 9. Synthesis of DuanPhos *via* optically resolution with (+)-DBTA.

Moreover, optical resolution has also been utilized in the synthesis *P*-chiral 1,2-diphosphines. Imamoto *et al*. reported the synthesis of conformationally rigid *P*-chiral 1,2-diphosphines *via* the aforementioned optical resolution method.[34] The initial racemic monophosphines were coupled to form a mixture of chiral and *meso* *P*-stereogenic diphosphines dimers. Subsequent separation of the diastereomers following by resolution of the enantiomers in the racemic mixture using DBTA afforded the individual 1,2-*P*-chiral diphosphines.

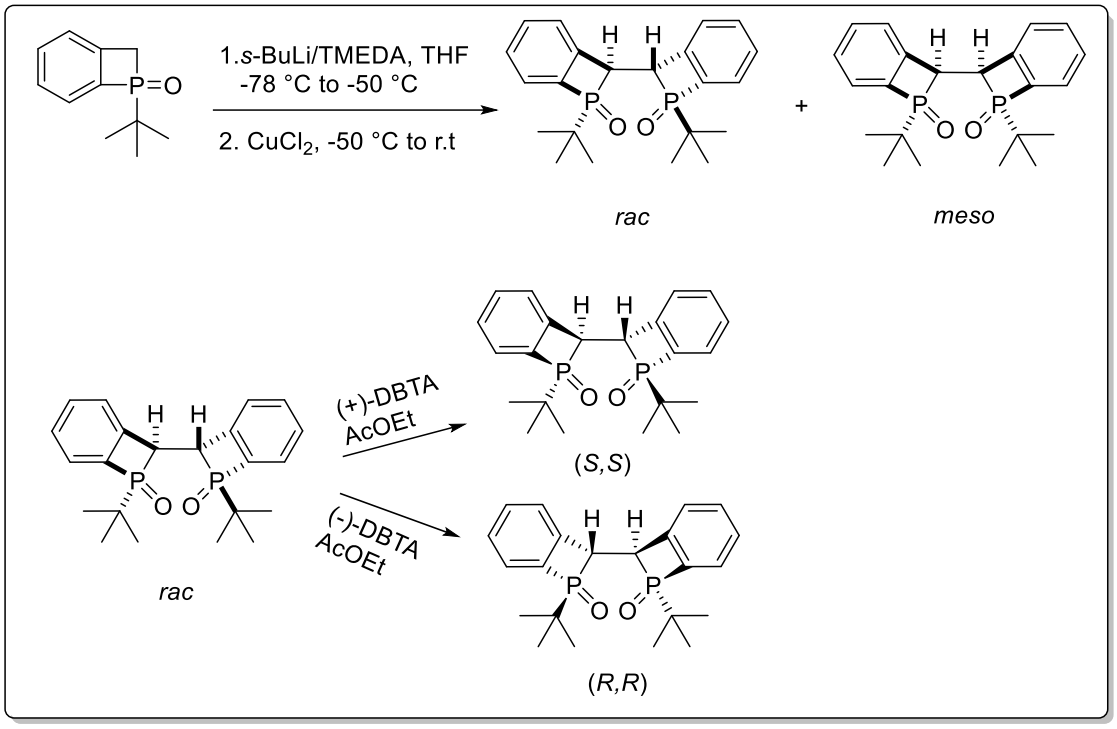

Scheme 10. Optical resolution in the synthesis of 1,2-*P*-chiral-diphosphine reported by Imamoto *et al*.

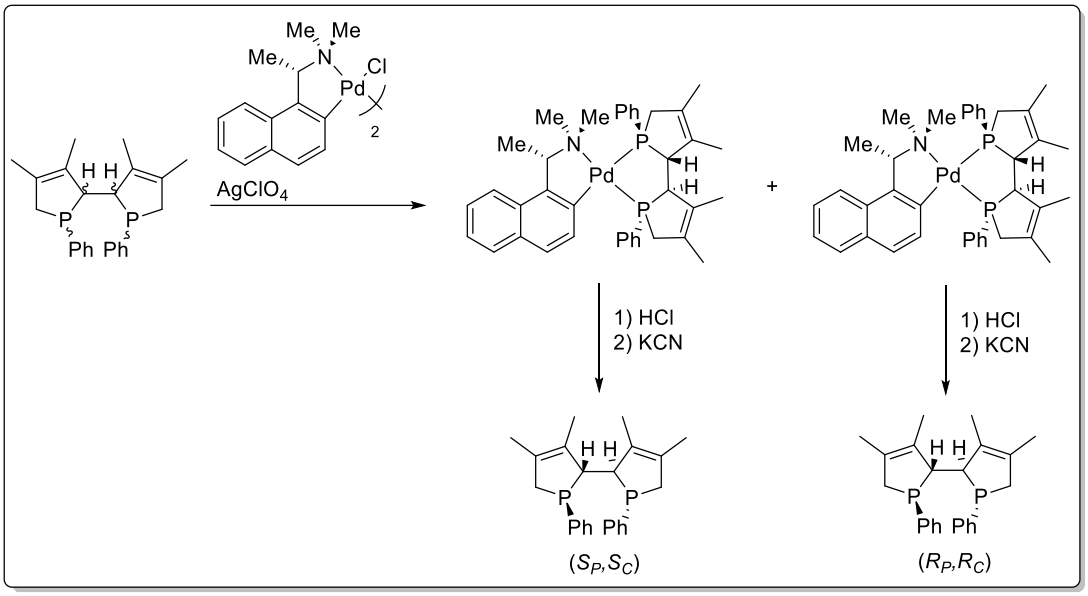

Scheme 11. Optical resolution in the synthesis of *P*-chiral-diphosphines reported by Leung *et al*.

Leung and co-workers separated racemic *P*-stereogenic heterocyclic diphosphines into their respective enantiopure variants through the use of a chiral metal template as the resolving agent before liberating the free diphosphines with KCN.[35]

In some cases, separation of the *P*-chiral 1,2-diphosphines diastereomers formed using optical resolution may be challenging. As such, the usage of chiral metal template, not as a resolving agent but as a chiral auxiliary, could be an alternative methodology. Leung *et al.* reported the use of a chiral auxiliary template in an asymmetric Diels-Alder reaction to access a variety of *P*-stereogenic diphosphines.[36]

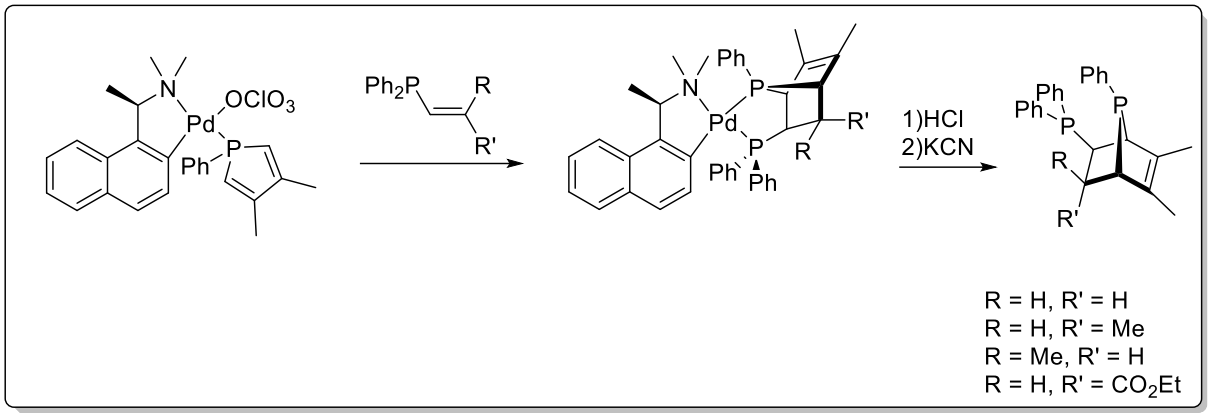

Scheme 12. Usage of chiral auxiliary template in the synthesis of *P*-chiral-diphosphines reported by Leung *et al*.

While numerous examples of chiral phosphines generated from the methods of chiral auxiliaries and optical resolution have been reported successfully to date, these two methods have their own limitations. Firstly, chiral auxiliaries are often expensive to generate or isolate. Secondly, the attachment and de-attachment of the auxiliaries on the racemic and chiral phosphines make the synthetic pathway time-consuming. In addition, the separation of diastereomers using physical means will take up additional time to produce the targeted chiral products. Thirdly, the removal of these auxiliaries generally entails chemical structural change to the auxiliaries which makes isolating and recovering of the same auxiliary almost impossible. As a result, additional unwanted waste and by-products may be generated by the reactions. Lastly, the auxiliaries used are often dependent on the specific compounds generated. Any slight change to the functional groups could render the auxiliaries useless. The above-mentioned limitations are in conflict with the twelve principles of green chemistry.[37]

1.3.3 Enantioselective Deprotonation

Initially reported by Raston *et al.*,[38] enantioselective deprotonation was combined with oxidative dimerization by Evans *et al.* for the development of C_2-symmetry *P*-chiral

diphosphines.[39] This idea was a combination of two established chemistry concepts. First, the possible deprotonation of methylphosphines at the methyl group with a strong base,[40] and second, the conversion of prochiral compounds to enantiopure variants using organolithium reagents in the presence of a chiral auxiliary for enantioselective deprotonation.[41] The oxidation of enantioenriched lithiated phosphine-borane complex using copper (II) salt to yield the corresponding borane-protected chiral diphosphines has been a notable protocol to access BisP*[42] and highly rigid and electron rich bisphospholane ligands.[34, 43]

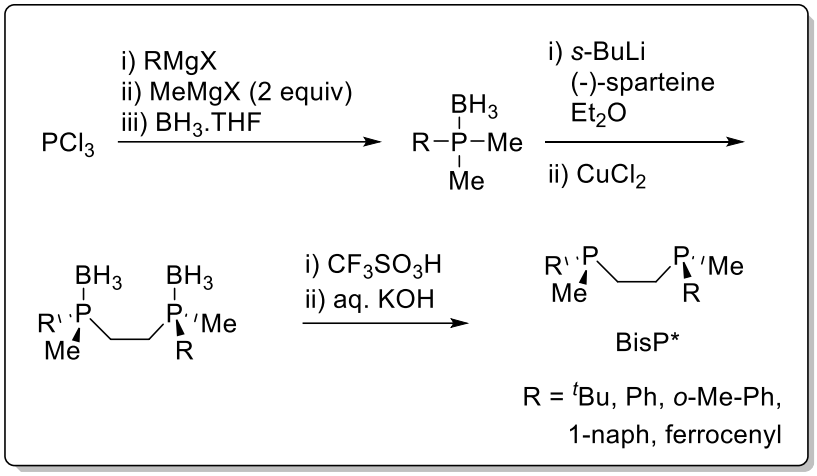

Scheme 13. Enantioselective deprotonation synthesis of BisP* diphosphines.

1.3.4 Asymmetric Synthesis of Optically Active Phosphines *via* Catalysis

The use of chiral catalysts to generate chiral phosphines in asymmetric syntheses has shown to be of significance to organophosphorus chemistry in recent years. The usage of this method has since overtaken other methods in the expansion of the library associated with optically active phosphines due to its simpler procedures and improved efficiency. Over the years, many phosphines bearing *C*-stereogenic centers, axial and planar chiralities have been synthesized due to their widespread applications in various catalytic reactions.[44] One such phosphine is the *C*-chiral PROPHOS, generated in the "self-breeding" catalytic system devised by Bosnich and co-worker.[24] This protocol involved the use of the target ligand to generate an

enantiomeric intermediate that could in turn lead to the regeneration of the ligand itself. This method yielded a significant amount of product ligand from a small catalytic amount of catalyst containing the chiral phosphine PROPHOS. The process began with the hydrogenation of readily available ethyl pyruvate to form (*S*)-ethyl O -acetyllactate **2** with the (*R*)-PROPHOS-containing rhodium catalyst. The subsequent reduction and toyslation of **2** gave ditosylate **3**. Further single recrystallization of the ditosylate improved the enantiomeric excess (*ee*) from 80% to 99%. Finally, nucleophilic substitution of the ditosylate using diphenylphosphide generated (*R*)-PROPHOS.

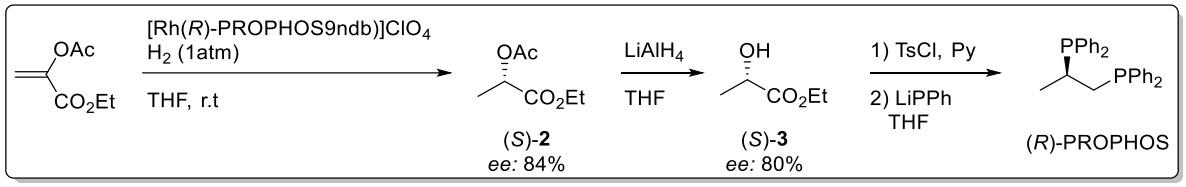

Scheme 14. "Self-Breeding" catalytic system.

Bosnich and co-workers successfully performed 'cross breeding' using (*S*,*S*)-SKEWPHOS as a ligand in a ruthenium complex system.[45] The use of SKEWPHOS ligand and a ruthenium precursor to form the desired SKEWPHOS containing ruthenium(II) catalyst was used in a asymmetric hydrogenation reaction to produce diol **4** from acetylacetone. The optically active diol further underwent mesylation and nucleophilic substitution using lithium phosphide salt to afford the opposite hand-form of *C*-chiral diphosphine, SKEWPHOS, with different aryl groups on the phosphorus atoms.

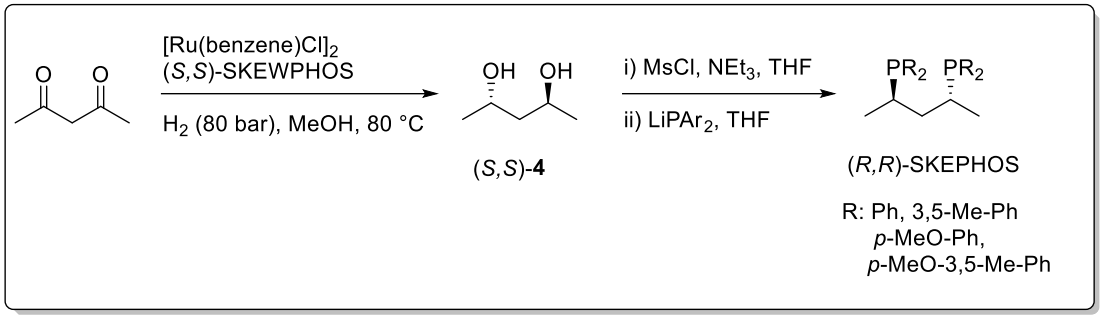

Scheme 15. 'Cross Breeding' of SKEPHOS ligand.

In the recent synthesis of axially chiral bisphosphobiarenes, Watson and co-workers conducted a nickel-catalyzed Ullmann coupling to access these privileged ligands.[46] *ortho*-(iodo)phosphonates was used in this report together with a nickel catalyst in tandem with manganese as the terminal reductant and cobalt phthalocyanine as the co-catalyst to furnish the desired product with high enantioselectivity and yield. These bisphosphonates could eventually be reduced to secondary chiral phosphines.

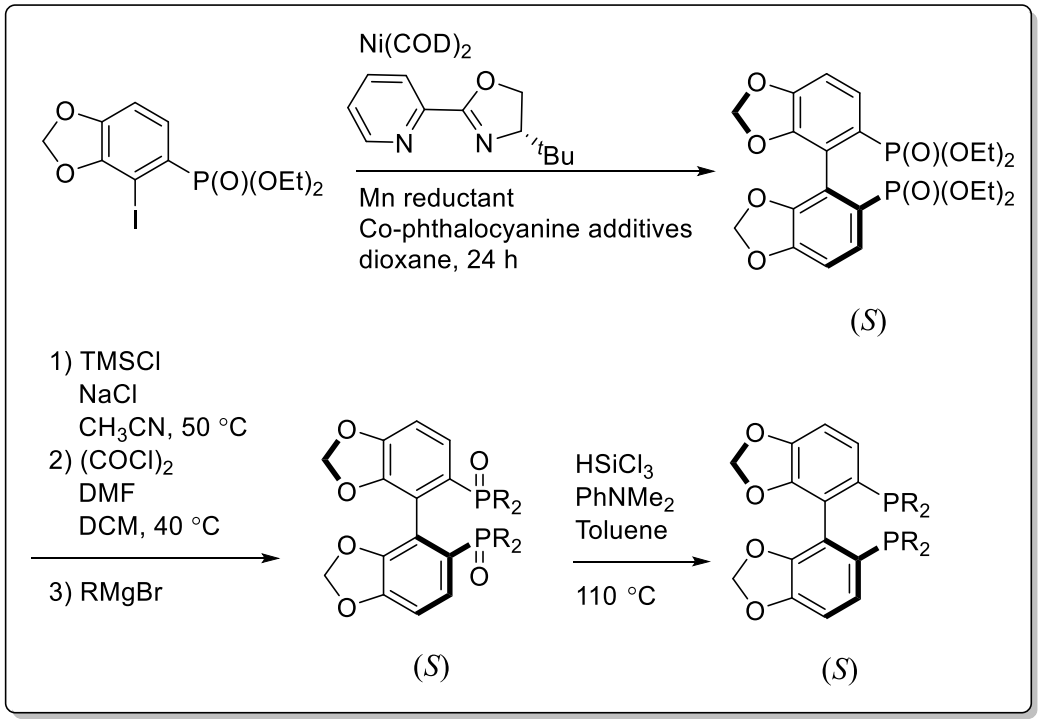

Scheme 16. Asymmetric Ullmann coupling reaction.

Another well-known asymmetric reaction that produced axially biaryl phosphines ligands was the Suzuki-Miyaura coupling reaction. However, unlike the Ullmann coupling reaction, Suzuki-Miyaura reaction could only generate biaryl phosphine ligands that were not sterically hindered or monophosphines.[47] One such example reported by Zhang and co-worker involved the synthesis of a series of axially chiral biaryl monophosphine oxides which could again be reduced with silanes to give free axially chiral biaryl monophosphines.[47c]

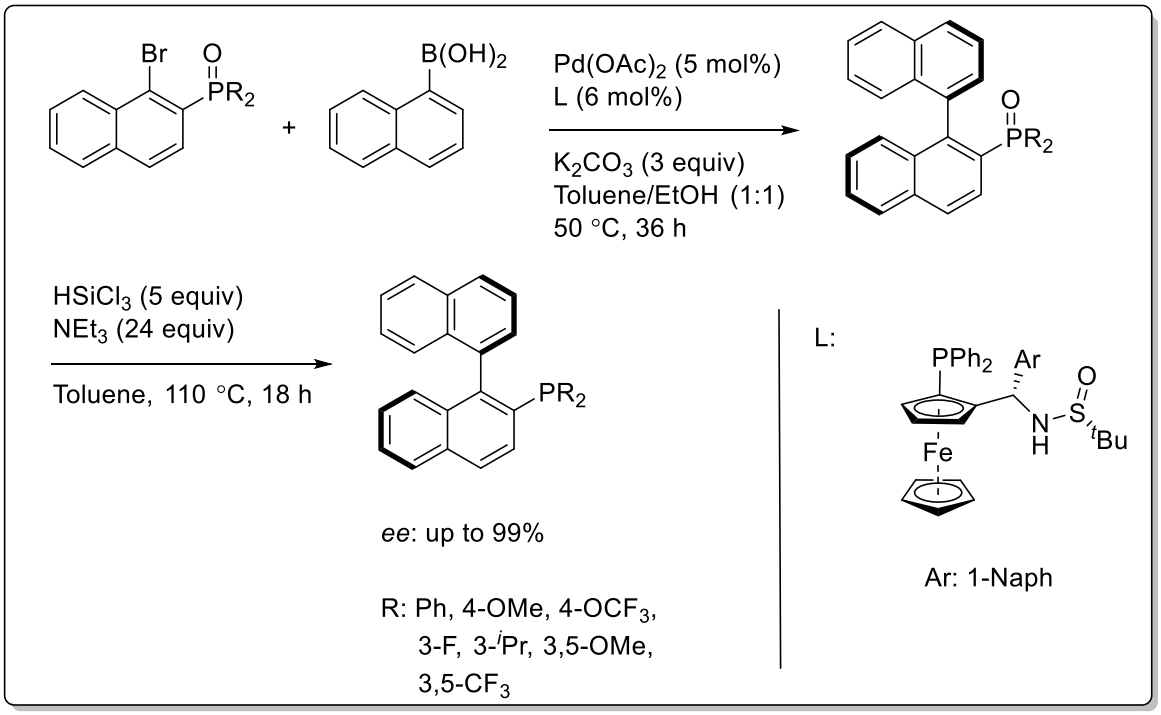

Scheme 17. Asymmetric Suzuki-Miyaura coupling reaction to produce axially chiral monophosphines.

Lastly, access to *P*-stereogenic diphosphines *via* the aforementioned established protocols are often non-versatile, time-consuming and costly. The multi-step processes make handling of the air-sensitive free secondary phosphines difficult. Whilst installation of protecting groups on these phosphines for easier manipulation is a viable option, additional steps to release the said moieties prior to coordination are required. Moreover, further purification procedures may be necessary and cumbersome. Asymmetric catalytic protocols promise solutions to the abovementioned issues by offering benefits such as simple one-step

procedures and inherent stereoselectivities. To the best of our knowledge, there exists only one such mentioned system to form *P*-stereogenic diphosphines – *metal-catalyzed asymmetric alkylation of secondary phosphines* – developed by Glueck in 2006.[48]

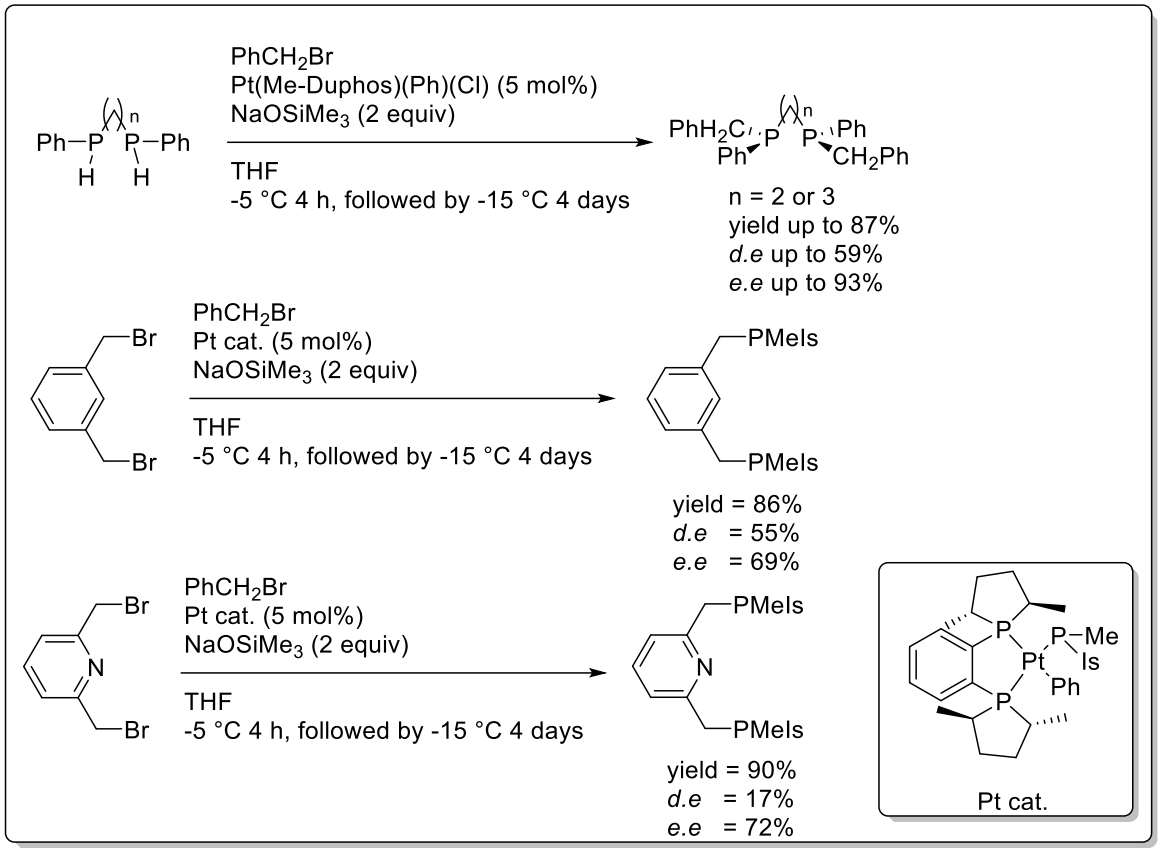

Scheme 18. Metal-catalyzed asymmetric alkylation of secondary phosphines.

1.4 Applications of Chiral Phosphines

1.4.1 Asymmetric Hydrogenation

The use of chiral phosphines as ligands in asymmetric catalytic reactions had been well established since the early breakthrough by Wilkinson *et al.* in 1966.[49] The first reported asymmetric catalysis utilizing these compounds was applied in the field of hydrogenation reaction on *α*-substituted acrylic acids using chiral methyl(isopropyl)phenylphosphine. Despite the fact that this reaction showed poor enantioselectivity (15% *ee* with α-phenylacrylic acid),[12-

[13] the utilization of chiral phosphines ligands in asymmetric hydrogenation still possessed great potential. Further modification to the methyl(isopropyl)phenylphosphine with *o*-anisyl group, in an attempt to increase the steric hindrance of the ligand, significantly improved the enantioselectivity of the hydrogenation reaction on α-dehydroamino acid.[17] Dimerization of PAMP to form the chelating diphosphine DIPAMP has proven to be more efficient in catalyzing the reaction to form L-DOPA, a drug for treating Parkinson's disease.[17, 29] Other successful optically active phosphines utilized in asymmetric C–H bond formation on C=C were (*S*,*S*)-CHIRAPHOS,[15j, 50] (*S*,*S*)-TangPHOS,[43, 51] (*S*,*S*)-FerroPHOS,[52] (*S*,*S*)-DuPHOS,[15f, 53] BINAP,[15f] and QuinoxP*.[54] .

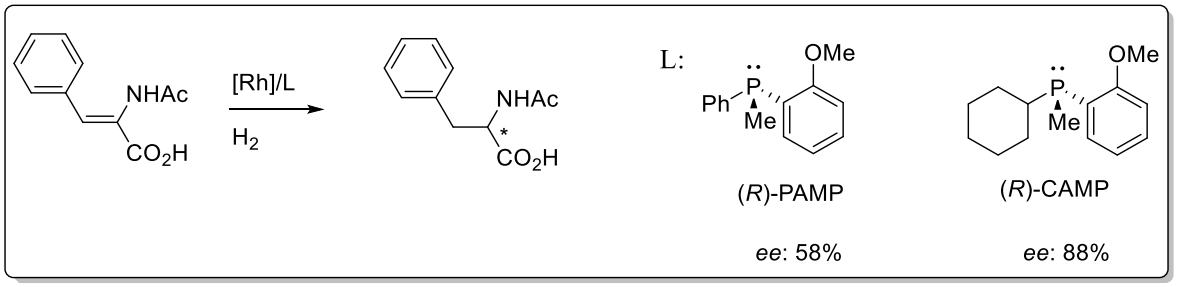

Scheme 19. Asymmetric hydrogenation reaction using chiral PAMP and CAMP as ligands.

In addition to asymmetric C–H bond formation reactions of C=C moiety, the scope of chiral phosphines found to be efficient as ligands in catalyzing hydrogenation reactions was expanded to include C=O moieties, *β*- and thiol esters, imines and amides. Noyori *et al.* had established the use of ruthenium-BINAP catalyst to hydrogenate β-esters *via* dynamic kinetic resolution.[55] This method has been used to widen the scope of enantiopure building blocks, which includes the production of Carbapenems **6** from the asymmetric hydrogenation of *rac*-**5**, by Takasago International Corporation,[56] and Fosfomycin,[57] both of which are antibiotics.

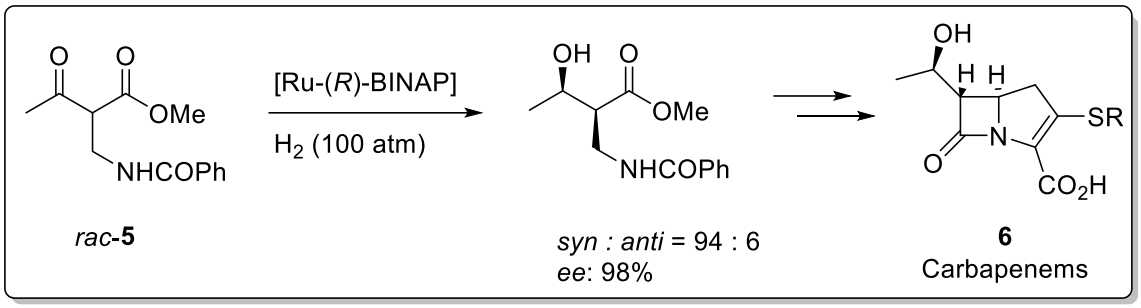

Scheme 20. Asymmetric hydrogenation reaction on C=O moiety in the synthesis of Carbapenems.

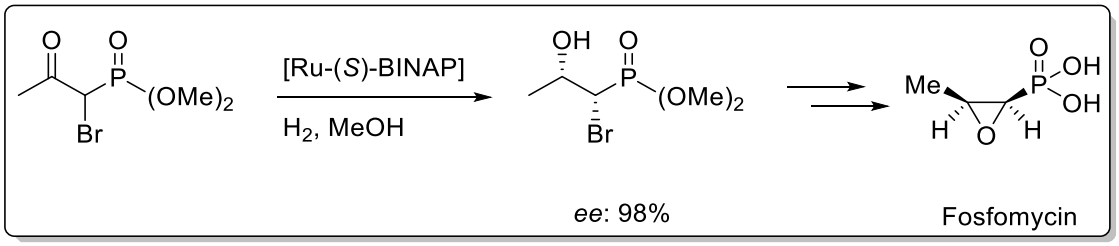

Scheme 21. Asymmetric hydrogenation reaction on C=O moiety in the synthesis of Fosfomycin.

Other efficient chiral phosphine ligands that have contributed to asymmetric hydrogenation of C=O functional group include (*S*)-SEGPhos,[58] (*S*)-SunPhos,[59] (*R*)-MeO-Biphep,[60] (*R*)-bisbenzodioxanPhos,[61] (S_C,R_P)-DuanPhos.[33]

Asymmetric C=N reduction presents an additional challenge due to the fact that the *E*/*Z* conformation of the imine will affect the reaction outcome and that some imines are susceptible to hydrolysis. Most of the successful asymmetric reactions involve the use of iridium complex containing diphosphines and phosphinooxazolines. This protocol has contributed significantly to the industrial process of producing Metolachlor, an active ingredient in the herbicide Dual,[62] and Dextromethorphan, an antitussive drug.[63] Another example worth mentioning is the asymmetric hydrogenation of unprotected imines to form unprotected simple chiral amines, developed by Merck, Zhang and co-workers.[64]

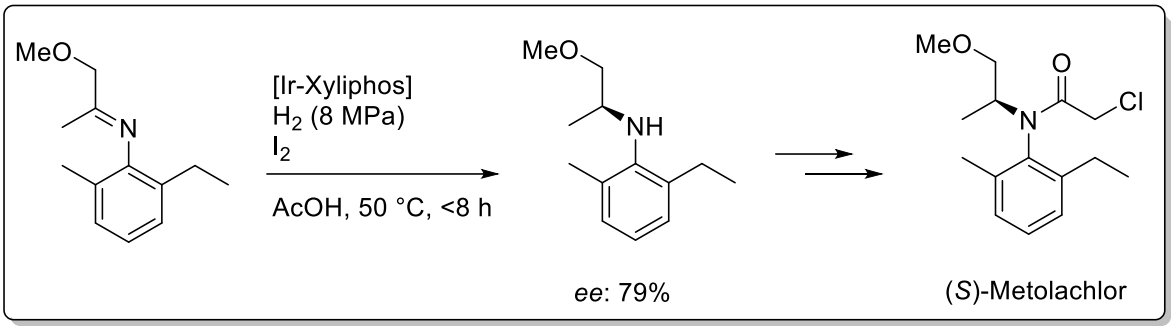

Scheme 22. Asymmetric hydrogenation reaction on C=N moiety in the synthesis of Metolachlor.

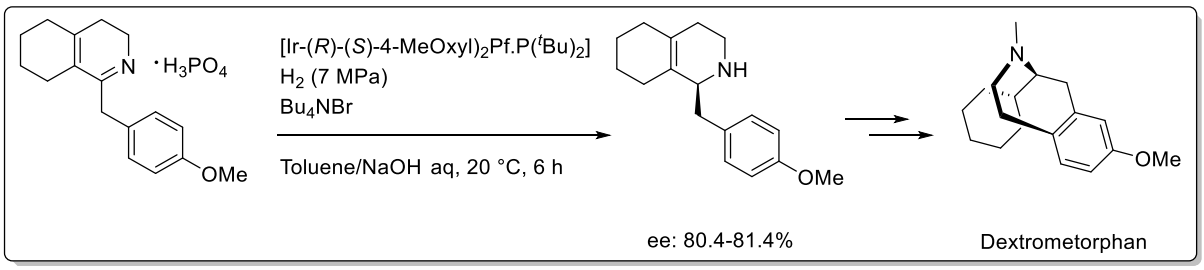

Scheme 23. Asymmetric hydrogenation reaction on C=N moiety in the synthesis of Dextrometorphan.

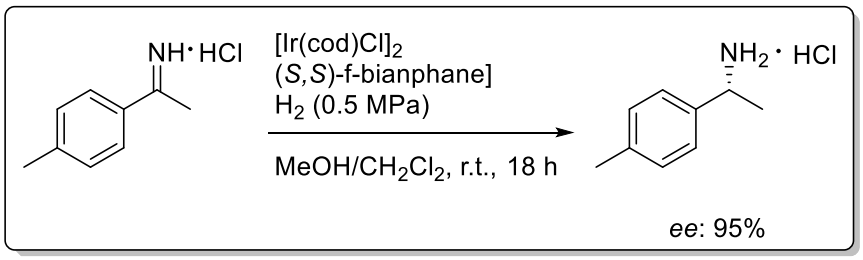

Scheme 24. Asymmetric hydrogenation of imines.

1.4.2 Asymmetric C–C Bond Formations

Besides asymmetric C–H bond formation reactions, chiral phosphines have also been widely utilized both as ligands in metal catalyzed reactions and as organocatalysts in asymmetric C–C bond formation. Application of chiral phosphines includes, but are not limited

to, asymmetric Michael addition,[65] Rauhut-Currier (RC) reaction,[65b] asymmetric 1,4-addition of arylboronic acids to *α,β*-unsaturated carbonyl compounds,[66] and asymmetric 1,4-addition of organometallic reagents to *α,β*-unsaturated carbonyl compounds.[67]

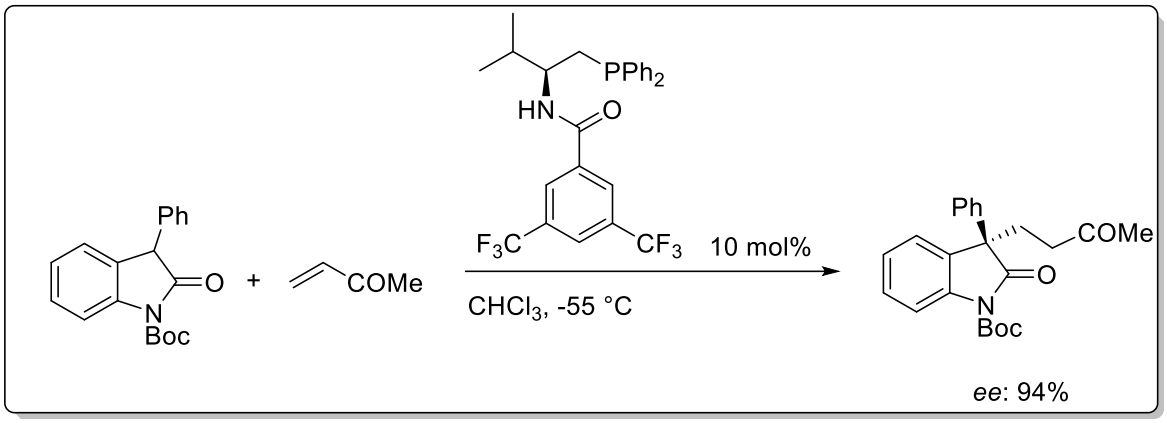

Scheme 25. Asymmetric Michael addition using chiral phosphine as organocatalysts.

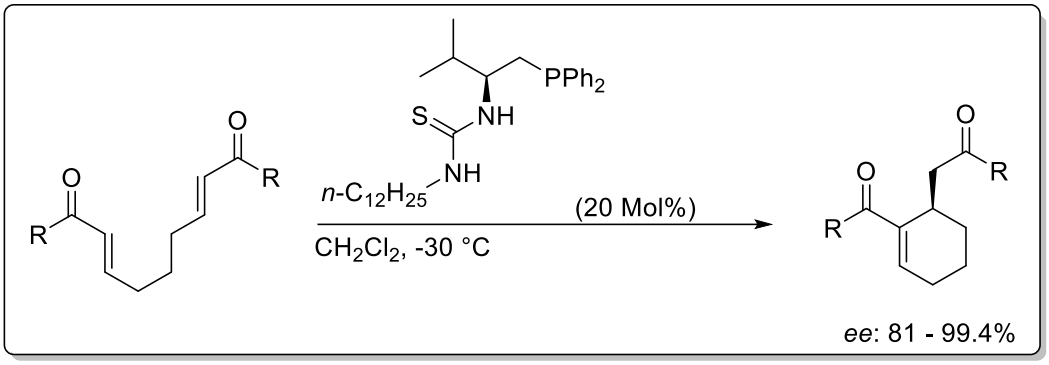

Scheme 26. Asymmetric Rauhut-Currier reaction using chiral phosphine as organocatalysts.

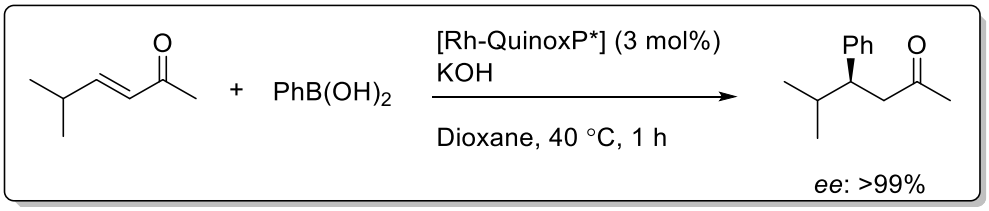

Scheme 27. Asymmetric 1,4-addition of phenyboronic acid to *α,β*-unsaturated carbonyl compound.

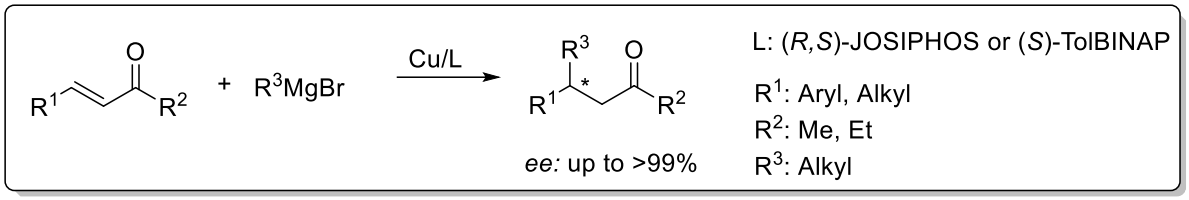

Scheme 28. Asymmetric 1,4-addition of grignard reagents to *α,β*-unsaturated carbonyl compounds.

1.4.3 Other Asymmetric Reactions

Apart from asymmetric C–H and C–C bond formation reactions in which the two main reactions chiral phosphines have played a significant role in, optically active phosphines have also been proven to be efficient in asymmetric C–X bond formation,[68] ring-opening reaction,[66, 69] hydrosilylation,[70] borylation,[71] *etc*.

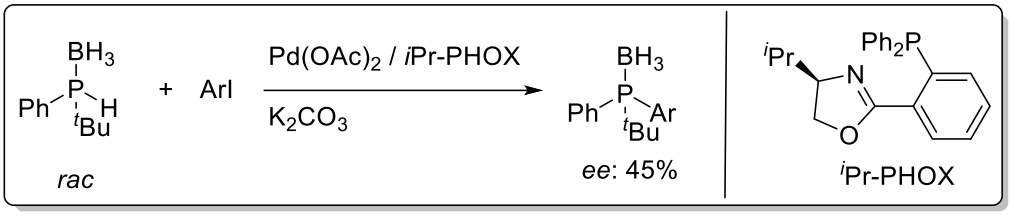

Scheme 29. Example of an asymmetric C–X (C–P) bond formation.

Asymmetric hydrosilylation has been successfully achieved with chiral bidentate ligands consisting of donor atoms such as nitrogen, sulfur and carbon. While some diphosphine ligands were not as efficient in improving the enantioselectivity of the reaction, it has been shown that *trans*-chelating diphosphine ligands were able to enhance the enantioselectivity of hydrosilylation reactions. Imamoto *et al.* designed a rhodium catalyst consisting of a chiral *P*-diphosphine as the ligand to aid in the asymmetric hydrosilylation of achiral ketone with up to 99 % enantioselectivity.[70]

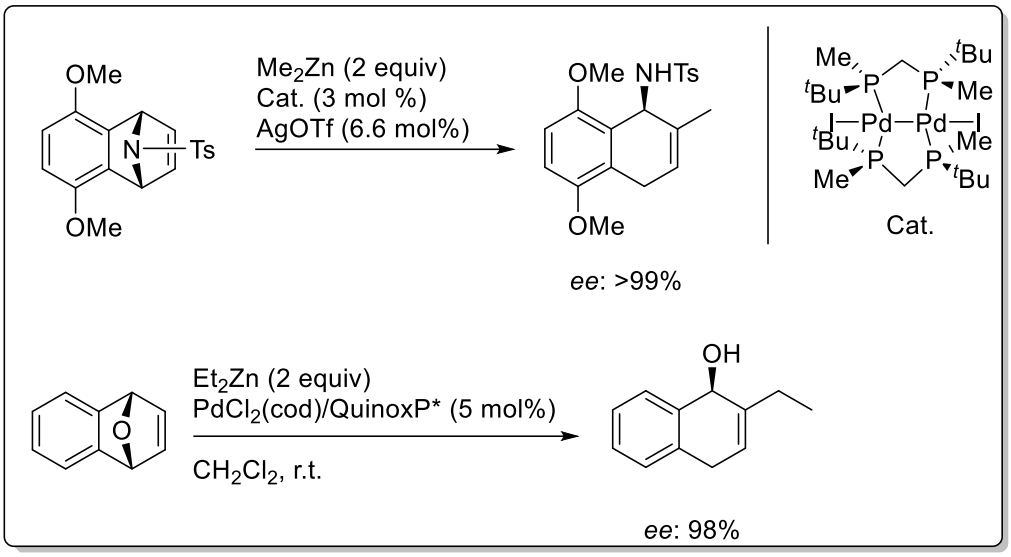

Scheme 30. Examples of asymmetric ring-opening reactions.

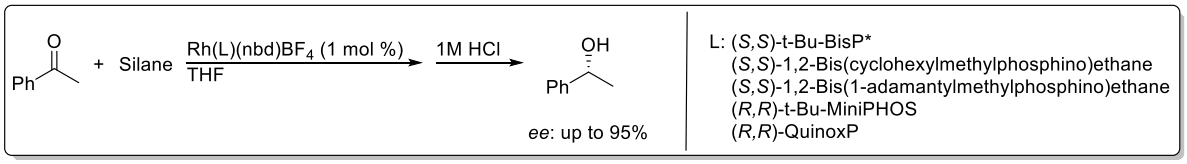

Scheme 31. Asymmetric hydrosilylation using Imamoto's rhodium catalysts.

Complexation of *P*-chiral diphosphines to a copper metal generated a copper(I) complex that was capable of catalyzing an asymmetric borylation reaction from alkenylsilane substrates.[71a] The enantioselectivity of this catalyst has shown to be more efficient as compared to chiral *N*-heterocyclic carbene-copper complexes.[71b]

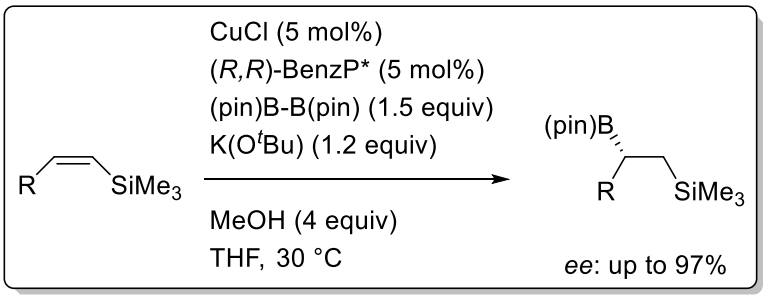

Scheme 32. Asymmetric hydroborylation of vinyl silane.

1.5 Aims of Thesis

Given the importance of chiral phosphines in asymmetric catalysis, decades of research have been dedicated to devise protocols and synthetic pathways to diligently expand the library associated with optically active phosphines. Amongst these chiral phosphines, optically active diphosphines have garnered much attention due to their prevalent usages in numerous asymmetric metal-assisted and organocatalytic reactions The chiral diphosphines employed in these systems typically consist of stereogenic centers either at the carbon backbone or on the phosphorus atoms. The presence of two chiral centers in close proximity to the metal center and the bidentate nature of diphosphines allows a more efficient transfer of chiral information from the ligand to the coordination sphere of the metal. As such, this thesis aims to introduce novel chiral diphosphines and provide general yet simple asymmetric pathways to synthesize challenging chiral diphosphines.

1.6 References

1. S. Mauskopf, CHAPTER 1 - A history of chirality. In *Chiral Analysis*, Busch, K. W.; Busch, M. A., Eds. Elsevier: Amsterdam, 2006; pp 3.

2. L. A. Nguyen; H. He; C. Pham-Huy, *Chiral drugs: an overview*, *Int J Biomed Sci* **2006**, *2*, 85.

3. Y. Chen; W. Ma, *The origin of biological homochirality along with the origin of life*, *PLoS Comput. Biol.* **2020**, *16*, e1007592.

4. T. Eriksson; S. Björkman; B. Roth; P. Höglund, *Intravenous formulations of the enantiomers of thalidomide: pharmacokinetic and initial pharmacodynamic characterization in man*, *The Journal of pharmacy and pharmacology* **2000**, *52*, 807.

5. R. S. Cahn; C. Ingold; V. Prelog, *Specification of Molecular Chirality*, *Angew. Chem. Int. Ed. Engl.* **1966**, *5*, 385.

6. S. Arae; M. Ogasawara, *ChemInform Abstract: Catalytic Asymmetric Synthesis of Planar-Chiral Transition-Metal Complexes*, *J. Syn. Org. Chem. Jpn.* **2012**, *70*, 593.

7. M. Rickhaus; M. Mayor; M. Juríček, *Strain-induced helical chirality in polyaromatic systems*, *Chem. Soc. Rev.* **2016**, *45*, 1542.

8. H. Förster; F. Vögtle, *Steric Interactions in Organic Chemistry: Spatial Requirements of Substituents*, *Angew. Chem. Int. Ed. Engl.* **1977**, *16*, 429.

9. (a) C. D. Montgomery, *Factors Affecting Energy Barriers for Pyramidal Inversion in Amines and Phosphines: A Computational Chemistry Lab Exercise*, *J. Chem. Educ.* **2013**, *90*, 661; (b) A. Rauk; L. C. Allen; K. Mislow, *Pyramidal Inversion*, *Angew. Chem. Int. Ed. Engl.* **1970**, *9*, 400; (c) J. B. Lambert; W. L. Oliver, *Nitrogen Inversion without Retarding Factors*, *J. Am. Chem. Soc.* **1969**, *91*, 7774; (d) F. A. L. Anet; R. D. Trepka; D. J. Cram, *Electrophilic Substitution at Saturated Carbon. XXXI. Effects of Attached Second-Row Elements on the Rates of Nitrogen Inversion in Aziridines*, *J. Am. Chem. Soc.* **1967**, *89*, 357; (e) C. Kölmel; C.

Ochsenfeld; R. Ahlrichs, *Anab initio investigation of structure and inversion barrier of triisopropylamine and related amines and phosphines, Theor. Chim. Acta* **1992**, *82*, 271.

10. (a) J. M. Lehn; B. Munsch, *Electronic structure and inversion barrier of phosphine. An ab initio SCF–LCAO–MO study, J. Chem. Soc. D* **1969**, 1327; (b) J. B. Lambert; G. F. Jackson; D. C. Mueller, *Substituent effects in the inversion-rotation process of diphosphines, J. Am. Chem. Soc.* **1970**, *92*, 3093.

11. L. Horner; H. Winkler; A. Rapp; A. Mentrup; H. Hoffmann; P. Beck, *Phosphororganische verbindungen optisch aktive tertiäre phosphine aus optisch aktiven quartären phosphoniumsalzen, Tetrahedron Lett.* **1961**, *2*, 161.

12. L. Horner; H. Siegel; H. Büthe, *Asymmetric Catalytic Hydrogenation with an Optically Active Phosphinerhodium Complex in Homogeneous Solution, Angew. Chem. Int. Ed. Engl.* **1968**, *7*, 942.

13. W. S. Knowles; M. J. Sabacky, *Catalytic asymmetric hydrogenation employing a soluble, optically active, rhodium complex, Chem. Commun. (London)* **1968**, 1445.

14. R. H. Crabtree; D. M. P. Mingos, *Comprehensive organometallic chemistry III.* Elsevier: Amsterdam ; Boston 2007.

15. (a) T. P. Dang; H. B. Kagan, *The asymmetric synthesis of hydratropic acid and amino-acids by homogeneous catalytic hydrogenation, J. Chem. Soc. D* **1971**, 481; (b) H. B. Kagan; T.-P. Dang, *Asymmetric catalytic reduction with transition metal complexes. I. Catalytic system of rhodium(I) with (-)-2,3-0-isopropylidene-2,3-dihydroxy-1,4-bis(diphenylphosphino)butane, a new chiral diphosphine, J. Am. Chem. Soc.* **1972**, *94*, 6429; (c) H. B. Kagan; N. Langlois; T. Phat Dang, *Reduction asymetrique catalysee par des complexes de metaux de transition IV. synthese d'amines chirales au moyen d'un complexe de rhodium et d'isopropylidene dihydroxy-2,3 bis(diphenylphosphino)-1,4 butane (diop), J. Organomet. Chem.* **1975**, *90*, 353; (d) B. D. Vineyard; W. S. Knowles; M. J. Sabacky; G. L.

Bachman; D. J. Weinkauff, *Asymmetric hydrogenation. Rhodium chiral bisphosphine catalyst*, *J. Am. Chem. Soc.* **1977**, *99*, 5946; (e) W. S. Knowles, *Asymmetric hydrogenation*, *Acc. Chem. Res.* **1983**, *16*, 106; (f) A. Miyashita; A. Yasuda; H. Takaya; K. Toriumi; T. Ito; T. Souchi; R. Noyori, *Synthesis of 2,2'-bis(diphenylphosphino)-1,1'-binaphthyl (BINAP), an atropisomeric chiral bis(triaryl)phosphine, and its use in the rhodium(I)-catalyzed asymmetric hydrogenation of .alpha.-(acylamino)acrylic acids*, *J. Am. Chem. Soc.* **1980**, *102*, 7932; (g) H. Takaya; K. Mashima; K. Koyano; M. Yagi; H. Kumobayashi; T. Taketomi; S. Akutagawa; R. Noyori, *Practical synthesis of (R)- or (S)-2,2'-bis(diarylphosphino)-1,1'-binaphthyls (BINAPs)*, *J. Org. Chem.* **1986**, *51*, 629; (h) R. Noyori, *Centenary Lecture. Chemical multiplication of chirality: science and applications*, *Chem. Soc. Rev.* **1989**, *18*, 187; (i) R. Noyori; H. Takaya, *BINAP: an efficient chiral element for asymmetric catalysis*, *Acc. Chem. Res.* **1990**, *23*, 345; (j) M. D. Fryzuk; B. Bosnich, *Asymmetric synthesis. Production of optically active amino acids by catalytic hydrogenation*, *J. Am. Chem. Soc.* **1977**, *99*, 6262.

16. R. Noyori, *Asymmetric Catalysis: Science and Opportunities (Nobel Lecture)*, *Angew. Chem. Int. Ed.* **2002**, *41*, 2008.

17. W. S. Knowles, *Asymmetric Hydrogenations (Nobel Lecture)*, *Angew. Chem. Int. Ed.* **2002**, *41*, 1998.

18. C. A. Tolman, *Electron donor-acceptor properties of phosphorus ligands. Substituent additivity*, *J. Am. Chem. Soc.* **1970**, *92*, 2953.

19. C. A. Tolman, *Steric effects of phosphorus ligands in organometallic chemistry and homogeneous catalysis*, *Chem. Rev.* **1977**, *77*, 313.

20. C. A. Tolman; W. C. Seidel; L. W. Gosser, *Formation of three-coordinate nickel(0) complexes by phosphorus ligand dissociation from NiL4*, *J. Am. Chem. Soc.* **1974**, *96*, 53.

21. (a) L. Horner; W. D. Balzer, *Phosphororganische verbindungen IXL zum sterischen verlauf der desoxygenierung von tertiären phosphinoxyden zu tertiären phosphinen mit*

trichlorsilan, Tetrahedron Lett. **1965**, *6*, 1157; (b) M. Stankevič; K. M. Pietrusiewicz, *An Expedient Reduction of sec-Phosphine Oxides to sec-Phosphine-boranes by BH3˙SMe2*, *Synlett* **2003**, *2003*, 1012; (c) T. Imamoto; S.-i. Kikuchi; T. Miura; Y. Wada, *Stereospecific Reduction of Phosphine Oxides to Phosphines by the Use of a Methylation Reagent and Lithium Aluminum Hydride, Org. Lett.* **2001**, *3*, 87; (d) D. Hérault; D. H. Nguyen; D. Nuel; G. Buono, *Reduction of secondary and tertiary phosphine oxides to phosphines, Chem. Soc. Rev.* **2015**, *44*, 2508; (e) C. Petit; A. Favre-Reguillon; B. Albela; L. Bonneviot; G. Mignani; M. Lemaire, *Mechanistic Insight into the Reduction of Tertiary Phosphine Oxides by Ti(OiPr)4/TMDS, Organometallics* **2009**, *28*, 6379.

22. K. Achiwa, *Asymmetric hydrogenation with new chiral functionalized bisphosphine-rhodium complexes, J. Am. Chem. Soc.* **1976**, *98*, 8265.

23. D. P. Riley; R. E. Shumate, *1,2-Bis(diphenylphosphino)-1-cyclohexylethane. A new chiral phosphine ligand for catalytic chiral hydrogenations, J. Org. Chem.* **1980**, *45*, 5187.

24. M. D. Fryzuk; B. Bosnich, *Asymmetric synthesis. An asymmetric homogeneous hydrogenation catalyst which breeds its own chirality, J. Am. Chem. Soc.* **1978**, *100*, 5491.

25. R. B. King; J. Bakos; C. D. Hoff; L. Marko, *1,2-Bis(diphenylphosphino)-1-phenylethane: a chiral ditertiary phosphine derived from mandelic acid used as a ligand in asymmetric homogeneous hydrogenation catalysts, J. Org. Chem.* **1979**, *44*, 1729.

26. O. Pàmies; G. Net; A. Ruiz; C. Claver, *A New Diphosphane Derived from Carbohydrates as an Effective Ligand for Asymmetric Hydrogenation, Eur. J. Inorg. Chem.* **2000**, *2000*, 2011.

27. M. Diéguez; O. Pàmies; A. Ruiz; S. Castillón; C. Claver, *Synthesis of novel diphosphines from d-(+)-glucose. Use in asymmetric hydrogenation, Tetrahedron Asymmetry* **2000**, *11*, 4701.

28. (a) S. Jugé, *Enantioselective Synthesis of P-Chirogenic Phosphorus Compounds via the Ephedrine-Borane Complex Methodology*, *Phosphorus Sulfur Silicon Relat. Elem.* **2008**, *183*, 233; (b) E. Rudzińska; Ł. Berlicki; P. Kafarski; M. Lämmerhofer; A. Mucha, *Cinchona alkaloids as privileged chiral solvating agents for the enantiodiscrimination of N-protected aminoalkanephosphonates—a comparative NMR study*, *Tetrahedron Asymmetry* **2009**, *20*, 2709; (c) K. M. Pietrusiewicz; M. Zablocka, *Preparation of Scalemic P-Chiral Phosphines and Their Derivatives*, *Chem. Rev.* **1994**, *94*, 1375.

29. W. S. Knowles; M. J. Sabacky; B. D. Vineyard; D. J. Weinkauff, *Asymmetric hydrogenation with a complex of rhodium and a chiral bisphosphine*, *J. Am. Chem. Soc.* **1975**, *97*, 2567.

30. R. Noyori; T. Ohkuma, *Asymmetric Catalysis by Architectural and Functional Molecular Engineering: Practical Chemo- and Stereoselective Hydrogenation of Ketones*, *Angew. Chem. Int. Ed.* **2001**, *40*, 40.

31. H. Brunner; W. Pieronczyk, *Asymmetric Hydrogenation of (Z)-α-(Acetylamino)-cinnamic Acid by a Rh/norphos Catalyst*, *Angew. Chem. Int. Ed. Engl.* **1979**, *18*, 620.

32. P. J. Pye; K. Rossen; R. A. Reamer; N. N. Tsou; R. P. Volante; P. J. Reider, *A New Planar Chiral Bisphosphine Ligand for Asymmetric Catalysis: Highly Enantioselective Hydrogenations under Mild Conditions*, *J. Am. Chem. Soc.* **1997**, *119*, 6207.

33. D. Liu; X. Zhang, *Practical P-Chiral Phosphane Ligand for Rh-Catalyzed Asymmetric Hydrogenation*, *European Journal of Organic Chemistry* **2005**, *2005*, 646.

34. T. Imamoto; K. V. L. Crépy; K. Katagiri, *Optically active 1,1'-di-tert-butyl-2,2'-dibenzophosphetenyl: a highly strained P-stereogenic diphosphine ligand*, *Tetrahedron Asymmetry* **2004**, *15*, 2213.

35. G. He; K. F. Mok; P.-H. Leung, *Optical Resolution, Configurational Stability, and Coordination Chemistry of the P-Chiral Heterocyclic Diphosphine 1,1'-Diphenyl-3,3',4,4'-tetramethyl- 2,2'-diphosphole-3,3'-diene*, *Organometallics* **1999**, *18*, 4027.

36. P.-H. Leung, *Asymmetric Synthesis and Organometallic Chemistry of Functionalized Phosphines Containing Stereogenic Phosphorus Centers*, *Acc. Chem. Res.* **2004**, *37*, 169.

37. P. T. Anastas; J. C. Warner, *Green Chemistry: Theory and Practice*. Oxford University Press: 2000.

38. L. T. Byrne; L. M. Engelhardt; G. E. Jacobsen; W.-P. Leung; R. I. Papasergio; C. L. Raston; B. W. Skelton; P. Twiss; A. H. White, *Synthesis of α-, γ-phosphorus functionalized alkyl lithium species; X-ray structures of [{Li(L)(Ch2PMeR)}2][L =NNN'N'-tetramethylethylenediamine (tmen), R = Me or Ph; L =(–)sparteine, R = Ph] and [Li(tmen){CH(SiMe3)C6H4PPh2-o}]*, *J. Chem. Soc., Dalton Trans.* **1989**, 105.

39. A. R. Muci; K. R. Campos; D. A. Evans, *Enantioselective Deprotonation as a Vehicle for the Asymmetric Synthesis of C2-Symmetric P-Chiral Diphosphines*, *J. Am. Chem. Soc.* **1995**, *117*, 9075.

40. C. A. Maryanoff; B. E. Maryanoff; R. Tang; K. Mislow, *One-step synthesis of optically pure 1,2-ethanobis(sulfoxides)and phosphine oxides via the copper-promoted oxidative dimerization of chiral sulfinyl and phosphinyl carbanions*, *J. Am. Chem. Soc.* **1973**, *95*, 5839.

41. P. Beak; A. Basu; D. J. Gallagher; Y. S. Park; S. Thayumanavan, *Regioselective, Diastereoselective, and Enantioselective Lithiation−Substitution Sequences: Reaction Pathways and Synthetic Applications*, *Acc. Chem. Res.* **1996**, *29*, 552.

42. T. Imamoto; J. Watanabe; Y. Wada; H. Masuda; H. Yamada; H. Tsuruta; S. Matsukawa; K. Yamaguchi, *P-Chiral Bis(trialkylphosphine) Ligands and Their Use in Highly Enantioselective Hydrogenation Reactions*, *J. Am. Chem. Soc.* **1998**, *120*, 1635.

43. W. Tang; X. Zhang, *A Chiral 1,2-Bisphospholane Ligand with a Novel Structural Motif: Applications in Highly Enantioselective Rh-Catalyzed Hydrogenations*, *Angew. Chem. Int. Ed.* **2002**, *41*, 1612.

44. W. Li; X. Zhang, Chiral Phosphines and Diphosphines. In *Phosphorus(III) Ligands in Homogeneous Catalysis: Design and Synthesis*, John Wiley & Sons, Ltd.: 2012; pp 27.

45. (a) P. A. MacNeil; N. K. Roberts; B. Bosnich, *Asymmetric synthesis. Asymmetric catalytic hydrogenation using chiral chelating six-membered ring diphosphines*, *J. Am. Chem. Soc.* **1981**, *103*, 2273; (b) H. Brunner; A. Terfort, *Enantioselective catalysis 95 An asymmetric hydrogenation system breeding its own counter-configurated ligand*, *Tetrahedron Asymmetry* **1995**, *6*, 919.

46. Z. Zuo; R. S. Kim; D. A. Watson, *Synthesis of Axially Chiral 2,2'-Bisphosphobiarenes via a Nickel-Catalyzed Asymmetric Ullmann Coupling: General Access to Privileged Chiral Ligands without Optical Resolution*, *J. Am. Chem. Soc.* **2021**, *143*, 1328.

47. (a) Y. Zhou; X. Zhang; H. Liang; Z. Cao; X. Zhao; Y. He; S. Wang; J. Pang; Z. Zhou; Z. Ke; L. Qiu, *Enantioselective Synthesis of Axially Chiral Biaryl Monophosphine Oxides via Direct Asymmetric Suzuki Coupling and DFT Investigations of the Enantioselectivity*, *ACS Catal.* **2014**, *4*, 1390; (b) W. Xia; Y. Li; Z. Zhou; H. Chen; H. Liang; S. Yu; X. He; Y. Zhang; J. Pang; Z. Zhou; L. Qiu, *Synthesis of Chiral-Bridged Atropisomeric Monophosphine Ligands with Tunable Dihedral Angles and their Applications in Asymmetric Suzuki–Miyaura Coupling Reactions*, *Adv. Synth. Catal.* **2017**, *359*, 1656; (c) W. Ji; H.-H. Wu; J. Zhang, *Axially Chiral Biaryl Monophosphine Oxides Enabled by Palladium/WJ-Phos-Catalyzed Asymmetric Suzuki–Miyaura Cross-coupling*, *ACS Catal.* **2020**, *10*, 1548; (d) T. Hayashi; K. Hayashizaki; T. Kiyoi; Y. Ito, *Asymmetric synthesis catalyzed by chiral ferrocenylphosphine-transition-metal complexes. 6. Practical asymmetric synthesis of 1,1'-binaphthyls via asymmetric cross-coupling with a chiral [(alkoxyalkyl)ferrocenyl]monophosphine/nickel catalyst*, *J. Am. Chem.*

Soc. **1988**, *110*, 8153; (e) J. Yin; S. L. Buchwald, *A Catalytic Asymmetric Suzuki Coupling for the Synthesis of Axially Chiral Biaryl Compounds*, *J. Am. Chem. Soc.* **2000**, *122*, 12051.

48. C. Scriban; D. S. Glueck, *Platinum-Catalyzed Asymmetric Alkylation of Secondary Phosphines: Enantioselective Synthesis of P-Stereogenic Phosphines*, *J. Am. Chem. Soc.* **2006**, *128*, 2788.

49. J. A. Osborn; F. H. Jardine; J. F. Young; G. Wilkinson, *The preparation and properties of tris(triphenylphosphine)halogenorhodium(I) and some reactions thereof including catalytic homogeneous hydrogenation of olefins and acetylenes and their derivatives*, *J. Chem. Soc.* **1966**, 1711.

50. M. D. Fryzuk; B. Bosnich, *Asymmetric synthesis. Preparation of chiral methyl chiral lactic acid by catalytic asymmetric hydrogenation*, *J. Am. Chem. Soc.* **1979**, *101*, 3043.

51. (a) J. Chen; W. Zhang; H. Geng; W. Li; G. Hou; A. Lei; X. Zhang, *Efficient Synthesis of Chiral β-Arylisopropylamines by Using Catalytic Asymmetric Hydrogenation*, *Angew. Chem. Int. Ed.* **2009**, *48*, 800; (b) G. Shang; Q. Yang; X. Zhang, *Rh-Catalyzed Asymmetric Hydrogenation of α-Aryl Imino Esters: An Efficient Enantioselective Synthesis of Aryl Glycine Derivatives*, *Angew. Chem. Int. Ed.* **2006**, *45*, 6360.

52. J. Kang; J. H. Lee; J. B. Kim; G. J. Kim, *Asymmetric modular synthesis of cylindrically chiral FerroPHOS ligands for the Rh-catalyzed asymmetric hydroboration*, *Chirality* **2000**, *12*, 378.

53. M. J. Burk; C. S. Kalberg; A. Pizzano, *Rh−DuPHOS-Catalyzed Enantioselective Hydrogenation of Enol Esters. Application to the Synthesis of Highly Enantioenriched α-Hydroxy Esters and 1,2-Diols*, *J. Am. Chem. Soc.* **1998**, *120*, 4345.

54. T. Imamoto; K. Tamura; Z. Zhang; Y. Horiuchi; M. Sugiya; K. Yoshida; A. Yanagisawa; I. D. Gridnev, *Rigid P-Chiral Phosphine Ligands with tert-Butylmethylphosphino*

Groups for Rhodium-Catalyzed Asymmetric Hydrogenation of Functionalized Alkenes, *J. Am. Chem. Soc.* **2012**, *134*, 1754.

55. (a) R. Noyori; T. Ohkuma; M. Kitamura; H. Takaya; N. Sayo; H. Kumobayashi; S. Akutagawa, *Asymmetric hydrogenation of .beta.-keto carboxylic esters. A practical, purely chemical access to .beta.-hydroxy esters in high enantiomeric purity*, *J. Am. Chem. Soc.* **1987**, *109*, 5856; (b) M. Kitamura; M. Tokunaga; R. Noyori, *Quantitative expression of dynamic kinetic resolution of chirally labile enantiomers: stereoselective hydrogenation of 2-substituted 3-oxo carboxylic esters catalyzed by BINAP-ruthenium(II) complexes*, *J. Am. Chem. Soc.* **1993**, *115*, 144.

56. (a) R. Noyori; T. Ikeda; T. Ohkuma; M. Widhalm; M. Kitamura; H. Takaya; S. Akutagawa; N. Sayo; T. Saito; T. Taketomi; H. Kumobayashi, *Stereoselective hydrogenation via dynamic kinetic resolution*, *J. Am. Chem. Soc.* **1989**, *111*, 9134; (b) T. Ohkuma; M. Kitamura; R. Noyori, Asymmetric Hydrogenation. In *Catalytic Asymmetric Synthesis*, 2000; pp 1.

57. M. Kitamura; M. Tokunaga; R. Noyori, *Asymmetric Hydrogenation of .beta.-Keto Phosphonates: A Practical Way to Fosfomycin*, *J. Am. Chem. Soc.* **1995**, *117*, 2931.

58. H. Shimizu; I. Nagasaki; K. Matsumura; N. Sayo; T. Saito, *Developments in Asymmetric Hydrogenation from an Industrial Perspective*, *Acc. Chem. Res.* **2007**, *40*, 1385.

59. M. Zhao; W. Li; X. Li; K. Ren; X. Tao; X. Xie; T. Ayad; V. Ratovelomanana-Vidal; Z. Zhang, *Enantioselective Ruthenium(II)/Xyl-SunPhos/Daipen-Catalyzed Hydrogenation of γ-Ketoamides*, *J. Org. Chem.* **2014**, *79*, 6164.

60. J. P. Genêt; V. Ratovelomanana-Vidal; M. C. Caño de Andrade; X. Pfister; P. Guerreiro; J. Y. Lenoir, *Practical asymmetric hydrogenation of β-keto esters at atmospheric pressure using chiral Ru (II) catalysts*, *Tetrahedron Lett.* **1995**, *36*, 4801.

61. C.-C. Pai; Y.-M. Li; Z.-Y. Zhou; A. S. C. Chan, *Synthesis of new chiral diphosphine ligand (BisbenzodioxanPhos) and its application in asymmetric catalytic hydrogenation*, *Tetrahedron Lett.* **2002**, *43*, 2789.

62. (a) H.-U. Blaser; R. Hanreich; H.-D. Schneider; F. Spindler; B. Steinacher, The Chiral Switch of Metolachlor: The Development of a Large-Scale Enantioselective Catalytic Process. In *Asymmetric Catalysis on Industrial Scale*, 2003; pp 55; (b) H.-U. Blaser, *The Chiral Switch of (S)-Metolachlor: A Personal Account of an Industrial Odyssey in Asymmetric Catalysis*, *Adv. Synth. Catal.* **2002**, *344*, 17.

63. J. F. McCarrity; W. Brieden; R. Fuchs; H.-P. Mettler; B. Schmidt; O. Werbitzky, Liberties and Constraints in the Development of Asymmetric Hydrogenations on a Technical Scale. In *Asymmetric Catalysis on Industrial Scale*, 2003; pp 283.

64. G. Hou; F. Gosselin; W. Li; J. C. McWilliams; Y. Sun; M. Weisel; P. D. O'Shea; C.-y. Chen; I. W. Davies; X. Zhang, *Enantioselective Hydrogenation of N−H Imines*, *J. Am. Chem. Soc.* **2009**, *131*, 9882.

65. (a) F. Zhong; X. Dou; X. Han; W. Yao; Q. Zhu; Y. Meng; Y. Lu, *Chiral Phosphine Catalyzed Asymmetric Michael Addition of Oxindoles*, *Angew. Chem. Int. Ed.* **2013**, *52*, 943; (b) B. Huang; C. Li; H. Wang; C. Wang; L. Liu; J. Zhang, *Phosphine-Catalyzed Diastereo- and Enantioselective Michael Addition of β-Carbonyl Esters to β-Trifluoromethyl and β-Ester Enones: Enhanced Reactivity by Inorganic Base*, *Org. Lett.* **2017**, *19*, 5102.

66. T. Imamoto; K. Sugita; K. Yoshida, *An Air-Stable P-Chiral Phosphine Ligand for Highly Enantioselective Transition-Metal-Catalyzed Reactions*, *J. Am. Chem. Soc.* **2005**, *127*, 11934.

67. (a) B. E. Rossiter; N. M. Swingle, *Asymmetric conjugate addition*, *Chem. Rev.* **1992**, *92*, 771; (b) M. P. Sibi; S. Manyem, *Enantioselective Conjugate Additions*, *Tetrahedron* **2000**, *56*, 8033; (c) F. López; S. R. Harutyunyan; A. Meetsma; A. J. Minnaard; B. L. Feringa, *Copper-*

Catalyzed Enantioselective Conjugate Addition of Grignard Reagents to α,β-Unsaturated Esters, *Angew. Chem. Int. Ed.* **2005**, *44*, 2752; (d) B. Maciá Ruiz; K. Geurts; M. Á. Fernández-Ibáñez; B. ter Horst; A. J. Minnaard; B. L. Feringa, *Highly Versatile Enantioselective Conjugate Addition of Grignard Reagents to α,β-Unsaturated Thioesters*, *Org. Lett.* **2007**, *9*, 5123.

68. S. Pican; A.-C. Gaumont, *Palladium catalysed enantioselective phosphination reactions using secondary phosphine-boranes and aryl iodide*, *Chem. Commun.* **2005**, 2393.

69. T. Ogura; K. Yoshida; A. Yanagisawa; T. Imamoto, *Optically Active Dinuclear Palladium Complexes Containing a Pd−Pd Bond: Preparation and Enantioinduction Ability in Asymmetric Ring-Opening Reactions*, *Org. Lett.* **2009**, *11*, 2245.

70. T. Imamoto; T. Itoh; Y. Yamanoi; R. Narui; K. Yoshida, *Highly enantioselective hydrosilylation of simple ketones catalyzed by rhodium complexes of P-chiral diphosphine ligands bearing tert-butylmethylphosphino groups*, *Tetrahedron Asymmetry* **2006**, *17*, 560.

71. (a) K. Kubota; E. Yamamoto; H. Ito, *Regio- and Enantioselective Monoborylation of Alkenylsilanes Catalyzed by an Electron-Donating Chiral Phosphine–Copper(I) Complex*, *Adv. Synth. Catal.* **2013**, *355*, 3527; (b) F. Meng; H. Jang; A. H. Hoveyda, *Exceptionally E- and β-Selective NHC–Cu-Catalyzed Proto-Silyl Additions to Terminal Alkynes and Site- and Enantioselective Proto-Boryl Additions to the Resulting Vinylsilanes: Synthesis of Enantiomerically Enriched Vicinal and Geminal Borosilanes*, *Chem. Eur. J.* **2013**, *19*, 3204.

Chapter II

C$_2$- Symmetric *P**-Diphosphines *via* Catalytic Asymmetric Hydrophosphination

2.1 Introduction

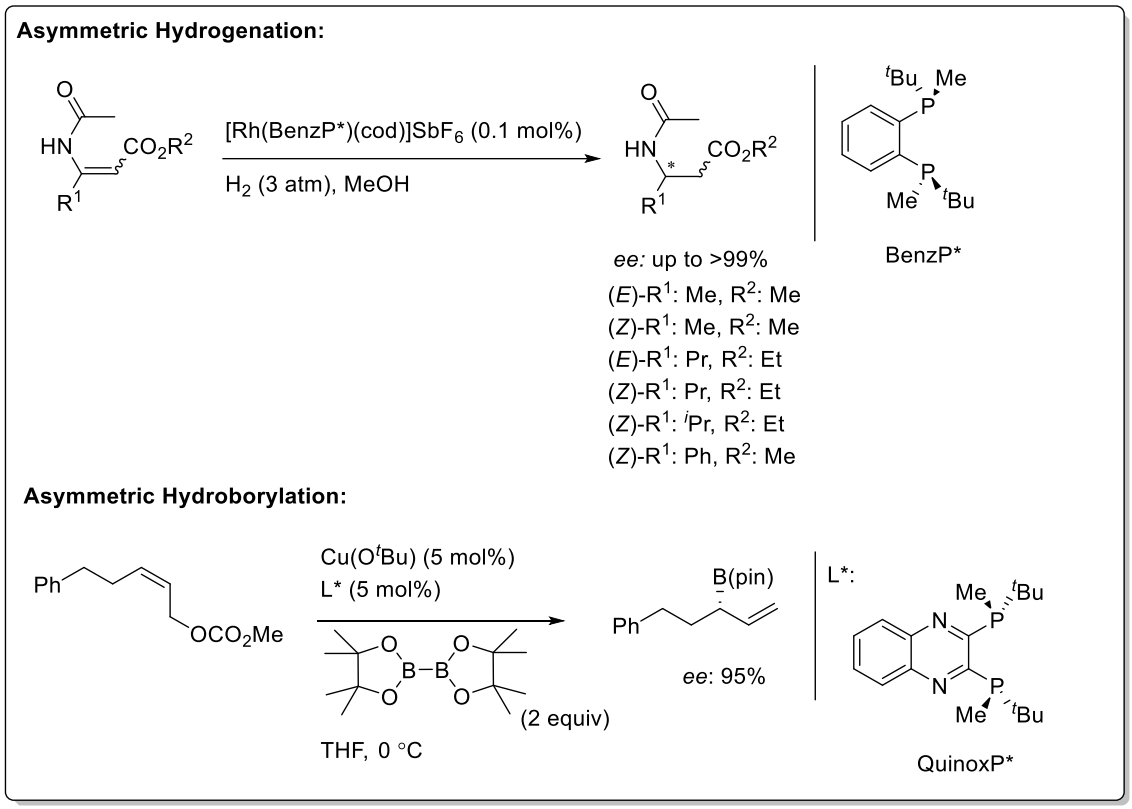

Scheme 33. Selected examples of applications using *P*-chiral diphosphines.

Optically active 1,2-diphosphines garnered much attention in metal-assisted asymmetric reactions due to their efficacy and ability to induce a high degree of stereoselectivity. In general, chiral 1,2-diphosphines contains stereogenic centers at the carbon and/or phosphorus. Amongst these, *P**-diphosphines are conspicuous ligands due to the fact that the chiral phosphorus donors lie in close proximity to the substrate coordination sites which consequentially allows the efficient transfer of chiral information from the substituents on the phosphorus atom to the ligated substrates *via* the metal center. The outcome of this phenomenon is better enantiocontrol in the catalytic reaction. It is well-known that *P*-

stereogenic diphosphines have been widely valorized as useful ligands in the pioneering studies of asymmetric hydrogenation reactions,[1] asymmetric hydrosilyation reactions[2] and asymmetric borylation reactions.[3]

2.1.1 Synthetic Methodologies

To date, while synthetic methodologies employed to synthesize *P*-chiral monophosphines are prevalent,[4] synthesis of *P*-chiral 1,2-diphosphines has been challenging as currently, only limited protocols are available. These protocols, which were discussed in section 1.3, include 1) optical resolution, 2) usage of chiral auxiliaries, 3) chiral pool synthesis and 4) enantioselective deprotonation. Consequently, in the early days of *P**-diphosphines discoveries, studies on the applications of these *P*-chirogenic diphosphines were not widespread.

2.1.2 Our Group Recent Development – Asymmetric Hydrophosphination

Our group has always been diligently developing novel synthetic protocols to access synthetically useful chiral phosphines. One prominent method developed over the years is the catalytic asymmetric hydrophosphination reaction. Asymmetric hydrophosphination reactions are simple, atom-economical, and readily afford the optically active phosphines in a single step. Our odyssey in this area of catalytic asymmetric C–P bond formation started with the use of chiral bisacetonitrile complex (*R*)-**7** with an activated olefin – *trans*-chalcone. The reaction afforded the corresponding chiral phosphine in quantitative yield and moderate *ee* (77%).[5]

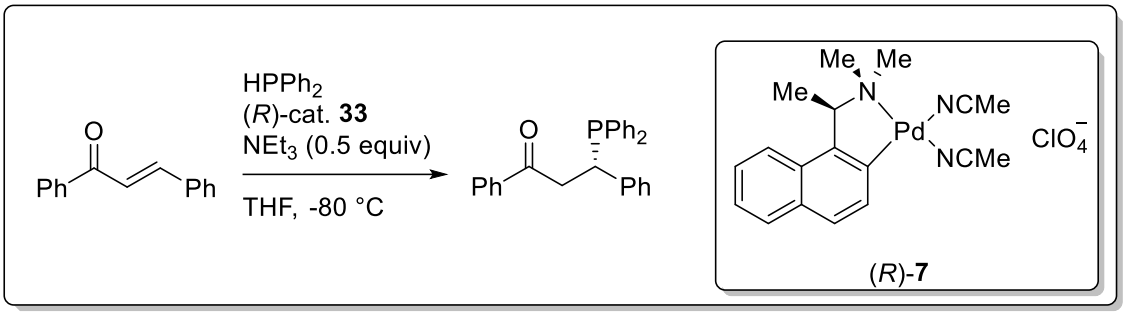

Scheme 34. Asymmetric hydrophosphination reaction using palladacycle (*R*)-**7**.

To further improve the enantioselectivity and rate of reactions of the reaction, palladacycle (*R*)-**8** was developed. By replacing the nitrogen donor with a phosphorus donor, a stronger *trans* effect could be exerted, establishing a more labile *trans* coordination site on the palladium metal center. In addition, greater steric induction was introduced with the two phenyl groups on the phosphorus atom. As a result of these changes to the bidentate ligand on the palladium center, complex **8** showed significant improvements in both reactivity and selectivity in the asymmetric hydrophosphination reaction.[6]

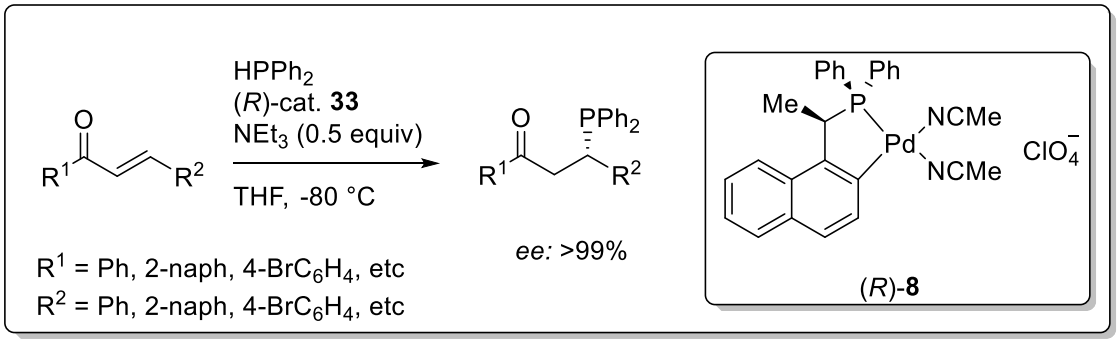

Scheme 35. Asymmetric hydrophosphination reaction using palladacycle (*R*)-**8**.

The superior performance of these two catalysts originated from both the steric lock of the five-membered palladacycle ring in the *Δ* conformation brought about by the interaction between the H^8-naphthylene and methyl group, and the *trans*-effect caused by the N and P donor atoms.

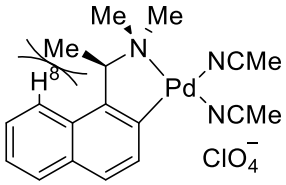

(*R*)-**7**

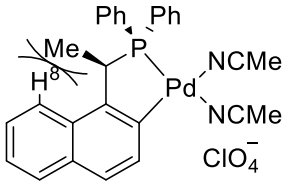

(*R*)-**8**

Duan *et al.* reported a similar hydrophosphination procedure catalyzed by pincer catalysts.[7] However, the pincer catalysts used by Duan *et al*. were generated through the chiral auxiliary method. Our group was able to synthesize a new generation of chiral tridentate pincer complexes from asymmetric hydrophosphination reaction. These pincer compounds conferred excellent stereoinductive properties and, prior to the development of (*R*,*R*)-complex **9**, have proven to be efficient catalysts in asymmetric hydrophosphination reactions.[7a] With these catalysts, a myriad of enantioenriched phosphines were synthesized by our group.[8]

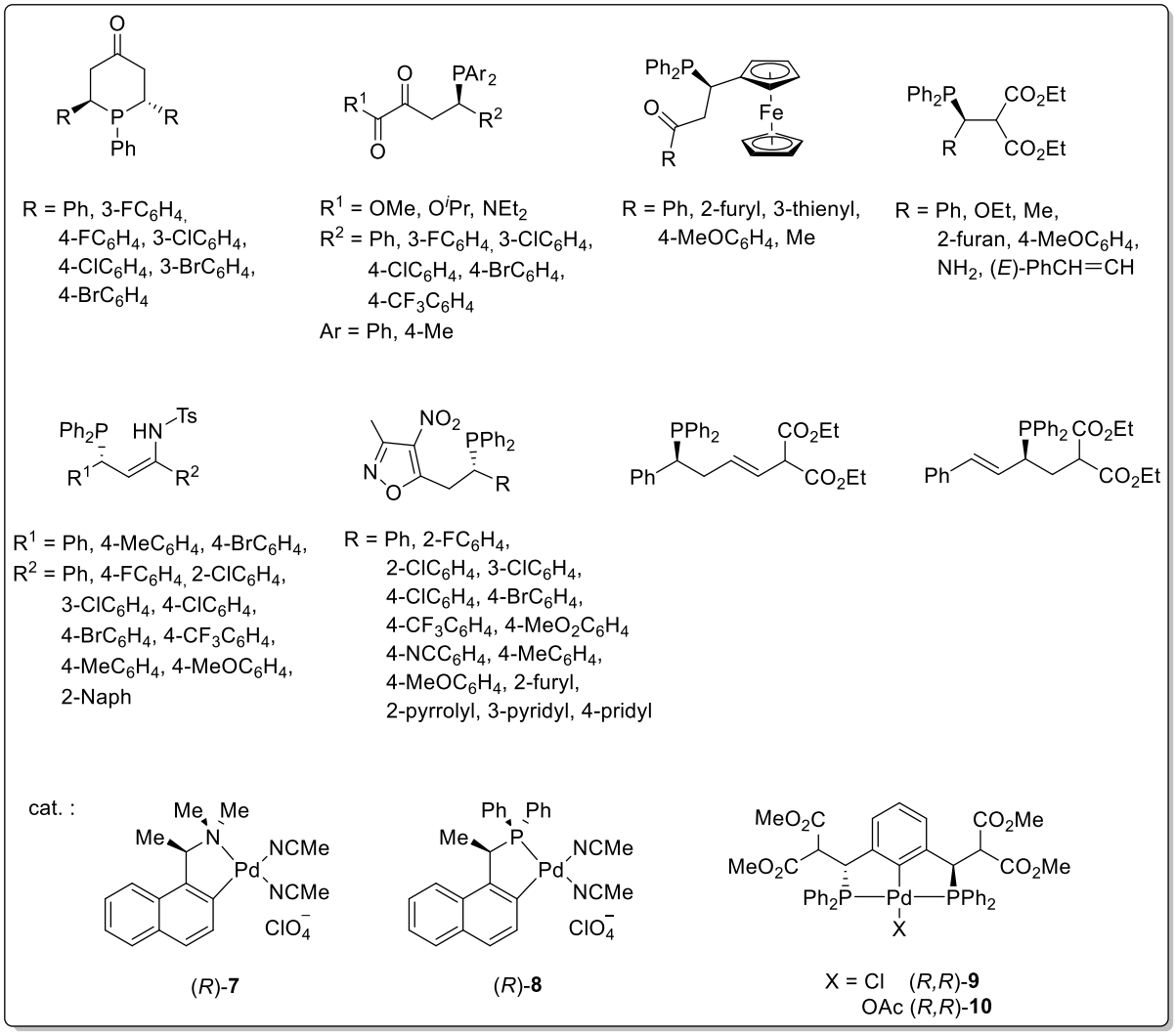

Figure 8. Asymmetric hydrophosphinated products developed by Leung and co-workers.

2.1.3 Research Objective

In marked contrast to previous hydrophosphination attempts by our group, we envisioned a strategy in which secondary 1,2-diphosphines themselves could be utilized as substrates in conjunction with olefin substrates for dihydrophosphination with the aim of creating an efficient general catalytic protocol to access C_2-symmetric tertiary *P*-chiral 1,2-diphosphines. According to a study done by Marynick and co-worker[9], theoretical calculation utilizing Hartree-Fock calculations and electron correlation concluded that coordinated-*phosphido* species have low inversion barrier in the order of 11-15 kcal/mol while free

phosphines have inversion barrier of about 35 kcal/mol. As such, reactions involving coordinated-*phosphido* species proceeded with a fast inversion at the chiral phosphorus center. It was also hypothesized that the rate of inversion of the metal-*phosphido* complex was faster than the rate of C–P bond formation with an electrophile predicted by Curtin-Hammett kinetics.[10] This fast inversion of the metal-*phosphido* complex allowed *meso*/*rac*-secondary diphosphine mixtures as the starting materials in the generation of chiral phosphines, thereby circumventing the need for enantiomerically pure organophosphorus precursors as reactants.

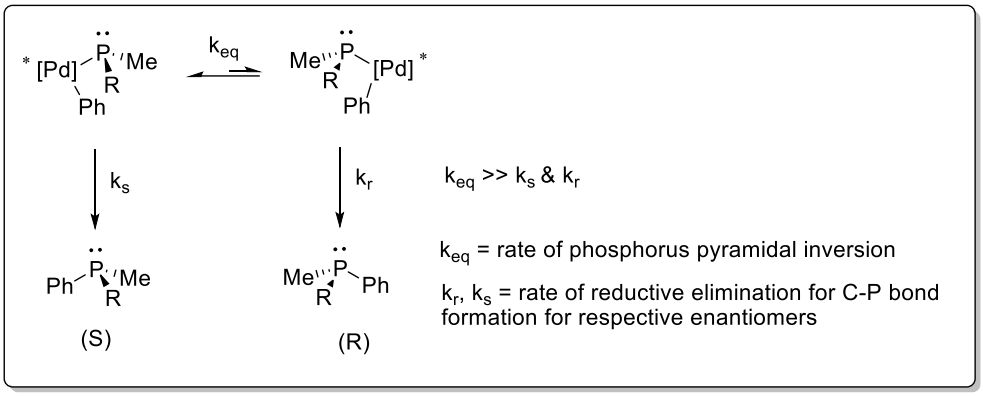

Figure 9. Formation of *P*-chiral phosphine based on Curtin-Hammett kinetics.

2.2 Results and Discussion

2.2.1 General Catalytic Protocol to Access Optically Enriched *C*$_2$-Symmetric *P*-Stereogenic Diphosphines.

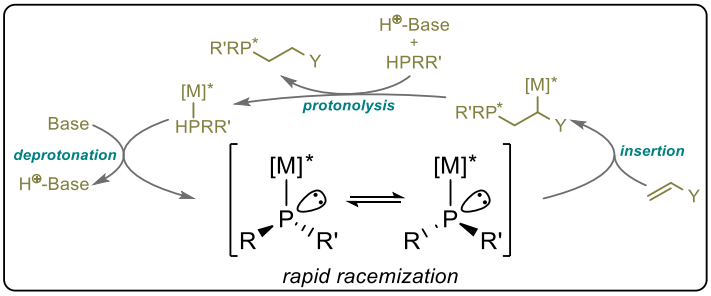

Figure 10. Racemization of the metal-*phosphido* intermediate in metal-catalyzed hydrophosphination.

Our preliminary investigation involved bis(phenylphosphino)ethane as the 1,2-diphosphine substrate for the dihydrophosphination reaction due to the presence of sterically different substituents on the phosphorus center. Bis(phenylphosphino)ethane can be synthesized from bis(diphenylphosphino)ethane *via* a lithium-induced phosphorus–carbon bond cleavage reaction.[11] This regioselectivity of this reaction is highly temperature dependent. This is due to the reversibility among the different species in the reaction, where the equilibrium is thermodynamic in nature.[11] Conducting the reaction at elevated temperature favours pathways **Ia** and **Ib**, while lowering the temperature favours pathways **IIa** and **IIb**. In addition, it has also been studied that maintaining the temperature for the hydrolysis of the lithium bis(phosphide) at low temperature was crucial as the formation of diphenylphosphine during the process of hydrolysis at elevated temperature is possible. As such, the whole synthesis process of bis(phenylphosphino)ethane was carried out at 0 °C.

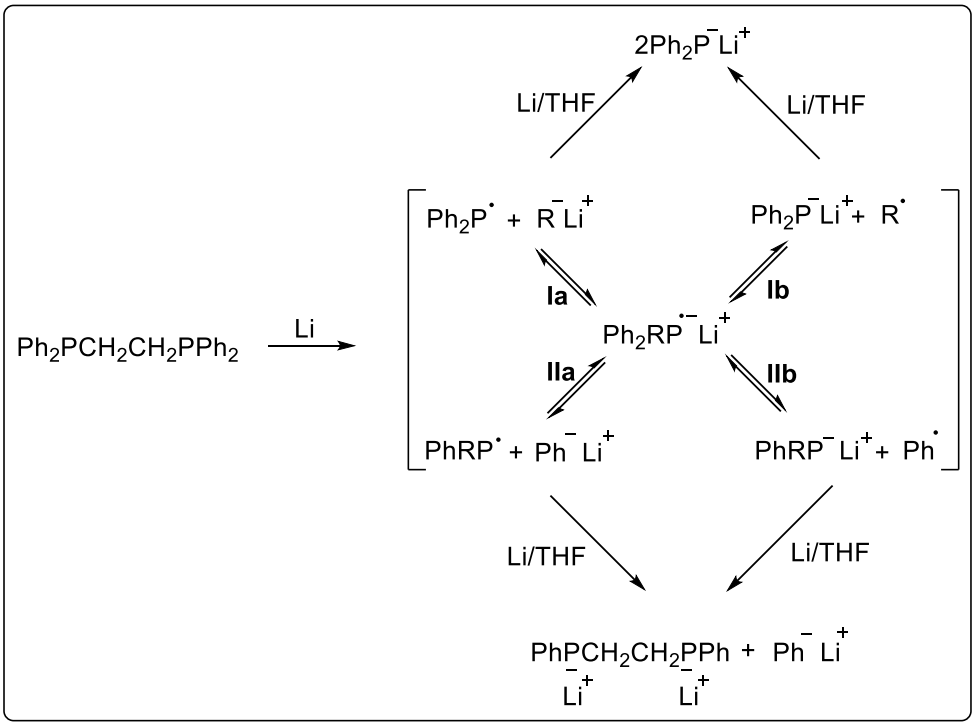

Scheme 36. Equilibrium of the cleavage of phenyl group from bis(diphenylphosphino)ethane.

During the evaluation of palladacycles for the asymmetric H–P addition reaction, Leung and co-workers had determined that two of these compounds, namely the naphthalene-based on the palladacyclic systems **7** and **8** respectively, portrayed excellent activity and stereoselectivity for the asymmetric procedure. Of specific mention was the presence of two vacant sites within the coordination sphere. We hypothesized that the utility of CN palladacycle **7** in the synthesis of the diphosphines may lead to catalyst poisoning due to the chelating effect of diphosphines onto the metal center, resulting in a stochiometric amount of complex required for the synthesis of chiral 1,2-diphosphines.[23] In view of this observation, PCP pincer-type complex **9**, given the presence of only one-vacant site, prohibits the two phosphorus centers from coordinating to the metal center simultaneously and this allows a step-wise nucleophilic addition to the olefinyl substrates. Hence, complex **9** was chosen for the development of the synthesis of *P*-chirogenic 1,2-diphosphine protocol. The C_2-symmetric pincer complex was confirmed to have a non-interconvertible conformational lock on the two five-membered

puckered rings, with only one conformer existing in both the solution and solid states.[24] This will result in a *Si*-face attack on the electrophile substrate being more favourable.[25]

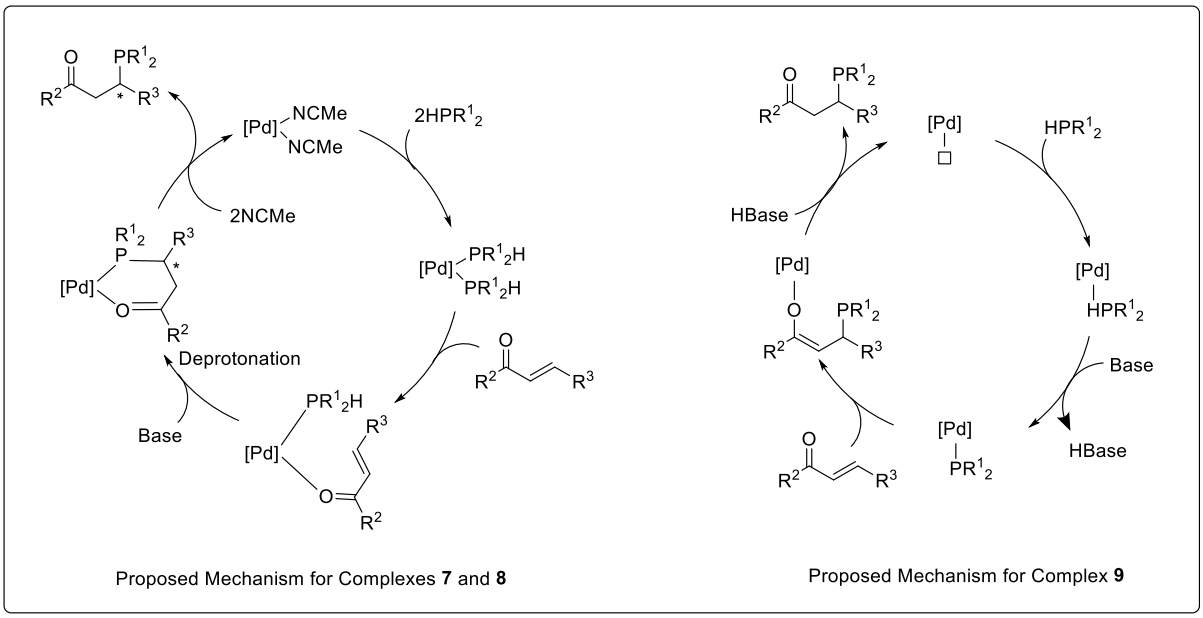

Scheme 37. Prosed mechanisms for complexes **7**, **8** and **9**.

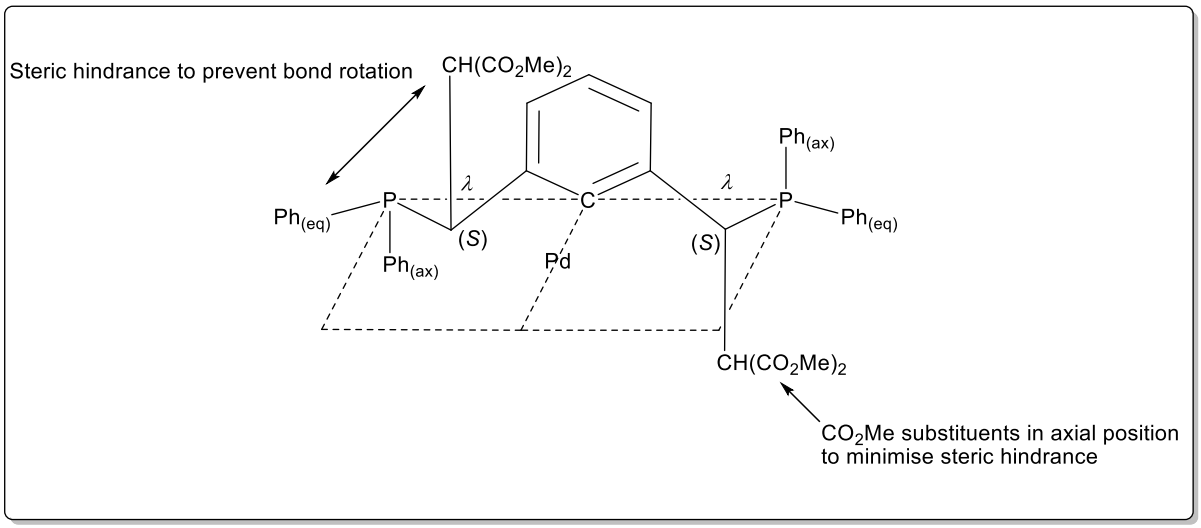

Figure 11. Non-interconvertible conformation lock for C_2-symmetric pincer complex.

Acrylonitrile was used as alkene substrate for the dihydrophosphination procedure as hydrophosphination requires the presence of a sufficiently strong electron-withdrawing group to be present in the alkene substrate for Michael addition.

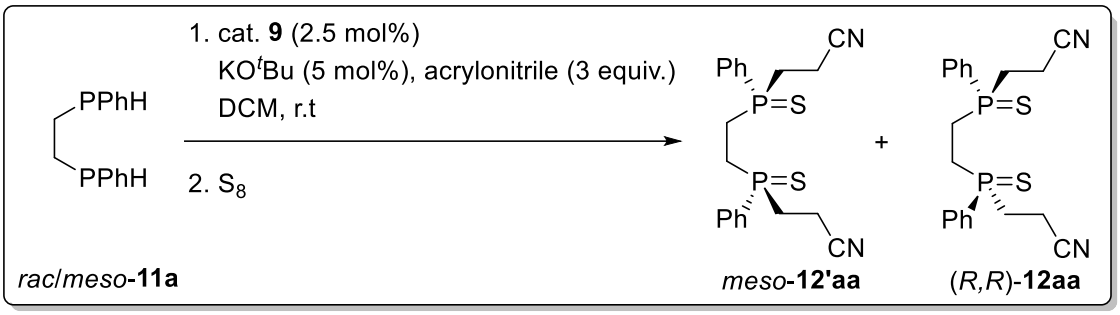

Scheme 38. Initial reaction condition for the asymmetric 1,2-dihydrophosphination reaction.

Preliminary dihydrophosphination reaction was done with bis(phenylphosphino)ethane and acrylonitrile, in dichloromethane at room temperature and KO^{t}Bu as the base. After an overnight reaction, a $^{31}P\{^1H\}$ NMR spectrum as obtained for the products from the reaction. Two new signals have emerged at chemical shifts δ –20.4 and –20.8. However, there were still unreacted starting material as seen in the $^{31}P\{^1H\}$ NMR at δ –46.4 (optically active) and –46.6 (*meso*). Even after 72 hours, the reaction remained incomplete. Upon further investigation, there existed a minute amount of diphenylphosphine in the prepared stock bis(phenylphosphino)ethane mixture. We hypothesized that diphenylphosphine may deactivate the catalyst once it has been attached to it as diphenylphosphine and acrylonitrile may not be compatible for hydrophosphination procedure due to the C=C bond within acrylonitrile being less activated. To prove our hypothesis, a reaction was conducted with diphenylphosphine and acrylonitrile under the same set of conditions. As expected, no reaction has occurred. Hence, it is crucial for bis(phenylphosphino)ethane to be extremely pure.

Another attempt was done with a pure pot of bis(phenylphosphino)ethane (Table 1, entry 1). Gratifyingly, the reaction furnished clean conversion of the substrate to diphosphines after 16 hours of reaction. The air-sensitive diphosphines were subsequently sulfurized for ease of purification and characterization. $^{31}P\{^1H\}$ NMR revealed that the ratio of **12aa** and **12'aa** was about 1:1, with *ee* at 5% for the chiral product. It should also be noted that sulfurization of

the free diphosphines mixture did not change the diastereomeric ratio. A range of protic and aprotic solvents were screened for reactivity and selectivity. All solvents, except acetone, provided clean conversion of the products at ambient temperature within 16 hours (Table 1, entries 2-6). Acetonitrile (Table 1, entry 5) offered the highest *ee* at 59%, albeit with poor diastereoselectivity (4% *de*). On the other hand, ethanol (Table 1, entry 2) gave higher proportion of the chiral C_2-symmetric isomer (14% *de*), but at a significantly lower *ee* at 30%.

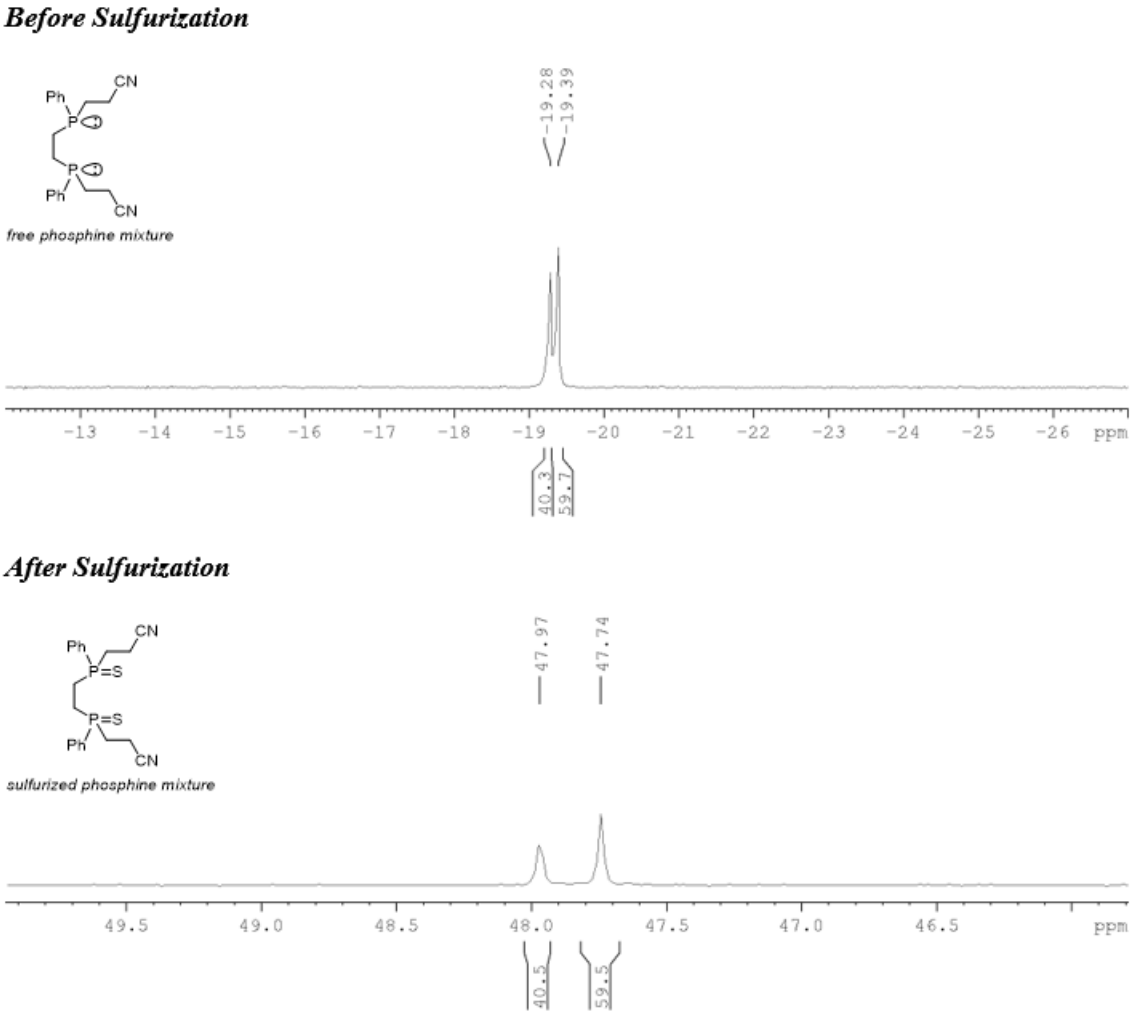

Figure 12. Diastereomeric integrity of diphosphine before and after sulfurization.

Subsequent reactions with a series of organic and inorganic bases in acetonitrile was investigated (Table 1, entries 7-15). Between the two classes, DBU was found to favour *meso* **12'aa** at 14% *de* and gave a racemic mixture. No pronounced deviations in selectivity or

reactivity were evident for the other bases. Nonetheless, sodium methoxide (Table 1, entry 8) and diisopropylamine (Table 1, entry 15) at ambient temperature were found to provide slightly improved diastereoselectivities and enhanced enantioselectivities at 68% and 65% respectively.

Table 1. Protocol optimization for the catalytic asymmetric 1,2-dihydrophosphination of acrylonitrile.[a]

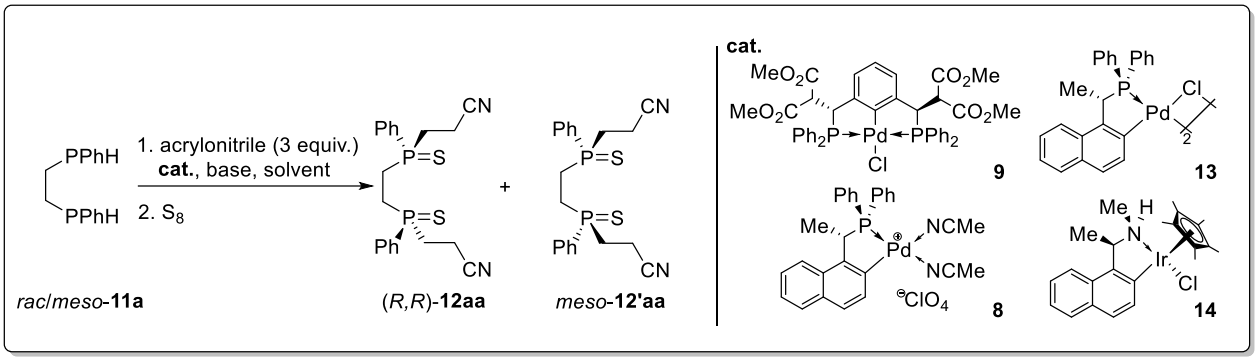

entry	*catalyst*	*cat./mol %*	*base*	*base/mol %*	*solvent*	*temp* (°C)	*dr*[b] (%)	*ee*[c] (%)
1	**9**	2.5	KO^{t}Bu	5	CH_2Cl_2	25	52:48	5
2	**9**	2.5	KO^{t}Bu	5	$CHCl_3$	25	46:54	33
3	**9**	2.5	KO^{t}Bu	5	MeOH	25	52:48	18
4	**9**	2.5	KO^{t}Bu	5	EtOH	25	57:43	30
5	**9**	2.5	KO^{t}Bu	5	MeCN	25	52:48	59
6[d]	**9**	2.5	KO^{t}Bu	5	$(CH_3)_2CO$	25	46:54	19
7	**9**	2.5	NaOH	5	MeCN	25	55:45	69
8	**9**	2.5	NaOMe	5	MeCN	25	58:42	68
9	**9**	2.5	NaOEt	5	MeCN	25	57:43	65
10	**9**	2.5	NaOAc	5	MeCN	25	56:44	63
11	**9**	2.5	CsF	5	MeCN	25	55:45	65
12	**9**	2.5	DIPEA	5	MeCN	25	56:44	64

13	**9**	2.5	DBU	5	MeCN	25	43:57	0
14	**9**	2.5	NEt_3	5	MeCN	25	59:41	65
15	**9**	2.5	$^{i}Pr_2NH$	5	MeCN	25	60:40	65
16	**9**	2.5	NaOMe	5	MeCN	0	59:41	87
17[e]	**9**	2.5	NaOMe	5	MeCN	–40	58:42	90
18	**9**	2.5	$^{i}Pr_2NH$	5	MeCN	0	57:43	85
19	**9**	2.5	$^{i}Pr_2NH$	5	MeCN	–40	59:41	94
20[f]	**9**	1.5	$^{i}Pr_2NH$	5	MeCN	–40	55:45	80
21	**9**	2	$^{i}Pr_2NH$	5	MeCN	–40	58:42	90
22	**9**	2	$^{i}Pr_2NH$	20	MeCN	–40	59:41	92
23	**9**	2	$^{i}Pr_2NH$	40	MeCN	–40	56:44	76
24	**13**	2	$^{i}Pr_2NH$	20	MeCN	–40	45:55	94
25	**8**	2	$^{i}Pr_2NH$	20	MeCN	–40	37:63	40
26[g]	**14**	2	$^{i}Pr_2NH$	20	MeCN	–40	45:55	>99

[a]Reactions were carried out with bis(phenylphosphino)ethane (0.16 mmol), acrylonitrile (0.49 mmol), catalyst and base in the listed solvent (3 mL) at stated temperature for 16 h. Unless otherwise stated, complete conversion to products **12aa** and *meso*-**12'aa** were observed. [b]Diastereomeric ratio (*dr*) of **12aa**:*meso*-**12'aa** determined from $^{31}P\{^{1}H\}$ NMR of sulfurized reaction mixture. [c]Determined by chiral HPLC. [d]NMR yield of **37aa**/*meso*-**37'aa** mixture at 60% upon complete conversion of *rac*/*meso*-**11a** (byproduct found to be the monophosphinated product). [e]22 h reaction time. [f]40 h reaction time. [g]Reaction was halted after 72 h. Conversion at 30%.

The reaction mixture containing diisopropylamine at reduced temperature (Table 1, entry 19) afforded the optically active product **12aa** at 94% *ee*, while the mixture with sodium

methoxide gave a slightly poorer selectivity of 90% *ee*, with little to no deviation of diastereoselectivity. Fine-tuning of catalyst loading to 2 mol% was the lowest under which the reaction can proceed before adverse effects on the reaction time was observed (Table 1, entry 20 – 21), and increasing the base loading to 20 mol% pushed the rate of reaction slightly, while maintaining the selectivity of the protocol (Table 1, entry 22). Further increase in base loading led to retardation of the reaction and reduced selectivity (Table 1, entry 23).

Finally, the procedure was screened with a range of catalysts known for asymmetric hydrophosphination.[6, 15] It was revealed that bidentate palladacycles gave modest to excellent enantioselectivities for the dihydrophosphination, although they were found to have preference for the *meso* isomer (Table 1, entries 24-25). When screened using a chiral-at-metal iridacycle **14**, an enantiomeric excess of 99% was observed (Table 1, entry 26). However, the reaction remained mostly incomplete (at 30% conversion) even after three days of reaction.

Recrystallization of the enantioenriched solution (in a mixture of *n*-hexane and dichloromethane) yielded colourless needle-like crystals of trigonal nature. The absolute stereochemistry at the phosphorus centers of diphosphine **12aa** was unambiguously confirmed by crystallographic analysis to be *R* and *R* at centers P1 and P2 respectively, with an absolute structure parameter of -0.02(4).

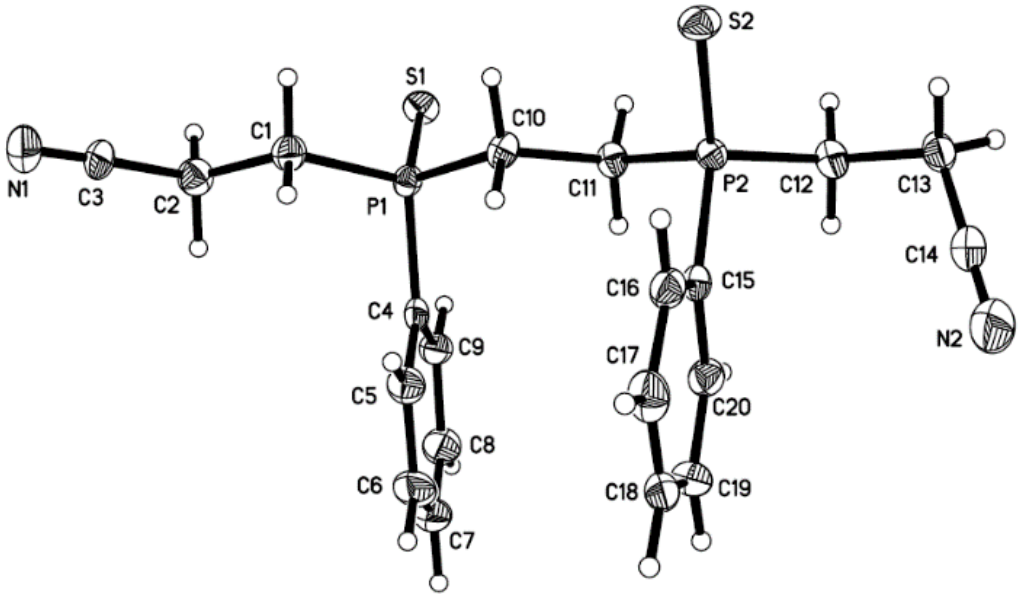

Figure 13. Molecular structure of sulfurized *P*-chiral 1,2-diphosphine (*R*,*R*)-**12aa** with thermal ellipsoids shown at 50% probability. Only one of two asymmetric units is shown.

Table 2. Substrate scope of the catalytic asymmetric dihydrophosphination of olefins.

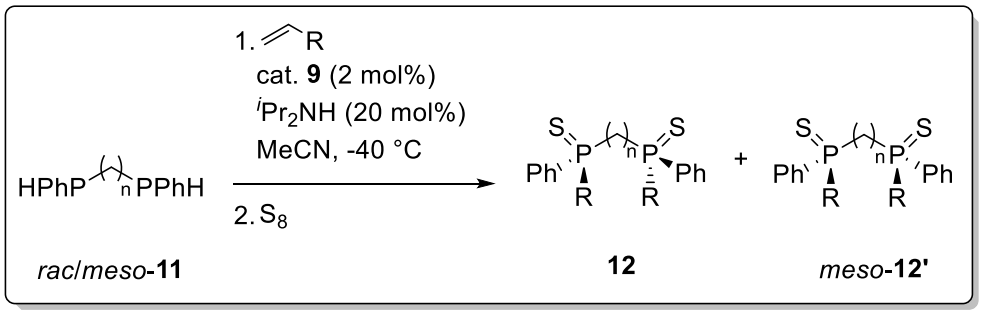

entry	*product*	*n*	*R*	*yield*[b] ***(12/12')***	*dr*[c]	*ee*[d] (%)
1	**12aa**	2	–CN	57 / 36	59:41	92
2	**12ab**	2	–CO_2Me	64 / 30	67:33	87
3	**12ac**	2	–CO_2Et	70 / 22	72:28	86
4	**12ad**	2	–(C=O)Me	45 / 44	49:51	62
5	**12ae**	2	–$(C=O)NH_2$	59 / 41[e]	59:41	99

6	**12af**	2	–(C=O)NMe_2	43 / 41[f]	49:51[g]	>99
7	**12ag**	2	–SO_2Ph	48 / 52[e]	48:52	81
8	**12ah**	2	–Ph	-	n.r.[h]	n.r.[h]
9	**12ai**	2	–*p*-CF_3-C_6H_4	-	n.r.[h]	n.r.[h]
10	**12ba**	3	–CN	62 / 38[f]	62:38	62

[a]Reactions were carried out with bis(phenylphosphino)ethane (0.16 mmol), olefin (0.49 mmol), catalyst **9** (2 mol%) and $^{i}Pr_2NH$ (20 mol%) in MeCN (3 mL) at –40 °C until completion of the reaction. [b]Isolated yield. [c]Diastereomeric ratio (*dr*) of **12**:*meso*-**12'** determined from $^{31}P\{^{1}H\}$ NMR of sulfurized reaction mixture. [d]Determined by chiral HPLC. [e]NMR yield determined from $^{31}P\{^{1}H\}$ NMR of reaction mixture. [f]Isolated yield of *chiral*-**13af** and *meso*-**13'af**. [g]Determined from $^{31}P\{^{1}H\}$ NMR of complexed reaction mixture. [h]No reaction.

Having identified the optimal reaction conditions, the scope of the catalytic dihydrophosphination was surveyed and the results are summarized in Table 2. As expected, activated olefins were compatible to hydrophosphination, rendering the desired optically active isomers in good to excellent enantioselectivities. Vinyl esters furnished their respective products in excellent *ee*, albeit with modest diastereoselectivity (Table 2, entries 2-3). A slight improvement in diastereomeric ratio was observed upon increasing the steric bulk of the alkyl substituent (from methyl to ethyl) within the ester moiety which is attributable to greater steric interactions between the substrate and ligand within the coordination sphere of the intermediate. Whilst a less activating olefin substrate – methyl vinyl ketone – could undergo the reaction, the procedure required excess substrate and longer reaction time to achieve high conversion (Table 2, entry 4). Both diastereoselectivity and enantioselectivity were also significantly affected. The employment of vinyl primary and tertiary amides as substrates returned favourable enantioselectivities of 99% *ee* (Table 2, entries 5-6). Disappointingly, the tertiary

amide gave equal proportions of diastereomers. We further examined the tolerance of the reaction to the sulfone group (Table 2, entry 7). Despite achieving a good enantioselectivity, the diastereomeric ratio obtained was similar at approximately 1:1. Unfortunately, the reaction condition was not suitable for substrates with low activating property as seen in our trials with styrene and *p*-trifluoromethyl vinyl benzene (Table 2, entries 8-9). Given that steric interactions may affect the selectivity of the reaction, we decided to extend the study to bis(phenylphosphino)propane (Table 2, entry 10). Diastereoselectivity was found to increase slightly to 24%, favouring the optically active product **12ba**. However, *ee* achieved in this instance was modest at 62%.

2.2.2 Access to *P*-, *C*-Stereogenic Diphosphine Using Developed Protocol

Taking advantage of the fact that the protocol may afford diphosphines with *P*- and *C*-stereogenic centers, we extended our study to include a non-terminal olefin substrate as a proof-of-concept. *trans*-Chalcone was chosen for the investigation due to its demonstrated efficiency and stereoselectivity in asymmetric hydrophosphination reactions.[6, 8g] When subjected to our reaction conditions, complete conversion was achieved within 24 h (Scheme 39). On the basis of crude $^{31}P\{^{1}H\}$ NMR studies, the presence of two significant stereoisomers were detected, one of which could be easily recrystallized from a solvent mixture of *n*-hexane and dichloromethane. The absolute stereochemistry of the crystalline compound **12aj** was confirmed by crystallographic analysis to be *R, R, R* and *S* at centers C9, C30, P2 and P1 respectively, with an absolute structure parameter of 0.05(4) (Figure 15). The remaining major isomer exhibited a singlet at δ 57.24, illustrating a symmetrical structure. While other minor isomers do exist within the crude sample, the ability of our protocol to generate preferentially two isomers with four stereogenic centers reflects on the potential of the developed protocol as an enantio- and diastereoselective methodology for this extremely challenging synthetic

scenario which entails simultaneous stereo-control of newly generated *C*- and *P*-stereocenters. It should once again be emphasized that this procedure is, to the best of our knowledge, the first catalytic protocol to achieve a direct synthesis of free *P*- and *C*-chiral 1,2-diphosphines.

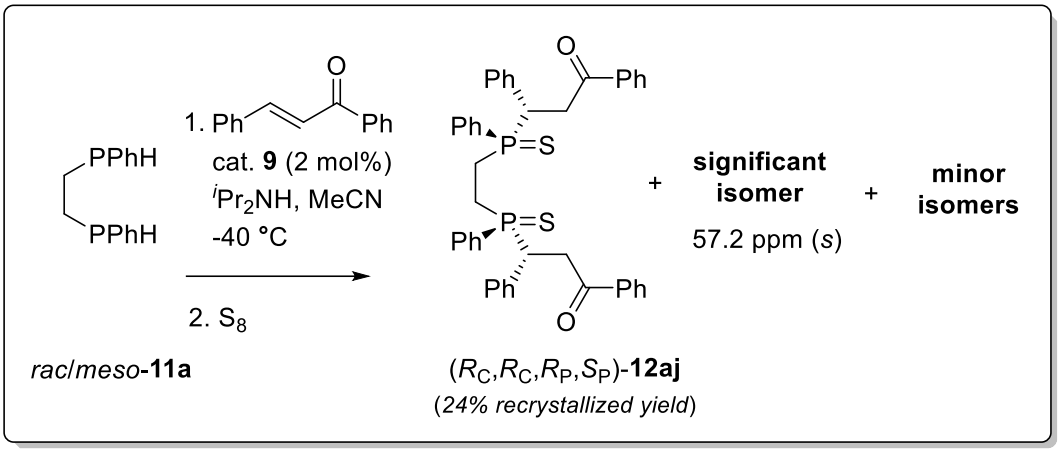

Scheme 39. Catalytic dihydrophosphination with *trans*-chalcone affording 1,2-diphosphines with both *P*- and *C*-stereogenic centers.

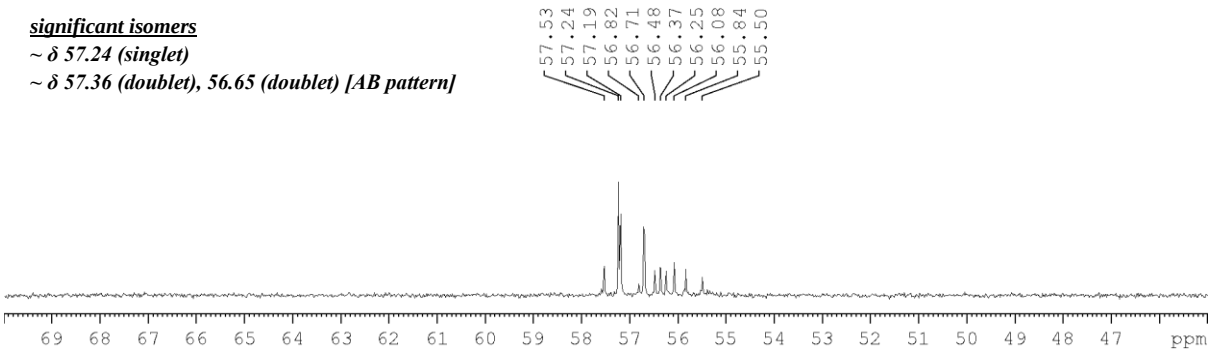

Figure 14. Crude reaction mixture $^{31}P\{^{1}H\}$ NMR spectrum of *rac/meso*-DPPE with *trans*-chalcone.

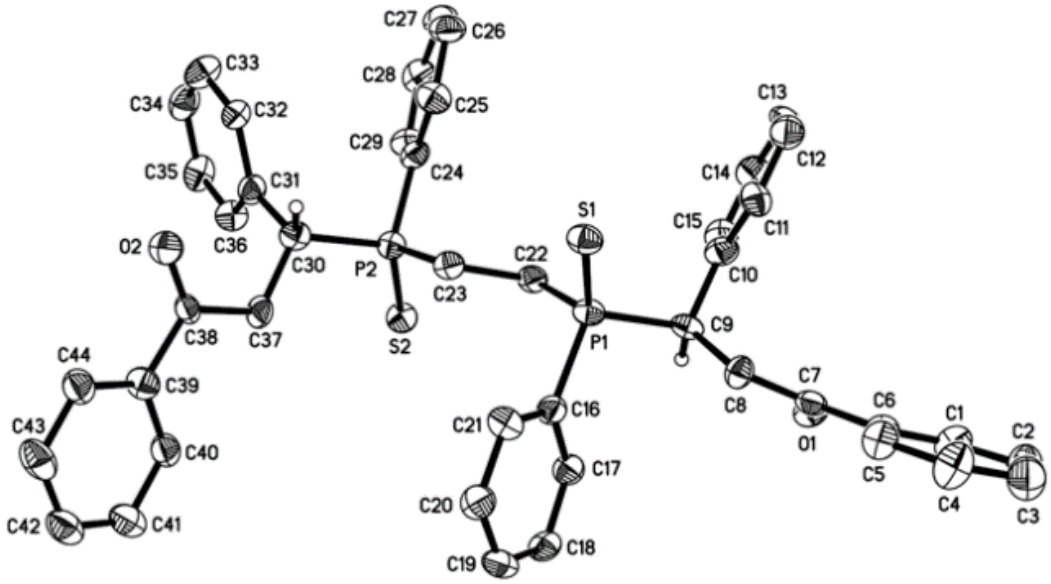

Figure 15. Molecular structure of sulfurized phosphine (R_C,R_C,R_P,S_P)-**12aj** with thermal ellipsoids shown at 50% probability. Hydrogen atoms except H(C9) and H(C30) were omitted for clarity.

2.2.3 Complexation of Optically Active 1,2-Diphosphines

Lastly, since 1,2-diphosphines could be utilized as ligands, we subjected the solvated free phosphines **12aa** and *meso*-**12'aa** to methanolic Li_2PdCl_4 in a one-pot procedure. The reaction was able to provide its corresponding chelated palladium complexes **13aa** and *meso*-**13'aa** quantitatively. These species can then be easily isolated *via* column chromatography. X-ray crystallographic analysis of the recrystallized complexes (*R*,*R*)-**13aa**, with an absolute structure parameter of -0.018(18), (Figure 16) and *meso*-**13'aa** indicated little variance in bond lengths and angles about the palladium center when compared against Pd(dppe)Cl_2,[16] although slight increment to Cl–Pd–Cl bond angles were observed (97.37° (*chiral*–**13aa**) and 96.27° (*meso*–**13'aa**) vs. 94.19° (Pd(dppe)Cl_2)). We further evaluated the ease of isolation of the metallated diphosphines with tertiary amide functionality. It should be noted that our attempts

at purifying the sulfurized diastereomers **12af** and *meso*-**12'af** *via* column chromatography were unfruitful. However, in the case of the chelated complexes **13af** and *meso*-**13'af**, chromatography could be performed with ease. This portrayed the versatility of the procedure to provide a direct and efficient method to access to a plethora of optically active diphosphine complexes for use in asymmetric applications.

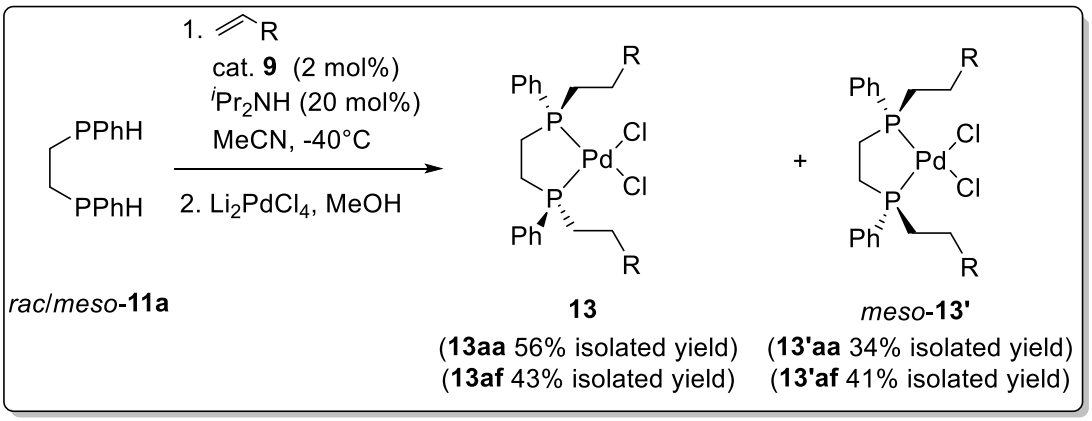

Scheme 40. One-pot direct catalytic dihydrophosphination complexation reaction.

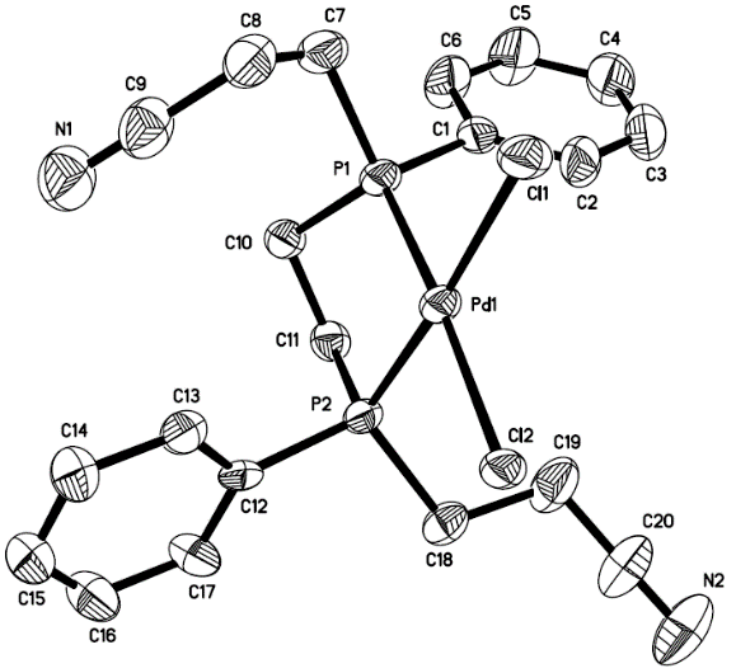

Figure 16. Molecular structure of *P*-chiral 1,2-diphosphine complex (*R*,*R*)-**13aa** with thermal ellipsoids shown at 50% probability. Hydrogen atoms except H(C9) and H(C30) were omitted for clarity. Selected bond lengths and angles: P(1)–Pd (2.2255(17) Å), P(2)–Pd (2.2281(17) Å), Cl(1)–Pd (2.3568(18) Å), Cl(2)–Pd (2.3817(15) Å), P(1)–Pd–P(2) (85.17(6)°), Cl(1)–Pd–Cl(2) (97.37(6)°).

2.2.4 Proposed Catalytic Cycle

Our experimental observation using the crude $^{31}P\{^{1}H\}$ NMR spectroscopy data showed evidence of stepwise hydrophosphination. We have proposed a catalytic cycle based on the mechanistic study of complexes **8** and **9** in asymmetric hydrophosphination reactions[5, 14] in line with our experimental observations (Figure 17). Between diphenylphosphine and bis(phenylphosphino)ethane, the former formed a more thermodynamically stable diphenylphosphide palladium complex in the presence of a base. Since diphenylphosphine is more acidic than bis(phenylphosphino)ethane, the palladium complex was trapped as the diphenylphosphide palladium complex. We also postulated that the formation of the first

chirality on the phosphorus center would affect the formation of the second chirality on the other phosphorus center. In general, weakly electron-withdrawing substituents on the substrates did not lead to any reaction as electrophilic activation of the substrates was poor (Table 2, entries 8 and 9), while stronger electron-withdrawing substituents led to quantitative conversions.

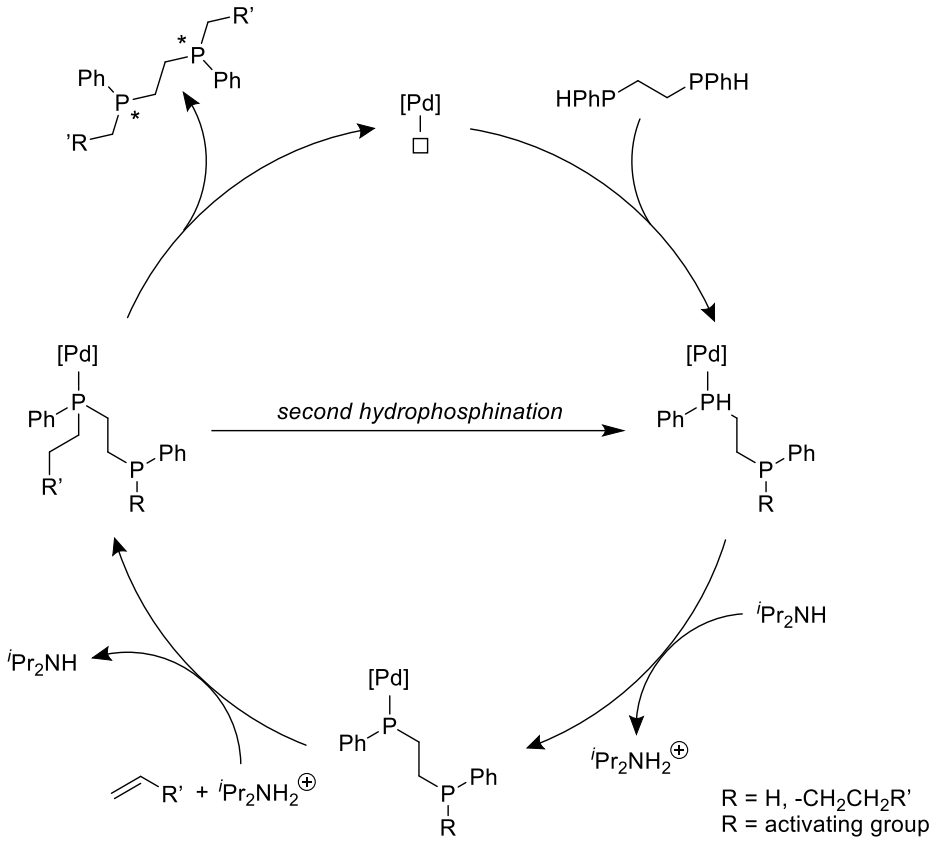

Figure 17. Proposed catalytic cycle to the asymmetric catalytic 1,2-dihydrophosphination of secondary 1,2-diphosphines.

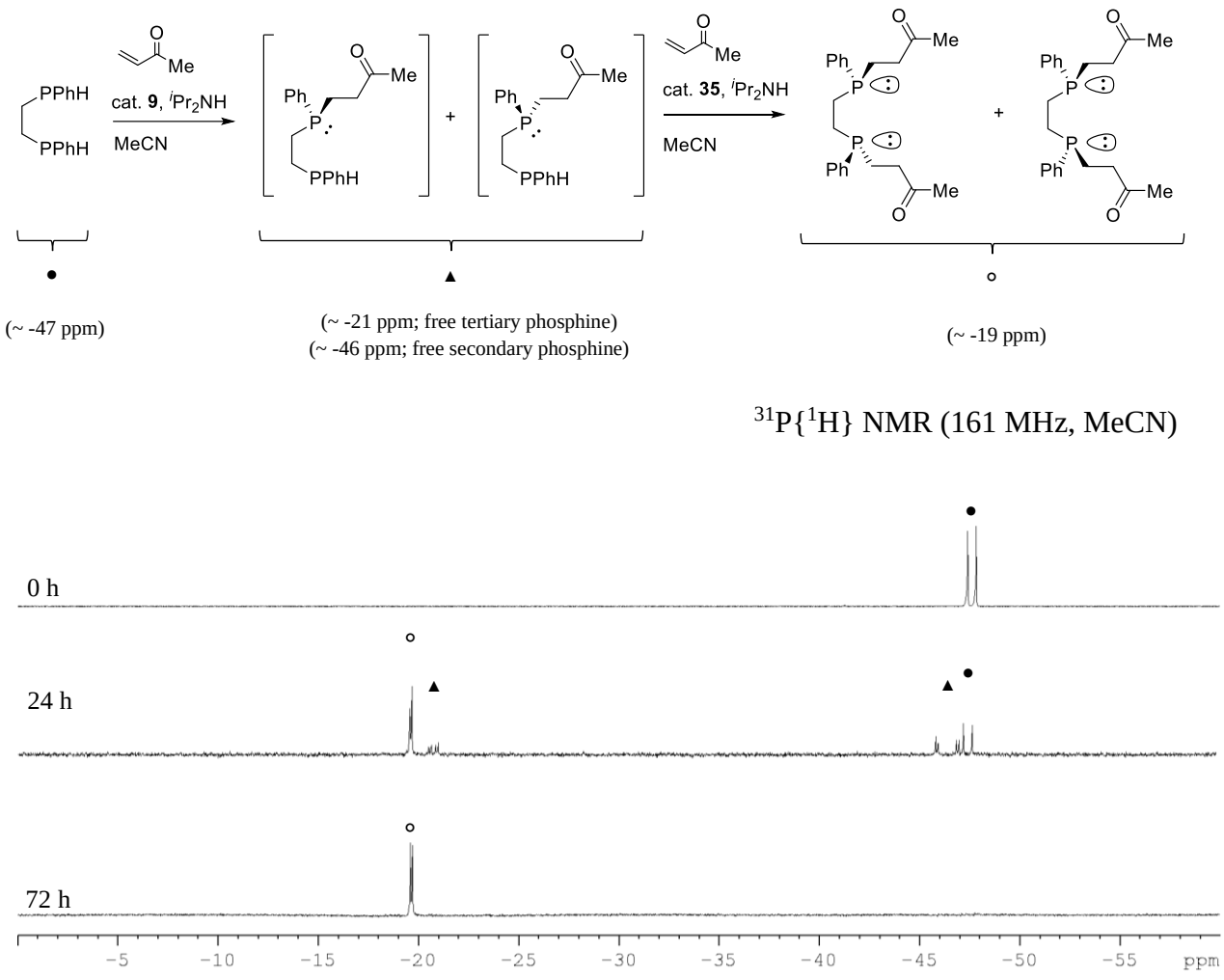

Figure 18. Evidence of stepwise hydrophosphination *via* $^{31}P\{^{1}H\}$ NMR spectroscopy.

2.3 Conclusion

In conclusion, we have developed a direct, efficient and atom-economical method in the synthesis of *P*-chiral diphosphines. The reaction was found to tolerate a variety of activated olefins to yield the corresponding diphosphines in good to excellent enantiomeric excesses. Disappointingly, only modest diastereoselectivities were attained since there could be conflicting influences between the chiral catalyst and the mono-hydrophosphinated species on the coordinated stereogenic *phosphido* substrate. Extension of this methodology to the synthesis of challenging *P,C*-chiral diphosphines, exemplified by hydrophosphination of *trans*-chalcone, was also demonstrated. Complexation to palladium proceeded smoothly, providing

a simple one-pot access to catalyst precursors. Given the substrate scope of the protocol, as well as its efficiency and effectiveness, we believe the procedure has immense synthetic potential in expanding the library of invaluable *P*-chiral and *P*,C**-diphosphines and their derivatives.

2.4 Experimental

Reactions involving air- or moisture-sensitive compounds were carried out by means of conventional Schlenk techniques under a positive pressure of nitrogen gas. Unless stated otherwise, chemicals and solvents were used as received from commercial vendors without further purification. Nuclear magnetic resonance (NMR) spectroscopy was recorded at Nanyang Technological University Division of Chemistry and Biological Chemistry Central Facilities Laboratory on the Bruker Avance 400 spectrometer at 400 MHz for ^{1}H NMR and 100 MHz for ^{13}C{^{1}H} NMR. Chemical shifts (δ) are quoted in ppm and referenced to chemical shifts of residual solvent peaks for ^{1}H and ^{13}C{^{1}H} NMR. Enantiomeric excess (*ee*) was determined with an Agilent 1200 series high performance liquid chromatography (HPLC) system fitted with Daicel Chiralpak® I-series analytical columns (250 mm), eluted with a solvent mixture of *n*-hexane and 2-propanol. High resolution mass spectrometry (HRMS) *via* electrospray ionization (ESI) was performed on the Waters Q-Tof Premier spectrometer. Unless stated otherwise, acetonitrile was used as the solvent for the dissolution of compounds. Optical rotation studies were measured on the Jasco P-1030 polarimeter in a 0.1 dm polarimetry cell at the specified temperature using the D-line of sodium (589 nm) as the source of light. Unless stated otherwise, dichloromethane was used as the solvent for the dissolution of compounds.

Optimization of Procedure for the Catalytic Asymmetric 1,2-Dihydrophosphination of Acrylonitrile, 12aa and 12'aa. To a degassed solution (3 mL) of bis(phenylphosphino)ethane (40 mg, 0.16 mmol) was added catalyst and base. The mixture was subsequently cooled to the listed temperature prior to addition of acrylonitrile (26 mg, 0.49 mmol). The reaction mixture was then stirred at the same temperature for 16 h. S_8 (13 mg, 0.41 mmol) was added to the crude mixture and stirred at ambient temperature for 2 h. The solution was purified directly by column chromatography on silica gel with dichloromethane as the eluent to provide the products.

General Procedure for the Catalytic Asymmetric Dihydrophosphination Reaction, 12, 12'. Catalyst **9** (2.8 mg, 2 mol%) and $^{i}Pr_2NH$ (3.2 mg, 20 mol%) were added to a solution of diphosphine *rac/meso*-**11** (0.16 mmol) in degassed MeCN (3 mL). The mixture was subsequent cooled to –40 °C prior to addition of the olefinic substrate (0.49 mmol). The reaction mixture was then stirred at the same temperature until the reaction was completed. S_8 (13 mg, 0.41 mmol) was added to the crude mixture and stirred at ambient temperature for 2 h. The solution was purified directly by column chromatography on silica gel to provide the products.

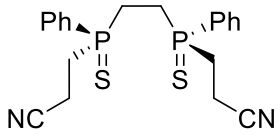

12aa

White solid; Eluent system (column chromatography): CH_2Cl_2; Yield: 38.6 mg (57%); $[\alpha]_D$ (21 °C) = 4.1°; ^{1}H NMR (400 MHz, CD*2*Cl*2*): δ 2.11-2.19 (m, 2H, PC*H*HC*H*HP), 2.35-2.45 (m, 6H, PC*H*HCH$_2$CN, PCH$_2$C*H*$_2$CN), 2.48-2.57 (m, 2H, PCH*H*CH*H*P), 2.74-2.85 (m, 2H, PCH*H*CH$_2$CN), 7.48-7.74 (m, 10H, Ar*H*); ^{13}C{^{1}H} NMR (100 MHz, CD2Cl2): δ 11.21 (s, *C*H$_2$CN), 25.79 (m, CH$_2$*C*H$_2$P), 29.06 (m, *C*H$_2$CH$_2$CN), 118.44 (t, J_{CP} = 8.5 Hz, *C*N), 128.33

(m, Ar*C*), 129.17 (t, J_{CP} = 6.2 Hz, Ar*C*), 131.07 (t, J_{CP} = 5.0 Hz, Ar*C*), 132.68 (s, Ar*C*); $^{31}P\{^{1}H\}$ NMR (161 MHz, CD2Cl2): δ 47.61; HRMS (ESI) m/z [negative mode] calcd. for $C_{20}N_2H_{21}P_2S_2$ 415.0621, found 415.0622.

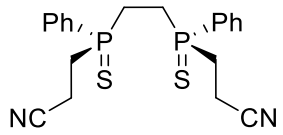

12'aa

White solid; Eluent system (column chromatography): CH_2Cl_2; Yield: 24.4 mg (36%); ^{1}H NMR (400 MHz, CD_2Cl_2): *δ* 1.91-1.96 (m, 2H, PC*H*HC*H*HP), 2.29-2.47 (m, 6H, PCH*H*CH*H*P, PC*H*$_2$CH$_2$CN), 2.65-2.78 (m, 4H, PCH$_2$C*H*$_2$CN), 7.56-7.65 (m, 6H, Ar*H*), 7.82-7.88 (m, 4H, Ar*H*); $^{13}C\{^{1}H\}$ NMR (100 MHz, CD_2Cl_2): *δ* 11.13 (s, *C*H$_2$CN), 25.67 (m, CH$_2$*C*H$_2$P), 29.23 (m, , *C*H$_2$CH$_2$CN), 118.35 (t, J_{CP} = 8.6 Hz, *C*N), 128.04 (m, Ar*C*), 129.28 (t, J_{CP} = 6.1 Hz, Ar*C*), 131.24 (t, J_{CP} = 5.1 Hz, Ar*C*), 132.77 (s, Ar*C*); $^{31}P\{^{1}H\}$ NMR (161 MHz, CD_2Cl_2): *δ* 47.84; HRMS (ESI) *m*/*z* [*negative mode*] calcd. for $C_{20}N_2H_{21}P_2S_2$ 415.0621, found 415.620.

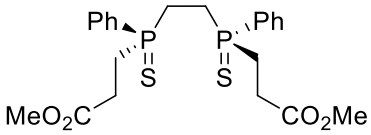

12ab

White solid; Eluent system (column chromatography): CH_2Cl_2; Yield: 50.2 mg (64%); $[\alpha]_D$ (20 °C) = -57.1°; ^{1}H NMR (400 MHz, CD_2Cl_2): *δ* 2.05-2.13 (m, 2H, PC*H*HC*H*HP), 2.32-2.51 (m, 8H, PCH*H*CH*H*P, PC*H*HCH$_2$CO$_2$Me, PCH$_2$C*H*$_2$CO$_2$Me), 2.67-2.74 (m, 2H, PCH*H*CH$_2$CO$_2$Me), 3.58 (s, 6H, OC*H*$_3$) 7.45-7.56 (m, 6H, Ar*H*), 7.69-7.74 (m, 4H, Ar*H*); $^{13}C\{^{1}H\}$ NMR (100 MHz, CD_2Cl_2): *δ* 26.02 (t, J_{CP} = 25.5 Hz, *C*H$_2$CH$_2$CO), 27.15 (s, *C*H$_3$), 28.34 (t, J_{CP} = 27.8 Hz, CH$_2$*C*H$_2$P), 51.91 (s, *C*H$_2$CO), 128.90 (t, J_{CP} = 5.7 Hz, Ar*C*), 129.66

(t, J_{CP} = 3.8 Hz, Ar*C*), 131.10 (t, J_{CP} = 4.8 Hz, Ar*C*), 132.10 (s, Ar*C*), 172.43 (t, J = 7.8 Hz, *C*O); $^{31}P\{^{1}H\}$ NMR (161 MHz, CD_2Cl_2): δ 48.57; HRMS (ESI) *m*/*z* [*positive mode*] calcd. for $C_{22}H_{29}P_2O_4S_2$ 483.0983, found 483.0998.

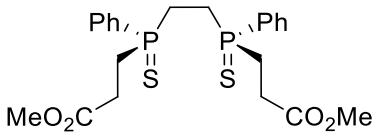

12'ab

White solid; Eluent system (column chromatography): CH_2Cl_2; Yield: 23.5 mg (30%); ^{1}H NMR (400 MHz, CD_2Cl_2): δ 1.77-1.82 (m, 2H, PC*H*HC*H*HP), 2.14-2.35 (m, 6H, PCH*H*CH*H*P, PC*H*$_2$CH$_2$CO$_2$Me), 2.48-2.58 (m, 4H, PCH$_2$C*H*$_2$CO$_2$Me), 3.44 (s, 6H, OC*H*$_3$) 7.42-7.50 (m, 6H, Ar*H*), 7.73-7.78 (m, 4H, Ar*H*); $^{13}C\{^{1}H\}$ NMR (100 MHz, CD_2Cl_2): δ 25.77 (t, J_{CP} = 25.5 Hz, *C*H$_2$CH$_2$CO), 27.01 (s, *C*H$_3$), 28.37 (t, J_{CP} = 28.0 Hz, CH$_2$*C*H$_2$P), 51.84 (s, *C*H$_2$CO), 128.92 (t, J_{CP} = 5.8 Hz, Ar*C*), 129.26 (t, J_{CP} = 1.4 Hz, Ar*C*), 131.19 (t, J_{CP} = 5.0 Hz, Ar*C*), 132.14 (s, Ar*C*), 172.31 (t, J_{CP} = 7.6 Hz, *C*O); $^{31}P\{^{1}H\}$ NMR (161 MHz, CD_2Cl_2): δ 48.79; HRMS (ESI) *m*/*z* [*positive mode*] calcd. for $C_{22}H_{29}P_2O_4S_2$ 483.0983, found 483.0986.

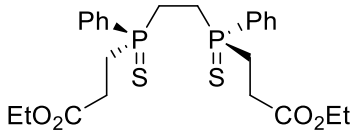

12ac

White solid; Eluent system (column chromatography): CH_2Cl_2; Yield: 58.1 mg (70%); $[\alpha]_D$ (20 °C) = 10.4°; ^{1}H NMR (400 MHz, CD_2Cl_2): δ 1.20 (t, 6H, J_{HH} = 7.1 Hz, CH$_2$C*H*$_3$), 2.04-2.13 (m, 2H, PC*H*HC*H*HP), 2.26-2.52 (m, 8H, PCH*H*CH*H*P, PC*H*HCH$_2$CO$_2$Et, PCH$_2$C*H*$_2$CO$_2$Et), 2.64-2.74 (m, 2H, PCH*H*CH$_2$CO$_2$Et) 4.04 (dq, 4H, J_{HH} = 1.1 Hz, J_{HH} = 7.1 Hz, C*H*$_2$CH$_3$), 7.44-7.56 (m, 6H, Ar*H*), 7.69-7.74 (m, 4H, Ar*H*); $^{13}C\{^{1}H\}$ NMR (100 MHz, CD_2Cl_2): δ 14.00 (s,

*C*H$_3$), 25.98 (t, J_{CP} = 25.1 Hz, *C*H$_2$CH$_2$CO), 27.36 (s, *C*H$_2$CO), 28.35 (t, J_{CP} = 27.4 Hz, CH$_2$*C*H$_2$P), 60.98 (s, *C*H$_2$CH$_3$), 128.87 (t, J_{CP} = 5.7 Hz, Ar*C*), 129.63 (t, J_{CP} = 36.9 Hz, Ar*C*), 131.09 (t, J_{CP} = 4.8 Hz, Ar*C*), 132.09 (s, Ar*C*), 171.98 (t, J_{CP} = 8.2 Hz, *C*O); $^{31}P\{^{1}H\}$ NMR (161 MHz, CD_2Cl_2): δ 48.62; HRMS (ESI) *m*/*z* [*positive mode*] calcd. for $C_{24}H_{33}O_4P_2S_2$ 511.1296, found 511.1306.

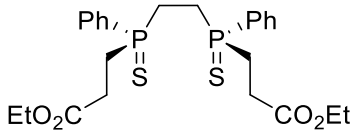

12'ac

White solid; Eluent system (column chromatography): CH_2Cl_2; Yield: 18.2 mg (22%); ^{1}H NMR (400 MHz, CD_2Cl_2): δ 1.17 (t, 6H, J_{HH} = 7.2 Hz, CH$_2$C*H*$_3$), 1.86-1.92 (m, 2H, PC*H*HC*H*HP), 2.22-2.44 (m, 6H, PCH*H*CH*H*P, PC*H*$_2$CH$_2$CO$_2$Et), 2.57-2.67 (m, 4H, PCH$_2$C*H*$_2$CO$_2$Et), 4.00 (q, 4H, J_{HH} = 7.1 Hz, C*H*$_2$CH$_3$), 7.52-7.61 (m, 6H, Ar*H*), 7.83-7.88 (m, 4H, Ar*H*); $^{13}C\{^{1}H\}$ NMR (100 MHz, CD_2Cl_2): δ 13.95 (s, *C*H$_3$), 25.77 (t, J_{CP} = 25.9 Hz, *C*H$_2$CH$_2$CO), 27.26 (s, *C*H$_2$CO), 28.45 (t, J_{CP} = 28.6 Hz, CH$_2$*C*H$_2$P), 60.92 (s, *C*H$_2$CH$_3$), 128.94 (t, J_{CP} = 5.9 Hz, Ar*C*), 129.67 (t, J = 37.4 Hz, Ar*C*), 131.22 (t, J_{CP} = 4.9 Hz, Ar*C*), 132.15 (s, Ar*C*), 171.90 (t, J_{CP} = 7.6 Hz, *C*O); $^{31}P\{^{1}H\}$ NMR (161 MHz, CD_2Cl_2): δ 48.86; HRMS (ESI) *m*/*z* [*positive mode*] calcd. for $C_{24}H_{33}O_4P_2S_2$ 511.1296, found 511.1313.

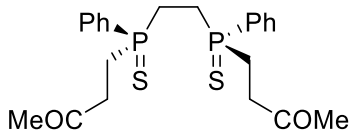

12ad

White solid; Eluent system (column chromatography): CH_2Cl_2; Yield: 32.9 mg (45%); $[\alpha]_D$ (20 °C) = 37.9°; ^{1}H NMR (400 MHz, CD_2Cl_2): δ 1.86-1.91 (m, 2H, PC*H*HC*H*HP), 2.04 (s, 6H,

C(=O)C*H*$_3$), 2.20-2.47 (m, 6H, PCH*H*CH*H*P, PCH$_2$C*H*$_2$C(=O)Me), 2.55-2.59 (m, 2H, PC*H*HCH$_2$C(=O)Me) 2.74-2.85 (m, 2H, PCH*H*CH$_2$C(=O)Me), 7.52-7.58 (m, 6H, Ar*H*), 7.82-7.86 (m, 4H, Ar*H*); ^{13}C{^{1}H} NMR (100 MHz, CD_2Cl_2): δ 26.22 (t, J_{CP} = 25.8 Hz, CH$_2$*C*H$_2$P), 26.76 (t, J_{CP} = 28.6 Hz, *C*H$_2$CH$_2$CO), 29.54 (s, *C*H$_3$), 36.11 (s, *C*H$_2$CO), 128.96 (t, J_{CP} = 5.8 Hz, Ar*C*), 129.79 (t, J_{CP} = 37.6 Hz, Ar*C*), 131.16 (t, J_{CP} = 4.8 Hz, Ar*C*), 132.10 (s, Ar*C*), 205.70 (t, J_{CP} = 6.8 Hz, *C*O); ^{31}P{^{1}H} NMR (161 MHz, CD_2Cl_2): δ 49.41; HRMS (ESI) *m*/*z* [*positive mode*] calcd. for $C_{22}H_{29}O_2P_2S_2$ 451.1084, found 415.1087.

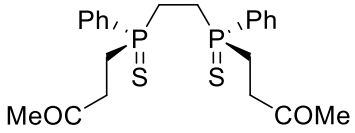

12'ad

White solid; Eluent system (column chromatography): CH_2Cl_2; Yield: 32.2 mg (44%); ^{1}H NMR (400 MHz, CD_2Cl_2): δ 2.00-2.03 (m, 2H, PC*H*HC*H*HP), 2.08 (s, 6H, C(=O)C*H*$_3$), 2.29-2.35 (m, 4H, PCH$_2$C*H*$_2$C(=O)Me), 2.41-2.55 (m, 4H, PCH*H*CH*H*P, PC*H*HCH$_2$C(=O)Me) 2.81-2.91 (m, 2H, PCH*H*CH$_2$C(=O)Me), 7.44-7.47 (m, 4H, Ar*H*), 7.52-7.56 (m, 2H, Ar*H*), 7.68-7.73 (m, 4H, Ar*H*); ^{13}C{^{1}H} NMR (100 MHz, CD_2Cl_2): δ 26.30 (t, J_{CP} = 25.9 Hz, CH$_2$*C*H$_2$P), 26.66 (t, J_{CP} = 28.6 Hz, *C*H$_2$CH$_2$CO), 29.58 (s, *C*H$_3$), 36.19 (s, *C*H$_2$CO), 128.88 (t, J_{CP} = 5.7 Hz, Ar*C*), 129.99 (t, J_{CP} = 37.8 Hz, Ar*C*), 131.06 (t, J_{CP} = 4.9 Hz, Ar*C*), 132.03 (s, Ar*C*), 205.75 (t, J_{CP} = 6.2 Hz, *C*O); ^{31}P{^{1}H} NMR (161 MHz, CD_2Cl_2): δ 49.22; HRMS (ESI) *m*/*z* [*positive mode*] calcd. for $C_{22}H_{29}O_2P_2S_2$ 451.1084, found 415.1088.

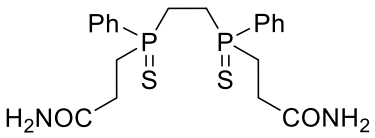

12ae/12'ae

White solid; Eluent system (column chromatography): EtOAc (*provides pure chiral*-**12ae** / *meso*-**12'ae** *mixture*); ^{1}H NMR (400 MHz, CD_3OD): δ 2.00-2.60 (m, -C*H*$_2$-), 7.48-7.59 (m, Ar*H*), 7.79-7.84 (m, Ar*H* (major product)), 7.92-7.93 (m, Ar*H* (minor product)); ^{31}P{^{1}H} NMR (161 MHz, CD_3OD): δ 50.02 (minor product), 50.12 (major product); HRMS (ESI) *m*/*z* [*positive mode*] calcd. for $C_{20}H_{27}N_2O_2P_2S_2$ 453.0989, found 453.0986.

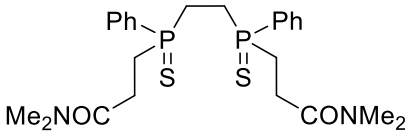

12af/12'af

White solid; Eluent system (column chromatography): EtOAc (*provides pure chiral*-**12af** / *meso*-**12'af** *mixture*); ^{1}H NMR (400 MHz, CD_2Cl_2): δ 1.91-2.72 (m, -C*H*$_2$-), 2.81 (s, NC*H*$_3$ (major product)), 2.84 (s, NC*H*$_3$ (minor product)), 2.86 (s, NC*H*$_3$ (major product)), 2.90 (s, NC*H*$_3$ (minor product)), 7.44-7.57 (m, Ar*H*), 7.71-7.76 (m, Ar*H* (minor product)), 7.83-7.88 (m, Ar*H* (major product)); ^{31}P{^{1}H} NMR (161 MHz, CD_2Cl_2): δ 49.41 (minor product), 49.58 (major product); HRMS (ESI) *m*/*z* [*positive mode*] calcd. for $C_{24}H_{35}N_2O_2P_2S_2$ 509.1615, found 509.1600. Note: ^{1}H and ^{31}P{^{1}H} NMR spectrum of isolated pure complexed *chiral*-**15af** and *meso*-**15'af** available below.

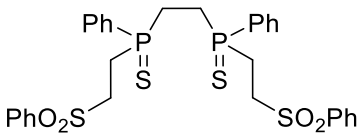

12ag/12'ag

White solid; Eluent system (column chromatography): CH_2Cl_2 (*provides pure chiral*-**12ag** */ meso*-**12'ag** *mixture*); ^{1}H NMR (400 MHz, CD_2Cl_2): δ 1.83-3.42 (m, -C*H*$_2$-), 7.43-7.83 (m, Ar*H*); ^{31}P{^{1}H} NMR (161 MHz, CD_2Cl_2): δ 47.43 (major product), 47.64 (minor product); HRMS (ESI) *m*/*z* [*positive mode*] calcd. for $C_{30}H_{33}O_4P_2S_4$ 647.0737, found 647.0735.

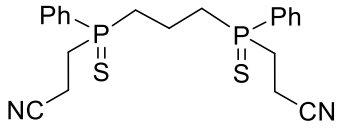

12ba/12'ba

White solid; Eluent system (column chromatography): CH_2Cl_2 (*provides pure chiral*-**12ba** */ meso*-**12'ba** *mixture*); ^{1}H NMR (400 MHz, CD_2Cl_2): δ 2.21-2.76 (m, -C*H*$_2$-), 7.47-7.83 (m, Ar*H*); ^{31}P{^{1}H} NMR (161 MHz, CD_2Cl_2): δ 49.01 (minor product), 49.10 (major product); HRMS (ESI) *m*/*z* [*positive mode*] calcd. for $C_{21}H_{25}N_2P_2S_2$ 431.0934, found 431.0937.

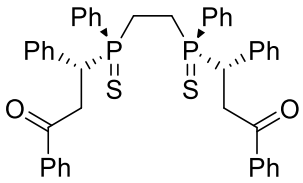

12aj

Colourless needles (recrystallized); Recrystallized from *n*-hexanes and $CHCl_2$; Yield: 28.3 mg (24%) (recrystallized yield); ^{1}H NMR (400 MHz, CD_2Cl_2): δ 1.66 (m, 1H, PC*H*HCH$_2$P), 1.92 (m, 1H, PCH*H*CH$_2$P), 2.15 (m, 1H, PCH$_2$C*H*HP), 2.54 (m, 1H, PCH$_2$CH*H*P), 3.18 (ddd, J_{HH}

= 18.1 Hz, J_{HP} = 11.4 Hz, J_{HH} = 3.0 Hz, 1H, C*H*HC(=O)Ph), 3.56 (m, 1H, CH*H*C(=O)Ph), 3.85 (m, 2H, C*HH*C(=O)Ph), 4.08 (dt, J_{HP} = 10.2 Hz, J_{HH} = 4.1 Hz, 1H, PC*H*(Ph)CH_2), 4.21 (dt, J_{HP} = 9.9 Hz, J_{HH} = 3.0 Hz, 1H, PC*H*(Ph)CH_2), 6.87 (d, J_{HP} = 8 Hz, 2H, Ar*H*), 7.07 (m, 3H, Ar*H*), 7.35-7.59 (m, 16H, Ar*H*), 7.77 (d, J_{HP} = 7.6 Hz, 2H, Ar*H*), 7.87 (d, J_{HP} = 7.6 Hz, 2H, Ar*H*), 7.98 (dd, J_{HP} = 11.3 Hz, J_{HH} = 8.0 Hz, 2H, Ar*H*); $^{13}C\{^1H\}$ NMR (100 MHz, CD_2Cl_2): δ 23.53 (d, J_{CP} = 48.8 Hz, *C*H_2CH_2CO), 24.24 (d, J_{CP} = 52.1 Hz, *C*H_2CH_2CO), 39.09 (d, J_{CP} = 6.5 Hz, *C*H_2CO), 39.11 (d, J_{CP} = 7.0 Hz, *C*H_2CO), 44.11 (dd, J_{CP} = 48.0 Hz, J_{CP} = 2.4 Hz, , CH_2CH_2P), 44.77 (dd, J_{CP} = 46.1 Hz, J_{CP} = 2.6 Hz, CH_2CH_2P), 127.31-136.74 (m, Ar*C*), 196.24 (d, J_{CP} = 14.1 Hz, *C*O), 196.60 (d, J_{CP} = 11.6 Hz, *C*O); $^{31}P\{^1H\}$ NMR (161 MHz, CD_2Cl_2): δ 56.46 (d, J_{PP} = 54.4 Hz), 57.28 (d, J_{PP} = 54.4 Hz).

One-Pot Direct Dihydrophosphination-Complexation of 1,2-Diphosphines, 13, 13'. Catalyst **9** (2.8 mg, 2 mol%) and $^{i}Pr_2NH$ (3.2 mg, 20 mol%) were added to a solution of bis(phenylphosphino)ethane *rac*/*meso*-**11a** (40 mg, 0.16 mmol) in degassed MeCN (3 mL). The mixture was subsequent cooled to –40 °C prior to addition of olefinic substrate (0.49 mmol). The reaction mixture was then stirred at the same temperature for 16 h. A methanolic solution (4 mL) of Li_2PdCl_4 (52.4 mg, 0.2 mmol) was added to the mixture and stirred for 2 h at ambient temperature. The crude mixture was concentrated prior to purification by column chromatography on silica gel to provide complexes **13** and *meso*-**13'**.

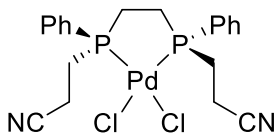

13aa

Colourless blocks (recrystallized); Eluent system (column chromatography): CH_2Cl_2/EtOAc (4:1); Yield: 48.2 mg (56%); $[\alpha]_D$ (21 °C) = -239.3°; ^1H NMR (400 MHz, CD_2Cl_2): δ 2.06-2.16

(m, 2H, PC*H*HC*H*HP), 2.61-2.98 (m, 10H, PCH*H*CH*H*P, PCH_2CH_2CN), 7.53-7.63 (m, 6H, Ar*H*), 8.03-8.08 (m, 4H, Ar*H*); ^{13}C{^{1}H} NMR (100 MHz, CD_2Cl_2): δ 13.45 (s, *C*H_2CN), 24.53 (m, *C*H_2CH$_2$CN), 26.21 (m, CH$_2$*C*H_2P), 118.47 (m, *C*N), 125.54 (dd, J = 2.2 Hz, J = 54.7 Hz, Ar*C*), 129.63 (m, Ar*C*), 133.08 (s, Ar*C*), 133.31 (m, Ar*C*); ^{31}P{^{1}H} NMR (161 MHz, CD_2Cl_2): δ 70.87; HRMS (ESI) *m*/*z* [*negative mode*] calcd for $C_{20}N_2H_{22}P_2Cl_2Pd$ 527.6970, found 527.9661.

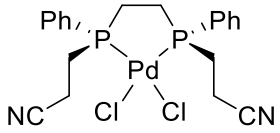

13'aa

Colourless plates (recrystallized); Eluent system (column chromatography): CH_2Cl_2/EtOAc (4:1); Yield: 29.3 mg (34%); ^{1}H NMR (400 MHz, d_6-DMSO): δ 2.19-2.37 (m, 2H, PC*H*HC*H*HP), 2.65-3.15 (m, 10H, PCH*H*CH*H*P, PCH_2CH_2CN), 7.50-7.60 (m, 6H, Ar*H*), 7.91-7.96 (m, 4H, Ar*H*); ^{13}C{^{1}H} NMR (100 MHz, d_6-DMSO): δ 12.54 (s, *C*H_2CN); 23.02 (m, *C*H_2CH$_2$CN), 26.57 (m, CH$_2$*C*H_2P), 119.54 (m, *C*N), 127.46 (dd, J = 1.5 Hz, J = 54.0 Hz, Ar*C*), 129.03 (m, Ar*C*), 132.28 (s, Ar*C*), 132.72 (m, Ar*C*); ^{31}P{^{1}H} NMR (161 MHz, d_6-DMSO): δ 73.45; HRMS (ESI) *m*/*z* [*negative mode*] calcd for $C_{20}N_2H_{22}P_2Cl_2Pd$ 527.6970, found 527.9672.

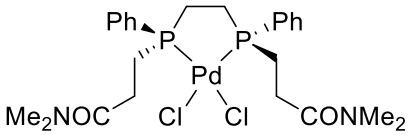

13af

White solid; Eluent system (column chromatography): Acetone/EtOAc (2:1); Yield: 43.4 mg (43%); ^{1}H NMR (400 MHz, CD_2Cl_2): δ 2.09-2.12 (m, 2H, PC*H*HC*H*HP), 2.36-2.50 (m, 2H,

PCH*H*CH*H*P), 2.60-2.71 (m, 4H, PCH$_2$C*H*$_2$CN), 2.75 (s, 6H, N(C*H*$_3$)Me), 2.80-2.88 (m, 4H, PC*H*$_2$CH$_2$CN), 2.91 (s, 6H, NMe(C*H*$_3$)), 7.51-7.59 (m, 6H, Ar*H*), 8.02-8.07 (m, 4H, Ar*H*); ^{13}C{^{1}H} NMR (100 MHz, CD_2Cl_2): δ 24.17 (m, *C*H$_2$CH$_2$CN), 26.81 (m, CH$_2$*C*H$_2$P), 29.23 (s, *C*H$_2$CN), 35.31 (s, *C*H$_3$), 37.08 (s, *C*H$_3$), 128.59 (m, Ar*C*), 129.17 (t, J_{CP} = 5.8 Hz, Ar*C*), 132.28 (s, Ar*C*), 133.27 (t, J_{CP} = 5.8 Hz, Ar*C*), 170.43 (t, J_{CP} = 5.2 Hz, *C*O); ^{31}P{^{1}H} NMR (161 MHz, CD_2Cl_2): δ 75.25.

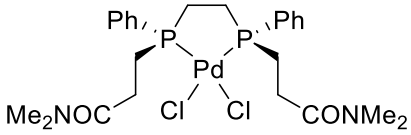

13'af

White solid; Eluent system (column chromatography): Acetone/EtOAc (2:1); Yield: 41.4 mg (41%); ^{1}H NMR (400 MHz, CD_2Cl_2): δ 2.12-2.14 (m, 2H, PC*H*HC*H*HP), 2.70-2.81 (m, 6H, PCH*H*CH*H*P, PCH$_2$C*H*$_2$CN), 2.92 (s, 6H, N(C*H*$_3$)Me), 3.01 (s, 6H, NMe(C*H*$_3$)); 3.13-3.22 (m, 4H, PC*H*$_2$CH$_2$CN), 7.43-7.51 (m, 6H, Ar*H*), 7.88-7.94 (m, 4H, Ar*H*); ^{13}C{^{1}H} NMR (100 MHz, CD_2Cl_2): δ 24.36 (m, *C*H$_2$CH$_2$CN), 29.08 (m, CH$_2$*C*H$_2$P), 29.27 (s, *C*H$_2$CN), 35.53 (s, *C*H$_3$), 37.25 (s, *C*H$_3$), 129.11 (t, J_{CP} = 5.2 Hz, Ar*C*), 129.70 (m, Ar*C*), 132.05 (s, Ar*C*), 132.92 (t, J_{CP} = 5.2 Hz, Ar*C*), 171.10 (t, J_{CP} = 4.8 Hz, *C*O); ^{31}P{^{1}H} NMR (161 MHz, CD_2Cl_2): δ 73.90.

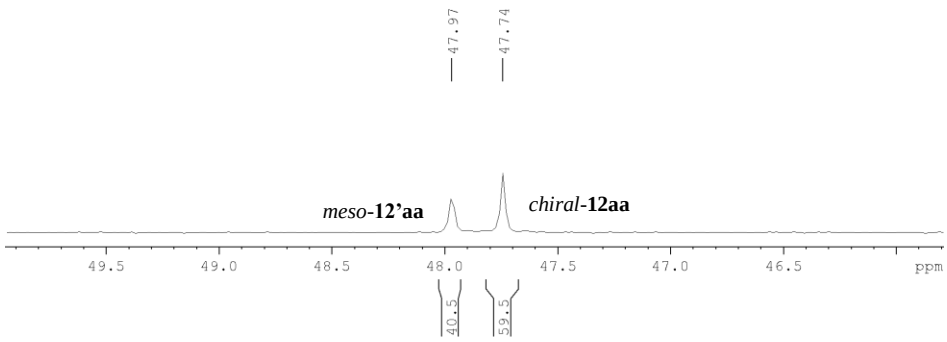

Figure 19. Determination of Diastereomeric Ratio of 12aa/12'aa

2.5 References

1. (a) W. S. Knowles; M. J. Sabacky; B. D. Vineyard; D. J. Weinkauff, *Asymmetric hydrogenation with a complex of rhodium and a chiral bisphosphine*, *J. Am. Chem. Soc.* **1975**, *97*, 2567; (b) T. Imamoto; K. Sugita; K. Yoshida, *An Air-Stable P-Chiral Phosphine Ligand for Highly Enantioselective Transition-Metal-Catalyzed Reactions*, *J. Am. Chem. Soc.* **2005**, *127*, 11934; (c) Y. Yamanoi; T. Imamoto, *Methylene-Bridged P-Chiral Diphosphines in Highly Enantioselective Reactions*, *J. Org. Chem.* **1999**, *64*, 2988; (d) T. P. Dang; H. B. Kagan, *The asymmetric synthesis of hydratropic acid and amino-acids by homogeneous catalytic hydrogenation*, *J. Chem. Soc. D* **1971**, 481; (e) T. Imamoto; K. Tamura; Z. Zhang; Y. Horiuchi; M. Sugiya; K. Yoshida; A. Yanagisawa; I. D. Gridnev, *Rigid P-Chiral Phosphine Ligands with tert-Butylmethylphosphino Groups for Rhodium-Catalyzed Asymmetric Hydrogenation of Functionalized Alkenes*, *J. Am. Chem. Soc.* **2012**, *134*, 1754.

2. T. Imamoto; T. Itoh; Y. Yamanoi; R. Narui; K. Yoshida, *Highly enantioselective hydrosilylation of simple ketones catalyzed by rhodium complexes of P-chiral diphosphine ligands bearing tert-butylmethylphosphino groups*, *Tetrahedron Asymmetry* **2006**, *17*, 560.

3. (a) H. Ito; S. Ito; Y. Sasaki; K. Matsuura; M. Sawamura, *Copper-Catalyzed Enantioselective Substitution of Allylic Carbonates with Diboron: An Efficient Route to Optically Active α-Chiral Allylboronates*, *J. Am. Chem. Soc.* **2007**, *129*, 14856; (b) I. H. Chen; L. Yin; W. Itano; M. Kanai; M. Shibasaki, *Catalytic Asymmetric Synthesis of Chiral Tertiary Organoboronic Esters through Conjugate Boration of β-Substituted Cyclic Enones*, *J. Am. Chem. Soc.* **2009**, *131*, 11664; (c) K. Kubota; E. Yamamoto; H. Ito, *Regio- and Enantioselective Monoborylation of Alkenylsilanes Catalyzed by an Electron-Donating Chiral Phosphine–Copper(I) Complex*, *Adv. Synth. Catal.* **2013**, *355*, 3527.

4. (a) G. Erre; S. Enthaler; K. Junge; S. Gladiali; M. Beller, *Synthesis and application of chiral monodentate phosphines in asymmetric hydrogenation*, *Coord. Chem. Rev.* **2008**, *252*,

471; (b) I. Wauters; W. Debrouwer; C. V. Stevens, *Preparation of phosphines through C–P bond formation*, *Beilstein J. Org. Chem.* **2014**, *10*, 1064.

5. Y. Huang; S. A. Pullarkat; Y. Li; P.-H. Leung, *Palladium(ii)-catalyzed asymmetric hydrophosphination of enones: efficient access to chiral tertiary phosphines*, *Chem. Commun.* **2010**, *46*, 6950.

6. Y. Huang; S. A. Pullarkat; Y. Li; P.-H. Leung, *Palladacycle-Catalyzed Asymmetric Hydrophosphination of Enones for Synthesis of C*- and P*-Chiral Tertiary Phosphines*, *Inorg. Chem.* **2012**, *51*, 2533.

7. (a) J.-J. Feng; X.-F. Chen; M. Shi; W.-L. Duan, *Palladium-Catalyzed Asymmetric Addition of Diarylphosphines to Enones toward the Synthesis of Chiral Phosphines*, *J. Am. Chem. Soc.* **2010**, *132*, 5562; (b) J. M. Longmire; X. Zhang, *Synthesis of chiral phosphine ligands with aromatic backbones and their applications in asymmetric catalysis*, *Tetrahedron Lett.* **1997**, *38*, 1725.

8. (a) Y. Huang; S. A. Pullarkat; S. Teong; R. J. Chew; Y. Li; P.-H. Leung, *Palladacycle-Catalyzed Asymmetric Intermolecular Construction of Chiral Tertiary P-Heterocycles by Stepwise Addition of H–P–H Bonds to Bis(enones)*, *Organometallics* **2012**, *31*, 4871; (b) R. J. Chew; K. Y. Teo; Y. Huang; B.-B. Li; Y. Li; S. A. Pullarkat; P.-H. Leung, *Enantioselective phospha-Michael addition of diarylphosphines to β,γ-unsaturated α-ketoesters and amides*, *Chem. Commun.* **2014**, *50*, 8768; (c) K. Gan; A. Sadeer; C. Xu; Y. Li; S. A. Pullarkat, *Asymmetric Construction of a Ferrocenyl Phosphapalladacycle from Achiral Enones and a Demonstration of Its Catalytic Potential*, *Organometallics* **2014**, *33*, 5074; (d) C. Xu; G. Jun Hao Kennard; F. Hennersdorf; Y. Li; S. A. Pullarkat; P.-H. Leung, *Chiral Phosphapalladacycles as Efficient Catalysts for the Asymmetric Hydrophosphination of Substituted Methylidenemalonate Esters: Direct Access to Functionalized Tertiary Chiral Phosphines*, *Organometallics* **2012**, *31*, 3022; (e) Y. Huang; R. J. Chew; S. A. Pullarkat; Y. Li;

P.-H. Leung, *Asymmetric Synthesis of Enaminophosphines via Palladacycle-Catalyzed Addition of Ph2PH to α,β-Unsaturated Imines*, *J. Org. Chem.* **2012**, *77*, 6849; (f) R. J. Chew; Y. Huang; Y. Li; S. A. Pullarkat; P.-H. Leung, *Enantioselective Addition of Diphenylphosphine to 3-Methyl-4-nitro-5-alkenylisoxazoles*, *Adv. Synth. Catal.* **2013**, *355*, 1403; (g) X.-Y. Yang; J. H. Gan; Y. Li; S. A. Pullarkat; P.-H. Leung, *Palladium catalyzed asymmetric hydrophosphination of α,β- and α,β,γ,δ-unsaturated malonate esters – efficient control of reactivity, stereo- and regio-selectivity*, *Dalton Trans.* **2015**, *44*, 1258.

9. J. R. Rogers; T. P. S. Wagner; D. S. Marynick, *Metal-Assisted Pyramidal Inversion in Metal-Phosphido Complexes*, *Inorg. Chem.* **1994**, *33*, 3104.

10. D. S. Glueck, *Metal-Catalyzed Asymmetric Synthesis of P-Stereogenic Phosphines*, *Synlett* **2007**, *2007*, 2627.

11. J. Dogan; J. B. Schulte; G. F. Swiegers; S. B. Wild, *Mechanism of Phosphorus−Carbon Bond Cleavage by Lithium in Tertiary Phosphines. An Optimized Synthesis of 1,2-Bis(phenylphosphino)ethane*, *J. Org. Chem.* **2000**, *65*, 951.

12. X.-R. Li; R. J. Chew; Y. Li; P.-H. Leung, *Investigation of Functional Group Effects on Palladium Catalysed Asymmetric P–H Addition*, *Aust. J. Chem.* **2016**, *69*, 499.

13. X.-Y. Yang; W. S. Tay; Y. Li; S. A. Pullarkat; P.-H. Leung, *Versatile Syntheses of Optically Pure PCE Pincer Ligands: Facile Modifications of the Pendant Arms and Ligand Backbones*, *Organometallics* **2015**, *34*, 1582.

14. X.-Y. Yang; Y.-X. Jia; W. S. Tay; Y. Li; S. A. Pullarkat; P.-H. Leung, *Mechanistic insights into the role of PC- and PCP-type palladium catalysts in asymmetric hydrophosphination of activated alkenes incorporating potential coordinating heteroatoms*, *Dalton Trans.* **2016**, *45*, 13449.

15. (a) H. J. Chen; R. H. X. Teo; J. Wong; Y. Li; S. A. Pullarkat; P.-H. Leung, *Challenges in cyclometalation: steric effects leading to competing pathways and η1,η2-cyclometalated*

iridium(iii) complexes, *Dalton Trans.* **2018**, *47*, 13046; (b) H. J. Chen; R. Hong Xiang Teo; Y. Li; S. A. Pullarkat; P.-H. Leung, *Stereogenic Lock in 1-Naphthylethanamine Complexes for Catalyst and Auxiliary Design: Structural and Reactivity Analysis for Cycloiridated Pseudotetrahedral Complexes*, *Organometallics* **2018**, *37*, 99; (c) J. K.-P. Ng; G.-K. Tan; J. J. Vittal; P.-H. Leung, *Optical Resolution and the Study of Ligand Effects on the Ortho-Metalation Reaction of Resolved (±)-Diphenyl[1-(1-naphthyl)ethyl]phosphine and Its Arsenic Analogue*, *Inorg. Chem.* **2003**, *42*, 7674.

16. W. L. Steffen; G. J. Palenik, *Crystal and molecular structures of dichloro[bis(diphenylphosphino)methane]palladium(II), dichloro[bis(diphenylphosphino)ethane]palladium(II), and dichloro[1,3-bis(diphenylphosphino)propane]palladium(II)*, *Inorg. Chem.* **1976**, *15*, 2432.

Chapter III

Catalytic Asymmetric Hydrophosphination as a Valuable Tool to Access Mono- and Di-Hydrophosphinated Curcuminoids

3.1 Introduction

3.1.1 Curcumin

Curcumin, chemically known as diferuloyl methane, is a ubiquitous dietary phytochemical found in the Indian spice turmeric. Turmeric has often been used in Indian system as traditional medicine, Ayurveda, to treat wounds, inflammations and growth of disease-causing microorganisms. Turmeric has a characteristic yellow color due to the presence of curcuminoids in it – curcumin (Cur), demethoxycurcumin (DMC) and bisdemethoxycurcumin (BDMC). These curcuminoids make up about 5% of turmeric, of which curcumin is the main biologically active component. Cur was first isolated in 1815 and its chemical structure was elucidated in 1910.[1] A drastic increase in the number of studies on curcumin as an anticancer agent was observed after epidemiological studies showed a reduction (10-15%) in occurrence of some types of cancer in patients who consumed turmeric regularly.[2] Over 3000 scientific researches have been published on the study of the chemical, photophysical, biological and anticancer effects of Cur, including uses as a chemo-preventive and therapeutic drug against chronic diseases such as Alzheimer, cancer, cardio-vascular, skin, inflammatory and neurological diseases.[3]

3.1.2 Curcumin Complexes

Although clinical studies on the effects of curcumin in humans have shown that mild side-effects only surfaced with high daily dosages of up to 12g, poor bioavailability of curcumin presented a more pertinent problem. The main factors limiting curcumin

bioavailability were the insolubility of Cur in water, rapid metabolism, systemic elimination and poor absorption.[4] One method to overcome this limitation was the incorporation of metals into the Cur backbone. The syntheses of metal–Cur complexes make use of the naturally occurring diketo moiety as a suitable bidentate chelate to bind to a variety of metals. The first reported curcumin complex was prepared by Beck *et al*[5] and the versatile method developed could be employed in the syntheses of many other complexes. The method involved the deprotonation of Cur with a strong base followed by complexation with metal halides. Initially used for the complexation of Cur with transition metals, the protocol has now been extended to include main-group elements.[6]

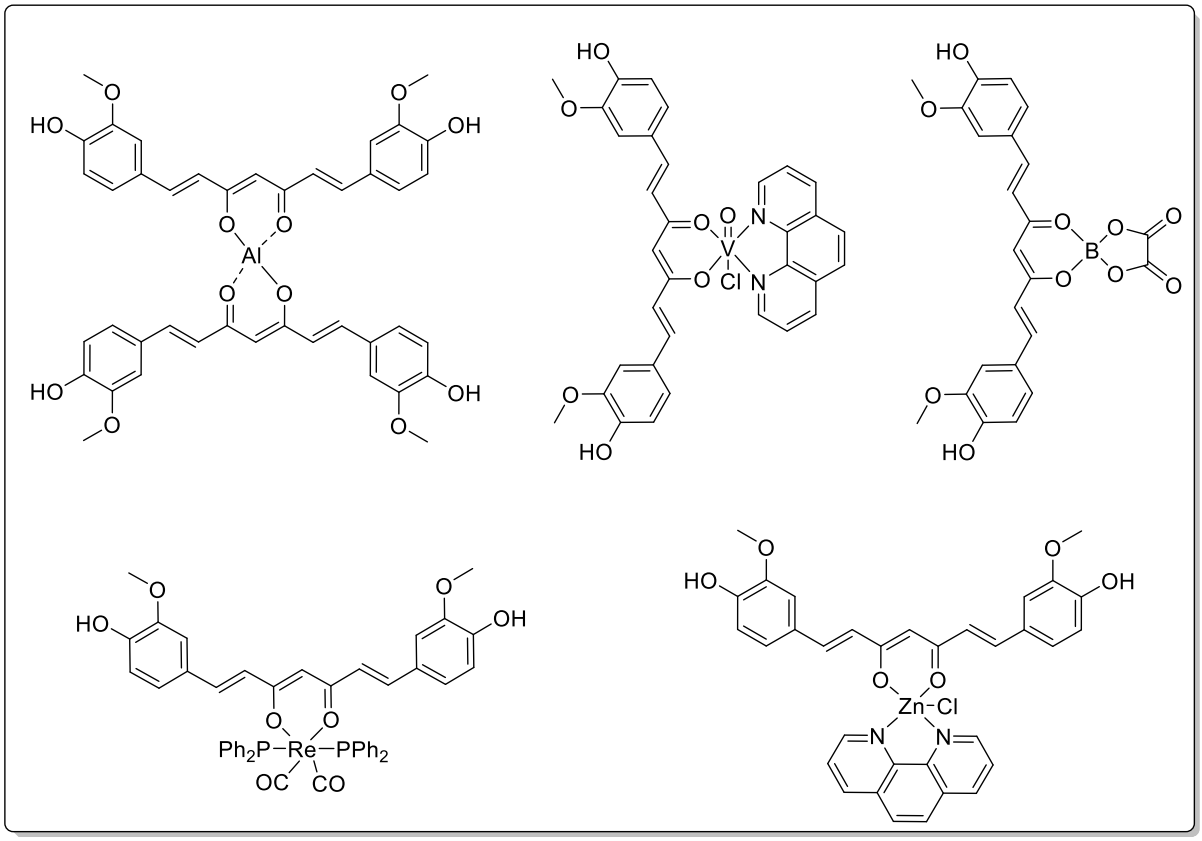

Figure 20. Selected examples of complexes containing Cur as ligand(s).

The first few reported curcumin complexes being tested for antitumor effects date back to 1998. Vanadium(IV), cobalt(II), nickel(II) and copper(II) complexes were among those that

have been tested *in vitro* and *in vivo* for antitumor effects, with copper(II) displaying the highest selective cytotoxicity and most significant reduction in solid tumor size in ascites tumor-bearing mice.[6b] In addition, these complexes exhibited antirheumatic activity, angiogenesis inhibition and anticancer potential.[7]

Besides being studied for its pharmacological effects as a potential chemo-preventive and therapeutic drug, Cur has also found utility in catalytic reactions, namely the Heck, Suzuki and Stille coupling reactions.[8] Japtap *et al.* used the naturally occurring Cur as a ligand in the complexation with palladium(II) for use as a catalyst in the coupling reactions.[8a] Jani and co-workers further improved the complex reusability by modifying boehmite surface with Cur to anchor palladium(II), producing Boehmite Nanoparticles Curcumin-Pd.[8b]

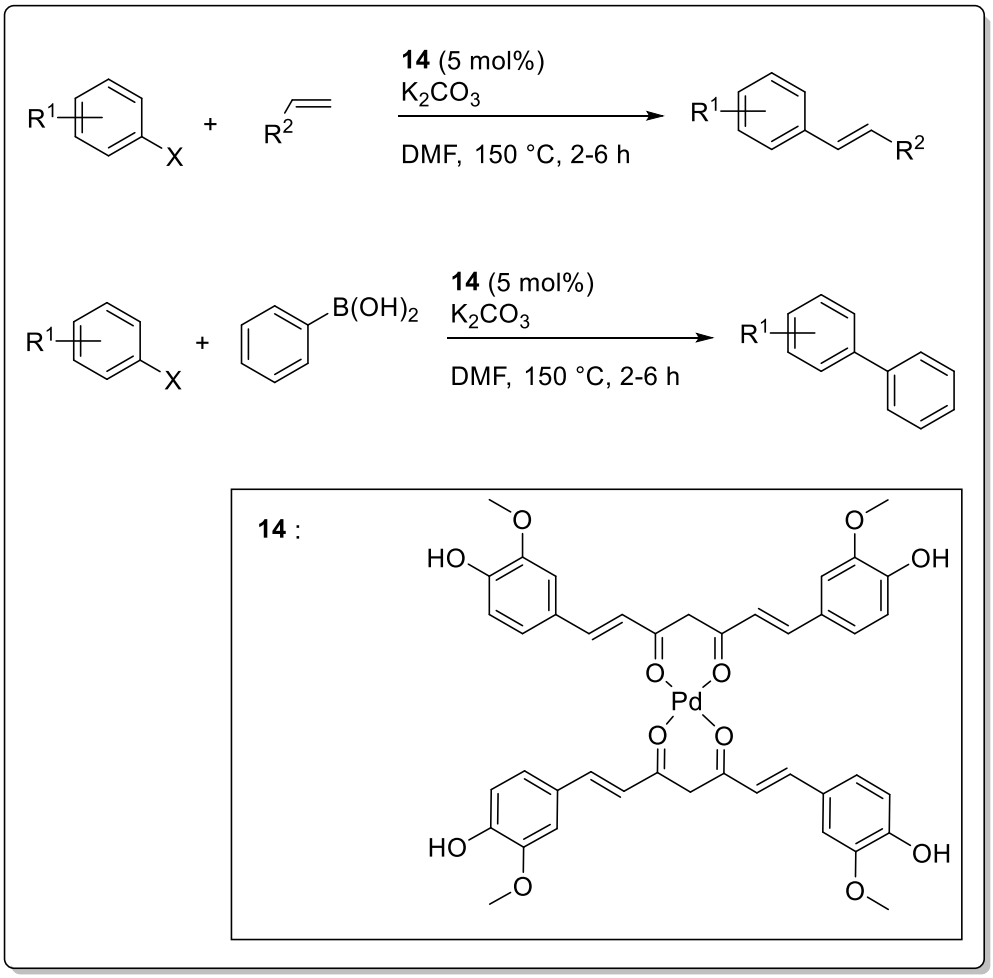

Scheme 41. Example of Heck and Suzuki reactions using palladium(II) Cur **14** as catalyst.

3.1.3 Functionalized Curcumin and Its Complexes

Structurally related compounds of curcumin have been synthesized and studied for the evaluation of their biological activities. The first reported semi-functionalized derivatives were done by Dutta *et al.* in which the keto group was replaced with nitrogen and sulfur as donors.[9] These compounds showed enhanced antioxidant activity, and when comparing the antiproliferative activity against Cur in breast cancer cell line MCF7, nitrogen and sulfur-functionalized Cur was found to be more potent than Cur, with a decrease in cell viability by 38%.[9-10] Hydrazinocurcuminoids, synthesized by Shim *et al.*, are potential antiangiogenic agents as nanomolar concentrations are able to inhibit the multiplication of bovine aortic endothelial cells without cytotoxicity.

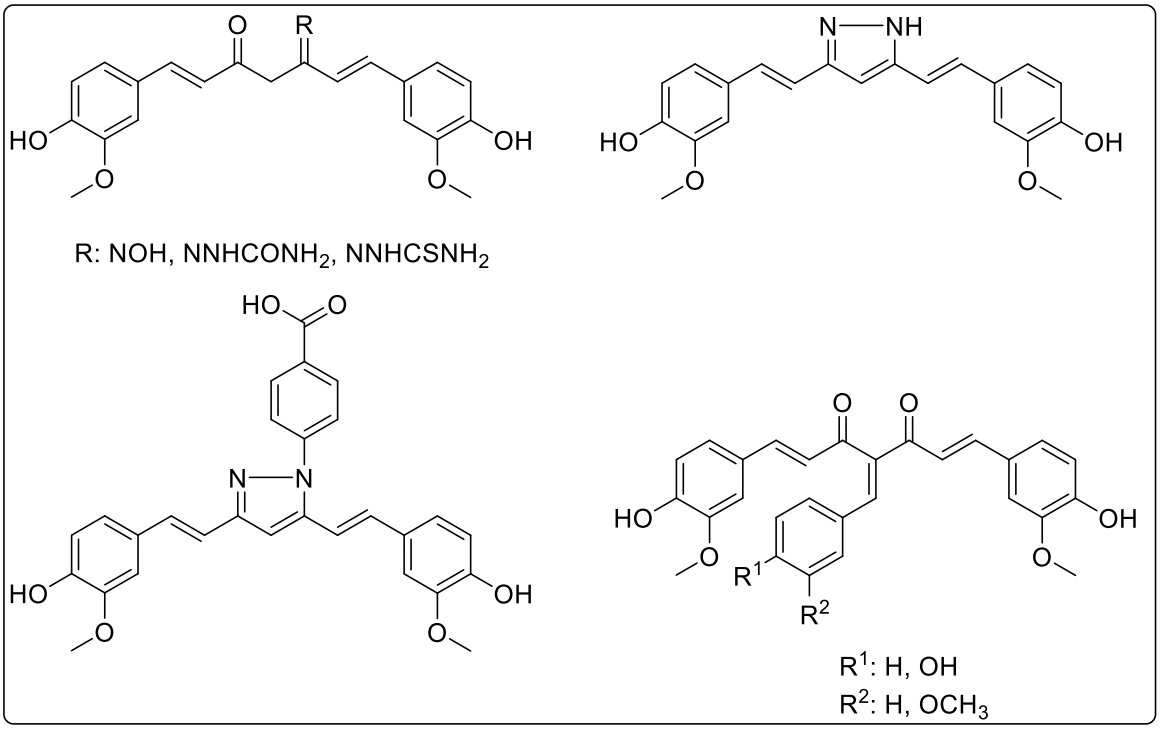

Figure 21. Selected examples of functionalized Cur in the carbon backbone.

A few novel Cur derivatives were synthesized by Mishra *et al*. and their *in vitro* inhibition of *Plasmodium falciparum* growth was evaluated. These derivatives exhibited

enhanced potencies towards inhibiting chloroquine sensitive *Plasmodium falciparum* due to the increase in cellular uptake, greater efficacies of inhibiting the target and greater retention by the parasite. Their studies also proved the need for the hydroxy group in Cur for antimalarial activity.[11]

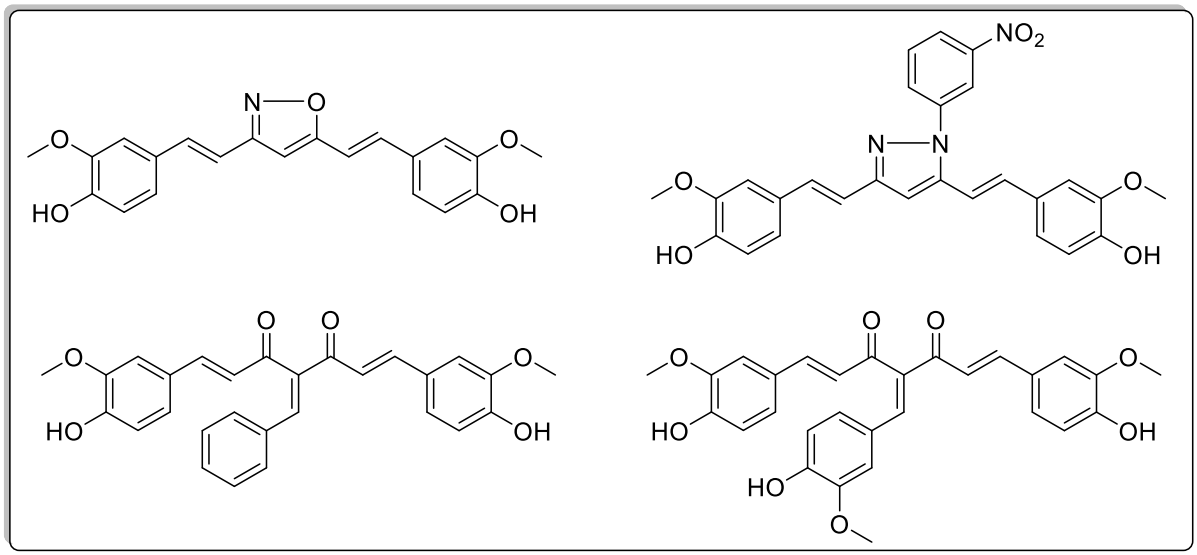

Figure 22. Examples of functionalized Cur on the aryl groups by Mishra *et al*.

In addition to functionalizing the carbon backbone, functionalization of the aryl region was also done. John *et al.* synthesized a series of Cur derivatives that was functionalized at the aryl rings. These compounds were further evaluated for their efficacies as antitumor drugs and cytotoxicity. Complexation of these curcuminoids to copper metal showed an increase in antitumor activity and were revealed to be cytotoxic to cultured L929 cells, with IC_{50} of about 2.7×10^{-5} M for the curcuminoids and 2×10^{-6} M for the copper complexes. Complexes containing phenolic group were the most active in the study, and an increase in conjugation along the carbon backbone showed an increased life span (ILS578.6%) of ascites tumor-bearing animals.[12]

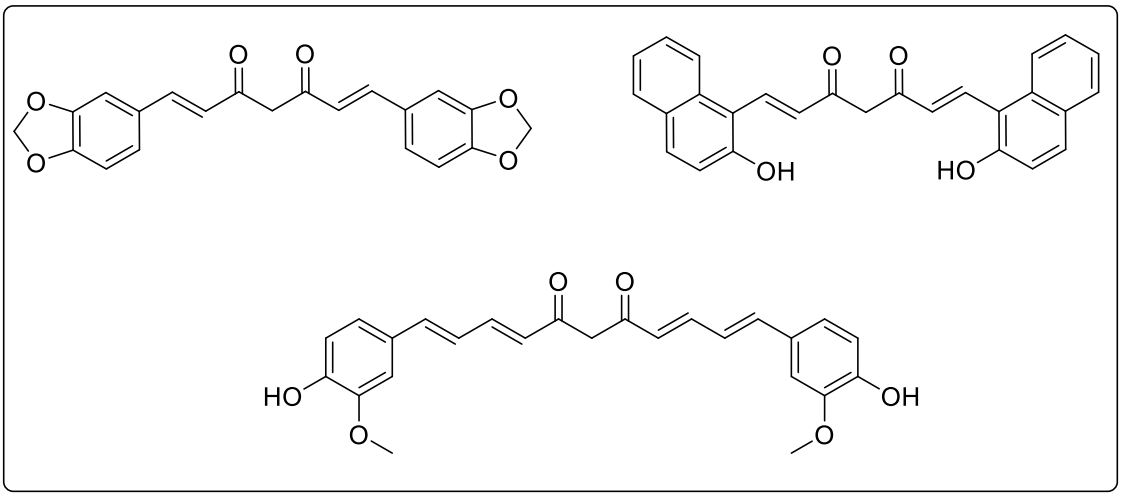

Figure 23. Examples of functionalized Cur on the aryl groups by John *et al*.

3.1.4 Research Objective

While numerous articles have reported successful results such as improved biological effects and significant cytotoxicity towards cancer cells associated with functionalized curcumins, the lack of research in the incorporation of phosphorus-based functional groups into the backbone of Cur remains extant. In addition, the conjugated enone motif in curcumin serves as an excellent electrophile for the introduction of numerous useful nucleophiles for post-modification of curcumin. The research gap in the studies pertaining to the methodology and study of new functionalized curcumins in a biological setting together with the ongoing interest of our group in asymmetric hydrophosphination of electrophilic substrates prompted us to consider hydrophosphination as a viable tool in the introduction of phosphine groups into Cur.

3.2 Results and Discussion

3.2.1 Preparation of Curcumin and Curcumin Derivative

Pure Cur can be obtained from commercially available curcuminoids consisting of roughly 75% Cur, 20% DMC and 5% BDMC (Merck source) through silica gel chromatography in a eluent system of chloroform and methanol.[13] However, the use of approximately 30L of solvents per 11g of curcuminoids required in this protocol is not the most efficient way of obtaining pure Cur. Instead, a more efficient method to produce pure Cur would be through aldol condensation between vanillin and acetylacetone.[14] In this methodology, acetylacetone was first reacted with boric anhydride **15** to form a less activated methylene synthon to prevent a *Knovenagel* condensation. Subsequently, the acetone-boric complex was subjected to a double aldol condensation with two equivalents of vanillin in the presence of a drying agent such as tributyl borate and a base such as *n*-butylamine, before being decomplexed with hydrochloric acid to produce pure Cur in 81% yield. In this reaction, the utilization of tributyl borate served two purposes. Firstly, it acted as a desiccant to provide a dry reaction condition, and secondly, it helped to kinetically activate the carbonyl carbon in vanillin. This same synthetic methodology could be employed to synthesize BDMC, but with 4-hydroxybenzaldehyde in place of vanillin.

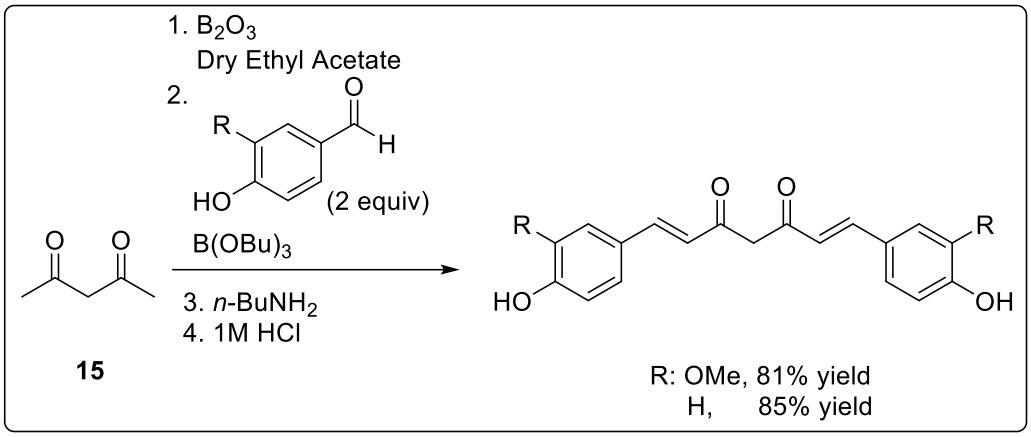

Scheme 42. Double aldol condensation to produce Cur and BDMC.

3.2.2 Catalytic Asymmetric Hydrophosphination

Chemically, Cur exists as a significant mixture of two tautomeric forms, a diketo and an enol form, due to the stabilization provided by the intramolecular hydrogen bonding between the carbonyl oxygens and the acidic proton abstracted from the 1,3-diketone framework. This enol-keto tautomerization has been studied and shown to be dependent on the type of solvent used. In aprotic solvents, Cur exists mainly in the less electrophilic enolic form, which is 5 to 8 kcal/mol more stabilized than its more electrophilic keto form due to the higher extent of conjugation. In protic solvents, however, this intramolecular hydrogen bond is disrupted by the competition for hydrogen bonding from the solvent and the diketo group, consequentially resulting in the keto form being the predominant state of curcumin.[3e] Since the proportion of individual tautomers can be adjusted through the use of solvents, we envisioned that asymmetric hydrophosphination could serve as a means to produce C_2-symmetric *C*-chirogenic monophosphine and diphosphines in protic solvents by selectively favoring the more electrophilic diketo form.

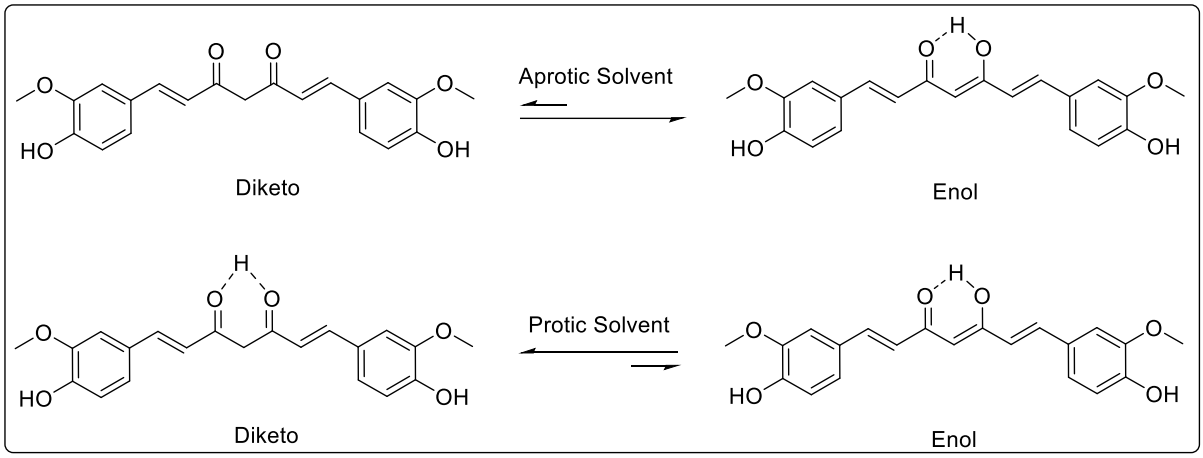

Figure 24. Enol-keto tautomerization of Cur in aprotic and protic solvents.

Our preliminary investigation involved the hydrophosphination of Cur with diphenylphosphine in the presence of catalyst **8** and base, diisopropylamine, in methanol. The aforementioned mixture furnished a mixture of monophosphine **17aa**, *C*-chiral diphosphine **17aa'** and *meso*-diphosphine **17aa"**. These air-sensitive products were subsequently sulfurized for purification and characterization. $^{31}P\{^{1}H\}$ NMR analysis revealed that chiral compound **17aa'** and *meso* compound **17aa"** existed in an approximately 1:1 ratio, with the optically active diphosphine species having good enantioselectivity of 71% *ee*. It is interesting to note that the poor diastereoselectivity of the reaction could be attributed to the poor enantioselectivity of the first hydrophosphination procedure, as observed by the 4% *ee* of the monophosphine **17aa**. It is also worth mentioning that there existed enol-keto tautomerization due to the presence of the diketo moiety in the three products. Due to the higher degree of conjugation in **17aa**, the enol form was favoured over the diketo form.

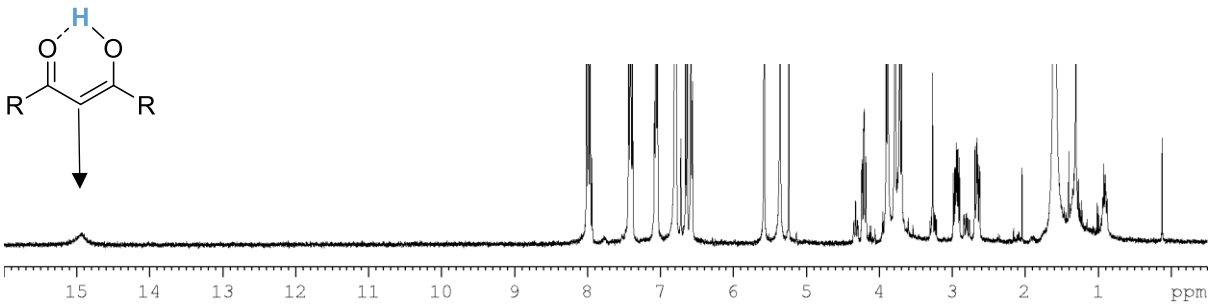

Figure 25. Characteristic signal of enolic proton in the ^{1}H NMR (CD_2Cl_2, 400 MHz) spectrum.

Firstly, solvent screening was conducted with a series of protic and aprotic solvents to determine their effects on the reactivity of curcumin and selectivity of the reaction. Due to the lengthy reaction time, all reactions were halted after 120 h. Expectedly, the major product produced when aprotic solvents were used was the monohydrophosphinated product while protic solvents afforded a mixture of three products. No reaction was observed in toluene (Table 3, entry 5) presumably due to the insolubility of Cur. Between the two protic solvents, methanol (Table 3, entry 1) offered a higher *ee* of 71% for the chiral diphosphine **17aa'** and an overall conversion of 90%, while ethanol (Table 3, entry 2) gave a diminished *ee* of 64% and an overall conversion of 83%. It is worth mentioning that the *ee* for the monohydrophosphinated product **17aa** was roughly 0%, implying that the selectivity of the dihydrophosphination reaction probably originated from the second hydrophosphination step due to the greater steric bulk of the monophosphine and consequently, affecting the diastereoselectivity of the reaction.

Table 3. Condition optimization for the asymmetric hydrophosphination of Cur.[a]

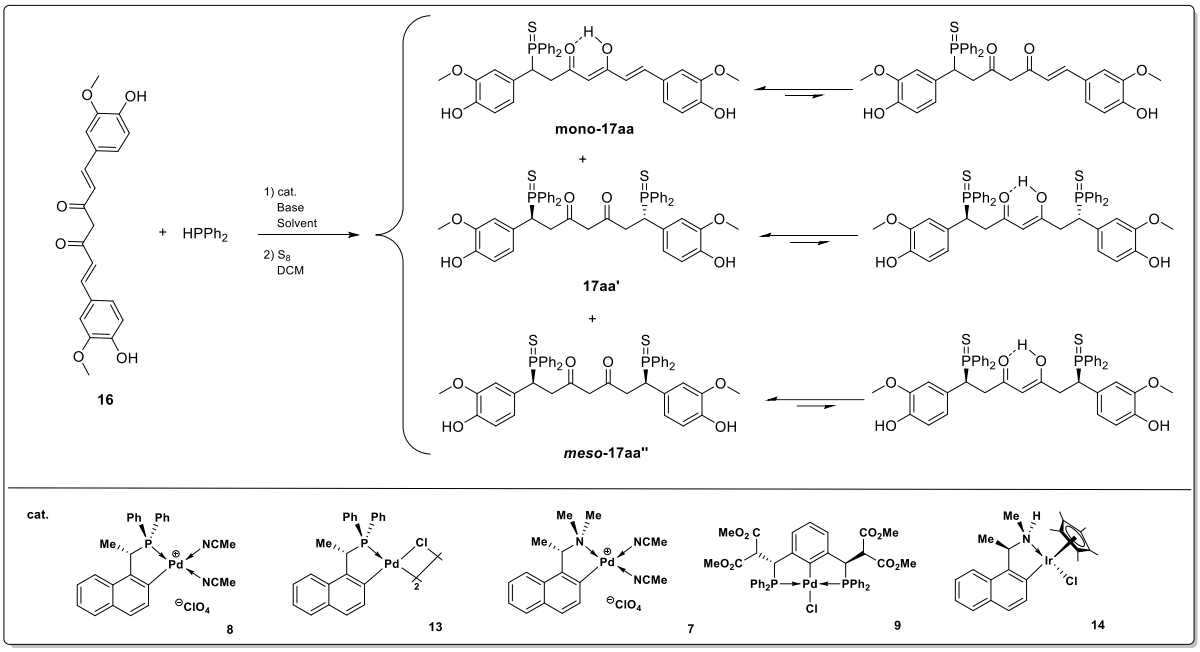

entry	*catalyst*	*cat. /mol%*	*base*	*Base/mol%*	*solvent*	*conversion (%)*[b]	*ee (%)*[c]
1	**8**	2	$^{i}Pr_2NH$	20	MeOH	90	71
2	**8**	2	$^{i}Pr_2NH$	20	EtOH	83	64
3	**8**	2	$^{i}Pr_2NH$	20	DCM	38[d]	n.d
4	**8**	2	$^{i}Pr_2NH$	20	MeCN	63[d]	n.d
5	**8**	2	$^{i}Pr_2NH$	20	Toluene	n.r	-
6	**8**	2	$^{i}Pr_2NH$	20	THF	n.r	-
7	**8**	2	NEt_3	20	MeOH	80	74
8	**8**	2	NaOAc	20	MeOH	88	71
9	**8**	2	DBU	20	MeOH	77	30
10	**8**	2	Cs_2CO_3	20	MeOH	64	65
11	**8**	2	CsF	20	MeOH	76	52
12	**8**	2	DIPEA	20	MeOH	81	66
13	**8**	1	NEt_3	20	MeOH	57	41

14	**8**	4	NEt_3	20	MeOH	85	79
15	**8**	2.5	NEt_3	20	MeOH	86	80
16	**8**	2.5	NEt_3	50	MeOH	80	66
17	**8**	2.5	NEt_3	100	MeOH	79	64
18	**13**	2.5	NEt_3	20	MeOH	83	52
19	**7**	2.5	NEt_3	20	MeOH	85	25
20	**9**	2.5	NEt_3	20	MeOH	78	34
21	**14**	2.5	NEt_3	20	MeOH	75	5
22[e]	**8**	2.5	NEt_3	20	MeOH	100	26
23[f]	**8**	2.5	NEt_3	20	MeOH	83	95

[a]Reactions were carried out with curcumin (0.14 mmol), diphenylphosphine (0.28 mmol), catalyst and base in the listed solvent (7.5 mL) at room temperature for 120 h. [b]Conversion was based on percentage of diphenylphosphine reacted. [c]Enantiomeric excess of chiral diphosphine determined by chiral HPLC. [d]Reaction furnished mostly monophosphine-**17aa**. [e]Reaction conducted at 50 °C for 60 h. [f]Reaction conducted at 0 °C for 120 h. *de* = 30%

Secondly, a range of organic and inorganic bases was investigated, and amongst them, triethylamine (Table 3, entry 7) gave an improved enantioselectivity of 74%, albeit a slightly poorer conversion, while sodium acetate (Table 3, entry 8) gave reactivity and selectivity results similar to that of diisopropylamine. Further fine-tuning of the catalyst and base loading (Table 3, entries 13-17) of the reaction was conducted. Increasing the catalyst loading to 2.5 mol% afforded improved selectivity with slight improvement in reaction rate (Table 3, entry 15). No significant change was observed to the overall conversion and with higher catalyst loading. Lastly, an increase in base loading resulted in a significant loss in enantioselectivity of the reaction.

Thirdly, catalysts[15] which were known to be active in asymmetric hydrophosphination reactions were screened. While there were no significant changes to the overall rate of reactions, the enantioselectivity of the reactions was the worst with iridacycle **14**. (Table 3, entry 21).

Finally, temperatures were adjusted in an attempt to shorten the reaction time. At 50°C, (Table 3, entry 22) the reaction time could be reduced successfully to 60 h as full conversion was attained but resulted in a significant drop in the *ee* to 26%. On the other hand, reducing the temperature to 0 °C led to only a slight decrease in conversion but a significant improvement in enantioselectivity of 95% (Table 3, entry 23). In addition, *ee* of the monophosphine-**17aa** was enhanced to 76%. Diastereoselectivity was also increased to 30%.

Table 4. Asymmetric dihydrophosphination reaction on different substrate scope.[a]

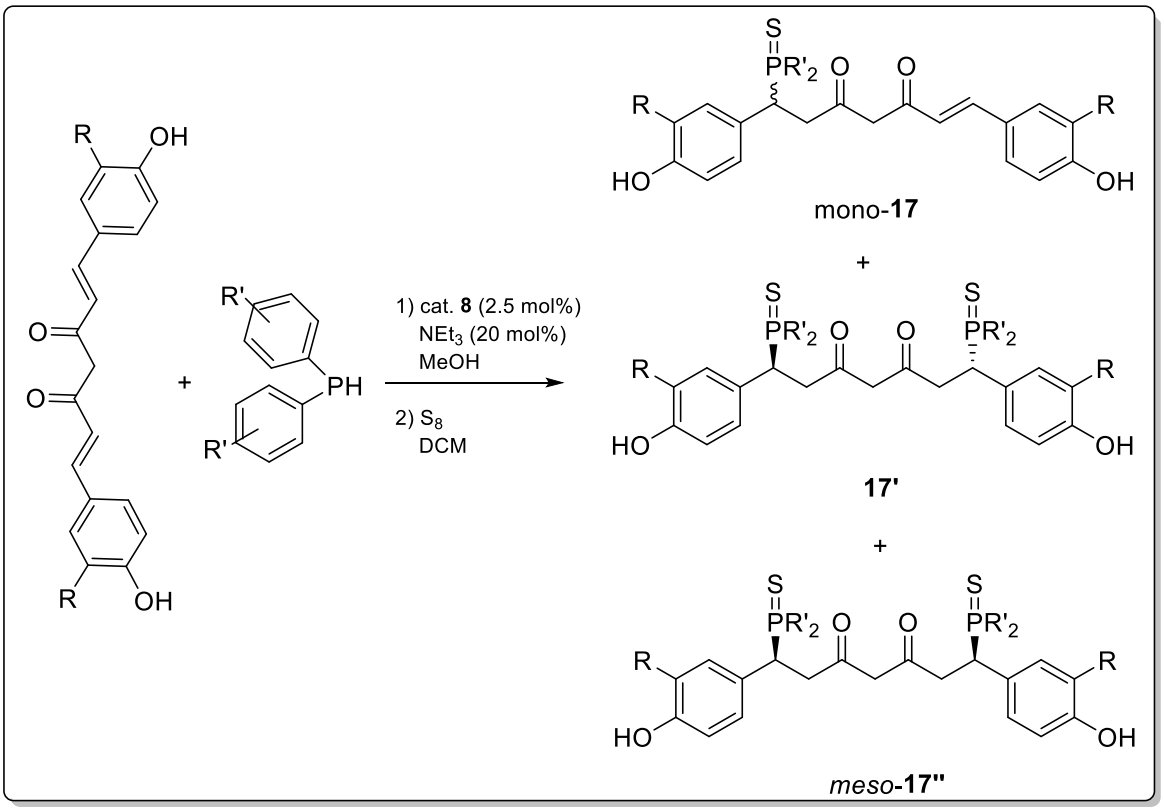

entry	Product	*R*	*R'*	*conversion (%)*[b]	*ee (%)*[c]
1	17ab	H	H	80	95
2	17ac	OMe	4-OMe	92	92
3	17ad	OMe	2-OMe	95	5
4	17ae	OMe	2-Me	17	2
5[d]	17af	OMe	3,5-CF_3	93	5
6	17ag	OMe	2,4,6-Me	n.r	-

[a]Reactions were carried out with secondary phosphine (0.14 mmol), Cur/BDMC (0.28 mmol), catalyst **8** (2 mol%) and NEt_3 (20 mol%) in dry MeOH (3 mL) at 0 °C for 120 h.

[b]Conversion based on amount of secondary phosphine reacted. [c]Determined by chiral HPLC. [d]Reaction conducted at room temperature for 288 h.

A variety of phosphine substrates and a curcumin derivative, BDMC, was surveyed for their tolerance for the optimized reaction conditions. (Table 4) As the biological application of interest in this article pertained to the biological roles the conjugation in pure curcumin and the phosphine-gold moieties played in anticancer therapies, partially hydrophosphinated curcumin and its derivatives, including the phosphine sulfides and phosphine-gold complexes, were not isolated and characterized. Asymmetric dihydrophosphination on BDMC provided comparable reactivity with excellent enantioenriched product at 95% *ee* (Table 4, entry 1). Conversions were enhanced when an electron-donating methoxy moiety was present in the secondary phosphines. However, methyl substituted secondary phosphine (Table 4, entry 4) required longer reaction time and tri-substituted aryl methyl group (Table 4, entry 6) did not furnish any products. This could be attributed to the increase in steric hindrance on the phosphine substrate. In addition, sterically demanding secondary phosphines greatly affected the selectivity of dihydrophosphination reaction, yielding close to 0% *ee* as compared to less sterically hindered bis(4-methoxyphenyl) phosphine (Table 4, entry 2), which produced an excellent *ee* of 92%.

In view of the promising results curcumin and phosphine gold complexes have on biological activities, we proceeded to extend our study of functionalized Cur to include Cur diphosphines gold complexes.[16] We subjected the solvated racemic diphosphines to two equivalents of $AuClSMe_2$. The reaction was able to generate the corresponding *rac*-**18aa** and *meso*-**18aa'**, which can be separated *via* simple column chromatography.

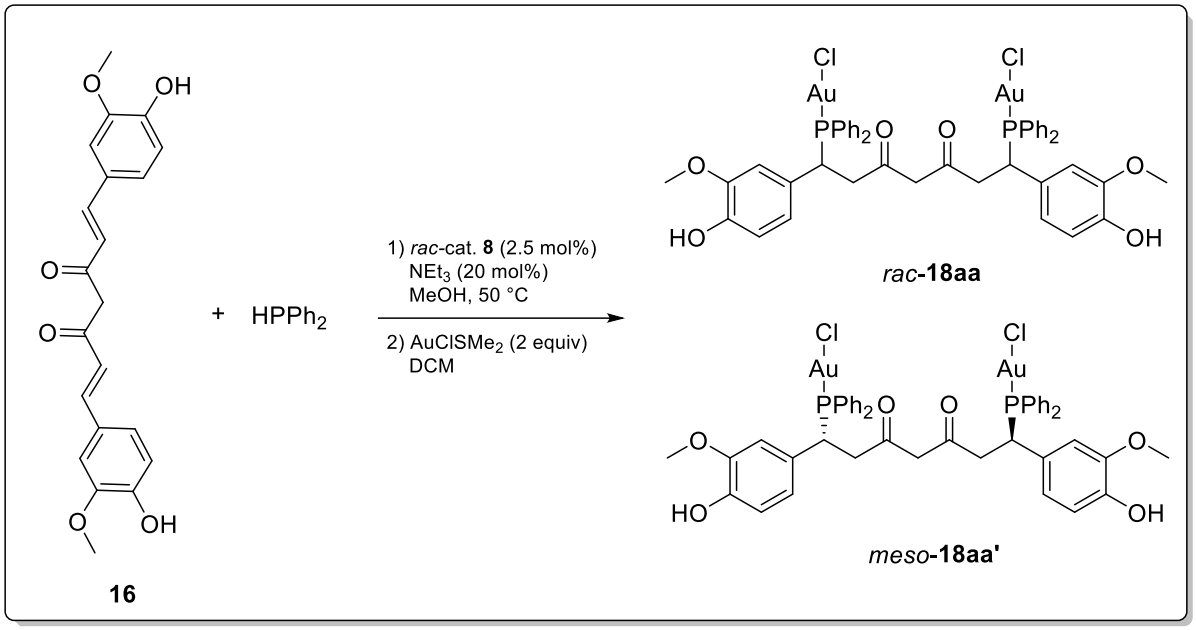

Scheme 43. Complexation of dihydrophosphinated-Cur with gold(I) complex.

3.2.3 Cancer Activity of Dihydrophosphinated Curcumin Gold(I) Complexes

Gold derivatives have been long used as drugs among the ancient Egyptians to treat pulmonary tuberculosis.[17] The development of the gold(I) phosphine complex, auranofin, shifted the attention of gold complexes to the treatment of rheumatoid arthritis.[18] Epidemiological study of patients being treated for rheumatoid arthritis using gold(I) drugs were observed to have lower anti-tumoral rate. This trend was similar to that of other anti-cancer drugs such as 6-mercaptopurine and cyclophosphamide,[16c] all of which spurred the rapid design and testing of gold(I) compounds for antitumor activity.

In some cases, free phosphines have been shown to exhibit antitumor activity and this has motivated the development of phosphine-gold complexes as anti-cancer drugs.[19] Studies have also shown that the main factors affecting patients' chemotherapy outcome are highly activated mitochondrial activity and the inactivity of mitochondrial inhibitors.[16b] In addition, mitochondrial functions are important to the survival of cancer cells.[20] Given that the

mechanism of action of gold(I)-phosphine complexes is based on their ability to selectively target mitochondria, these drugs provide an alternative towards anti-cancer research as selective anti-mitochondrial drugs. The direct coordination of gold(I) ion to the selenolate domain, found in the active site of the mitochondrial thioredoxin reductase, from the highly lipophilic neutral gold(I) complexes will help in the enhanced uptake of these drugs into the mitochondria. This will result in an increase in both the swelling and inner mitochondrial membrane potential (IMMP),[21] which then leads to cell apoptosis. Mitochondria consists primarily of two layers that are connected by the membrane permeability transition pore (PTP). PTP is controlled by the potential between the inner and outer membrane layers, and in situation where cells are exposed to cell death signal, the formation of reactive oxygen species and Bax/Bcl-2 ratio is increased to elevate the difference in potential between the inner and outer membranes, resulting in the increase in permeability of the outer membrane that allows the release of proteins responsible for programmed cell death. This mechanism is followed by the production of apoptotic protease activating factor (APAF-1) cell death complexes and the cell death signaling cascade, without affecting the surrounding tissues.[22]

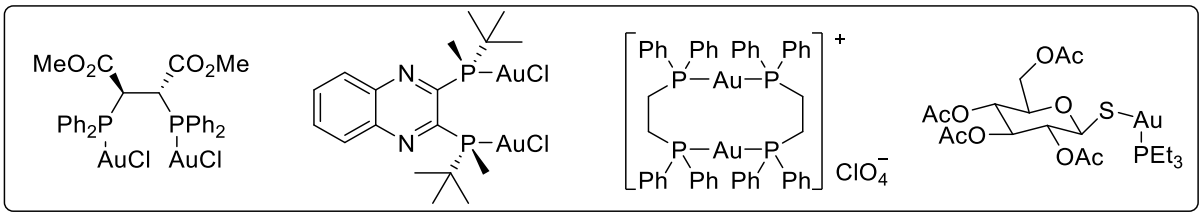

Figure 26. Examples of phosphine-gold(I) Complexes.

We examined the anti-cancer efficacies of the new dihydrophosphinated Cur gold complexes with curcumin using stomach (MKN74) and breast cancer (MCF7) cell lines at various timepoints. The well-established chemotherapy drug cisplatin was used as a reference positive control (Figures 27 and 28). Relative AUCs were calculated for the complexes across time and compared to cisplatin.

From Figure 27, by comparing the anti-cancer properties of the drugs at concentrations above 10^{-9} M, cisplatin fared the best in both the cancer cell lines and at all timepoints. *Rac*-**18aa** and *meso*-**18aa'** showed better anti-cancer properties against MKN74 at the 24h and 48h timelines and MCF7 at 24h timeline as compared to Cur. This implies that the phosphine gold moiety could have exerted some biological effects on the cancer cells.

From figure 28, after 24 hours of treatment, Cur was shown to be equally or more effective than cisplatin in reducing MKN74 and MCF7 cell viability. Such effects were negated after 40- to 72 hours. *Meso*-**18aa'** was comparable in efficacy to cisplatin against MKN74 cells at the 24 hours timepoint and begun to diminish after prolong incubation. *Meso*-**18aa'** was less effective against MCF7 when compared with cisplatin. The *rac*-**18aa** was the least effective among the examined compound when compared with cisplatin.

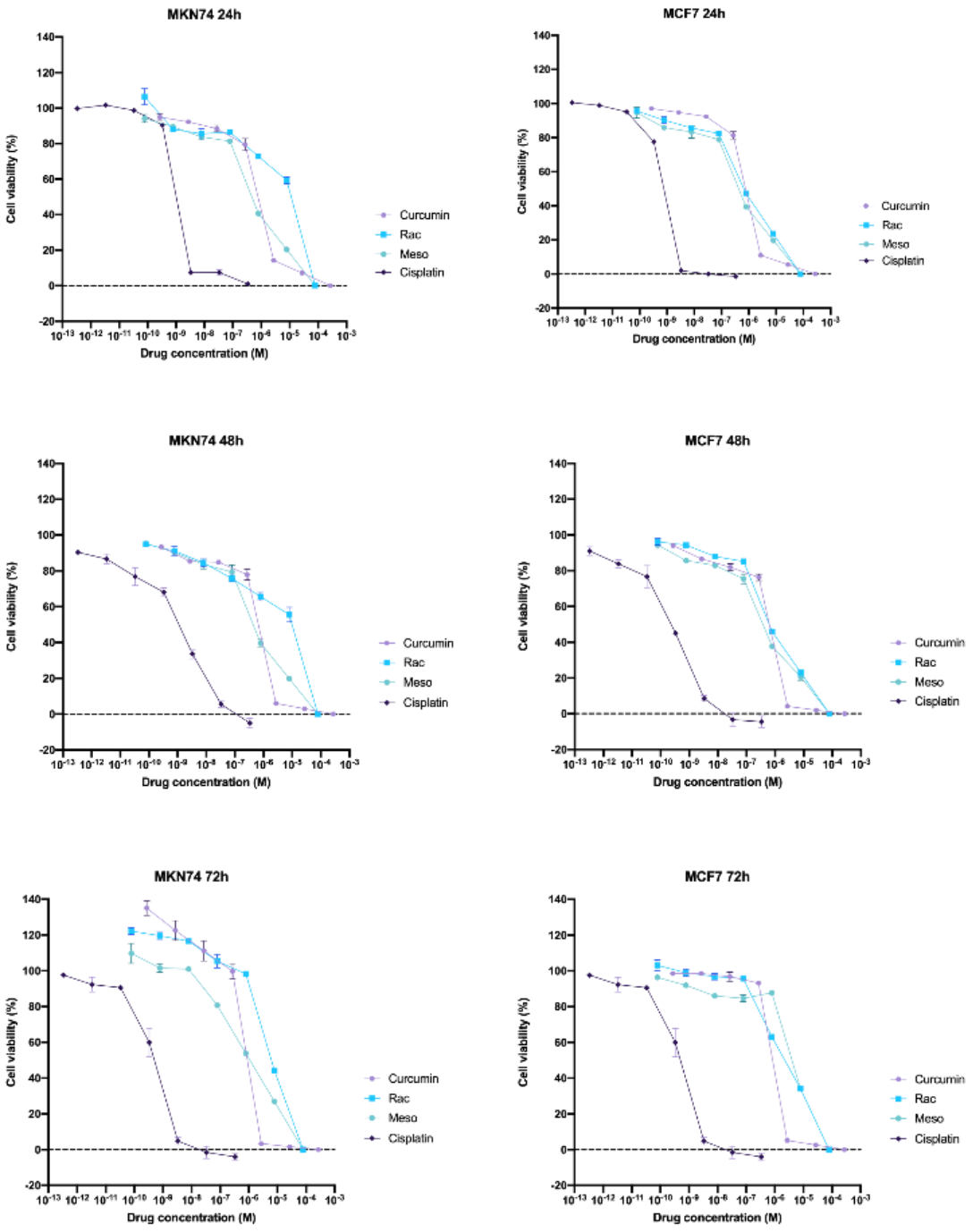

Figure 27. Measured cell viability (%) of MKN74 and MCF7 cultured cancer cells normalized to untreated group upon exposure to different drug compounds. Compound labels read: Rac(*rac*-**18aa**), Meso(*meso*-**18aa'**).

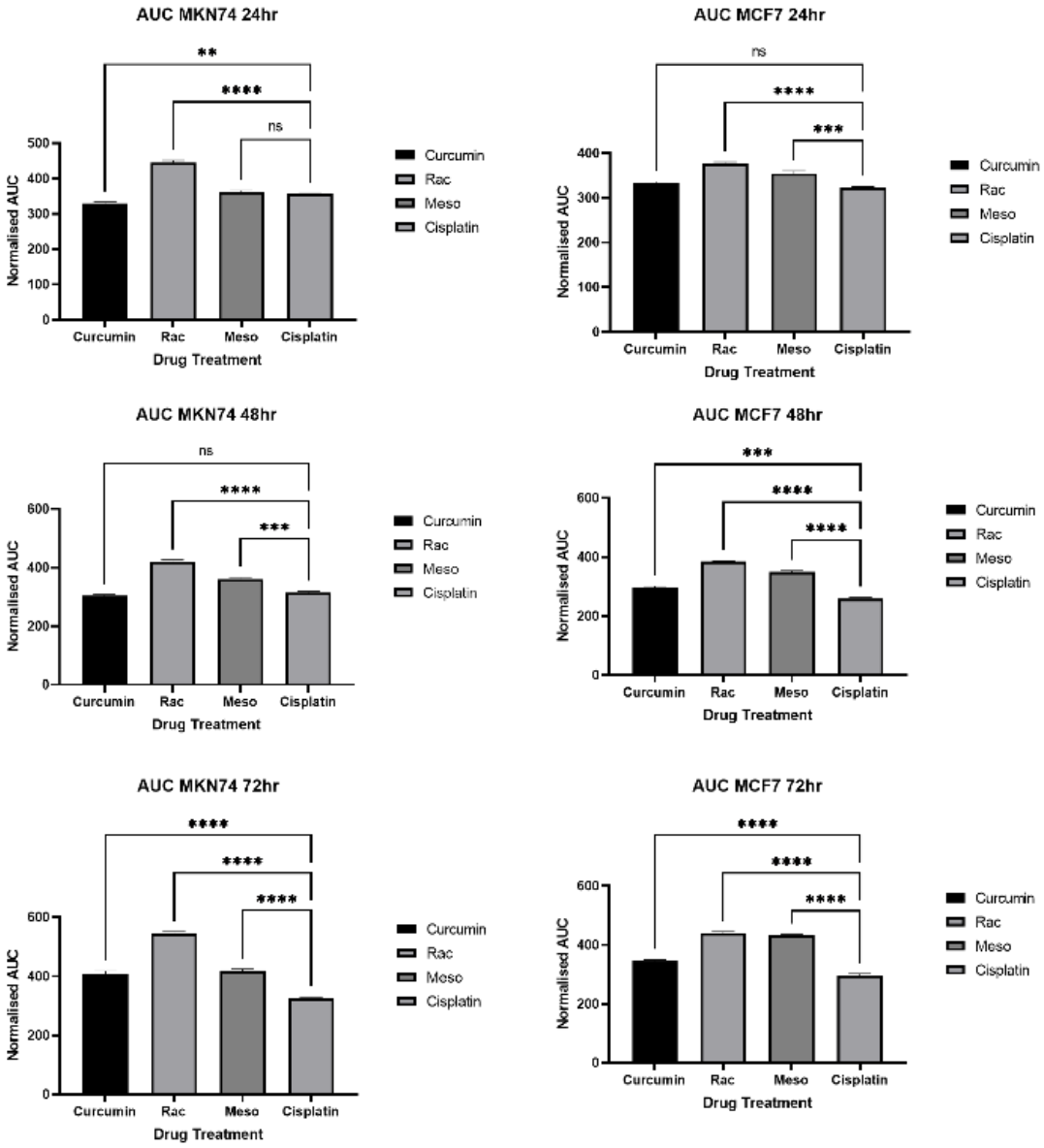

Figure 28. Normalized area under curve (AUC) of various drug compounds contrasted against cisplatin. Compound labels read: Rac(*rac*-**18aa**), Meso(*meso*-**18aa'**)

3.3 Conclusion

In conclusion, catalytic asymmetric hydrophosphination has proven to be a viable tool to access dihydrophosphinated Cur and its derivatives with excellent enantioselectivites of up to 95% *ee*. Gold(I) complexes of the dihydrophosphinated Cur were successfully prepared *in-situ* and their efficacies as anticancer drugs were evaluated using the MKN74 and MCF7 cell-lines.

3.4 Experimental

Optimization of Procedure for the Catalytic Asymmetric Dihydrophosphination of Curcumin, 17aa' and 17aa". To a degassed solution (7.5 mL) of diphenylphosphine (52.1 mg, 0.28 mmol) was added catalyst. The mixture was subsequently cooled to the listed temperature prior to addition of curcumin (51.6 mg, 0.14 mmol) and base. The reaction mixture was then stirred at the same temperature for 120 h. S_8 (9.92 mg, 0.31 mmol) was added to the crude mixture and stirred at ambient temperature for 2 h. The solution was purified directly by column chromatography on silica gel with 199:1 dichloromethane/MeOH as the eluent to provide the products.

General Procedure for the Catalytic Asymmetric Dihydrophosphination Reaction, 17' and 17". Catalyst **8** (2.51 mg, 2.5 mol%) was added to a solution of secondary phosphines (0.16 mmol) in dry and degassed MeOH (7.5 mL). The mixture was subsequently cooled to 0 °C before the addition of substrate **16** (0.08 mmol) and NEt_3 (4.46 mg, 20 mol%). The reaction mixture was then stirred for 120 h. S_8 (5.76 mg, 0.18 mmol) was added to the crude mixture and stirred until the reaction completed. The solution was purified directly by preparatory thin layer chromatography (PTLC) to provide the products.

Secondary Phosphine: Diphenylphosphine

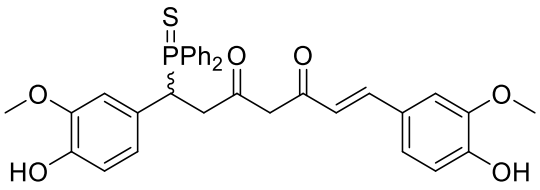

17aa

Yellow Solid; Eluent system (PTLC): DCM/MeOH (199:1); Yield: 3.75 mg (4%); $[\alpha]_D$ (22 °C) = -82.1°; ^{1}H NMR (400 MHz, CD_2Cl_2): δ 2.90 (ddd, 1H, J_{HH} = 16.2 Hz, J_{HP} = 10.7 Hz, J_{HH} = 3.1 Hz, PCHC*H*HCO), 3.24 (ddd, 1H, J_{HH} = 16.1 Hz, J_{HH} = 11.0 Hz, J_{HP} = 6.9 Hz, PC*H*CH$_2$), 3.68 (s, 3H, C*H*$_3$OAr), 3.91 (s, 3H, C*H*$_3$OAr), 4.56 (ddd, 1H, J_{HH} = 10.4 Hz, J_{HP} = 10.2 Hz, J_{HH} = 2.7 Hz, PCHC*H*HCO), 5.50 (s, 1H, O*H*), 5.51 (s, 1H, O*H*), 5.93 (s, 1H, COC*H*CO), 6.23 (d, 1H, J_{HH} = 15.8 Hz, COCHC*H*), 6.63-6.88 (m, 4H, Ar*H*), 7.02-7.04 (m, 2H, Ar*H*), 7.26-7.38 (m, 3H, Ar*H*), 7.48 (d, 1H, J_{HH} = 15.8 Hz, COC*H*CH), 7.53-7.58 (m, 5H, Ar*H*), 8.13-8.18 (m, 2H, Ar*H*), 15.02 (bs, 1H, O*H*O); ^{13}C{^{1}H} NMR (100 MHz, CD_2Cl_2): 41.16 (s, CH$_2$*C*H$_2$CO), 42.08 (s, *C*H$_3$), 42.01 (s, *C*H$_3$), 56.38 (d, J_{CP} = 11.0 Hz, *C*H$_2$P), 101.53 (s, CO*C*H$_2$CO), 109.84 (s, Ar*C*), 113.09 (d, J_{CP} = 4.7 Hz, Ar*C*), 113.86 (d, J_{CP} = 3.4 Hz, Ar*C*), 114.99 (s, Ar*C*), 120.09 (s, Ar*C*), 123.19 (s, Ar*C*), 123.24 (s, Ar*C*), 126.62 (d, J_{CP} = 3.7 Hz, Ar*C*), 127.98 (s, *C*HCH), 128.37 (d, J_{CP} = 12.0 Hz, Ar*C*), 129.23 (d, J_{CP} = 11.5 Hz, Ar*C*), 131.63 (d, J_{CP} = 2.4 Hz, Ar*C*), 132.02 (d, J_{CP} = 9.5 Hz, Ar*C*), 132.31 (d, J_{CP} = 9.3 Hz, Ar*C*), 140.47 (s, *C*HCH), 145.50 (d, J_{CP} = 3.0 Hz, Ar*C*), 146.32 (s, Ar*C*), 146.34 (s, Ar*C*) 147.38 (s, Ar*C*), 148.35 (s, Ar*C*), 153.04 (s, Ar*C*), 156.85 (s, *C*O), 197.92 (d, J_{CP} = 15.4 Hz, *C*O); ^{31}P{^{1}H} NMR (161 MHz, CD_2Cl_2): δ 50.82; HRMS (ESI)m/z[positive mode] calcd. for C33H32O6PS 587.1657, found 587.1657.

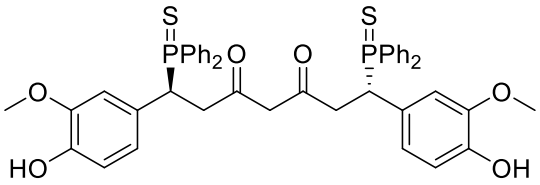

***chiral*-17aa'**

White Solid; Eluent system (PTLC): DCM/MeOH (199:1); Yield: 48.9 mg (38%); $[\alpha]_D$ (22 °C) = -50.8°; ^{1}H NMR (400 MHz, CD_2Cl_2): δ 2.67 (ddd, 1H, J_{HH} = 15.7 Hz, J_{HP} = 10.0 Hz, J_{HH} = 3.2 Hz, PCHC*H*HCO), 2.95 (ddd, 1H, J_{HH} = 15.8 Hz, J_{HH} = 11.2 Hz, J_{HP} = 7.1 Hz, PC*H*CH$_2$CO), 3.65 (s, 6H, C*H*$_3$OAr), 4.31 (ddd, 1H, J_{HH} = 10.6 Hz, J_{HP} = 10.6 Hz, J_{HH} = 3.1 Hz, PCHC*H*HCO), 5.53 (s, 2H, O*H*), 6.55-6.61 (m, 4H, Ar*H*), 6.73 (s, 2H, COC*H*$_2$CO), 7.23-7.55 (m, 18H, Ar*H*), 8.03-8.08 (m, 4H Ar*H*); ^{13}C{^{1}H} NMR (100 MHz, CD_2Cl_2): δ 39.05 (d, J = 3.9 Hz, *C*H$_2$P), 42.35 (s, CH$_2$*C*H$_2$CO), 42.87 (s, *C*H$_3$), 56.03 (s, CO*C*H$_2$CO), 102.12 (s, Ar*C*), 112.82 (d, J = 4.7 Hz, Ar*C*), 113.80 (d, J = 2.3 Hz, Ar*C*), 123.22 (d, J = 6.1 Hz, Ar*C*), 126.08 (d, J = 4.6 Hz, Ar*C*), 128.35 (d, J = 12.0 Hz, Ar*C*), 129.18 (d, J = 11.5 Hz, Ar*C*), 130.88 (s), 131.35 (s, Ar*C*), 131.64 (s, Ar*C*), 131.94 (d, J = 9.8 Hz, Ar*C*), 132.17 (d, J = 9.1 Hz, Ar*C*), 145.51 (d, J = 3.1 Hz, Ar*C*), 146.31 (d, J = 2.5 Hz, Ar*C*) 190.84 (d, J = 15.7 Hz, *C*O); ^{31}P{^{1}H} NMR (161 MHz, CD_2Cl_2): δ 50.55; HRMS (ESI)m/z[positive mode] calcd. for $C_{45}H_{43}O_6P_2S_2$ 805.1976, found 805.1976.

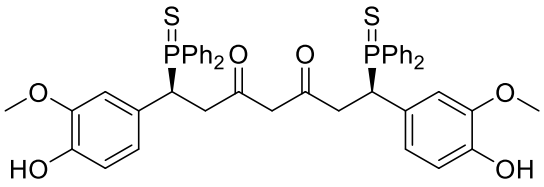

***meso*-17aa"**

White Solid; Eluent system (PTLC): DCM/MeOH (199:1); Yield: 30.9 mg (24%); ^{1}H NMR (400 MHz, CD_2Cl_2): δ 2.69 (ddd, 1H, J_{HH} = 15.8 Hz, J_{HP} = 10.0 Hz, J_{HH} = 3.5 Hz,

PCHC*H*HCO), 2.92 (ddd, 1H, J_{HH} = 15.8 Hz, J_{HH} = 10.8 Hz, J_{HP} = 7.7 Hz, PC*H*CH_2CO), 3.61 (s, 6H, CH_3OAr), 4.31 (ddd, 1H, J_{HH} = 10.5 Hz, J_{HP} = 10.5 Hz, J_{HH} = 3.4 Hz, PCHC*H*HCO), 5.59 (s, 2H, O*H*), 6.52-6.58 (m, 4H, Ar*H*), 6.68 (s, 2H, COCH_2CO), 7.23-7.37 (m, 7H, Ar*H*), 7.46-7.56 (m, 11H, Ar*H*) 8.05-8.10 (m, 4H Ar*H*); $^{13}C\{^1H\}$ NMR (100 MHz, CD_2Cl_2): δ 39.08 (d, J = 3.5 Hz, *C*H_2P), 42.29 (s, CH_2*C*H_2CO). 42.81 (s, *C*H_3), 56.22 (s, CO*C*H_2CO), 102.22 (s, Ar*C*), 112.71 (d, J = 4.7 Hz, Ar*C*), 113.89 (d, J = 2.7 Hz, Ar*C*), 123.08 (d, J = 6.1 Hz, Ar*C*), 126.10 (d, J = 4.6 Hz, Ar*C*), 128.35 (d, J = 11.7 Hz, Ar*C*), 129.16 (d, J = 11.5 Hz, Ar*C*) 131.00 (s, Ar*C*), 131.35 (s, Ar*C*), 131.63 (d, J = 3.2 Hz, Ar*C*), 131.95 (d, J = 9.9 Hz, Ar*C*), 132.23 (d, J = 9.4 Hz, Ar*C*), 146.44 (d, J = 3.0 Hz, Ar*C*), 146.32 (d, J = 2.4 Hz, Ar*C*), 190.80 (d, J = 15.4 Hz, *C*O); $^{31}P\{^1H\}$ NMR (161 MHz, CD_2Cl_2): δ 50.52; HRMS (ESI)m/z[positive mode] calcd. for $C_{45}H_{43}O_6P_2S_2$ 805.1976, found 805.1976.

Olefinic Substrate: bisdimethoxycurcumin

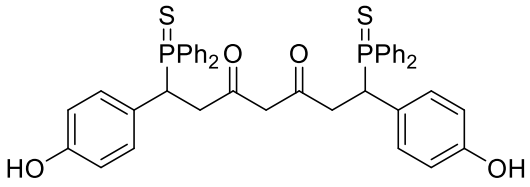

17ab'/17ab" (reported as an inseparable diastereomeric mixture)

White Solid; Eluent system (PTLC): Chloroform/MeOH (400:1) (*provides pure chiral*-**17ab** */ meso*-**17ab"** *mixture*); ^1H NMR (400 MHz, CD_2Cl_2): δ 1.66 (bs, -O*H*), 2.57-2.71 (m, -C*H*H-), 2.86-2.97 (m, -C*H*H-), 3.16-3.25 (m, -C*H*H-), 4.28-4.43 (m, -C*H*H-), 6.48-8.08 (m, Ar*H*); $^{31}P\{^1H\}$ NMR (161 MHz, CD_2Cl_2): δ 50.18, 50.46; HRMS (ESI) *m/z* [*positive mode*] calcd. for $C_{43}H_{39}O_4P_2S_2$ 745.1765, found 745.1765.

Secondary Phosphine: bis(4-methoxyphenyl)phosphine

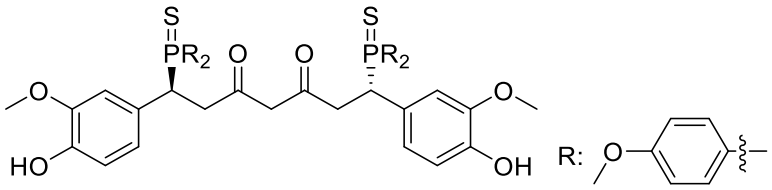

17ac'

White Solid; Eluent system (PTLC): DCM/MeOH (199:1); Yield: 39.6 mg (41%); $[\alpha]_D$ (22 °C) = -105.8°; ^{1}H NMR (400 MHz, CD_2Cl_2): δ 2.62 (ddd, 2H, J_{HH} = 15.7 Hz, J_{HP} = 9.8 Hz, J_{HH} = 3.1 Hz, PCHC*H*HCO), 2.90 (ddd, 2H, J_{HH} = 15.7 Hz, J_{HH} = 11.4 Hz, J_{HP} = 6.7 Hz, PC*H*CH_2CO), 3.68 (s, 6H, C*H*$_3$OAr), 3.74 (s, 6H, C*H*$_3$OAr), 3.84 (s, 6H, C*H*$_3$OAr), 4.17 (ddd, 2H, J_{HH} = 10.8 Hz, J_{HP} = 10.6 Hz, J_{HH} = 3.0 Hz, PCHC*H*HCO), 5.54 (s, 2H, O*H*), 6.52-6.55 (m, 2H, Ar*H*), 6.59 (s, 1H, COC*H*$_2$CO), 6.61 (s, 1H, COC*H*$_2$CO), 6.74-6.77 (m, 7H, Ar*H*), 7.00-7.02 (m, 4H Ar*H*), 7.35-7.40 (m, 5H Ar*H*), 7.92-7.97 (m, 4H Ar*H*); ^{13}C{^{1}H} NMR (100 MHz, CD_2Cl_2): δ 39.07 (d, J_{CP} = 3.3 Hz, *C*H_2P), 43.10 (s, CH_2*C*H_2CO), 43.63 (s, *C*H$_3$), 55.72 (s, *C*H$_3$), 55.88 (s, *C*H$_3$), 56.30 (s, CO*C*H_2CO), 102.08 (s, Ar*C*), 112.80 (d, J_{CP} = 4.3, Ar*C*), 113.80 (d, J_{CP} = 13.0, Ar*C*), 114.67 (d, J_{CP} = 12.5, Ar*C*), 121.84 (s, Ar*C*), 122.68 (d, J_{CP} = 3.9, Ar*C*), 123.24 (d, J_{CP} = 6.1, Ar*C*), 126.44 (d, J_{CP} = 4.8, Ar*C*), 133.77 (d, J_{CP} = 11.2, Ar*C*), 133.99 (d, J_{CP} = 10.4, Ar*C*), 145.43 (d, J_{CP} = 3.0, Ar*C*), 146.31 (d, J_{CP} = 2.1, Ar*C*), 162.43 (d, J_{CP} = 2.4, Ar*C*), 162.88 (d, J_{CP} = 2.4, Ar*C*), 191.17 (d, J_{CP} = 16.2, *C*O); ^{31}P{^{1}H} NMR (161 MHz, CD_2Cl_2): δ 49.03; HRMS (ESI)m/z[positive mode] calcd. for $C_{49}H_{51}O_{10}P_2S_2$ 925.2399, found 925.2399.

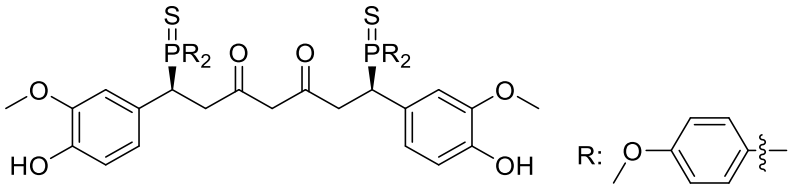

17ac”

White Solid; Eluent system (PTLC): DCM/MeOH (199:1); Yield: 21.2 mg (22%); ^{1}H NMR (400 MHz, CD_2Cl_2): δ 2.66 (ddd, 2H, J_{HH} = 15.7 Hz, J_{HP} = 10.1 Hz, J_{HH} = 3.4 Hz, PCHC*H*HCO), 2.87 (ddd, 2H, J_{HH} = 15.8 Hz, J_{HH} = 11.0 Hz, J_{HP} = 7.6 Hz, PC*H*CH_2CO), 3.64 (s, 6H, CH_3OAr), 3.74 (s, 6H, CH_3OAr), 3.84 (s, 6H, CH_3OAr), 4.17 (ddd, 2H, J_{HH} = 10.7 Hz, J_{HP} = 10.6 Hz, J_{HH} = 3.0 Hz, PCHC*H*HCO), 5.57 (s, 2H, O*H*), 6.49-6.52 (m, 2H, Ar*H*), 6.59 (s, 1H, COCH_2CO), 6.61 (s, 1H, COCH_2CO), 6.74-6.77 (m, 7H, Ar*H*), 7.00-7.02 (m, 4H Ar*H*), 7.35-7.40 (m, 5H Ar*H*), 7.92-7.97 (m, 4H Ar*H*); ^{13}C{^{1}H} NMR (100 MHz, CD_2Cl_2): δ 39.13 (d, J_{CP} = 4.1 Hz, *C*H_2P), 43.02 (s, CH_2*C*H_2CO), 43.55 (s, *C*H_3), 55.73 (s, *C*H_3), 55.88 (s, *C*H_3), 56.23 (s, CO*C*H_2CO), 102.14 (s, Ar*C*), 112.70 (d, J_{CP} = 4.6, Ar*C*), 113.80 (d, J_{CP} = 13.0, Ar*C*), 114.62 (d, J_{CP} = 12.6, Ar*C*), 121.91 (s, Ar*C*), 122.71 (d, J_{CP} = 2.2, Ar*C*), 123.11 (d, J_{CP} = 6.1, Ar*C*), 126.50 (d, J_{CP} = 4.6, Ar*C*), 133.78 (d, J_{CP} = 11.0, Ar*C*), 134.60 (d, J_{CP} = 10.4, Ar*C*), 145.37 (d, J_{CP} = 3.1, Ar*C*), 146.32 (d, J_{CP} = 2.5, Ar*C*), 162.42 (d, J_{CP} = 2.6, Ar*C*), 162.87 (d, J_{CP} = 3.1, Ar*C*), 191.13 (d, J_{CP} = 15.6, *C*O); ^{31}P{^{1}H} NMR (161 MHz, CD_2Cl_2): δ 49.04; HRMS (ESI)m/z[positive mode] calcd. for $C_{49}H_{51}O_{10}P_2S_2$ 925.2399, found 925.2413.

Secondary Phosphine: bis(2-methoxyphenyl)phosphine

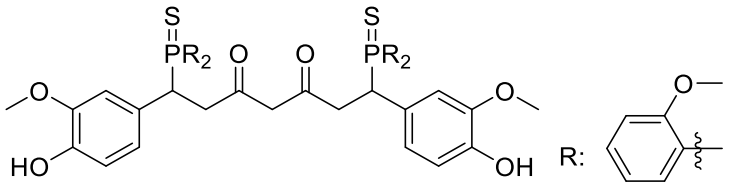

2ad'/2ad" (reported as an inseparable diastereomeric mixture)

White Solid; Eluent system (PTLC): DCM/MeOH (199:1) (*provides pure chiral*-**2ad** / *meso*-**2ad"** *mixture*); ^{1}H NMR (400 MHz, CD_2Cl_2): δ 3.12-3.19 (m, -C*H*-), 3.53-3.60 (m, -C*H*-), 3.63 (s, -CH_3-), 3.65-3.69 ((m, -CH_2-), 3.67 (s, -CH_3-), 3.69 (s, -CH_3-), 3.74 (s, -CH_3-), 4.28-4.43 (m, -CH_2-), 6.44-7.89 (m, Ar*H*); ^{31}P{^{1}H} NMR (161 MHz, CD_2Cl_2): δ 50.18, 50.46; HRMS (ESI) *m*/*z* [*positive mode*] calcd. for $C_{49}H_{51}O_{10}P_2S_2$ 925.2399, found 925.2399.

Secondary Phosphine: bis(2-methylphenyl)phosphine

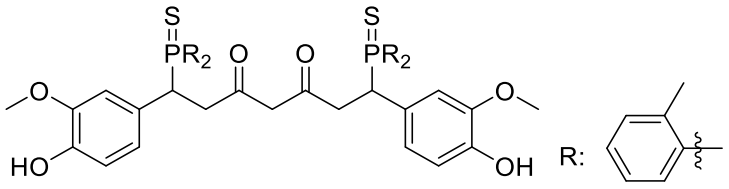

17ae'/17ae" (reported as an inseparable diastereomeric mixture)

White Solid; Eluent system (PTLC): DCM/Hex/MeOH (99.5:99.5:1) (*provides pure chiral*-**17ae** / *meso*-**17ae"** *mixture*); ^{1}H NMR (400 MHz, CD_2Cl_2): δ 1.92 (s, -CH_3-), 1.94 (s, -CH_3-), 2.10 (s, -CH_3-), 3.19-3.24 (m, -C*H*-), 3.65 (s, -CH_3-), 3.68 (s, -CH_3-), 3.71 (s, -CH_3-), 4.52-4.68 ((m, -CH_2-), 5.37 (s, -O*H*-), 6.42-8.02 (m, Ar*H*); ^{31}P{^{1}H} NMR (161 MHz, CD_2Cl_2): δ 47.15 (overlap of two signals); HRMS (ESI) *m*/*z* [*positive mode*] calcd. for $C_{49}H_{51}O_6P_2S_2$ 861.2602, found 861.2602.

Secondary Phosphine: bis(3,5-trifluoromethylphenyl)phosphine

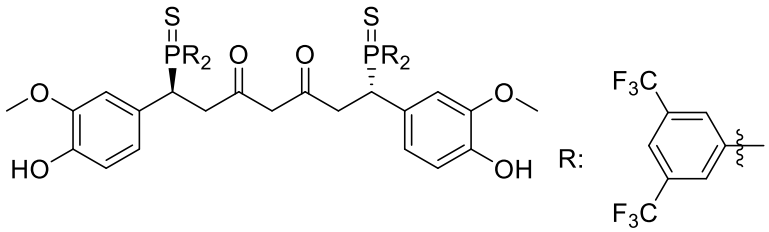

17af'

White Solid; Eluent system (PTLC): DCM/Hex/MeOH (70:30:0.5); Yield: 26.1 mg (23%); $[\alpha]_D$ (23 °C) = 0.4°; ^{1}H NMR (400 MHz, CD_2Cl_2): δ 2.77 (ddd, 2H, J_{HH} = 16.3 Hz, J_{HP} = 12.6 Hz, J_{HH} = 4.0 Hz, PCHC*H*HCO), 2.87-2.98 (m, 2H, PC*H*CH_2CO), 3.73 (s, 6H, C*H*$_3$OAr), 4.47 (ddd, 2H, J_{HH} = 9.4 Hz, J_{HP} = 9.4 Hz, J_{HH} = 4.2 Hz, PCHC*H*HCO), 5.61 (s, 2H, O*H*), 6.63-6.68 (m, 5H, Ar*H*), 6.79 (s, 2H, COC*H*$_2$CO), 7.85-7.91 (m, 7H, Ar*H*), 8.08-8.16 (m, 2H Ar*H*), 8.55 (d, 4H, J_{HH} = 11.6 Hz, Ar*H*); ^{13}C{^{1}H} NMR (100 MHz, CD_2Cl_2): δ 39.44 (d, J_{CP} = 3.9 Hz, *C*H_2P), 41.94 (s, CH_2*C*H_2CO), 42.47 (s, *C*H_3), 56.30 (s, CO*C*H_2CO), 102.12 (s, Ar*C*), 112.24 (d, J_{CP} = 4.5 Hz, Ar*C*), 114.55 (d, J_{CP} = 2.1 Hz, Ar*C*), 121.77 (d, J_{CP} = 14.1 Hz, Ar*C*), 123.06 (d, J_{CP} = 6.9 Hz, Ar*C*), 124.56 (d, J_{CF} = 28.4 Hz, *C*H_3), 124.65 (d, J_{CF} = 20.6 Hz, *C*H_3), 126.00 (d, J_{CP} = 3.2 Hz, Ar*C*), 126.76 (d, J_{CP} = 7.8 Hz, Ar*C*), 131.80 (d, J_{CP} = 12.0 Hz, Ar*C*), 132.52 (d, J_{CP} = 10.3 Hz, Ar*C*), 133.16 (d, J_{CF} = 189.9 Hz, *C*H_3), 133.52 (s, Ar*C*), 133.97 (d, J_{CF} = 189.5 Hz, *C*H_3), 134.24 (s, Ar*C*), 146.46 (d, J_{CP} = 2.7, Ar*C*), 146.96 (d, J_{CP} = 1.9, Ar*C*), 189.50 (d, J_{CP} = 13.7, *C*O); ^{31}P{^{1}H} NMR (161 MHz, CD_2Cl_2): δ 49.44; ^{19}F NMR (376 MHz, CD_2Cl_2) δ -63.47, -63.24; HRMS (ESI) m/z [positive mode] calcd. for $C_{53}H_{35}F_{24}O_6P_2S_2$ 1349.0967, found 1349.1034.

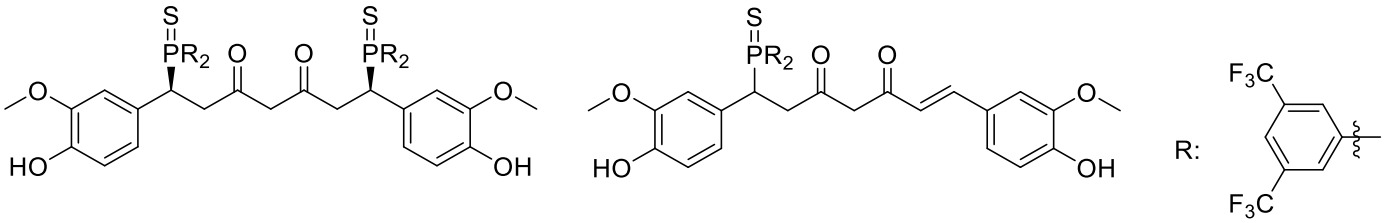

17af/17af" (reported as an inseparable mixture with mono product)

Yellowish white Solid; Eluent system (PTLC): DCM/Hex/MeOH (70:30:0.5) (*provides pure mono*-**2af** and *meso*-**2af"** / *mixture*); ^{1}H **NMR** (400 MHz, CD_2Cl_2): ^{1}H NMR (400 MHz, CD_2Cl_2): δ 2.74 (ddd, 2H, J_{HH} = 16.2 Hz, J_{HP} = 11.9 Hz, J_{HH} = 4.4 Hz, PCHC*H*HCO), 2.88-2.97 (m, 2H, PC*H*CH_2CO), 3.69 (s, 6H, CH_3OAr), 4.42-4.48 (m, 2H, PCHC*H*HCO), 5.64 (s, 2H, O*H*), 6.60-6.75 (m, 7H, Ar*H*, COCH_2CO), 7.86-7.91 (m, 7H, Ar*H*), 8.10-8.12 (m, 2H Ar*H*), 8.57 (d, 4H, J_{HH} = 11.6 Hz, Ar*H*); ^{31}P{^{1}H} NMR (161 MHz, CD_2Cl_2): δ 49.14 (*meso*); ^{19}F NMR (376 MHz, CD_2Cl_2) δ -63.48, -63.33; HRMS (ESI) *m*/*z* [*positive mode*] calcd. for $C_{53}H_{35}F_{24}O_6P_2S_2$ 1349.0967, found 1349.1006, $C_{37}H_{28}F_{12}O_6PS$ 859.1153, found 859.1172.

One-Pot Direct Dihydrophosphination-Complexation of Diphosphines, 18aa and 18aa'. To a degassed solution (7.5 mL) of diphenylphosphine (52.1 mg, 0.28 mmol) was added *rac*-catalyst **C1**. Curcumin (51.6 mg, 0.14 mmol) and NEt_3 (5.7 mg, 0.056 mmol) were subsequently added into the reaction mixture. The reaction mixture was then stirred at the 50 °C for 48 h. $AuClSMe_2$ (82.5 mg, 0.28 mmol) was added to the crude mixture and stirred at ambient temperature for 8 h. The solution was purified directly by column chromatography on silica gel with 99:1 dichloromethane/ethyl acetate as the eluent to provide the products.

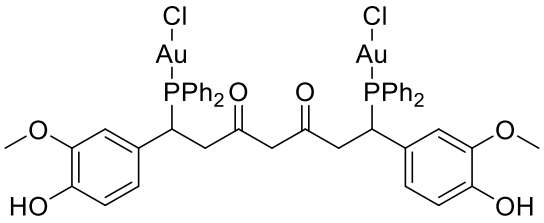

rac-**18aa**

White Solid; Eluent system (column chromatography): DCM/EA (99:1); Yield: 141.8 mg (42%); ^{1}H NMR (400 MHz, CD_2Cl_2): δ 2.72 (ddd, 2H, J_{HH} = 15.6 Hz, J_{HP} = 10.2 Hz, J_{HH} = 3.5 Hz, PCHC*H*HCO), 2.97 (ddd, 2H, J_{HH} = 15.7 Hz, J_{HP} = 11.0 Hz, J_{HH} = 8.6 Hz, PC*H*CH$_2$CO), 3.77 (s, 6H, C*H*$_3$OAr), 4.28 (ddd, 2H, J_{HH} = 12.7 Hz, J_{HP} = 12.7 Hz, J_{HH} = 3.4 Hz, PCHC*H*HCO), 5.63 (s, 2H, O*H*), 6.50-6.54 (m, 2H, Ar*H*), 6.61 (s, 1H, COC*H*$_2$CO), 6.63 (s, 1H, COC*H*$_2$CO), 6.80-6.87 (m, 2H, Ar*H*), 7.27-7.41 (m, 11H Ar*H*), 7.50-7.62 (m, 7H, Ar*H*), 7.87-7.94 (m, 4H, Ar*H*); ^{13}C{^{1}H} NMR (100 MHz, CD_2Cl_2): δ 40.40 (t, J_{CP} = 5.4 Hz, *C*H$_2$P), 40.76 (s, CH$_2$*C*H$_2$CO), 56.14 (s, CO*C*H$_2$CO), 101.64 (s, *C*H$_3$), 111.94 (d, J_{CP} = 6.4 Hz, Ar*C*), 114.20 (d, J_{CP} = 2.4 Hz, Ar*C*), 122.89 (d, J_{CP} = 6.4 Hz, Ar*C*), 125.99 (s, Ar*C*), 127.08 (s, Ar*C*), 127.62 (s, Ar*C*), 128.76 (d, J_{CP} = 11.6 Hz, Ar*C*), 129.58 (d, J_{CP} = 11.1 Hz, Ar*C*), 131.93 (d, J_{CP} = 2.0 Hz, Ar*C*), 132.62 (d, J_{CP} = 2.7 Hz, Ar*C*), 133.90 (d, J_{CP} = 12.8 Hz, Ar*C*), 134.30 (d, J_{CP} = 13.2 Hz, Ar*C*), 145.39 (d, J_{CP} = 3.3 Hz, Ar*C*), 146.81 (d, J_{CP} = 2.1 Hz, Ar*C*), 189.35 (d, J_{CP} = 16.1, *C*O); ^{31}P{^{1}H} NMR (161 MHz, CD_2Cl_2): δ 45.11; HRMS (ESI)m/z[positive mode] calcd. for $C_{45}H_{43}O_6P_2Cl_2Au_2$ 1205.1243, found 1205.1243.

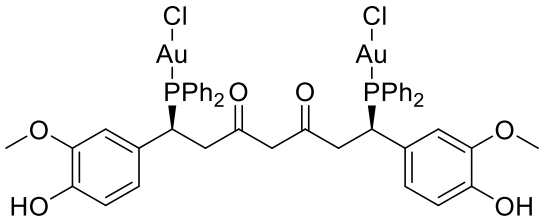

meso-**18aa'**

White Solid; Eluent system (column chromatography): DCM/EA (99:1); Yield: 108.0 mg (32%); ^{1}H NMR (400 MHz, CD_2Cl_2): δ 2.69-2.79 (m, 2H, PCHC*H*HCO), 2.91-3.00 (m, 2H, PC*H*CH$_2$CO), 3.74 (s, 6H, C*H*$_3$OAr), 4.23-4.30 (m, 2H, PCHC*H*HCO), 5.68 (bs, 2H, O*H*), 6.47-6.68 (m, 4H, Ar*H*), 6.82 (s, 2H, COC*H*$_2$CO), 7.28-7.41 (m, 12H, Ar*H*), 7.55-7.56 (m, 6H Ar*H*), 7.91-7.95 (m, 4H, Ar*H*); ^{13}C{^{1}H} NMR (100 MHz, CD_2Cl_2): δ 40.77 (s, *C*H$_2$P), 41.14 (s, CH$_2$*C*H$_2$CO), 56.42 (s, CO*C*H$_2$CO), 102.05 (s, *C*H$_3$), 112.14 (d, J_{CP} = 6.3 Hz, Ar*C*), 114.62 (s, Ar*C*), 123.16 (d, J_{CP} = 6.5 Hz, Ar*C*), 126.26 (s, Ar*C*), 127.53 (s, Ar*C*), 128.02 (d, J_{CP} = 9.6 Hz, Ar*C*), 129.10 (d, J_{CP} = 11.7 Hz, Ar*C*), 129.94 (d, J_{CP} = 11.1 Hz, Ar*C*), 132.28 (d, J_{CP} = 2.3 Hz, Ar*C*), 132.95 (d, J_{CP} = 2.3 Hz, Ar*C*), 134.25 (d, J_{CP} = 12.8 Hz, Ar*C*), 134.68 (d, J_{CP} = 13.1 Hz, Ar*C*), 145.69 (d, J_{CP} = 3.3 Hz, Ar*C*), 147.17 (d, J_{CP} = 2.3 Hz, Ar*C*), 189.71 (d, J_{CP} = 16.4 Hz, *C*O); ^{31}P{^{1}H} NMR (161 MHz, CD_2Cl_2): δ 44.99; HRMS (ESI)m/z[positive mode] calcd. for $C_{45}H_{43}O_6P_2Cl_2Au_2$ 1205.1243, found 1205.1243.

Cell culture

Non-invasive, estrogen receptor positive and progesterone receptor positive human breast carcinoma, MCF7 and well-differentiated gastric adenocarcinoma, MKN74 cells were from American Type Culture Collection (ATCC, USA) and Japanese Cancer Research Resources Bank (JCRB, Japan), respectively. Both cell lines were cultured in Roswell Park Memorial Institute 1640 (RPMI) medium (GE Healthcare, USA) supplemented with 10% Fetal Bovine Serum (FBS) (GE Healthcare) in a humified incubator of 5% CO2 at 37°C.

Drug treatment

Cells were seeded at a density of 10000cells/ml (3125cells/cm2) in 96 wells plate 48 h before cell treatment. The drug complexes were resuspended in Dimethyl sulfide (DMSO) (Sigma Aldrich, USA) before drug treatment at various concentrations (0.1pM to 1mM) in fresh culture medium for 24 hours to 72 hours.

AlamarBlue Assay

After the drug treatment, treatment medium was replaced with 10µL of AlamarBlue cell viability reagent and 90µL of fresh culture medium to obtain a final ratio of 1:9 of AlamarBlue: fresh culture medium before 1 h incubation at 37°C. The absorbance of the test and control wells was read at 570 nm and 600 nm with a spectrometer (Biotek Synergy H1) (Biotek, USA). The percentage of AlamarBlue reduction was calculated as followed:

$$\text{Percentage of Alamar Blue reduction} = \frac{(\text{O2 x A1}) - (\text{O1 x A2})}{(\text{R1 x N2}) - (\text{R2 x N1})} \text{ x } 100\%$$

Percentage of Alamar Blue reduction= ((O2 x A1)-(O1 x A2))/((R1 x N2)-(R2 x N1)) x 100%

O1 = Molar extinction coefficient (E) of oxidised AlamarBlue at 570 nm

O2 = E of oxidised AlamarBlue at 600 nm

R1 = E of reduced AlamarBlue at 570 nm

R2 = E of reduced AlamarBlue at 600nm

A1 = absorbance of test wells at 570 nm

A2 = absorbance of test wells at 600 nm

N1 = absorbance of negative control well (culture medium and AlmarBlue without cells) at 570nm

N2 = absorbance of positive control well (culture medium and AlmarBlue without cells) at 600nm

Statistical Analysis

Statistical analyses were performed using 1-way ANOVA via GraphPad Prism 9.1.2 (La Jolla, USA). P-values < 0.05 is considered significant.

3.5 References

1. J. Miłobędzka; S. v. Kostanecki; V. Lampe, *Zur Kenntnis des Curcumins, Chem. Ber.* **1910**, *43*, 2163.

2. A. Carter, *Curry Compound Fights Cancer in the Clinic, J. Natl. Cancer Inst.* **2008**, *100*, 616.

3. (a) B. B. Aggarwal; A. Kumar; A. C. Bharti, *Anticancer potential of curcumin: preclinical and clinical studies*, *Anticancer Res* **2003**, *23*, 363; (b) P. Anand; S. G. Thomas; A. B. Kunnumakkara; C. Sundaram; K. B. Harikumar; B. Sung; S. T. Tharakan; K. Misra; I. K. Priyadarsini; K. N. Rajasekharan; B. B. Aggarwal, *Biological activities of curcumin and its analogues (Congeners) made by man and Mother Nature*, *Biochem. Pharmacol.* **2008**, *76*, 1590; (c) R. A. Sharma; A. J. Gescher; W. P. Steward, *Curcumin: The story so far*, *Eur. J. Cancer* **2005**, *41*, 1955; (d) P. Anand; A. B. Kunnumakkara; R. A. Newman; B. B. Aggarwal, *Bioavailability of Curcumin: Problems and Promises*, *Mol. Pharm.* **2007**, *4*, 807; (e) K. I. Priyadarsini, *Photophysics, photochemistry and photobiology of curcumin: Studies from organic solutions, bio-mimetics and living cells*, *J. Photochem. Photobiol. C* **2009**, *10*, 81; (f) R. Yadav; G. Tarun, *Versatility of turmeric: A review the golden spice of life*, *J. Pharmacogn. Phytochem.* **2017**, *6*, 41; (g) D. Shrishail; H. Harish K; H. Ravichandra; G.Tulsianand; S. D. Shruthi, *TURMERIC: NATURE'S PRECIOUS MEDICINE*, *Asian J. Pharm. Clin. Res.* **2013**, *6*, 10.

4. A. Goel; A. B. Kunnumakkara; B. B. Aggarwal, *Curcumin as "Curecumin": from kitchen to clinic*, *Biochem Pharmacol* **2008**, *75*, 787.

5. F. Kühlwein; K. Polborn; W. Beck, *Metallkomplexe von Farbstoffen. VIII Übergangsmetallkomplexe des Curcumins und seiner Derivate*, *Z. Anorg. Allg. Chem.* **1997**, *623*, 1211.

6. (a) A. Beneduci; G. A. Corrente; T. Marino; D. Aiello; L. Bartella; L. Di Donna; A. Napoli; N. Russo; I. Romeo; E. Furia, *Insight on the chelation of aluminum(III) and iron(III) by curcumin in aqueous solution*, *J. Mol. Liq.* **2019**, *296*, 111805; (b) S. Wanninger; V. Lorenz; A. Subhan; F. T. Edelmann, *Metal complexes of curcumin – synthetic strategies, structures and medicinal applications*, *Chem. Soc. Rev.* **2015**, *44*, 4986; (c) R. Pallikkavil; M. B. Ummathur; S. Sreedharan; K. Krishnankutty, *Synthesis, characterization and antimicrobial studies of Cd(II), Hg(II), Pb(II), Sn(II) and Ca(II) complexes of curcumin*, *Main Group Met. Chem.* **2013**, *36*, 123.

7. K. Mohammadi; K. H. Thompson; B. O. Patrick; T. Storr; C. Martins; E. Polishchuk; V. G. Yuen; J. H. McNeill; C. Orvig, *Synthesis and characterization of dual function vanadyl, gallium and indium curcumin complexes for medicinal applications*, *Journal of inorganic biochemistry* **2005**, *99*, 2217.

8. (a) D. S. Bhange; N. K. Rasal; R. B. Sonawane; S. V. Jagtap, *Application of Curcumin as Ligand in [Pd(Curc-H)2] Catalyst for Carbon-Carbon Bond Formation in Heck and Suzuki Coupling Reactions*, *ChemistrySelect* **2018**, *3*, 11230; (b) M. A. Jani; K. Bahrami, *BNPs@Cur-Pd as a versatile and recyclable green nanocatalyst for Suzuki, Heck and Stille coupling reactions*, *J. Exp. Nanosci.* **2020**, *15*, 182.

9. S. Dutta; A. Murugkar; N. Gandhe; S. Padhye, *Enhanced antioxidant activities of metal conjugates of curcumin derivatives*, *Met Based Drugs* **2001**, *8*, 183.

10. S. Dutta; S. Padhye; K. I. Priyadarsini; C. Newton, *Antioxidant and antiproliferative activity of curcumin semicarbazone*, *Bioorganic & medicinal chemistry letters* **2005**, *15*, 2738.

11. (a) S. Mishra; N. Kapoor; A. Mubarak Ali; B. V. Pardhasaradhi; A. L. Kumari; A. Khar; K. Misra, *Differential apoptotic and redox regulatory activities of curcumin and its derivatives*, *Free radical biology & medicine* **2005**, *38*, 1353; (b) S. Mishra; K. Karmodiya; N. Surolia; A.

Surolia, *Synthesis and exploration of novel curcumin analogues as anti-malarial agents*, *Bioorganic & medicinal chemistry* **2008**, *16*, 2894.

12. V. D. John; G. Kuttan; K. Krishnankutty, *Anti-tumour studies of metal chelates of synthetic curcuminoids*, *Journal of experimental & clinical cancer research : CR* **2002**, *21*, 219.

13. C. Heffernan; M. Ukrainczyk; R. K. Gamidi; B. K. Hodnett; Å. C. Rasmuson, *Extraction and Purification of Curcuminoids from Crude Curcumin by a Combination of Crystallization and Chromatography*, *Org. Process Res. Dev.* **2017**, *21*, 821.

14. W. Wichitnithad; U. Nimmannit; S. Wacharasindhu; P. Rojsitthisak, *Synthesis, Characterization and Biological Evaluation of Succinate Prodrugs of Curcuminoids for Colon Cancer Treatment*, *Molecules* **2011**, *16*, 1888.

15. (a) H. J. Chen; R. Hong Xiang Teo; Y. Li; S. A. Pullarkat; P.-H. Leung, *Stereogenic Lock in 1-Naphthylethanamine Complexes for Catalyst and Auxiliary Design: Structural and Reactivity Analysis for Cycloiridated Pseudotetrahedral Complexes*, *Organometallics* **2018**, *37*, 99; (b) Y. Huang; R. J. Chew; Y. Li; S. A. Pullarkat; P.-H. Leung, *Direct Synthesis of Chiral Tertiary Diphosphines via Pd(II)-Catalyzed Asymmetric Hydrophosphination of Dienones*, *Org. Lett.* **2011**, *13*, 5862; (c) J. K.-P. Ng; G.-K. Tan; J. J. Vittal; P.-H. Leung, *Optical Resolution and the Study of Ligand Effects on the Ortho-Metalation Reaction of Resolved (±)-Diphenyl[1-(1-naphthyl)ethyl]phosphine and Its Arsenic Analogue*, *Inorg. Chem.* **2003**, *42*, 7674.

16. (a) B.-B. Li; Y.-X. Jia; P.-C. Zhu; R. J. Chew; Y. Li; N. S. Tan; P.-H. Leung, *Highly selective anti-cancer properties of ester functionalized enantiopure dinuclear gold (I)-diphosphine*, *European journal of medicinal chemistry* **2015**, *98*, 250; (b) M. P. Rigobello; G. Scutari; R. Boscolo; A. Bindoli, *Induction of mitochondrial permeability transition by auranofin, a gold(I)-phosphine derivative*, *British journal of pharmacology* **2002**, *136*, 1162;

(c) E. R. T. Tiekink, *Gold derivatives for the treatment of cancer*, *Crit. Rev. Oncol. Hematol.* **2002**, *42*, 225.

17. C. F. Shaw, *Gold-Based Therapeutic Agents*, *Chem. Rev.* **1999**, *99*, 2589.

18. B. M. Sutton, *Gold compounds for rheumatoid arthritis*, *Gold Bull.* **1986**, *19*, 15.

19. C. K. Mirabelli; D. T. Hill; L. F. Faucette; F. L. McCabe; G. R. Girard; D. B. Bryan; B. M. Sutton; J. O. L. Barus; S. T. Crooke; R. K. Johnson, *Antitumor activity of bis(diphenylphosphino)alkanes, their gold(I) coordination complexes, and related compounds*, *J. Med. Chem.* **1987**, *30*, 2181.

20. (a) M. T. Villanueva, *The mitochondria thief*, *Nat. Rev. Cancer* **2015**, *15*, 70; (b) S. S. Sabharwal; P. T. Schumacker, *Mitochondrial ROS in cancer: initiators, amplifiers or an Achilles' heel?*, *Nat. Rev. Cancer* **2014**, *14*, 709; (c) D. C. Wallace, *Mitochondria and cancer*, *Nat. Rev. Cancer* **2012**, *12*, 685.

21. (a) S. J. Berners-Price; A. Filipovska, *Gold compounds as therapeutic agents for human diseases*, *Metallomics : integrated biometal science* **2011**, *3*, 863; (b) W. F. Kean; I. R. Kean, *Clinical pharmacology of gold*, *Inflammopharmacology* **2008**, *16*, 112.

22. (a) G. D. Hoke; G. F. Rush; G. F. Bossard; J. V. McArdle; B. D. Jensen; C. K. Mirabelli, *Mechanism of alterations in isolated rat liver mitochondrial function induced by gold complexes of bidentate phosphines*, *J. Biol. Chem.* **1988**, *263*, 11203; (b) G. Kroemer; L. Galluzzi; C. Brenner, *Mitochondrial Membrane Permeabilization in Cell Death*, *Physiol. Rev.* **2007**, *87*, 99; (c) D. R. Green; G. Kroemer, *Pharmacological manipulation of cell death: clinical applications in sight?*, *J. Clin. Investig.* **2005**, *115*, 2610.

Chapter IV

Synthesis, Complexation and Application of Phosphine-(Phosphino Chalcogenide) Ligands

4.1 Introduction

4.1.1 Non-C_2 Symmetrical Chiral Bidentate Ligands

The importance of rotational symmetry in the design of chiral ligands was recognized by Kagan in his introduction of C_2-symmetric phosphines for asymmetric hydrogenation reactions.[1] Chiral phosphorus bidentate ligands comprising of a large substituent and a small substituent at the phosphorus center have been shown to induce more efficient enantioselectivities,[2] and in the past decades, C_2-symmetrical chiral bidentate ligands have been utilized extensively in transition metal-catalyzed asymmetric reactions owing to their stereodifferentiation abilities and synthetic accessibilities.[1, 3] In addition, the presence of a C_2 symmetry axis greatly reduces the possibility of generating a large number of stereoisomeric transition states.[4]

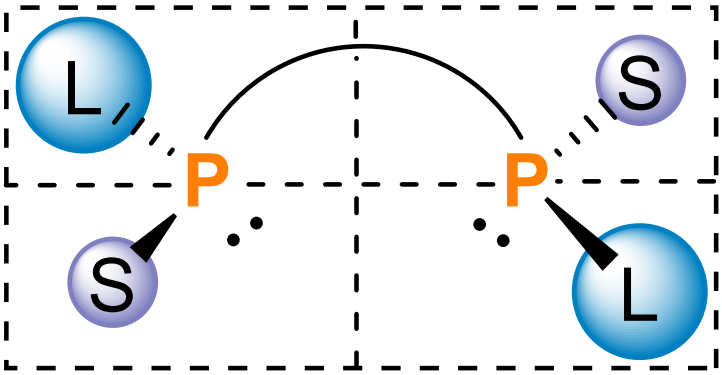

Figure 29. Illustration of the quadrant rule of bidentate ligands – C_2-symmetric chiral environment made possible by a pair of sterically hindered ligands on opposite sides of a quadrant (for example top left and bottom right in the figure).

While the advantages associated with symmetrical chiral bidentate ligands have been attributed mainly to the existence of rotational symmetry within the ligands, other factors pertaining to the electronics of the donor atoms and steric interactions of the reactive intermediates have also been shown to contribute significantly to the effectiveness of such ligands. Building on this, hybrid chiral bidentate ligands bearing two hetero-donor atoms arranged in a non-C_2-symmetrical manner have since been shown to be effective ligands in many transition metal-mediated reactions as well. One main advantage of using such hybrid ligands is the ability to harness the innate differences in electronic and steric attributes of the heteroatoms to diversify their reactivity and stereoinduction. Recent advancements in the applications of non-symmetrical ligands have also shown that C_2-symmetry is not an absolute prerequisite in ensuring efficient relay of chiral information[5] and in some situations, C_1-symmetrical chiral ligands with two different donor atoms have better stereocontrol than their C_2-symmetrical chiral analogues.[6]

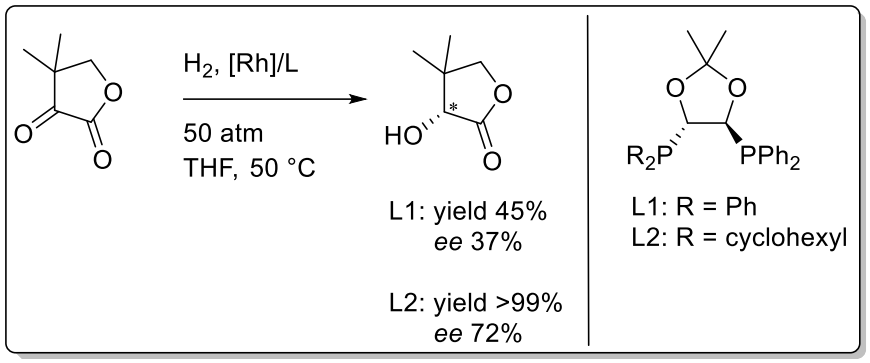

Scheme 44. Achiwa and co-worker hydrogenation studies with desymmetrized DIOP.

4.1.2 Hemilabile Chiral Bidentate Ligands and Their Applications

Hemilabile chiral ligands are defined as a group of chiral ligands consisting of a strongly bonded anchor donor and a weakly bonded labile group on a common metal center. These chelating chiral ligands have been of interest to researchers due to their ability to provide an open site on the metal center during reaction that would otherwise be absent in the ground state structure of a complex bearing non-hemilabile bidentate ligands. Hemilabile chiral ligands have been found to be catalytically useful in a broad range of reactions including hydrogenation,[7] hydroformylation,[8] carbonylation[9] and ring-opening metathesis polymerization.[10]

Gao *et al.* designed the polydentate chiral ligand consisting of two 'soft' phosphorus donors and two 'hard' nitrogen donors complexed to a Rh(I) metal center. This complex was subsequently used as a catalyst in the asymmetric transfer hydrogenation reaction of aromatic ketones, affording up to 99% yield and 94% *ee*. [7b]

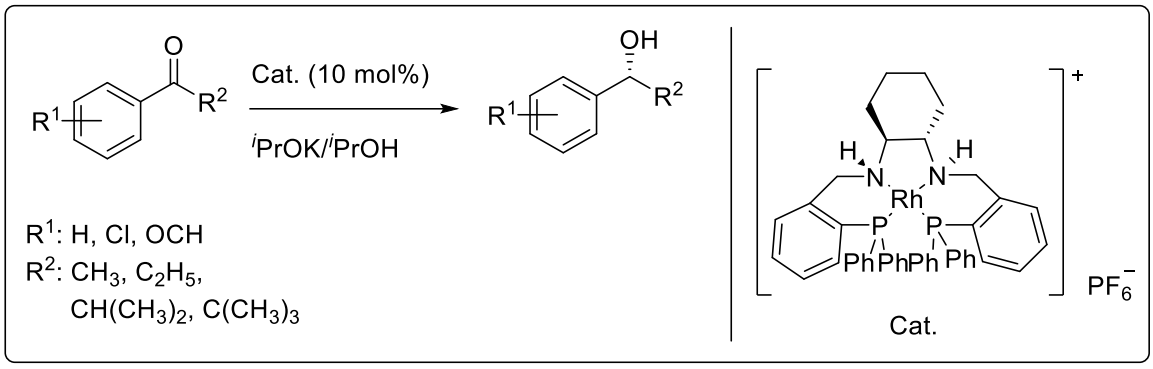

Scheme 45. Asymmetric transfer hydrogenation of aromatic ketones using hemilabile polydentate ligand.

Gladiali *et al.* subjected styrene to a hydroformylation reaction with the aid of a Rh(I) complex containing a chiral *P*,*O*-chelating ligand.[8a] Full conversion was observed within 15h of the reaction with a small catalyst loading of 0.05 mol%; this was comparable to many hydroformylation of styrene catalyzed by chiral bidentate diphosphites and diphosphines metal complexes.[11]

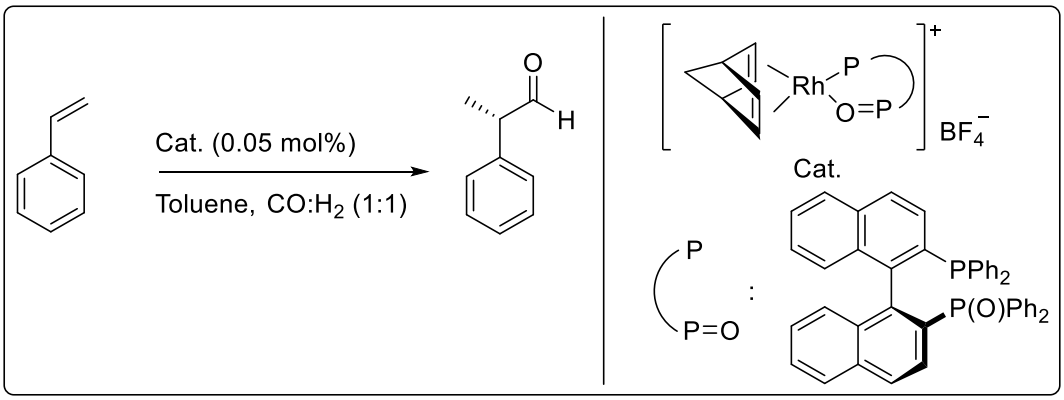

Scheme 46. Hydroformylation of styrene using *P*,*O*-hemilabile ligand.

4.1.3 Research Objective

The benefits of non-symmetrical chiral ligands having two heteroatoms as donors include their potential in influencing the electronics of the *trans* reaction sites on the metal

center. However, research on the designs and applications of hemilabile chiral heteroatoms bidentate ligands have been limited and as such, our group aimed to utilize our expertise in asymmetric hydrophosphination to devise a new strategy to form chiral C_1-symmetric ligands bearing two heteroatoms, specifically chiral phosphine-phosphino sulfide bidentate ligands.

4.2 Results and Discussion

4.2.1 Initial Attempt

Asymmetric hydrophosphination reactions generally require highly activated olefins as substrates, such as a carbonyl, ester or an amide group. In view of this, we attempted the enantioselective transformation of an activated olefin, specifically one that bears a conjugated phosphino-sulfide as the activator, into a chiral bidentate phosphine-phosphino-sulfide ligand through asymmetric hydrophosphination. The phosphino-sulfide olefin was synthesized from *β*-bromostyrene and diphenylphosphine oxide *via* an addition-elimination reaction[12] followed by thionation of the phosphine oxide product **19** using Lawesson's Reagent.[13]

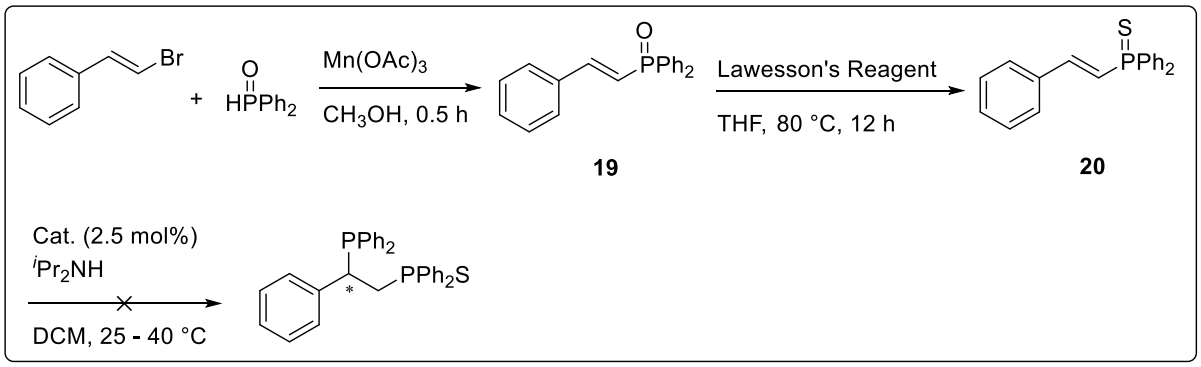

Scheme 47. Formation of activated olefin containing phosphine-sulfide functional group and attempted catalytic asymmetric hydrophosphination using phosphino-sulfide olefin.

In the initial trials of the asymmetric hydrophosphination of **20**, substrate **20** was reacted with diphenylphosphine in the presence of catalyst **8** and diisopropyl amine as the base

at room temperature. However, no reaction was observed after 24 hours. Further heating of the reaction mixture to 40 °C yielded no product. No reaction was also observed when the reaction was repeated with complex **9** as the catalyst. This result could be explained by the fact that P=S was a weaker activating group than C=O.

4.2.2 Synthesis of Substrate 21

To increase the extent of electrophilic activation in substrate **20**, an additional carbonyl group was incorporated. This new substrate, compound **21**, bearing two activating groups could be obtained from either **22** in an addition (hydrophosphination) reaction or from **23** in a nucleophilic substitution (phosphination) reaction. In addition, **23** could be obtained from **22** in a simple hydrohalogenation process. With this new retrosynthetic strategy in mind, the syntheses of substrates **22** and **23** were attempted and the feasibility of their conversion to the desired substrate **21** for asymmetric hydrophosphination was subsequently evaluated.

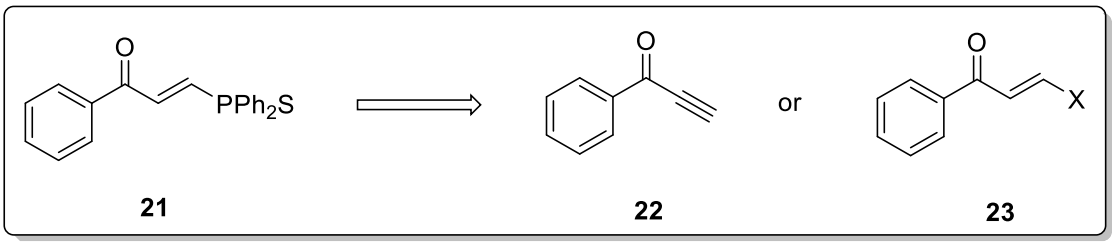

Scheme 48. Retrosynthesis of substrate **21**.

From benzaldehyde, the intermediatory alkyne ketone **22** could be formed *via* a Grignard reaction followed by an oxidation using the oxidant Dess-Martin Periodinane (DMP).

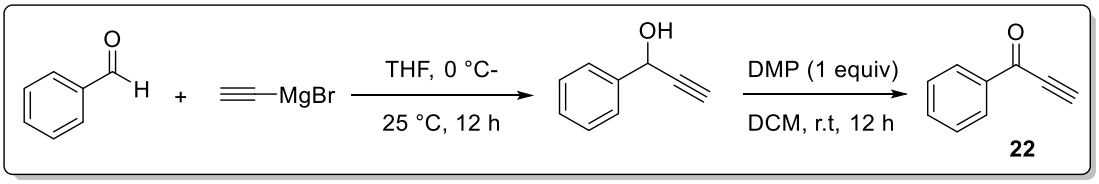

Scheme 49. Synthesis of alkyne ketone **22** from benzaldehyde.

Hydrophosphination of intermediate **22** with one equivalent of diphenylphosphine was immediately carried out but unfortunately, the reaction consistently afforded only the *di*hydrophosphinated product and not the desired new substrate **21**.

Moving forward, we turned our attention to the synthesis of the next candidate, compound **23**. Compound **23** was synthesized from **22** using sodium bromide (X=Br) in a mixed ACN/^{t}BuOH solvent system in the presence of aluminum chloride.[14] As usual, the phosphination of **23** was immediately carried out with diphenylphosphine in the presence of a base and fortunately, compound **23** afforded the desired substrate **21** after the product was sulfurized.

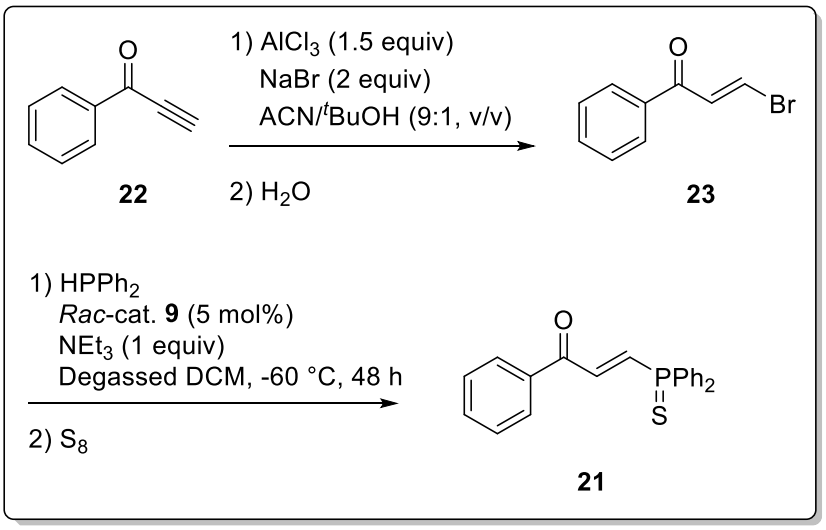

Scheme 50. Hydrobromination and nucleophilic substitution reactions of alkyne ketone.

4.2.3 Challenges Associated with the Asymmetric Hydrophosphination of 21

With the new substrate bearing two electron-withdrawing functional groups, a carbonyl and a conjugate phosphino-sulifde group, the preliminary asymmetric hydrophosphination reaction was conducted. In an initial run, **21** was reacted with bis(4-methoxyphenyl)phosphine in the presence of catalytic amount of **8** and triethylamine at room temperature. The reaction furnished within two hours the phosphine-phosphino-sulfide product **24**. The air-sensitive product was sulfurized to facilitate post-analyses such as the determination of enantiomeric excess and characterization. Unfortunately, HPLC data revealed that the product was obtained as a racemate even though the chiral catalyst **8** was employed. Conducting the reaction at -80 °C reduced the rate of reaction but still provided 0% *ee*. In addition, replacing catalyst **8** with catalyst **9** did not change the outcome of the enantioselectivity of the reaction and a possible reason for the lack of enantioselectivity in the hydrophosphination could be catalyst poisoning, either by the deactivation of the chiral catalyst by substrate **21** or product **24** or an extremely rapid uncatalyzed background reaction, involving the substrate and secondary phosphine without the need for a catalyst.

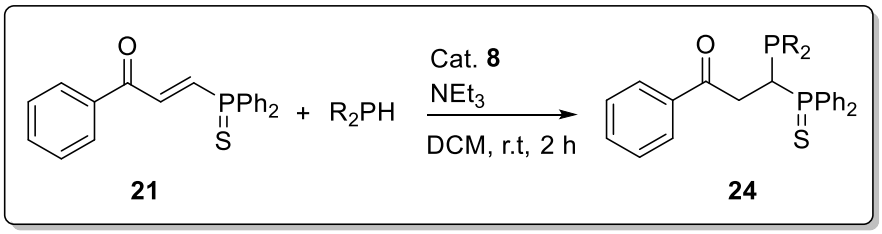

Scheme 51. Initial synthesis of product **24**.

In order to verify the hypothesis on catalyst poisoning, a reaction was conducted at room temperature with substrate **21**, chemical shift at δ35.86, in the presence of only 1 equivalent of catalyst **8**, chemical shift at δ63.41.[15] From this reaction, there was evidence of substrate coordination to the palladium metal center based on the shift in the $^{31}P\{^{1}H\}$ signals

of both catalyst **8** and substrate **21**. Subsequent addition of bis(4-methoxyphenyl)phosphine in the reaction mixture revealed further changes to the signals but there was no signal corresponding to the chemical shift of product **24**. The postulated structure of the product, based on the $^{31}P\{^{1}H\}$ NMR resonances and coupling constant, is shown in figure 32. The results from this experiment precluded the use of catalyst **8** in the enantioselective synthesis of **24**, as such an attempt to synthesize a racemic mixture of **24** was attempted in another reaction. In this second reaction, product **24** was formed quantitatively.

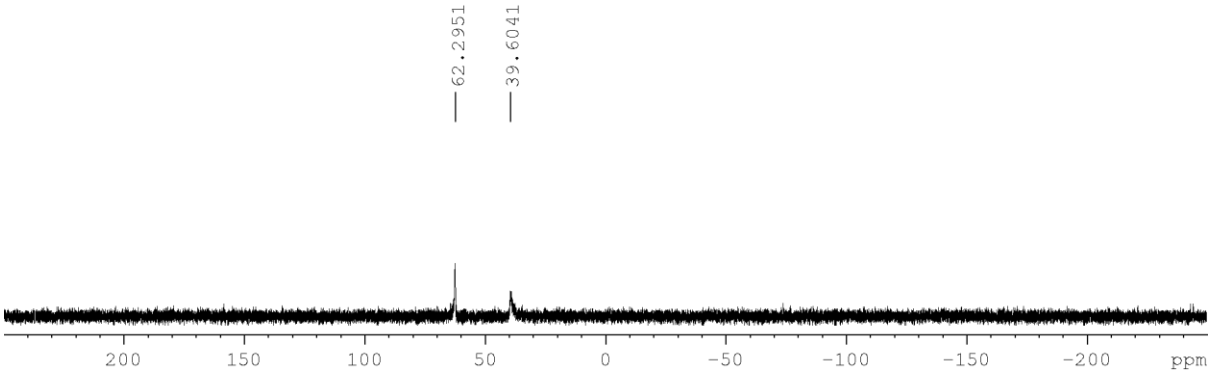

Figure 30. $^{31}P\{^{1}H\}$ NMR spectrum of the first reaction, before the addition of bis(4-methoxyphenyl)phosphine.

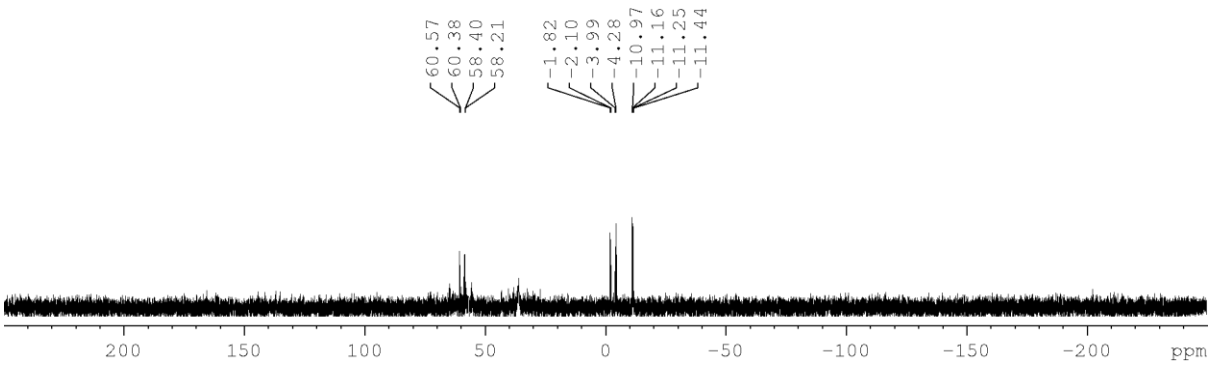

Figure 31. $^{31}P\{^{1}H\}$ NMR spectrum of the first reaction, after the addition of bis(4-methoxyphenyl)phosphine.

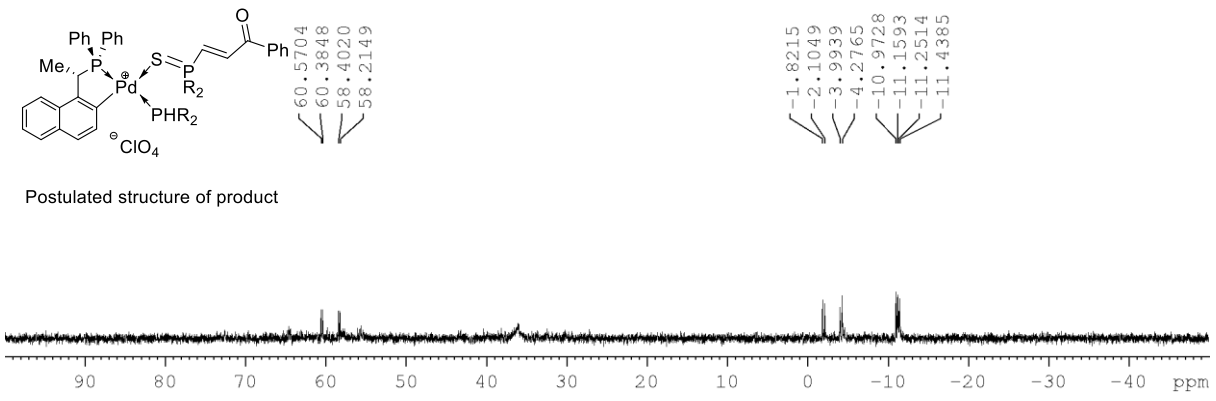

Postulated structure of product

Figure 32. Zoomed $^{31}P\{^{1}H\}$ NMR spectrum of the first reaction, after the addition of bis(4-methoxyphenyl)phosphine.

4.2.4 Syntheses of Racemic Phosphine-(Phosphino Chalcogenide) Complexes

Due to the phenomenon of catalysts poisoning as investigated in previous studies, attention has to be, unfortunately, shifted to the synthesis of *racemic* phosphine-phosphino-sulfide ligands and their lighter and heavier analogues, specifically phosphine-phosphino-oxide and selenide ligands, instead. Reaction between compounds **21** or **25** with secondary arylphosphines could be completed within two to nine hours to furnish racemic mixtures of phosphine-phosphino chalcogenides. In the substrate screening stage, a series of secondary phosphines containing withdrawing and donating aryl groups was used for the reaction shown in scheme 52. Secondary phosphines with aryl groups substituted at the 2 or 3 positions required the use of triethylamine for the reaction to proceed. This could be due to the presence of steric hindrance between the substrates and hence a more nucleophilic phosphide might be required for the nucleophilic addition step to occur successfully in the reaction. $PdCl_2(NCMe)_2$ then added to these crude mixtures to furnish the racemic phosphine-phosphino chalogenide palladium(II) complexes **26** to **33.**

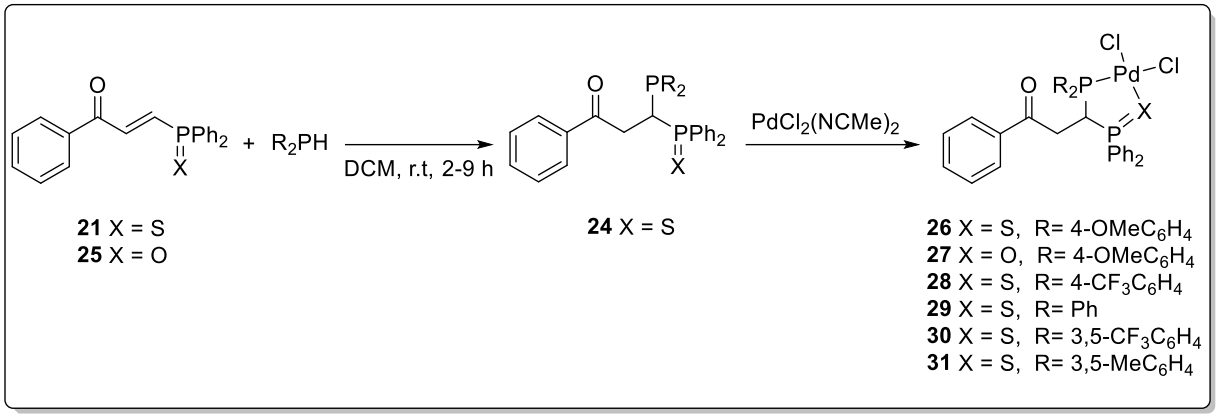

Scheme 52. Synthesis of phosphine-(phosphino chalcogenide) palladium(II) complexes.

Table 5. Relevant bond lengths and bond angle of solid state complexes.[a]

Complex	X / R	Pd-P	Pd-X	Pd-$Cl_{trans\text{-}X}$	Pd-$Cl_{trans\text{-}P}$	P-Pd-X
26	S/4-$OMeC_6H_4$	2.2155(10)	2.2800(10)	2.3176(10)	2.3427(10)	94.07(4)
27	O/4-$OMeC_6H_4$	2.2290(13)	2.090(3)	2.2616(12)	2.3476(12)	90.27(9)
28	S/4-$CF_3C_6H_4$	2.2205(17)	2.309(2)	2.323(2)	2.3308(18)	94.04(7)
29	S/Ph	2.2418(7)	2.3083(6)	2.2998(6)	2.3595(6)	94.65(2)
30	S/3,5-$CF_3C_6H_3$	2.2219(10)	2.2931(11)	2.3187(11)	2.3333(10)	93.29(4)
31	S/3,5-MeC_6H_3	2.2434(12)	2.3059(12)	2.3189(12)	2.3543(12)	94.56(4)
33	Se/Ph	2.2393(16)	2.3928(8)	2.3175(17)	2.3627(16)	95.20(5)
34	Se/4-$OMeC_6H_4$	2.2479(8)	2.4198(4)	2.3243(8)	2.3494(8)	93.72(2)

[a]Bond lengths and bond angle can be found in appendix and are given in Å and ° respectively.

The effects of the substituents on phosphine and the identity of the phosphine chalcogenide on the solid-state parameters such as bond lengths and angles were studied using the single crystal X-ray structures obtained from complexes **26** to **33**. In Table 5, it can be seen that the P-Pd bond generally was not affected greatly by the identity of the chalcogen and the substituent on the phosphine. For the Pd-Cl bond *trans* to the chalcogen, the bond was longer and weaker when the chalcogen was either sulfur or selenium; this was due to increased competition for π donation between the less electronegative sulfur or selenium atom (as compared to oxygen) and *trans* chloride into the vacant orbitals of Pd. Lastly, the P-Pd-X bite angle was bigger in **26** than **27** and **33** as the bulker sulfur/selenium atom causes more significant geometric distortion away from the ideal square planar angle due to a greater degree of steric influence. It is worth noting that the substituents on the phosphine did not exert any significant influence on the bite angle even though they are close to the coordination sphere of palladium (complexes **28** to **33**).

Table 6. Chemical Shifts and Coupling Constants of Complexes in Solution.[a]

Complex	X / R	^{31}P of PR_2	^{31}P of PPh_2	$^{2}J_{PP}$	$\Delta^{31}P$ of PR_2	$\Delta^{31}P$ of PPh_2
26	S/4-$OMeC_6H_4$	62.4424	41.7063	52	+80.0446	-10.0777
27	O/4-$OMeC_6H_4$	67.5886	30.1572	28	+84.3099	-3.6599
28	S/4-$CF_3C_6H_4$	63.1044	42.0149	57	+77.1755	-9.2942
29	S/Ph	62.9739	43.6581	55	+76.4902	-8.7613
30	S/3,5-$CF_3C_6H_3$	63.0348	41.3090	62	+75.8673	-8.8605
31	S/3,5-MeC_6H_3	62.7204	43.8736	52	+76.328	-8.5312

[a]Chemical shifts and coupling constants are given in ppm and Hz respectively.

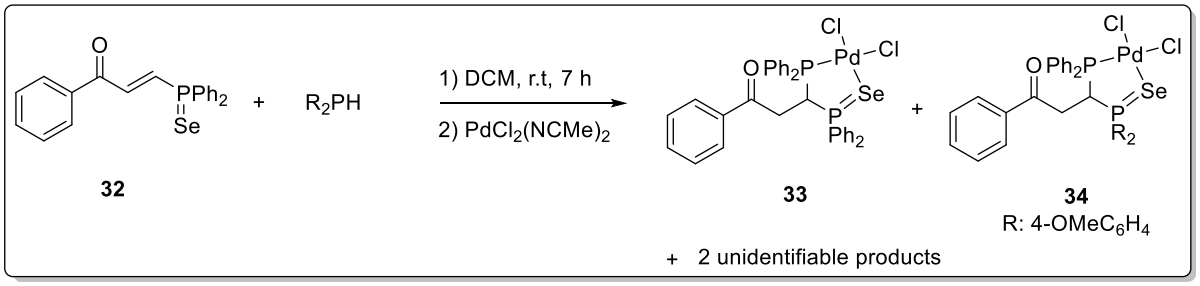

Scheme 53. Hydrophosphination reaction using phosphine-selenide substrate.

The hydrophosphination reaction with phosphine-selenide **32** and bis(4-methoxyphenyl)phosphine showed interesting and unexpected results. After an hour of reaction, diphenylphosphine could be observed in the $^{31}P\{^{1}H\}$ NMR spectrum of the crude mixture but no further change was observed in the crude spectrum after an additional six hours of reaction. Next, bis(acetonitrile)palladium(II) chloride was added to the ligand solution for complexation. Subsequent purification on silica gel and recrystallisation from DCM/Hex

afforded complexes **33** and **34**, amongst other unidentified products. The transfer of selenium atom from one phosphorus atom to another has also been observed by Cross *et al.*[16]

4.2.5 Stability of Complexes 26 And 27

In order to probe the stability of the phosphine-palladium bonds in complexes **26** and **27**, the complexes were reacted with hydrogen peroxide and sulfur separately. In both scenarios with both complexes, no oxidation was observed and this ascertained the inertness of the phosphine-palladium bonds with respect to hydrogen peroxide and sulfur as oxidants.

To probe the hemilability of the phosphino-chalcogenide-palladium bond in complexes **26** and **27**, one equivalent of triphenylphosphine was added to both complexes in dichloromethane and the mixtures were stirred overnight. The complexes were found to react with triphenylphosphine as confirmed from the $^{31}P\{^{1}H\}$ NMR spectra of the crude mixture. In the case of complex **26**, instead of a substitution of the phosphine sulfide ligand by the incoming triphenylphosphine ligand, the chloride ligand was displaced by triphenylphosphine and both the *cis*- and *trans*- forms of the product were detected. The hemilability of the phosphino-sulfide-palladium bond was thus not observed. In addition, in the crude mixture, it was observed that *cis*-**35** was formed in greater proportion as compared to *trans*-**36**. This implies that the phosphine sulfide ligand exhibited a stronger *trans* effect than the phosphine ligand. In the case of complex **27**, addition of triphenylphosphine to the complex in dichloromethane resulted in numerous messy signals in the $^{31}P\{^{1}H\}$ NMR spectrum which could not be identified despite enormous efforts.

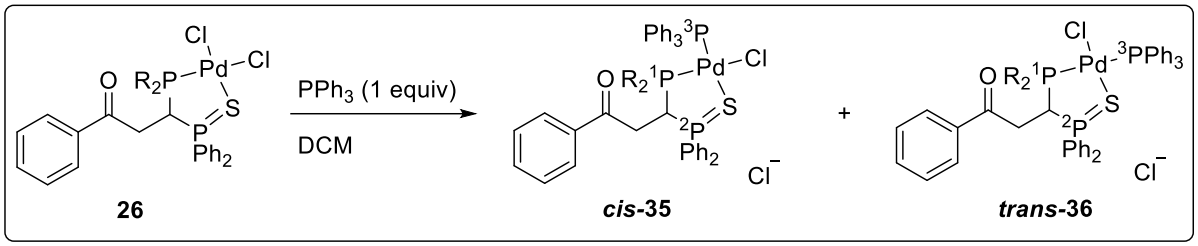

Scheme 54. Investigating the stability of the bidentate ligand using triphenylphosphine.

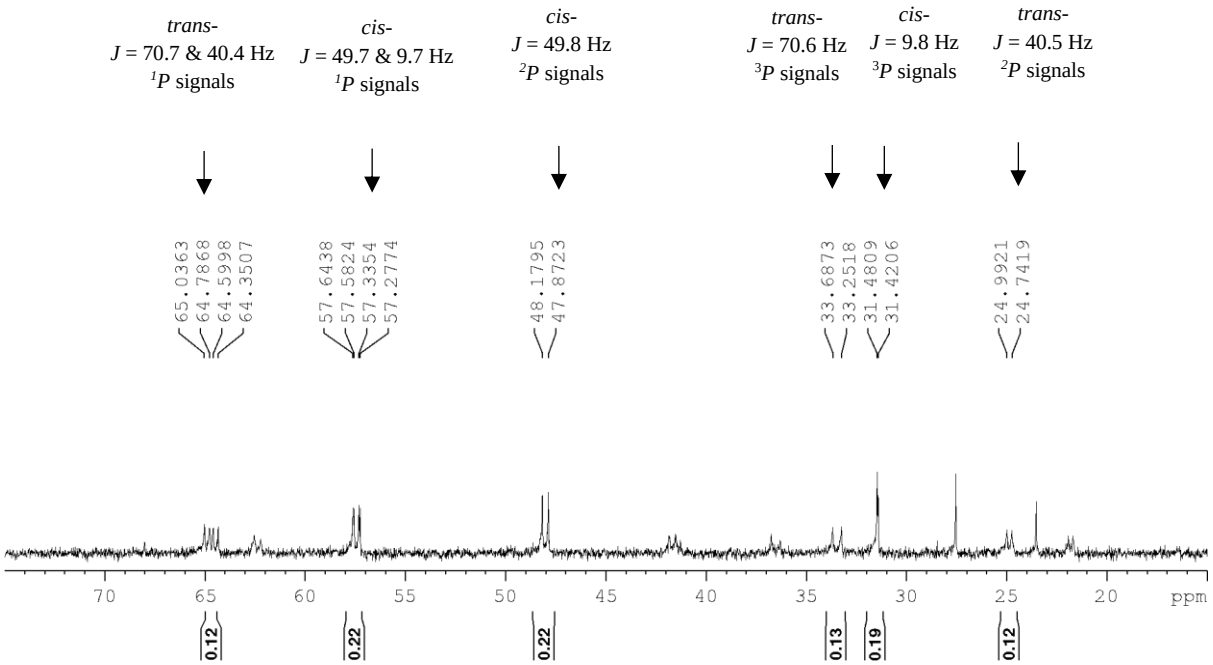

Figure 33. Evidence of *cis*- and *trans*- isomers.

4.2.6 Application – Synthesis of *N*-Heterocyclic Enaminones

Enaminones are enamines containing *β*-carbonyl functional group which exhibit high versatility as intermediates in many organic synthetic reactions,[17] as pharmaceuticals[17a, 18] and in heterocyclic syntheses.[19] For example, enaminones are ubiquitous structural motifs found in alkaloids including analogues of quinolone antibacterial and in mesembrine which is an important serotonin reuptake inhibitor.[20] Most recently and interestingly, Leung *et al.* employed enaminones as starting materials to generate novel *N*-heterocyclic carbene complexes.[17d] Traditionally, the syntheses of enaminones involve the use of tedious protecting

groups, energy-consuming protocols requiring elevated or low temperatures and leaving groups which contribute to a low atom economy and sometimes toxic waste generation. A slightly more environmentally friendly method involving the direct addition of nucleophiles to activated unsaturated functional groups has been reported although the number of examples remains scarce (Selected examples shown in scheme 55).

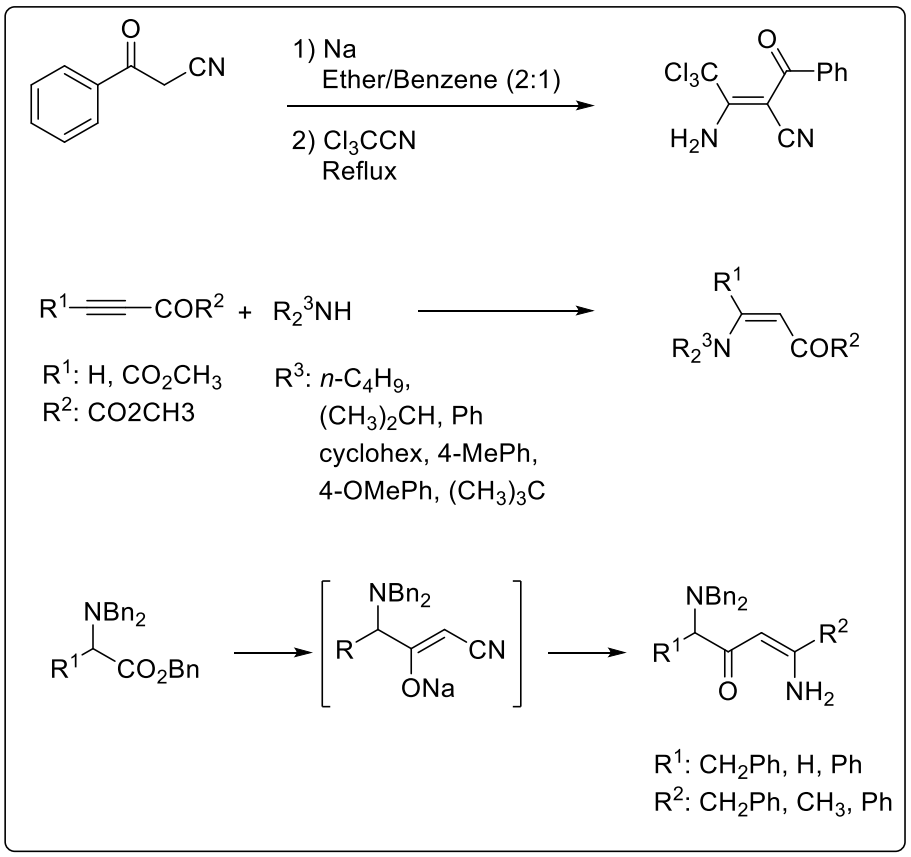

Scheme 55. Selected examples of the formation of enaminones *via* conjugate addition.

Given the widespread applications of enaminones, we attempted the facile synthesis of said compounds under mild reaction conditions using complex **26**. The advantages offered by this system include a simple one-step protocol, high atom economy and the use of benign reagents which are environmentally friendly. In a preliminary study carried out to probe the catalytic activity of complex **26**, a series of activated alkyne ketones and *N*-heterocycles were

employed as substrates in a Pd-catalyzed conjugate addition in the presence of a silver(I) salt and weak base.

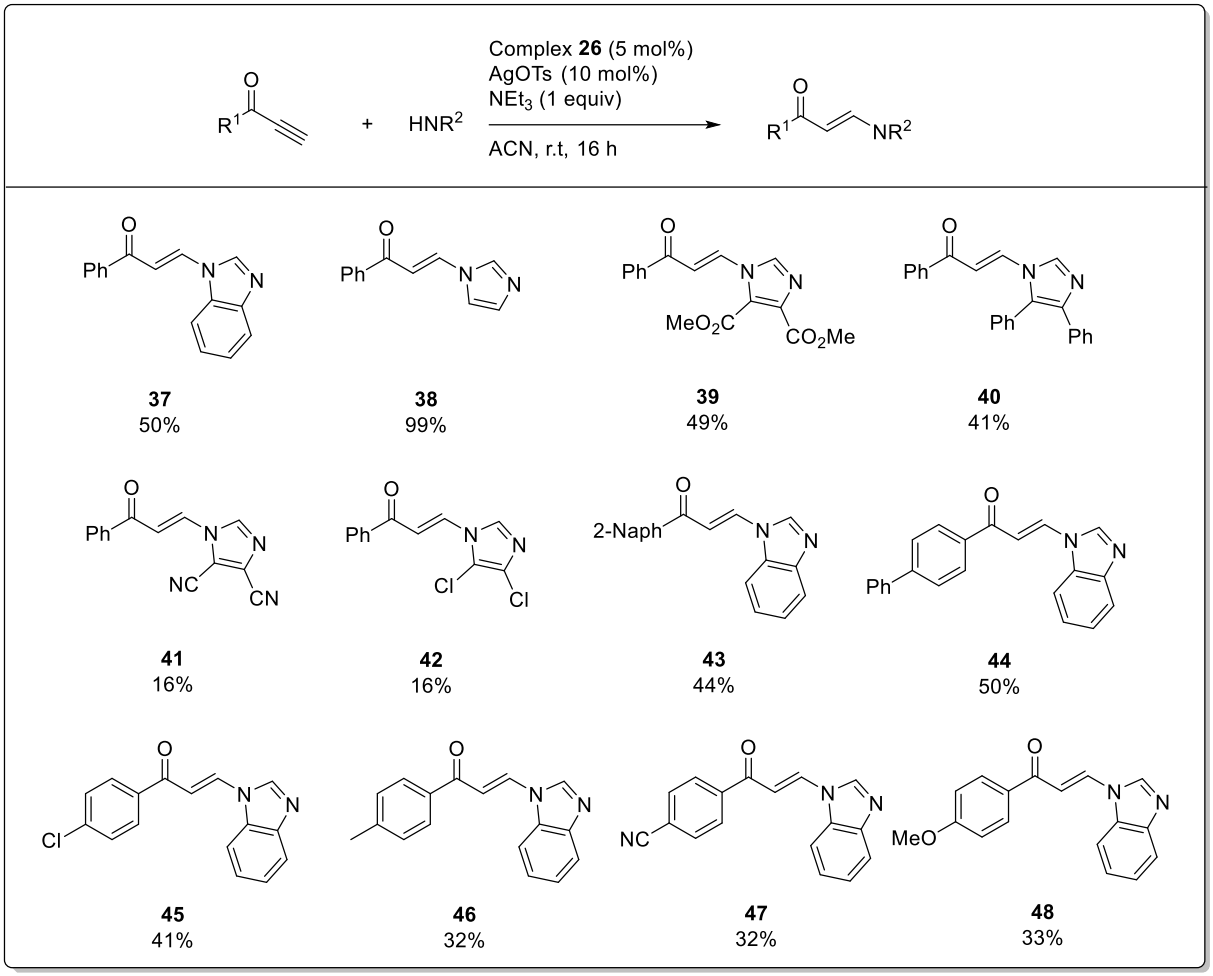

Scheme 56. Synthesis of enaminones *via* catalyzed conjugate addition.

The Pd-catalyzed conjugate addition was able to tolerate a range of alkyne ketone and imidazole substrates and the yields obtained for these products were also comparable to those reported by Leung *et al.*[17d] Electron-withdrawing groups (compounds **41** and **42**) or bulky substituents (compound **40**) on the azole moiety generally reduced the yield of the products. Furthermore, the variation in electronic properties of the substituents on the aryl end did not lead to a drastic change in the reaction yield, probably because these substituents were situated too far away from the olefin reaction site. The yields of the products were not quantitative

despite the full conversion of the reactants into the products. This loss in product yield could be attributed to the coordination of the product to the acidic silica during the purification process *via* silica chromatography.

4.3 Conclusion

In conclusion, we have successfully developed a direct and efficient protocol for the synthesis of C_1-symmetric, hetereodonor racemic bidentate ligands. Strong coordination of the reactants led to catalyst poisoning and hence the products could not be obtained in an enantioenriched form. A racemic phosphine-phosphino-sulfide palladium complex generated *via* the above protocol was applied successfully as a catalyst in the synthesis of a series of enaminones under mild conditions.

4.4 Experimental

General Procedure for the Synthesis of Substrates, 21, 25 and 32. *Rac*-catalyst **9** (7.00 mg, 5 mol%) was added to a solution of diphenylphosphine (29.8 mg, 0.16 mmol) in dry and degassed DCM (5 mL). The mixture was subsequently cooled to -60 °C before the addition of substrate **24** (0.16 mmol) and NEt_3 (16.2 mg, 0.16 mmol). The reaction mixture was then stirred for 48 h. S_8, Se or H_2O_2 (0.18 mmol) was added to the crude mixture and stirred until the reaction completed. The solution was purified directly by column chromatography on silica gel to provide the products.

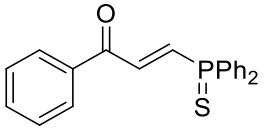

21

White Solid; Eluent system (silica column chromatography): DCM/Hex (1:1); Yield: (60%) ^{1}H NMR (400 MHz, CD_2Cl_2): δ 7.50-7.66 (m, 9H, Ar*H*, HCC*H*), 7.73-7.85 (m, 5H, Ar*H*), 8.00-8.09 (m, 3H, Ar*H*); ^{13}C{^{1}H} NMR (100 MHz, CD_2Cl_2): δ 129.24 (d, J_{CP} = 4.9 Hz, CO*C*HCH), 129.32 (d, J_{CP} = 4.9 Hz, COCH*C*H), 131.82 (d, J_{CP} = 10.8 Hz), 132.10 (s, Ar*C*), 132.41 (d, J_{CP} = 3.0 Hz, Ar*C*), 132.97 (s, Ar*C*), 134.24 (s, Ar*C*), 137.00 (s, Ar*C*), 137.21 (s, Ar*C*), 137.98 (s, Ar*C*), 140.47 (d, J_{CP} = 5.4 Hz, Ar*C*), 188.69 (d, J_{CP} = 18.0 Hz, *C*O); ^{31}P{^{1}H} NMR (161 MHz, CD_2Cl_2): δ 35.86; HRMS (ESI)m/z[positive mode] calcd. for $C_{21}H_{18}OPS$ 349.0816, found 349.0816.

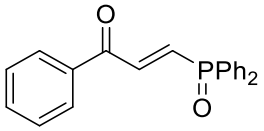

25

White Solid; Eluent system (silica column chromatography): DCM/Hex (1:1); Yield: (60%) ^{1}H NMR (400 MHz, CD_2Cl_2): δ 7.50-7.66 (m, 10H, Ar*H*, HCC*H*), 7.71-7.76 (m, 4H, Ar*H*), 7.93-8.03 (m, 3H, Ar*H*); ^{13}C{^{1}H} NMR (100 MHz, CD_2Cl_2): δ 129.24 (d, J_{CP} = 7.9 Hz, CO*C*HCH), 129.32 (s, Ar*C*), 131.59 (d, J_{CP} = 10.0 Hz, COCH*C*H), 131.82 (s, Ar*C*), 132.70 (d, J_{CP} = 2.7 Hz, Ar*C*), 134.21 (s, Ar*C*), 136.74 (s, Ar*C*), 136.92 (s, Ar*C*), 137.67 (s, Ar*C*), 139.84 (d, J_{CP} = 2.0 Hz, Ar*C*), 188.59 (d, J_{CP} = 16.4 Hz, *C*O); ^{31}P{^{1}H} NMR (161 MHz, CD_2Cl_2): δ 21.38; HRMS (ESI)m/z[positive mode] calcd. for $C_{21}H_{18}O_2P$ 333.1044, found 333.1044.

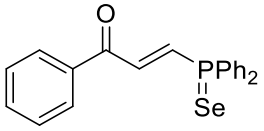

32

White Solid; Eluent system (silica column chromatography): DCM/Hex (1:1); Yield: (60%) ^{1}H NMR (400 MHz, CD_2Cl_2): δ 7.48-7.66 (m, 9H, Ar*H*, HCC*H*), 7.70-7.99 (m, 8H, Ar*H*); ^{13}C{^{1}H} NMR (100 MHz, CD_2Cl_2): δ 129.26 (s, Ar*C*), 129.34 (d, J_{CP} = 6.1 Hz, CO*C*HCH), 131.68 (s, Ar*C*), 132.31 (d, J_{CP} = 11.1 Hz, COCH*C*H), 132.48 (d, J_{CP} = 3.0 Hz, Ar*C*), 134.27 (s, Ar*C*), 136.17 (s, Ar*C*), 136.86 (s, Ar*C*), 136.98 (d, J_{CP} = 1.3 Hz, Ar*C*), 141.32 (d, J_{CP} = 6.0 Hz, Ar*C*), 188.60 (d, J_{CP} = 18.5 Hz, *C*O); ^{31}P{^{1}H} NMR (161 MHz, CD_2Cl_2): δ 27.96; HRMS (ESI)m/z[positive mode] calcd. for $C_{21}H_{18}OPSe$ 397.0260, found 397.0265.

General Procedure for the Synthesis of Complexes, 26–29, 33 and 34. Chalcogenide substrate (0.16 mmol) was added to a solution of secondary phosphines (0.16 mmol) in dry and degassed DCM (3 mL). The reaction mixture was then stirred for 2 h. $PdCl_2(NCMe)_2$ (41.5 mg, 0.16 mmol) was added to the crude mixture and stirred until the reaction completed. The solution was purified directly by column chromatography on silica gel to provide the products.

General Procedure for the Synthesis of Substrates, 30 and 31. Substrate **21** (55.7 mg, 0.16 mmol) was added to a solution of secondary phosphines (0.16 mmol) in dry and degassed DCM (3 mL). The reaction mixture was then stirred for 9 h. $PdCl_2(NCMe)_2$ (41.5 mg, 0.16 mmol) was added to the crude mixture and stirred until the reaction completed. The solution was purified directly by column chromatography on silica gel to provide the products.

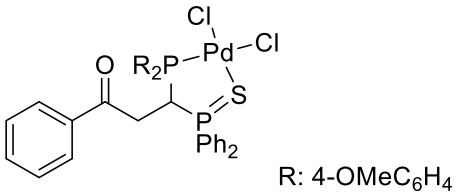

26

Yellow Solid; Eluent system (silica column chromatography): DCM; Yield: 111.2 mg (90%); ^{1}H NMR (400 MHz, CD_2Cl_2): δ 2.89-3.03 (m, 1H, C*H*H), 3.51 (s, 3H, C*H*$_3$), 3.71-3.86 (m, 4H, C*H*$_3$, C*H*), 5.10-5.17 (m, 1H, C*H*H), 6.57 (dd, J_{HH} = 8.9 Hz, J_{HH} = 2.1, Ar*H*), 6.83 (dd, J_{HH} = 8.9 Hz, J_{HH} = 2.1, Hz Ar*H*), 7.29-7.91 (m, 17H, Ar*H*), 8.07-8.12 (m, 2H, Ar*H*); ^{13}C{^{1}H} NMR (100 MHz, CD_2Cl_2): δ 35.45 (s, CO*C*H$_2$CH), 45.70 (s, COCH$_2$*C*H), 50.88 (s, *C*H$_3$), 55.53 (s, *C*H$_3$), 55.98 (s, Ar*C*), 114.17 (d, J_{CP} = 13.4 Hz, Ar*C*), 114.93(d, J_{CP} = 13.0 Hz, Ar*C*), 116.31 (s, Ar*C*), 116.95 (s, Ar*C*), 123.85 (s, Ar*C*), 124.29 (s, Ar*C*), 125.13 (s, Ar*C*) 128.28 (s, Ar*C*), 128.69 (s, Ar*C*), 129.52 (d, J_{CP} = 13.1 Hz, Ar*C*), 130.21 (d, J_{CP} = 12.4 Hz, Ar*C*), 132.58 (d, J_{CP} = 9.8 Hz, Ar*C*), 132.80 (d, J_{CP} = 10.4 Hz, Ar*C*), 133.71 (d, J_{CP} = 3.0 Hz, Ar*C*), 134.36(s, Ar*C*), 134.98 (s, Ar*C*), 137.19 (d, J_{CP} = 13.4 Hz, Ar*C*), 138.00 (d, J_{CP} = 13.2 Hz, Ar*C*), 162.85 (d, J_{CP} = 27.0 Hz, Ar*C*), 194.47 (s, *C*O); ^{31}P{^{1}H} NMR (161 MHz, CD_2Cl_2): δ 41.67 (d, J_{PP} = 52.1 Hz, *P*=S), 62.37 (d, J_{PP} = 52.2 Hz, *P*–Pd); HRMS (ESI)m/z[positive mode] calcd. for $C_{35}H_{33}O_3P_2SCl_2Pd$ 771.0038, found 771.0044.

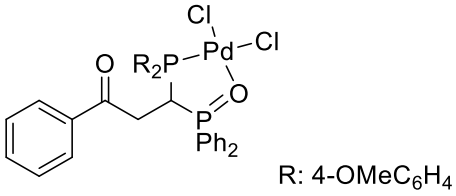

27

Orange Solid; Eluent system (silica column chromatography): DCM/MeOH (49:1); Yield: 114.9 mg (95%); ^{1}H NMR (400 MHz, CD_2Cl_2): δ 2.82-2.96 (m, 1H, C*H*H), 3.53 (s, 3H, C*H*$_3$),

3.63-3.75 (m, 1H, C*H*), 3.85 (s, 3H, C*H*$_3$), 4.36-4.43 (m, 1H, C*H*H), 6.59 (dd, J_{HH} = 8.9 Hz, J_{HH} = 2.1 Hz, Ar*H*), 6.88 (dd, J_{HH} = 8.9 Hz, J_{HH} = 2.1 Hz, Ar*H*), 7.31-7.58 (m, 11H, Ar*H*), 7.76-7.91 (m, 6H, Ar*H*), 8.10-8.15 (m, 2H, Ar*H*); $^{13}C\{^1H\}$ NMR (100 MHz, CD_2Cl_2): δ 34.57 (s, CO*C*H$_2$CH), 39.30 (d, J_{CP} = 14.6 Hz, COCH$_2$*C*H), 39.95 (d, J_{CP} = 14.9 Hz, Ar*C*), 55.60 (s, *C*H$_3$), 56.00 (s, *C*H$_3$), 114.31 (d, J_{CP} = 13.7 Hz, Ar*C*), 115.06 (d, J_{CP} = 13.0 Hz, Ar*C*), 116.41 (s, Ar*C*), 128.22 (s, Ar*C*), 128.68 (s, Ar*C*), 129.58 (d, J_{CP} = 12.5 Hz, Ar*C*), 129.93 (d, J_{CP} = 12.8 Hz, Ar*C*), 131.83 (d, J_{CP} = 9.9 Hz, Ar*C*), 132.06 (d, J_{CP} = 10.3 Hz, Ar*C*), 133.89 (d, J_{CP} = 2.5 H, Ar*C* z), 134.30 (s, Ar*C*), 134.40 (d, J_{CP} = 2.5 H, Ar*C* z), 134.97 (s, Ar*C*), 137.26 (s, Ar*C*), 137.38 (s, Ar*C*), 137.51 (s, Ar*C*), 163.08 (d, J_{CP} = 2.7 Hz, Ar*C*), 163.14 (d, J_{CP} = 2.8 Hz, Ar*C*), 194.62 (d, J_{CP} = 2.1 Hz, Ar*C*), 194.73 (d, J_{CP} = 2.0 Hz, *C*O); $^{31}P\{^1H\}$ NMR (161 MHz, CD_2Cl_2): δ 29.99 (d, J_{PP} = 29.7 Hz, *P*=O), 67.50 (d, J_{PP} = 30.1 Hz, *P*–Pd); HRMS (ESI)m/z[positive mode] calcd. for $C_{35}H_{33}O_4P_2Cl_2Pd$ 755.0266, found 755.0270.

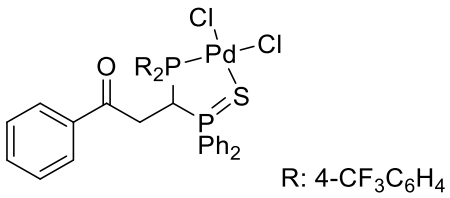

28

Yellow Solid; Eluent system (silica column chromatography): DCM; Yield: 40.7 mg (30%); ^1H NMR (400 MHz, CD_2Cl_2): δ 2.99-3.13 (m, 1H, C*H*H), 3.88-3.98 (m, 1H, C*H*H), 5.18-5.26 (m, 1H, C*H*), 7.27-7.65 (m, 15H, Ar*H*), 7.84-8.02 (m, 6H, Ar*H*), 8.40-8.45 (m, 2H, Ar*H*); $^{13}C\{^1H\}$ NMR (100 MHz, CD_2Cl_2): δ 35.31 (s, CO*C*H$_2$CH), 45.19 (s, COCH$_2$*C*H), 45.38 (s, *C*F$_3$), 45.71 (s, *C*F$_3$), 45.90 (s, Ar*C*), 123.53 (d, J_{CP} = 11.9 Hz, Ar*C*), 123.55 (s, Ar*C*), 125.38 (d, J_{CP} = 3.7 Hz, Ar*C*), 125.50 (d, J_{CP} = 3.7 Hz, Ar*C*), 126.11 (d, J_{CP} = 3.7 Hz, Ar*C*), 126.23 (d, J_{CP} = 3.7 Hz, Ar*C*), 128.09 (s, Ar*C*), 129.04 (s, Ar*C*), 129.79 (d, J_{CP} = 12.8 Hz, Ar*C*), 130.50 (d, J_{CP} = 12.5 Hz, Ar*C*), 132.74 (d, J_{CP} = 10.1 Hz, Ar*C*), 133.10 (d, J_{CP} = 10.3 Hz, Ar*C*), 133.63

(d, J_{CP} = 3.5 Hz, Ar*C*), 133.96 (d, J_{CP} = 3.1 Hz, Ar*C*),134.42 (s, Ar*C*), 134.92 (d, J_{CP} = 3.0 Hz, Ar*C*), 134.97 (s, Ar*C*), 135.87 (d, J_{CP} = 12.6 Hz, Ar*C*), 137.12 (d, J_{CP} = 12.3 Hz, Ar*C*), 194.22 (d, J_{CP} = 12.6 Hz, *C*O); $^{31}P\{^{1}H\}$ NMR (161 MHz, CD_2Cl_2): δ 42.01 (d, J_{PP} = 57.3 Hz, *P*=S), 63.10 (d, J_{PP} = 57.3 Hz, *P*–Pd); $^{19}F\{^{1}H\}$ (376 MHz, CD_2Cl_2) -63.89 (s), -63.84 (s); HRMS (ESI)m/z[positive mode] calcd. for $C_{35}H_{27}OP_2SCl_2PdF_6$ 846.9574, found 846.9581.

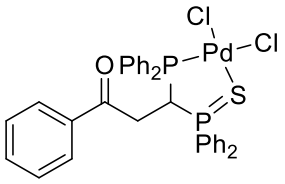

29

Yellow Solid; Eluent system (silica column chromatography): DCM; Yield: 96.8 mg (85%) ^{1}H NMR (400 MHz, CD_2Cl_2): δ 2.98-3.12 (m, 1H, C*H*H), 3.72-3.83 (m, 1H, C*H*H), 5.18-5.26 (m, 1H, C*H*), 7.07-7.14 (m, 3H, Ar*H*), 7.25-7.56 (m, 14H, Ar*H*), 7.79-7.91 (m, 6H, Ar*H*), 8.18-8.23 (m, 2H, Ar*H*); $^{13}C\{^{1}H\}$ NMR (100 MHz, CD_2Cl_2): δ 35.53 (s, CO*C*H_2CH), 44.57 (s, COCH$_2$*C*H), 44.77 (s, Ar*C*), 45.09 (s, Ar*C*), 45.29 (s, Ar*C*), 123.81 (s, Ar*C*), 125.46 (s, Ar*C*) 128.19 (s, Ar*C*), 128.63 (d, J_{CP} = 12.1 Hz, Ar*C*), 128.78 (s, Ar*C*), 129.30 (d, J_{CP} = 11.6 Hz, Ar*C*), 129.60 (d, J_{CP} = 12.9 Hz, Ar*C*), 130.23 (d, J_{CP} = 12.4 Hz, Ar*C*), 132.24 (d, J_{CP} = 2.8 Hz, Ar*C*), 132.63 (d, J_{CP} = 3.0 Hz, Ar*C*), 132.64 (d, J_{CP} = 10.0 Hz, Ar*C*), 132.85 (d, J_{CP} = 10.4 Hz, Ar*C*), 134.03 (d, J_{CP} = 3.0 Hz, Ar*C*), 134.48 (s, Ar*C*), 134.83 (s, Ar*C*), 135.41 (d, J_{CP} = 11.8 Hz, Ar*C*), 136.27 (d, J_{CP} = 11.5 Hz, Ar*C*), 194.24 (d, J_{CP} = 10.8 Hz, *C*O); $^{31}P\{^{1}H\}$ NMR (161 MHz, CD_2Cl_2): δ 43.66 (d, J_{PP} = 51.7 Hz, *P*=S), 62.97 (d, J_{PP} = 54.8 Hz, *P*–Pd); HRMS (ESI)m/z[positive mode] calcd. for $C_{33}H_{29}OP_2SCl_2Pd$ 710.9826, found 710.9832.

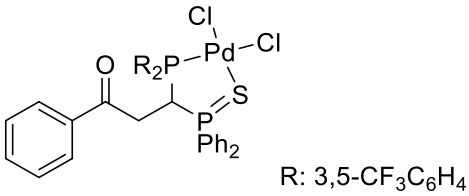

30

Yellow Solid; Eluent system (silica column chromatography): DCM/EA (19:1); Yield: 85.0 mg (54%) ^{1}H NMR (400 MHz, CD_2Cl_2): δ 3.04-3.19 (m, 1H, C*H*H), 3.81-3.91 (m, 1H, C*H*H), 5.22-5.29 (m, 1H, C*H*), 7.31-7.69 (m, 12H, Ar*H*), 7.88-8.04 (m, 5H, Ar*H*), 8.16 (d, 2H, J_{HH} = 12.2 Hz, Ar*H*), 8.80 (d, 2H, J_{HH} = 11.4 Hz, Ar*H*); ^{13}C{^{1}H} NMR (100 MHz, CD_2Cl_2): δ 35.13 (s, CO*C*H$_2$CH), 45.40 (s, COCH$_2$*C*H), 45.60 (s, *C*F$_3$), 45.92 (s, *C*F$_3$), 46.12 (s, *C*F$_3$), 123.26 (s, *C*F$_3$), 123.99 (d, J_{CP} = 14.9 Hz, Ar*C*), 126.44 (d, J_{CP} = 4.4 Hz, Ar*C*), 127.02 (d, J_{CP} = 3.5 Hz, Ar*C*), 128.12 (s, Ar*C*), 129.27 (s, Ar*C*), 130.00 (d, J_{CP} = 12.9 Hz, Ar*C*), 130.74 (d, J_{CP} = 12.7 Hz, Ar*C*), 131.78 (d, J_{CP} = 12.2 Hz, Ar*C*), 132.12 (d, J_{CP} = 12.3 Hz, Ar*C*), 132.79 (d, J_{CP} = 10.4 Hz, Ar*C*), 133.26 (d, J_{CP} = 10.2 Hz, Ar*C*), 133.80 (s, Ar*C*), 135.01 (s, Ar*C*), 135.17 (s, Ar*C*), 135.37 (d, J_{CP} = 3.0 Hz, Ar*C*), 135.53 (s, Ar*C*), 136.02 (d, J_{CP} = 4.1 Hz, Ar*C*), 136.15 (d, J_{CP} = 2.8 Hz, Ar*C*), 194.12 (d, J_{CP} = 12.2 Hz, *C*O); ^{31}P{^{1}H} NMR (161 MHz, CD_2Cl_2): δ 41.31 (d, J_{PP} = 62.4 Hz, *P*=S), 63.03 (d, J_{PP} = 59.6 Hz, *P*–Pd); ^{19}F{^{1}H} (376 MHz, CD_2Cl_2) -63.48 (s), -63.23 (s); HRMS (ESI)m/z[positive mode] calcd. for $C_{37}H_{25}OP_2SCl_2PdF_{12}$ 982.9322, found 982.9329.

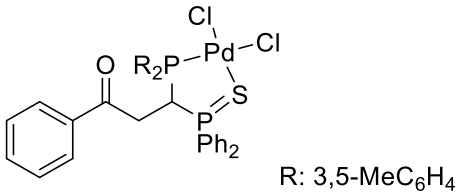

31

Yellow Solid; Eluent system (silica column chromatography): DCM; Yield: 79.9 mg (65%) ^{1}H NMR (400 MHz, CD_2Cl_2): δ 2.03 (s, 3H, C*H*$_3$), 2.32 (s, 3H, C*H*$_3$), 2.89-3.03 (m, 1H, C*H*H), 3.84-3.95 (m, 1H, C*H*H), 5.12-5.19 (m, 1H, C*H*), 6.63 (s, 1H, Ar*H*), 6.7.04 (s, 1H, Ar*H*), 7.27-7.31 (m, 2H, Ar*H*), 7.34-7.40 (m, 5H, Ar*H*), 7.48-7.58 (m, 6H, Ar*H*), 7.71-7.89 (m, 6H, Ar*H*); ^{13}C{^{1}H} NMR (100 MHz, CD_2Cl_2): δ 21.18 (s, *C*H$_3$), 21.47 (s, *C*H$_3$), 35.56 (s, CO*C*H$_2$CH), 45.21 (s, *C*H$_3$), 45.54 (s, *C*H$_3$), 45.78 (d, J_{CP} = 7.2 Hz, COCH$_2$*C*H), 127.99 (s, Ar*C*), 128.75 (s, Ar*C*), 129.07 (d, J_{CP} = 13.2 Hz, Ar*C*), 130.22 (d, J_{CP} = 12.4 Hz, Ar*C*), 130.24 (s, Ar*C*), 132.57 (s, Ar*C*), 132.67 (s, Ar*C*), 132.69 (s, Ar*C*), 132.80 (s, Ar*C*), 133.71 (d, J_{CP} = 11.2 Hz, Ar*C*), 133.73 (s, Ar*C*), 134.02 (d, J_{CP} = 2.5 Hz, Ar*C*), 134.36 (s, Ar*C*), 134.40 (s, Ar*C*), 134.46 (d, J_{CP} = 2.6 Hz, Ar*C*), 135.10 (s, Ar*C*), 138.67 (d, J_{CP} = 12.4 Hz, Ar*C*), 139.03 (d, J_{CP} = 12.3 Hz, Ar*C*), 193.95 (d, J_{CP} = 12.2 Hz, *C*O); ^{31}P{^{1}H} NMR (161 MHz, CD_2Cl_2): δ 43.87 (d, J_{PP} = 52.0 Hz, *P*=S), 62.72 (d, J_{PP} = 52.3 Hz, *P*–Pd); HRMS (ESI)m/z[positive mode] calcd. for $C_{37}H_{37}OP_2SCl_2Pd$ 767.0452, found 767.0460.

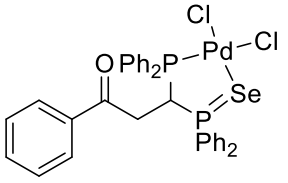

33

Yellow Solid; Eluent system (silica column chromatography): DCM; Recrystallized from *n*-hexanes and $CHCl_2$: Yield: 9.7 mg (8%)(recrystallized yield); ^{1}H NMR (400 MHz, CD_2Cl_2): δ

3.05-3.20 (m, 1H, C*H*H), 3.71-3.81 (m, 1H, C*H*), 5.72-5.80 (m, 1H, C*H*H), 6.71-7.53 (m, 16H, Ar*H*), 7.75-8.21 (m, 9H, Ar*H*); $^{31}P\{^{1}H\}$ NMR (161 MHz, CD_2Cl_2): δ 45.56 (d, J_{PP} = 62 Hz, *P*=Se), 49.03 (d, J_{PP} = 62 Hz, *P*–Pd); HRMS (ESI)m/z[positive mode] calcd. for $C_{33}H_{29}OP_2Cl_2SePd$ 758.9271, found 758.9279.

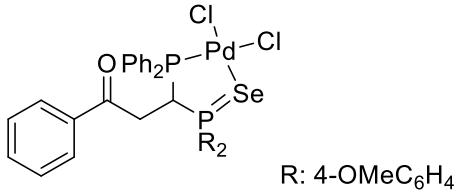

34

Yellow Solid; Eluent system (silica column chromatography): DCM/MeOH (99:1); Yield: 21.0 mg (16%)(recrystallized yield); ^{1}H NMR (400 MHz, CD_2Cl_2): δ 3.09-3.23 (m, 1H, C*H*H), 3.61-3.71 (m, 1H, C*H*), 3.74 (s, 3H, CH_3), 3.82 (s, 3H, CH_3), 5.55-5.62 (m, 1H, C*H*H), 6.73 (dd, J_{HH} = 8.9 Hz, J_{HH} = 2.7 Hz, Ar*H*), 6.89 (dd, J_{HH} = 9.0 Hz, J_{HH} = 2.6 Hz, Ar*H*), 7.10-7.16 (m, 3H, Ar*H*), 7.32-7.55 (m, 8H, Ar*H*), 7.65-7.89 (m, 6H, Ar*H*), 8.14-8.19 (m, 2H, Ar*H*); $^{13}C\{^{1}H\}$ NMR (100 MHz, CD_2Cl_2): δ 36.13 (s, CO*C*H_2CH), 46.71 (s, COCH$_2$*C*H), 46.91 (s, *C*H_3), 56.09 (s, *C*H_3), 115.22 (d, J_{CP} = 13.9 Hz, Ar*C*), 115.69 (d, J_{CP} = 13.6 Hz, Ar*C*),126.15 (s, Ar*C*), 126.72 (s, Ar*C*), 128.19 (s, Ar*C*), 128.56 (d, J_{CP} = 11.7 Hz, Ar*C*), 128.77 (s, Ar*C*), 129.09 (d, J_{CP} = 11.5 Hz, Ar*C*), 132.00 (d, J_{CP} = 2.1 Hz, Ar*C*), 132.18 (d, J_{CP} = 2.2 Hz, Ar*C*), 134.41 (s, Ar*C*), 135.00 (s, Ar*C*), 135.11 (s, Ar*C*), 135.24 (d, J_{CP} = 2.4 Hz, Ar*C*), 135.37 (s, Ar*C*), 135.66 (d, J_{CP} = 11.9 Hz, Ar*C*), 136.23 (d, J_{CP} = 11.5 Hz, Ar*C*), 164.04 (d, J_{CP} = 3.3 Hz, Ar*C*), 164.51 (d, J_{CP} = 2.2 Hz, Ar*C*), 194.21 (d, J_{CP} = 2.5 Hz, Ar*C*), 194.30 (d, J_{CP} = 3.3 Hz, *C*O); $^{31}P\{^{1}H\}$ NMR (161 MHz, CD_2Cl_2): δ 44.74 (d, J_{PP} = 59.9 Hz, *P*=Se), 46.33 (d, J_{PP} = 62.1 Hz, *P*–Pd); HRMS (ESI)m/z[positive mode] calcd. for $C_{35}H_{33}O_3P_2Cl_2PdSe$ 818.9482 found 818.9493.

4.5 References

1. H. B. Kagan; T.-P. Dang, *Asymmetric catalytic reduction with transition metal complexes. I. Catalytic system of rhodium(I) with (-)-2,3-0-isopropylidene-2,3-dihydroxy-1,4-bis(diphenylphosphino)butane, a new chiral diphosphine*, *J. Am. Chem. Soc.* **1972**, *94*, 6429.

2. T. Imamoto, *Searching for Practically Useful P-Chirogenic Phosphine Ligands*, *Chem. Rec.* **2016**, *16*, 2659.

3. (a) B. D. Vineyard; W. S. Knowles; M. J. Sabacky; G. L. Bachman; D. J. Weinkauff, *Asymmetric hydrogenation. Rhodium chiral bisphosphine catalyst, J. Am. Chem. Soc.* **1977**, *99*, 5946; (b) A. Miyashita; A. Yasuda; H. Takaya; K. Toriumi; T. Ito; T. Souchi; R. Noyori, *Synthesis of 2,2'-bis(diphenylphosphino)-1,1'-binaphthyl (BINAP), an atropisomeric chiral bis(triaryl)phosphine, and its use in the rhodium(I)-catalyzed asymmetric hydrogenation of .alpha.-(acylamino)acrylic acids*, *J. Am. Chem. Soc.* **1980**, *102*, 7932; (c) M. J. Burk; C. S. Kalberg; A. Pizzano, *Rh−DuPHOS-Catalyzed Enantioselective Hydrogenation of Enol Esters. Application to the Synthesis of Highly Enantioenriched α-Hydroxy Esters and 1,2-Diols*, *J. Am. Chem. Soc.* **1998**, *120*, 4345; (d) M. J. Burk, *C2-symmetric bis(phospholanes) and their use in highly enantioselective hydrogenation reactions*, *J. Am. Chem. Soc.* **1991**, *113*, 8518; (e) Q. Jiang; Y. Jiang; D. Xiao; P. Cao; X. Zhang, *Highly Enantioselective Hydrogenation of Simple Ketones Catalyzed by a Rh–PennPhos Complex, Angew. Chem. Int. Ed.* **1998**, *37*, 1100.

4. J. K. Whitesell, *C2 symmetry and asymmetric induction*, *Chem. Rev.* **1989**, *89*, 1581.

5. (a) D. Gleich; W. A. Herrmann, *Why Do Many C2-Symmetric Bisphosphine Ligands Fail in Asymmetric Hydroformylation? Theory in Front of Experiment*, *Organometallics* **1999**, *18*, 4354; (b) V. A. Pavlov, *The central chirality of the metal atom and configurational relations in asymmetric reactions catalysed by metal complexes*, *Russ. Chem. Rev.* **2004**, *73*, 1173; (c) V. A. Pavlov, *C2 and C1 Symmetry of chiral auxiliaries in catalytic reactions on metal complexes*, *Tetrahedron* **2008**, *64*, 1147.

6. (a) G. Consiglio; R. M. Waymouth, *Enantioselective homogeneous catalysis involving transition-metal-allyl intermediates*, *Chem. Rev.* **1989**, *89*, 257; (b) M. Diéguez; O. Pàmies; A. Ruiz; Y. Díaz; S. Castillón; C. Claver, *Carbohydrate derivative ligands in asymmetric catalysis*, *Coord. Chem. Rev.* **2004**, *248*, 2165; (c) N. Sakai; S. Mano; K. Nozaki; H. Takaya, *Highly enantioselective hydroformylation of olefins catalyzed by new phosphine phosphite-rhodium(I) complexes*, *J. Am. Chem. Soc.* **1993**, *115*, 7033; (d) A. Pfaltz; W. J. Drury, *Design of chiral ligands for asymmetric catalysis: From C2-symmetric P,P- and N,N-ligands to sterically and electronically nonsymmetrical P,N-ligands*, *Proceedings of the National Academy of Sciences of the United States of America* **2004**, *101*, 5723.

7. (a) J. Holz; R. Kadyrov*; S. Borns; D. Heller; A. Börner*, *Cooperative attractive interactions in asymmetric hydrogenations with dihydroxydiphosphine Rh(I) catalysts — a competition study*, *J. Organomet. Chem.* **2000**, *603*, 61; (b) J.-X. Gao; X.-D. Yi; P.-P. Xu; C.-L. Tang; H.-L. Wan; T. Ikariya, *New chiral cationic rhodium–aminophosphine complexes for asymmetric transfer hydrogenation of aromatic ketones*, *J. Organomet. Chem.* **1999**, *592*, 290.

8. (a) S. Gladiali; S. Medici; T. Kégl; L. Kollàr, *Synthesis, Characterization, and Catalytic Activity of Rh(I) Complexes with (S)-BINAPO, an Axially Chiral Inducer Capable of Hemilabile P,O-Heterobidentate Coordination*, *Monatsh. Chem.* **2000**, *131*, 1351; (b) R. Weber; U. Englert; B. Ganter; W. Keim; M. Möthrath, *Hydroformylation of epoxides catalyzed by cobalt and hemilabile P–O ligands*, *Chem. Commun.* **2000**, 1419.

9. (a) P. Braunstein; M. D. Fryzuk; M. Le Dall; F. Naud; S. J. Rettig; F. Speiser, *Synthesis and structure of Pd(II) complexes containing chelating (phosphinomethyl)oxazoline P,N-type ligands; copolymerisation of ethylene/CO*, *J. Chem. Soc., Dalton Trans.* **2000**, 1067; (b) J. Andrieu; P. Braunstein; F. Naud; R. D. Adams, *Cationic palladium complexes with ketophosphine and phosphino enolate ligands and their reactivity towards C□C coupling*

reactions. Crystal structures of [PdMe{Ph2PCH2C(O)Ph}(PCy3)](PF6) and [Pd{Ph2PCH···C(···Ō)Ph}(SMe2)2](PF6), *J. Organomet. Chem.* **2000**, *601*, 43.

10. E. Lindner; S. Pautz; R. Fawzi; M. Steimann, *Behavior of (Ether−phosphine)ruthenium(II) Complexes [(η6-C6Me6)RuH(P⌒O)][BF4] Containing Reactive Ru−O and Ru−H Bonds toward Various Small Molecules and Their Application in Ring-Opening Metathesis Polymerization*, *Organometallics* **1998**, *17*, 3006.

11. (a) F. Agbossou; J.-F. Carpentier; A. Mortreux, *Asymmetric Hydroformylation*, *Chem. Rev.* **1995**, *95*, 2485; (b) S. Gladiali; J. Carles Bayón; C. Claver, *Recent advances in enantioselective hydroformylation*, *Tetrahedron Asymmetry* **1995**, *6*, 1453.

12. G.-Y. Zhang; C.-K. Li; D.-P. Li; R.-S. Zeng; A. Shoberu; J.-P. Zou, *Solvent-controlled direct radical oxyphosphorylation of styrenes mediated by Manganese(III)*, *Tetrahedron* **2016**, *72*, 2972.

13. X.-L. Wang; J.-X. Chen; X.-S. Jia; L. Yin, *Synthesis of α,β-Unsaturated Phosphine Sulfides*, *Synthesis* **2020**, *52*, 141.

14. L. Feray; P. Perfetti; M. Bertrand, *AlCl3–NaI(NaBr)–t-BuOH: mild, chemo- and stereoselective reagents for hydrohalogenation of propiolic derivatives*, *Tetrahedron* **2009**, *65*, 8733.

15. Y. Huang; R. J. Chew; Y. Li; S. A. Pullarkat; P.-H. Leung, *Direct Synthesis of Chiral Tertiary Diphosphines via Pd(II)-Catalyzed Asymmetric Hydrophosphination of Dienones*, *Org. Lett.* **2011**, *13*, 5862.

16. D. H. Brown; R. J. Cross; R. Keat, *Rapid transfer for selenium from tertiary phosphine selenides to tertiary phosphines*, *J. Chem. Soc., Dalton Trans.* **1980**, 871.

17. (a) A.-Z. Elassar; A. El-Khair, *Recent Developments in the Chemistry of Enaminones*, *Tetrahedron* **2003**, *59*, 8463; (b) Y. Huang a; R. W. Hartmann, *The Improved Preparation of 7,8-Dihydro-Quinoline-5(6H)-One and 6,7-Dihydro-5H-1-Pyrindin-5-one*, *Synth. Commun.*

1998, *28*, 1197; (c) N. D. Eddington; D. S. Cox; R. R. Roberts; J. P. Stables; C. B. Powell; K. R. Scott, *Enaminones-versatile therapeutic pharmacophores. Further advances*, *Current medicinal chemistry* **2000**, *7*, 417; (d) J. W. K. Seah; Y. Li; S. A. Pullarkat; P.-H. Leung, *Access to a Chiral Phosphine–NHC Palladium(II) Complex via the Asymmetric Hydrophosphination of Achiral Vinyl Azoles*, *Organometallics* **2021**, *40*, 2118.

18. (a) C. P. Cartaya-Marin; D. G. Henderson; R. W. Soeder; A. J. Zapata, *Synthesis of Enaminones Using Trimethylsilyl Trifluoromethanesulfonate as an Activator*, *Synth. Commun.* **1997**, *27*, 4275; (b) D. Mulzac; K. R. Scott, *Profile of anticonvulsant activity and minimal toxicity of methyl 4-[(p-chlorophenyl)amino]-6-methyl-2-oxo-cyclohex-3-en-1-oate and some prototype antiepileptic drugs in mice and rats*, *Epilepsia* **1993**, *34*, 1141.

19. P. G. Baraldi; D. Simoni; S. Manfredini, *An Improved Preparation of Enaminones from 1,3-Diketones and Ammonium Acetate or Amine Acetates*, *Synthesis* **1983**, *1983*, 902.

20. J. P. Michael; C. B. d. Koning; D. Gravestock; G. D. Hosken; A. S. Howard; C. M. Jungmann; R. W. M. Krause; A. S. Parsons; S. C. Pelly; T. V. Stanbury, *Enaminones: versatile intermediates for natural product synthesis*, *Pure Appl. Chem.* **1999**, *71*, 979.

Chapter V

Conclusion and Future Work

5.1 Conclusions

Asymmetic hydrophosphination was successfully employed as an unprecedented tool in the syntheses of *P**-chiral diphosphines. Optimization of the reaction conditions was successful and the generation of *P** chiral diphosphines in high yields and enantioselectivities was achieved. In addition, application of the methodology was extended to natural diketones such as curcumin and its derivatives to afford chiral diphosphines which were then transformed into the corresponding gold complexes. These gold complexes were evaluated against cisplatin in a biological study as cytotoxic agents in two selected cancer cell lines.

5.1.1 C_2- Symmetric *P**-Diphosphines *via* Catalytic Asymmetric Hydrophosphination

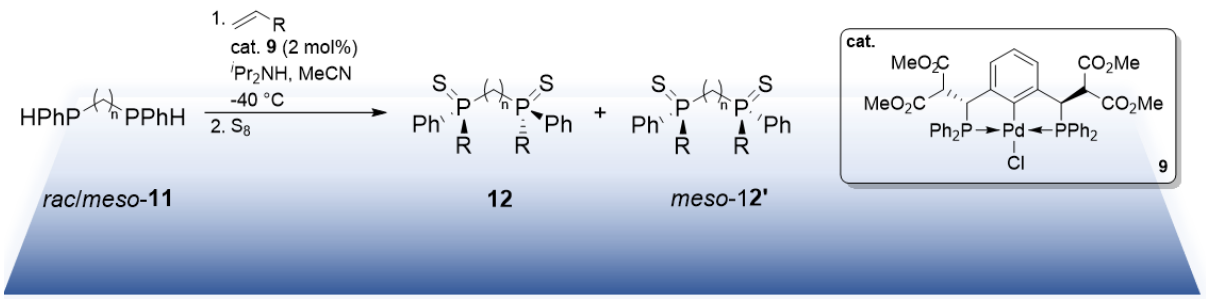

- *Generation of chiral free 1,2-diphosphines from rac/meso secondary diphosphines*
- *Up to >99% e.e. and 44% d.e.*
- *Can be extended to free P- and C-chiral 1,2-diphosphines*
- *One-pot two-step access to chiral 1,2-diphosphine complexes*

Scheme 57. Catalytic asymmetric dihydrophosphination reaction to generate *P*-chiral diphosphines.

Enantioenriched diphosphines of up to 99% *ee* and 44% *de* were obtained in the catalytic asymmetric hydrophosphination of activated olefins by *rac*-diphosphines catalyzed by **9**. The free diphosphines products were successfully complexed to palladium(II) metal center in a one-pot manner and the chiral complexes were separated from the *meso* complexes *via* simple silica column chromatography. This direct, efficient and atom economical protocol could tolerate a variety of activated olefins and be extended to the synthesis of challenging *P,C*-chiral diphosphines.

5.1.2 Catalytic Asymmetric Hydrophosphination as a Valuable Tool to Access Mono- and Di-Hydrophosphinated Curcuminoids

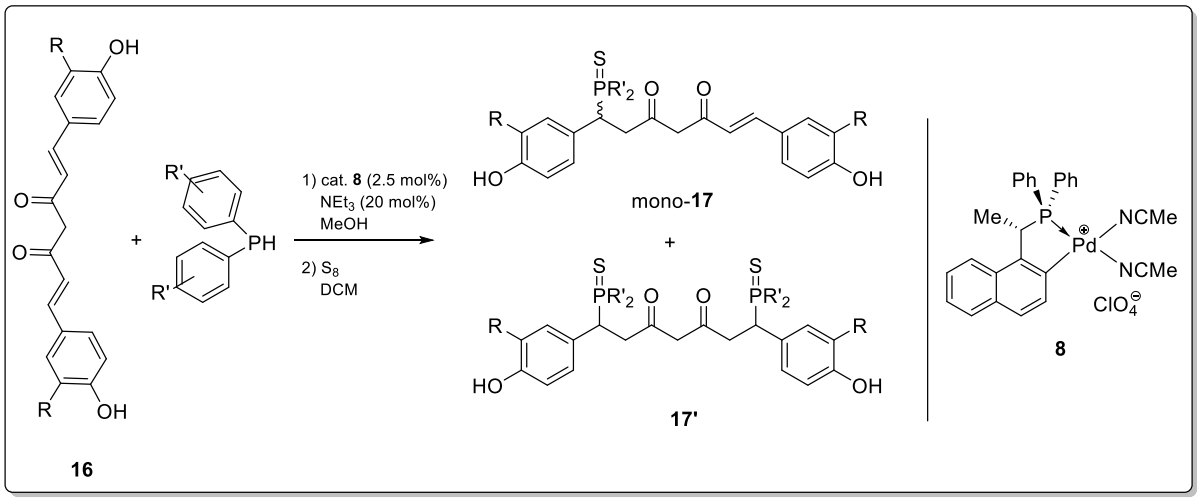

Scheme 58. Catalytic asymmetric mono– and di-hydrophosphination reactions to generate functionalized Cur compounds.

The incorporation of phosphorus-based functional groups into the carbon-backbone of Cur and BDMC was successfully achieved with the concomitant generation of two chiral centers. The asymmetric dihydrophosphination reaction genearted functionalized Cur of up to 95% *ee*. *Meso* diphenylphosphine-functionalized Cur gold(I) complex **18aa**' was also found to exhibit high anti-cancer activity against stomach cancer cells (MKN47), comparable to that of

pure Cur and cisplatin at the 24-hour standpoint. On the other hand, *rac* diphenylphosphine-functionalized Cur gold(I) complex **18aa** was not effective in reducing both MKN47 and MCF-7 cell viability.

5.1.3 Synthesis and Application of Phosphine-(Phosphino Chalcogenide) Ligands

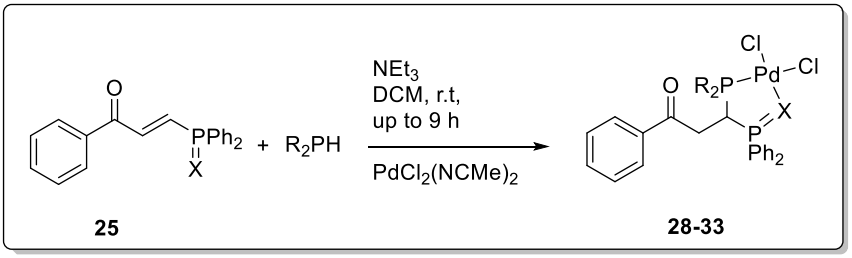

Scheme 59. Hydrophosphination reactions to generate heteroatoms diphosphines.

C$_1$-symmetrical bidentate ligands consisting of phosphorus and phosphino-chalcogenide donor atoms were synthesized under mild reaction conditions within nine hours. Interesting result was observed for the phosphine-selenide hydrophosphination reaction as selenium migration was detected alongside the formation of four other products. Tests performed on complex **26** showed that the phosphine-palladium bond was stable to oxidants and that the sulfur donor was a strong *trans*-effecter that readily labilized the *trans* chloride ligand. Lastly, complex **26** showed moderate catalytic activities in the synthesis of enaminones *via* a direct metal-catalyzed Michael addition under very mild reaction conditions.

5.2 Future Work – Asymmetric Boronic Acid Conjugate Addition

The syntheses of palladium(II) complexes in chapter II could find utility in the generation of *β*-substituted carbonyl compounds *via* catalytic asymmetric boronic acid addition reactions. There has been extensive research being devoted to the development of the asymmetric syntheses of *β*-substituted carbonyl compounds due to their valuable synthetic intermediatory status.[1] Many synthetic protocols of such carbonyl compounds require the use

of either highly reactive copper-based organometallic reagents,[1a] which necessitates the use of cryogenic temperatures and rigorously anhydrous conditions, or rhodium catalysts, which are costly and air sensitive.[2] Currently, palladium–catalyzed asymmetric boronic acid conjugate addition reactions are less well-known than their rhodium and copper counterparts and given the high atmospheric stability and tolerance of palladium complexes towards a wide range of boronic acids, these complexes are slowly finding applications in boronic acid conjugate addition reactions.[2] In view of this slow progress, the suitability of palladium(II) complexes containing *P*-chiral diphosphines in the asymmetric catalysis of boronic acid conjugate addition should be assessed and be compared to existing catalysts so as to expand the current methodologies associated with this class of reaction. Our group has reported the use of palladium catalyst in the asymmetric coupling reaction boronic acid and imine,[3] and this represents a promising application of our palladium catalyst

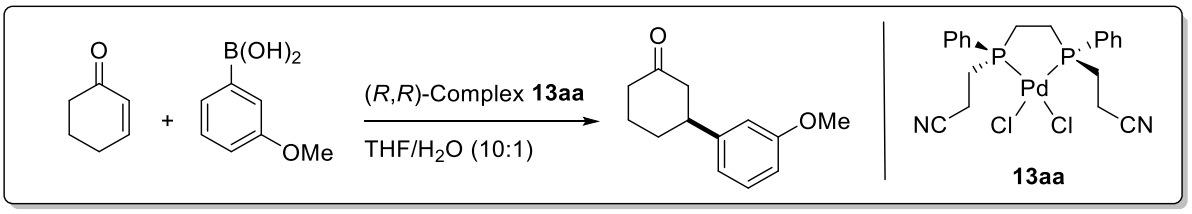

Scheme 60. Catalytic asymmetric conjugation addition reaction.

5.3 References

1. (a) T. Nishikata; Y. Yamamoto; I. D. Gridnev; N. Miyaura, *Enantioselective 1,4-Addition of Ar3Bi, [ArBF3]K, and ArSiF3 to Enones Catalyzed by a Dicationic Palladium(II)−Chiraphos or −Dipamp Complex*, *Organometallics* **2005**, *24*, 5025; (b) K. Majima; R. Takita; A. Okada; T. Ohshima; M. Shibasaki, *Catalytic Asymmetric Michael Reaction of β-Keto Esters: Effects of the Linker Heteroatom in Linked-BINOL*, *J. Am. Chem. Soc.* **2003**, *125*, 15837.

2. S. E. Shockley; J. C. Holder; B. M. Stoltz, *Palladium-Catalyzed Asymmetric Conjugate Addition of Arylboronic Acids to α,β-Unsaturated Cyclic Electrophiles*, *Org. Process Res. Dev.* **2015**, *19*, 974.

3. Y. Huang; L. Wang; J. Li; H. Qiu; P.-H. Leung, *Enantioselective C,P-Palladacycle-Catalyzed Arylation of Imines*, *ACS Omega* **2020**, *5*, 15936.

Appendix

Crystallographic Data

Crystallographic data for compound chiral-12aa

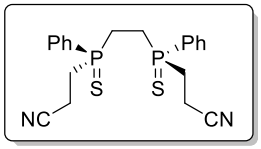

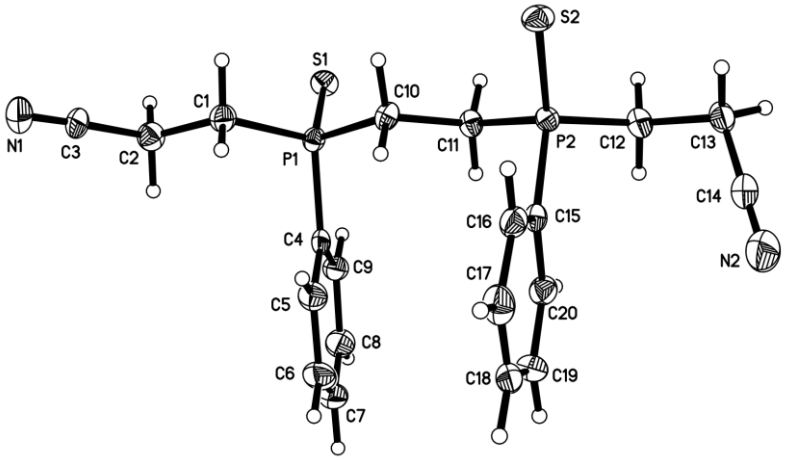

Identification code	leung974m	
Chemical formula	$C_{20}H_{22}N_2P_2S_2$	
Formula weight	416.45 g/mol	
Temperature	100(2) K	
Wavelength	0.71073 Å	
Crystal size	0.040 x 0.080 x 0.340 mm	
Crystal habit	colorless needle	
Crystal system	trigonal	
Space group	P 31	
Unit cell dimensions	a = 14.0913(3) Å	α = 90°
	b = 14.0913(3) Å	β = 90°
	c = 18.7668(3) Å	γ = 120°
Volume	3227.18(15) $Å^3$	
Z	6	
Density (calculated)	1.286 g/cm^3	
Absorption coefficient	0.403 mm^{-1}	
F(000)	1308	

Theta range for data collection	2.74 to 31.02°

Index ranges	-18<=h<=20, -20<=k<=17, -26<=l<=27	
Reflections collected	46046	
Independent reflections	13660 [R(int) = 0.0794]	
Coverage of independent reflections	99.9%	
Absorption correction	Multi-Scan	
Max. and min. transmission	0.9840 and 0.8750	
Structure solution technique	direct methods	
Structure solution program	XT, VERSION 2014/5	
Refinement method	Full-matrix least-squares on F^2	
Refinement program	SHELXL-2016/6 (Sheldrick, 2016)	
Function minimized	$\Sigma\ w(F_o^2 - F_c^2)^2$	
Data / restraints / parameters	13660 / 1 / 470	
Goodness-of-fit on F^2	1.059	
Final R indices	11152 data; $I>2\sigma(I)$	R1 = 0.0498, wR2 = 0.0791
	all data	R1 = 0.0768, wR2 = 0.0911
Weighting scheme	$w=1/[\sigma^2(F_o^2)+(0.0268P)^2]$ where $P=(F_o^2+2F_c^2)/3$	
Absolute structure parameter	-0.02(4)	
Largest diff. peak and hole	0.430 and -0.393 eÅ^{-3}	
R.M.S. deviation from mean	0.085 eÅ^{-3}	

Bond lengths (Å) of compound chiral-12aa

C1-C2	1.498(7)	C1-P1	1.822(6)
C1-H1A	0.99	C1-H1B	0.99
C2-C3	1.489(8)	C2-H2A	0.99
C2-H2B	0.99	C3-N1	1.146(8)
C4-C9	1.388(8)	C4-C5	1.409(7)
C4-P1	1.805(5)	C5-C6	1.390(8)
C5-H5	0.95	C6-C7	1.386(9)
C6-H6	0.95	C7-C8	1.374(9)
C7-H7	0.95	C8-C9	1.390(7)

C8-H8	0.95	C9-H9	0.95
C10-C11	1.521(7)	C10-P1	1.808(5)
C10-H10A	0.99	C10-H10B	0.99
C11-P2	1.814(6)	C11-H11A	0.99
C11-H11B	0.99	C12-C13	1.527(7)
C12-P2	1.809(6)	C12-H12A	0.99
C12-H12B	0.99	C13-C14	1.457(7)
C13-H13A	0.99	C13-H13B	0.99
C14-N2	1.139(7)	C15-C16	1.386(8)
C15-C20	1.398(7)	C15-P2	1.810(5)
C16-C17	1.392(8)	C16-H16	0.95
C17-C18	1.373(9)	C17-H17	0.95
C18-C19	1.375(9)	C18-H18	0.95
C19-C20	1.386(8)	C19-H19	0.95
C20-H20	0.95	C21-N3	1.134(7)
C21-C22	1.488(8)	C22-C23	1.494(7)
C22-H22A	0.99	C22-H22B	0.99
C23-P3	1.823(5)	C23-H23A	0.99
C23-H23B	0.99	C24-C29	1.380(7)
C24-C25	1.383(7)	C24-P3	1.814(5)
C25-C26	1.398(7)	C25-H25	0.95
C26-C27	1.390(9)	C26-H26	0.95
C27-C28	1.375(8)	C27-H27	0.95
C28-C29	1.401(7)	C28-H28	0.95
C29-H29	0.95	C30-C31	1.533(7)
C30-P3	1.817(5)	C30-H30A	0.99
C30-H30B	0.99	C31-P4	1.821(5)
C31-H31A	0.99	C31-H31B	0.99
C32-C33	1.529(7)	C32-P4	1.809(5)
C32-H32A	0.99	C32-H32B	0.99
C33-C34	1.455(7)	C33-H33A	0.99
C33-H33B	0.99	C34-N4	1.128(6)
C35-C40	1.377(7)	C35-C36	1.388(7)
C35-P4	1.810(5)	C36-C37	1.387(8)
C36-H36	0.95	C37-C38	1.381(9)
C37-H37	0.95	C38-C39	1.365(9)
C38-H38	0.95	C39-C40	1.383(7)
C39-H39	0.95	C40-H40	0.95
P1-S1	1.9514(18)	P2-S2	1.956(2)
P3-S3	1.9534(18)	P4-S4	1.9569(19)

Bond angles (°) of compound chiral-12aa

C2-C1-P1	114.3(4)	C2-C1-H1A	108.7
P1-C1-H1A	108.7	C2-C1-H1B	108.7
P1-C1-H1B	108.7	H1A-C1-H1B	107.6
C3-C2-C1	108.1(5)	C3-C2-H2A	110.1
C1-C2-H2A	110.1	C3-C2-H2B	110.1
C1-C2-H2B	110.1	H2A-C2-H2B	108.4
N1-C3-C2	176.2(6)	C9-C4-C5	119.5(5)
C9-C4-P1	120.8(4)	C5-C4-P1	119.6(4)
C6-C5-C4	119.7(6)	C6-C5-H5	120.1
C4-C5-H5	120.1	C7-C6-C5	119.5(5)
C7-C6-H6	120.3	C5-C6-H6	120.3
C8-C7-C6	121.2(5)	C8-C7-H7	119.4
C6-C7-H7	119.4	C7-C8-C9	119.8(6)
C7-C8-H8	120.1	C9-C8-H8	120.1
C4-C9-C8	120.2(5)	C4-C9-H9	119.9
C8-C9-H9	119.9	C11-C10-P1	113.4(4)
C11-C10-H10A	108.9	P1-C10-H10A	108.9
C11-C10-H10B	108.9	P1-C10-H10B	108.9
H10A-C10-H10B	107.7	C10-C11-P2	109.9(4)
C10-C11-H11A	109.7	P2-C11-H11A	109.7
C10-C11-H11B	109.7	P2-C11-H11B	109.7
H11A-C11-H11B	108.2	C13-C12-P2	115.5(4)
C13-C12-H12A	108.4	P2-C12-H12A	108.4
C13-C12-H12B	108.4	P2-C12-H12B	108.4
H12A-C12-H12B	107.5	C14-C13-C12	114.9(5)
C14-C13-H13A	108.6	C12-C13-H13A	108.6
C14-C13-H13B	108.6	C12-C13-H13B	108.6
H13A-C13-H13B	107.5	N2-C14-C13	178.8(7)
C16-C15-C20	119.8(5)	C16-C15-P2	120.2(4)
C20-C15-P2	120.0(4)	C15-C16-C17	120.1(5)
C15-C16-H16	120.0	C17-C16-H16	120.0
C18-C17-C16	119.8(6)	C18-C17-H17	120.1
C16-C17-H17	120.1	C17-C18-C19	120.5(5)
C17-C18-H18	119.8	C19-C18-H18	119.8
C18-C19-C20	120.6(6)	C18-C19-H19	119.7
C20-C19-H19	119.7	C19-C20-C15	119.2(6)
C19-C20-H20	120.4	C15-C20-H20	120.4
N3-C21-C22	178.7(6)	C21-C22-C23	110.1(5)
C21-C22-H22A	109.6	C23-C22-H22A	109.6

C21-C22-H22B	109.6	C23-C22-H22B	109.6
H22A-C22-H22B	108.1	C22-C23-P3	113.3(4)
C22-C23-H23A	108.9	P3-C23-H23A	108.9
C22-C23-H23B	108.9	P3-C23-H23B	108.9
H23A-C23-H23B	107.7	C29-C24-C25	120.8(5)
C29-C24-P3	119.5(4)	C25-C24-P3	119.7(4)
C24-C25-C26	120.1(5)	C24-C25-H25	119.9
C26-C25-H25	119.9	C27-C26-C25	118.8(5)
C27-C26-H26	120.6	C25-C26-H26	120.6
C28-C27-C26	120.9(5)	C28-C27-H27	119.5
C26-C27-H27	119.5	C27-C28-C29	120.1(6)
C27-C28-H28	120.0	C29-C28-H28	120.0
C24-C29-C28	119.2(5)	C24-C29-H29	120.4
C28-C29-H29	120.4	C31-C30-P3	110.5(3)
C31-C30-H30A	109.5	P3-C30-H30A	109.5
C31-C30-H30B	109.5	P3-C30-H30B	109.5
H30A-C30-H30B	108.1	C30-C31-P4	111.3(4)
C30-C31-H31A	109.4	P4-C31-H31A	109.4
C30-C31-H31B	109.4	P4-C31-H31B	109.4
H31A-C31-H31B	108.0	C33-C32-P4	114.5(4)
C33-C32-H32A	108.6	P4-C32-H32A	108.6
C33-C32-H32B	108.6	P4-C32-H32B	108.6
H32A-C32-H32B	107.6	C34-C33-C32	114.5(4)
C34-C33-H33A	108.6	C32-C33-H33A	108.6
C34-C33-H33B	108.6	C32-C33-H33B	108.6
H33A-C33-H33B	107.6	N4-C34-C33	177.9(7)
C40-C35-C36	119.5(5)	C40-C35-P4	120.7(4)
C36-C35-P4	119.7(4)	C37-C36-C35	120.4(5)
C37-C36-H36	119.8	C35-C36-H36	119.8
C38-C37-C36	119.0(6)	C38-C37-H37	120.5
C36-C37-H37	120.5	C39-C38-C37	120.9(5)
C39-C38-H38	119.5	C37-C38-H38	119.5
C38-C39-C40	120.1(6)	C38-C39-H39	119.9
C40-C39-H39	119.9	C35-C40-C39	120.1(6)
C35-C40-H40	119.9	C39-C40-H40	119.9
C4-P1-C10	105.0(2)	C4-P1-C1	108.4(2)
C10-P1-C1	99.4(2)	C4-P1-S1	113.4(2)
C10-P1-S1	115.10(19)	C1-P1-S1	114.34(18)
C12-P2-C15	108.1(3)	C12-P2-C11	103.3(2)
C15-P2-C11	104.0(2)	C12-P2-S2	113.93(19)
C15-P2-S2	113.44(19)	C11-P2-S2	113.17(18)

C24-P3-C30	104.6(2)	C24-P3-C23	103.9(2)
C30-P3-C23	106.0(3)	C24-P3-S3	114.66(19)
C30-P3-S3	112.97(17)	C23-P3-S3	113.72(19)
C32-P4-C35	107.3(2)	C32-P4-C31	103.9(2)
C35-P4-C31	104.1(2)	C32-P4-S4	113.44(18)
C35-P4-S4	113.81(19)	C31-P4-S4	113.39(19)

Crystallographic data for compound meso-12'aa

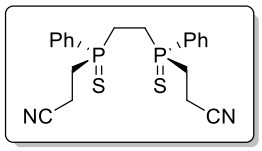

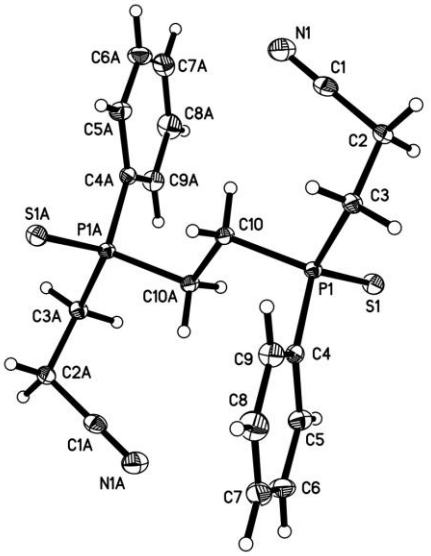

Identification code	leung973m
Chemical formula	$C_{20}H_{22}N_2P_2S_2$
Formula weight	416.45 g/mol
Temperature	112(2) K
Wavelength	0.71073 Å
Crystal size	0.040 x 0.100 x 0.120 mm
Crystal habit	colorless plate
Crystal system	triclinic
Space group	P -1
Unit cell dimensions	a = 7.1712(3) Å α = 63.0714(14)°
	b = 9.0800(4) Å β = 70.4805(14)°
	c = 9.5278(4) Å γ = 87.7152(16)°
Volume	516.73(4) $Å^3$
Z	1
Density (calculated)	1.338 g/cm^3
Absorption coefficient	0.419 mm^{-1}
F(000)	218

Theta range for data collection	2.54 to 37.87°
Index ranges	-12<=h<=12, -15<=k<=15, -16<=l<=16
Reflections collected	22394
Independent reflections	5570 [R(int) = 0.0744]
Coverage of independent reflections	99.6%

Absorption correction	Multi-Scan	
Max. and min. transmission	0.9830 and 0.9510	
Structure solution technique	direct methods	
Structure solution program	SHELXT 2014/5 (Sheldrick, 2014)	
Refinement method	Full-matrix least-squares on F^2	
Refinement program	SHELXL-2016/6 (Sheldrick, 2016)	
Function minimized	$\Sigma\ w(F_o^2 - F_c^2)^2$	
Data / restraints / parameters	5570 / 0 / 118	
Goodness-of-fit on F^2	1.066	
Δ/σ_{max}	0.001	
Final R indices	3818 data; $I>2\sigma(I)$	R1 = 0.0572, wR2 = 0.0957
	all data	R1 = 0.0994, wR2 = 0.1104
Weighting scheme	$w=1/[\sigma^2(F_o^2)+(0.0263P)^2+0.2633P]$ where $P=(F_o^2+2F_c^2)/3$	
Largest diff. peak and hole	0.572 and -0.585 $eÅ^{-3}$	
R.M.S. deviation from mean	0.101 $eÅ^{-3}$	

Bond lengths (Å) of compound meso-12'aa

C1-N1	1.144(2)	C1-C2	1.467(2)
C2-C3	1.536(2)	C2-H2A	0.99
C2-H2B	0.99	C3-P1	1.8239(14)
C3-H3A	0.99	C3-H3B	0.99
C4-C9	1.394(2)	C4-C5	1.401(2)
C4-P1	1.8096(14)	C5-C6	1.388(2)
C5-H5	0.95	C6-C7	1.381(3)
C6-H6	0.95	C7-C8	1.387(3)
C7-H7	0.95	C8-C9	1.389(2)
C8-H8	0.95	C9-H9	0.95
C10-C10	1.524(3)	C10-P1	1.8220(14)
C10-H10A	0.99	C10-H10B	0.99
P1-S1	1.9550(5)		

Bond angles (°) of compound meso-12'aa

N1-C1-C2	179.16(18)	C1-C2-C3	113.66(12)
C1-C2-H2A	108.8	C3-C2-H2A	108.8
C1-C2-H2B	108.8	C3-C2-H2B	108.8
H2A-C2-H2B	107.7	C2-C3-P1	113.87(10)
C2-C3-H3A	108.8	P1-C3-H3A	108.8
C2-C3-H3B	108.8	P1-C3-H3B	108.8
H3A-C3-H3B	107.7	C9-C4-C5	119.45(14)
C9-C4-P1	121.82(11)	C5-C4-P1	118.68(11)
C6-C5-C4	119.98(15)	C6-C5-H5	120.0
C4-C5-H5	120.0	C7-C6-C5	120.25(16)
C7-C6-H6	119.9	C5-C6-H6	119.9
C6-C7-C8	120.08(15)	C6-C7-H7	120.0
C8-C7-H7	120.0	C7-C8-C9	120.29(16)
C7-C8-H8	119.9	C9-C8-H8	119.9
C8-C9-C4	119.93(15)	C8-C9-H9	120.0
C4-C9-H9	120.0	C10-C10-P1	111.69(13)
C10-C10-H10A	109.3	P1-C10-H10A	109.3
C10-C10-H10B	109.3	P1-C10-H10B	109.3
H10A-C10-H10B	107.9	C4-P1-C10	104.67(7)
C4-P1-C3	105.47(7)	C10-P1-C3	105.84(7)
C4-P1-S1	114.11(5)	C10-P1-S1	113.01(5)
C3-P1-S1	112.94(5)		

Crystallographic data for compound 12aj

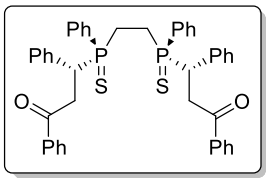

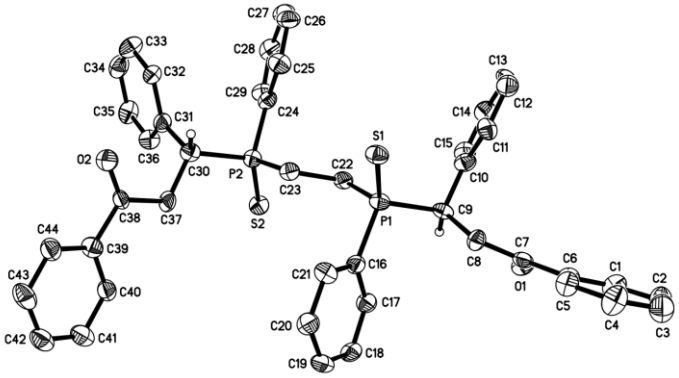

Identification code	leung966s	
Chemical formula	$C_{44}H_{40}O_2P_2S_2$	
Formula weight	726.82 g/mol	
Temperature	103(2) K	
Wavelength	1.54178 Å	
Crystal size	0.020 x 0.040 x 0.320 mm	
Crystal habit	colorless needle	
Crystal system	monoclinic	
Space group	P 1 21 1	
Unit cell dimensions	a = 6.1143(4) Å	α = 90°
	b = 17.0098(11) Å	β = 94.163(6)°
	c = 18.0673(11) Å	γ = 90°
Volume	1874.1(2) $Å^3$	
Z	2	
Density (calculated)	1.288 g/cm^3	
Absorption coefficient	2.379 mm^{-1}	
F(000)	764	

Theta range for data collection	2.45 to 66.69°
Index ranges	-6<=h<=7, -20<=k<=20, -21<=l<=19
Reflections collected	20211
Independent reflections	6538 [R(int) = 0.1608]
Coverage of independent reflections	99.0%
Absorption correction	Multi-Scan
Max. and min. transmission	0.9540 and 0.5170

Structure solution technique	direct methods	
Structure solution program	XT, VERSION 2014/5	
Refinement method	Full-matrix least-squares on F^2	
Refinement program	SHELXL-2014/7 (Sheldrick, 2014)	
Function minimized	$\Sigma\ w(F_o^2 - F_c^2)^2$	
Data / restraints / parameters	6538 / 1 / 452	
Goodness-of-fit on F^2	1.038	
Final R indices	4174 data; $I>2\sigma(I)$	R1 = 0.0756, wR2 = 0.1577
	all data	R1 = 0.1197, wR2 = 0.1836
Weighting scheme	$w=1/[\sigma^2(F_o^2)+(0.0411P)^2]$ where $P=(F_o^2+2F_c^2)/3$	
Absolute structure parameter	0.05(4)	
Extinction coefficient	0.0021(4)	
Largest diff. peak and hole	0.540 and -0.686 eÅ^{-3}	
R.M.S. deviation from mean	0.090 eÅ^{-3}	

Bond lengths (Å) of compound 12aj

C1-C6	1.402(14)	C1-C2	1.405(17)
C1-H1	0.95	C2-C3	1.368(17)
C2-H2	0.95	C3-C4	1.372(17)
C3-H3	0.95	C4-C5	1.395(16)
C4-H4	0.95	C5-C6	1.381(16)
C5-H5	0.95	C6-C7	1.513(15)
C7-O1	1.222(13)	C7-C8	1.516(14)
C8-C9	1.537(14)	C8-H8A	0.99
C8-H8B	0.99	C9-C10	1.533(15)
C9-P1	1.855(10)	C9-H9	1.0
C10-C15	1.374(16)	C10-C11	1.379(16)
C11-C12	1.389(16)	C11-H11	0.95
C12-C13	1.382(17)	C12-H12	0.95
C13-C14	1.377(16)	C13-H13	0.95
C14-C15	1.409(16)	C14-H14	0.95
C15-H15	0.95	C16-C17	1.368(15)
C16-C21	1.385(15)	C16-P1	1.818(11)
C17-C18	1.401(16)	C17-H17	0.95

C18-C19	1.380(16)	C18-H18	0.95
C19-C20	1.390(16)	C19-H19	0.95
C20-C21	1.391(16)	C20-H20	0.95
C21-H21	0.95	C22-C23	1.542(12)
C22-P1	1.807(11)	C22-H22A	0.99
C22-H22B	0.99	C23-P2	1.803(10)
C23-H23A	0.99	C23-H23B	0.99
C24-C25	1.397(16)	C24-C29	1.400(15)
C24-P2	1.817(11)	C25-C26	1.391(16)
C25-H25	0.95	C26-C27	1.407(18)
C26-H26	0.95	C27-C28	1.399(18)
C27-H27	0.95	C28-C29	1.389(16)
C28-H28	0.95	C29-H29	0.95
C30-C31	1.508(15)	C30-C37	1.520(15)
C30-P2	1.847(10)	C30-H30	1.0
C31-C36	1.373(15)	C31-C32	1.413(16)
C32-C33	1.389(16)	C32-H32	0.95
C33-C34	1.370(16)	C33-H33	0.95
C34-C35	1.406(17)	C34-H34	0.95
C35-C36	1.401(15)	C35-H35	0.95
C36-H36	0.95	C37-C38	1.501(14)
C37-H37A	0.99	C37-H37B	0.99
C38-O2	1.223(13)	C38-C39	1.500(15)
C39-C40	1.395(16)	C39-C44	1.403(15)
C40-C41	1.393(15)	C40-H40	0.95
C41-C42	1.391(17)	C41-H41	0.95
C42-C43	1.380(18)	C42-H42	0.95
C43-C44	1.392(16)	C43-H43	0.95
C44-H44	0.95	P1-S1	1.957(4)
P2-S2	1.955(4)		

Bond angles (°) of compound 12aj

C6-C1-C2	118.4(11)	C6-C1-H1	120.8
C2-C1-H1	120.8	C3-C2-C1	120.7(11)
C3-C2-H2	119.6	C1-C2-H2	119.6
C2-C3-C4	120.8(13)	C2-C3-H3	119.6
C4-C3-H3	119.6	C3-C4-C5	119.7(12)
C3-C4-H4	120.1	C5-C4-H4	120.1
C6-C5-C4	120.3(11)	C6-C5-H5	119.8

C4-C5-H5	119.8	C5-C6-C1	120.0(11)
C5-C6-C7	122.1(10)	C1-C6-C7	117.9(10)
O1-C7-C6	120.7(10)	O1-C7-C8	122.0(10)
C6-C7-C8	117.1(10)	C7-C8-C9	111.2(9)
C7-C8-H8A	109.4	C9-C8-H8A	109.4
C7-C8-H8B	109.4	C9-C8-H8B	109.4
H8A-C8-H8B	108.0	C10-C9-C8	113.7(9)
C10-C9-P1	111.0(7)	C8-C9-P1	109.4(7)
C10-C9-H9	107.5	C8-C9-H9	107.5
P1-C9-H9	107.5	C15-C10-C11	119.5(11)
C15-C10-C9	119.6(11)	C11-C10-C9	120.9(10)
C10-C11-C12	119.8(11)	C10-C11-H11	120.1
C12-C11-H11	120.1	C13-C12-C11	121.2(11)
C13-C12-H12	119.4	C11-C12-H12	119.4
C14-C13-C12	119.2(11)	C14-C13-H13	120.4
C12-C13-H13	120.4	C13-C14-C15	119.5(11)
C13-C14-H14	120.3	C15-C14-H14	120.3
C10-C15-C14	120.8(12)	C10-C15-H15	119.6
C14-C15-H15	119.6	C17-C16-C21	120.3(10)
C17-C16-P1	121.1(8)	C21-C16-P1	118.6(8)
C16-C17-C18	120.2(10)	C16-C17-H17	119.9
C18-C17-H17	119.9	C19-C18-C17	119.4(10)
C19-C18-H18	120.3	C17-C18-H18	120.3
C18-C19-C20	120.4(11)	C18-C19-H19	119.8
C20-C19-H19	119.8	C19-C20-C21	119.5(10)
C19-C20-H20	120.3	C21-C20-H20	120.3
C16-C21-C20	120.0(10)	C16-C21-H21	120.0
C20-C21-H21	120.0	C23-C22-P1	111.1(7)
C23-C22-H22A	109.4	P1-C22-H22A	109.4
C23-C22-H22B	109.4	P1-C22-H22B	109.4
H22A-C22-H22B	108.0	C22-C23-P2	114.8(7)
C22-C23-H23A	108.6	P2-C23-H23A	108.6
C22-C23-H23B	108.6	P2-C23-H23B	108.6
H23A-C23-H23B	107.6	C25-C24-C29	121.7(11)
C25-C24-P2	120.7(9)	C29-C24-P2	117.4(9)
C26-C25-C24	118.6(12)	C26-C25-H25	120.7
C24-C25-H25	120.7	C25-C26-C27	120.8(12)
C25-C26-H26	119.6	C27-C26-H26	119.6
C28-C27-C26	119.4(11)	C28-C27-H27	120.3
C26-C27-H27	120.3	C29-C28-C27	120.6(12)
C29-C28-H28	119.7	C27-C28-H28	119.7

C28-C29-C24	118.9(11)	C28-C29-H29	120.5
C24-C29-H29	120.5	C31-C30-C37	113.6(10)
C31-C30-P2	110.3(7)	C37-C30-P2	111.2(7)
C31-C30-H30	107.2	C37-C30-H30	107.2
P2-C30-H30	107.2	C36-C31-C32	118.0(11)
C36-C31-C30	122.7(10)	C32-C31-C30	119.1(11)
C33-C32-C31	120.6(12)	C33-C32-H32	119.7
C31-C32-H32	119.7	C34-C33-C32	120.5(12)
C34-C33-H33	119.7	C32-C33-H33	119.7
C33-C34-C35	120.1(11)	C33-C34-H34	119.9
C35-C34-H34	119.9	C36-C35-C34	118.6(11)
C36-C35-H35	120.7	C34-C35-H35	120.7
C31-C36-C35	122.1(11)	C31-C36-H36	119.0
C35-C36-H36	119.0	C38-C37-C30	113.1(9)
C38-C37-H37A	109.0	C30-C37-H37A	109.0
C38-C37-H37B	109.0	C30-C37-H37B	109.0
H37A-C37-H37B	107.8	O2-C38-C39	120.7(9)
O2-C38-C37	120.9(10)	C39-C38-C37	118.3(9)
C40-C39-C44	119.6(10)	C40-C39-C38	121.3(9)
C44-C39-C38	118.8(10)	C41-C40-C39	119.3(11)
C41-C40-H40	120.3	C39-C40-H40	120.3
C42-C41-C40	120.6(12)	C42-C41-H41	119.7
C40-C41-H41	119.7	C43-C42-C41	120.4(11)
C43-C42-H42	119.8	C41-C42-H42	119.8
C42-C43-C44	119.5(11)	C42-C43-H43	120.3
C44-C43-H43	120.3	C43-C44-C39	120.5(11)
C43-C44-H44	119.7	C39-C44-H44	119.7
C22-P1-C16	105.5(5)	C22-P1-C9	107.0(5)
C16-P1-C9	105.8(5)	C22-P1-S1	112.4(4)
C16-P1-S1	112.5(4)	C9-P1-S1	113.1(4)
C23-P2-C24	106.8(5)	C23-P2-C30	105.4(5)
C24-P2-C30	103.9(5)	C23-P2-S2	112.2(4)
C24-P2-S2	113.9(4)	C30-P2-S2	113.9(4)

Crystallographic data for compound chiral-13aa

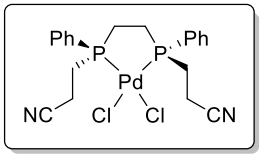

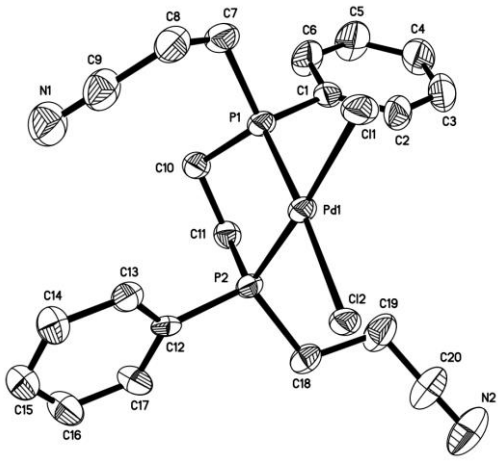

Identification code	leung1085m
Chemical formula	$C_{20}H_{22}Cl_2N_2P_2Pd$
Formula weight	529.63 g/mol
Temperature	100(2) K
Wavelength	0.71073 Å
Crystal size	0.160 x 0.240 x 0.300 mm
Crystal habit	colorless block
Crystal system	monoclinic
Space group	P 1 21 1
Unit cell dimensions	a = 10.3392(5) Å α = 90°
	b = 14.2907(6) Å β = 103.424(2)°
	c = 15.2301(7) Å γ = 90°
Volume	2188.83(17) $Å^3$
Z	4
Density (calculated)	1.607 g/cm^3
Absorption coefficient	1.246 mm^{-1}
F(000)	1064

Theta range for data collection	2.17 to 31.52°
Index ranges	-15<=h<=15, -17<=k<=21, -22<=l<=22
Reflections collected	26618
Independent reflections	12998 [R(int) = 0.0458]
Coverage of independent reflections	99.4%
Absorption correction	Multi-Scan
Max. and min. transmission	0.8260 and 0.7060

Structure solution technique	direct methods	
Structure solution program	XT, VERSION 2014/5	
Refinement method	Full-matrix least-squares on F^2	
Refinement program	SHELXL-2016/6 (Sheldrick, 2016)	
Function minimized	$\Sigma\ w(F_o^2 - F_c^2)^2$	
Data / restraints / parameters	12998 / 1808 / 738	
Goodness-of-fit on F^2	1.047	
Δ/σ_{max}	0.001	
Final R indices	10358 data; $I>2\sigma(I)$	R1 = 0.0546, wR2 = 0.1050
	all data	R1 = 0.0751, wR2 = 0.1196
Weighting scheme	$w=1/[\sigma^2(F_o^2)+(0.0255P)^2+3.6768P]$ where $P=(F_o^2+2F_c^2)/3$	
Absolute structure parameter	-0.018(18)	
Largest diff. peak and hole	0.746 and -1.027 eÅ^{-3}	
R.M.S. deviation from mean	0.116 eÅ^{-3}	

Bond lengths (Å) of compound chiral-13aa

C1-C2	1.386(8)	C1-C6	1.399(8)
C1-P1	1.806(6)	C2-C3	1.387(8)
C2-H2	0.95	C3-C4	1.387(9)
C3-H3	0.95	C4-C5	1.386(9)
C4-H4	0.95	C5-C6	1.381(9)
C5-H5	0.95	C6-H6	0.95
C7-C8	1.532(10)	C7-P1	1.830(7)
C7-H7A	0.99	C7-H7B	0.99
C8-C9	1.463(10)	C8-H8A	0.99
C8-H8B	0.99	C9-N1	1.135(9)
C10-C11	1.536(8)	C10-P1	1.824(6)
C10-H10A	0.99	C10-H10B	0.99
C11-P2	1.822(6)	C11-H11A	0.99
C11-H11B	0.99	C12-C13	1.39
C12-C17	1.39	C12-P2	1.778(6)
C13-C14	1.39	C13-H13	0.95

C14-C15	1.39	C14-H14	0.95
C15-C16	1.39	C15-H15	0.95
C16-C17	1.39	C16-H16	0.95
C17-H17	0.95	C18-C19	1.517(9)
C18-P2	1.827(6)	C18-H18A	0.99
C18-H18B	0.99	C19-C20	1.434(10)
C19-H19A	0.99	C19-H19B	0.99
C20-N2	1.140(9)	Cl1-Pd1	2.3568(18)
Cl2-Pd1	2.3817(15)	P1-Pd1	2.2255(17)
P2-C12A	1.828(8)	P2-Pd1	2.2281(17)
C21-C22	1.39	C21-C26	1.39
C21-P3	1.808(8)	C22-C23	1.39
C22-H22	0.95	C23-C24	1.39
C23-H23	0.95	C24-C25	1.39
C24-H24	0.95	C25-C26	1.39
C25-H25	0.95	C26-H26	0.95
C27-C28	1.533(12)	C27-P3	1.832(10)
C27-H27A	0.99	C27-H27B	0.99
C28-C29	1.462(13)	C28-H28A	0.99
C28-H28B	0.99	C29-N3	1.134(12)
C30-C31	1.553(12)	C30-P3	1.832(10)
C30-H30A	0.99	C30-H30B	0.99
C31-P4	1.832(10)	C31-H31A	0.99
C31-H31B	0.99	C32-C33	1.39
C32-C37	1.39	C32-P4	1.798(7)
C33-C34	1.39	C33-H33	0.95
C34-C35	1.39	C34-H34	0.95
C35-C36	1.39	C35-H35	0.95
C36-C37	1.39	C36-H36	0.95
C37-H37	0.95	C38-C39	1.516(13)
C38-P4	1.828(11)	C38-H38A	0.99
C38-H38B	0.99	C39-C40	1.446(13)
C39-H39A	0.99	C39-H39B	0.99
C40-N4	1.145(13)	Cl3-Pd2	2.358(4)
Cl4-Pd2	2.375(4)	P3-Pd2	2.233(6)
P4-Pd2	2.229(4)	C21A-C26A	1.373(11)
C21A-C22A	1.400(11)	C21A-P3A	1.807(10)
C22A-C23A	1.385(11)	C22A-H22A	0.95
C23A-C24A	1.385(11)	C23A-H23A	0.95
C24A-C25A	1.403(11)	C24A-H24A	0.95
C25A-C26A	1.387(11)	C25A-H25A	0.95

C26A-H26A	0.95	C27A-C28A	1.528(13)
C27A-P3A	1.834(11)	C27A-H27C	0.99
C27A-H27D	0.99	C28A-C29A	1.461(13)
C28A-H28C	0.99	C28A-H28D	0.99
C29A-N3A	1.132(13)	C30A-C31A	1.520(12)
C30A-P3A	1.794(11)	C30A-H30C	0.99
C30A-H30D	0.99	C31A-P4A	1.821(11)
C31A-H31C	0.99	C31A-H31D	0.99
C32A-C33A	1.379(10)	C32A-C37A	1.400(10)
C32A-P4A	1.790(10)	C33A-C34A	1.387(10)
C33A-H33A	0.95	C34A-C35A	1.386(10)
C34A-H34A	0.95	C35A-C36A	1.380(10)
C35A-H35A	0.95	C36A-C37A	1.396(10)
C36A-H36A	0.95	C37A-H37A	0.95
C38A-C39A	1.516(13)	C38A-P4A	1.833(11)
C38A-H38C	0.99	C38A-H38D	0.99
C39A-C40A	1.437(14)	C39A-H39C	0.99
C39A-H39D	0.99	C40A-N4A	1.144(13)
Cl3A-Pd2A	2.366(6)	Cl4A-Pd2A	2.367(5)
P3A-Pd2A	2.220(7)	P4A-Pd2A	2.232(5)
C12A-C13A	1.39	C12A-C17A	1.39
C13A-C14A	1.39	C13A-H13A	0.95
C14A-C15A	1.39	C14A-H14A	0.95
C15A-C16A	1.39	C15A-H15A	0.95
C16A-C17A	1.39	C16A-H16A	0.95
C17A-H17A	0.95		

Bond angles (°) of compound chiral-13aa

C2-C1-C6	119.4(6)	C2-C1-P1	120.4(5)
C6-C1-P1	120.1(5)	C1-C2-C3	119.3(6)
C1-C2-H2	120.3	C3-C2-H2	120.3
C4-C3-C2	121.0(7)	C4-C3-H3	119.5
C2-C3-H3	119.5	C5-C4-C3	119.8(7)
C5-C4-H4	120.1	C3-C4-H4	120.1
C6-C5-C4	119.4(7)	C6-C5-H5	120.3
C4-C5-H5	120.3	C5-C6-C1	121.0(7)
C5-C6-H6	119.5	C1-C6-H6	119.5
C8-C7-P1	115.2(5)	C8-C7-H7A	108.5
P1-C7-H7A	108.5	C8-C7-H7B	108.5

P1-C7-H7B	108.5	H7A-C7-H7B	107.5
C9-C8-C7	114.3(7)	C9-C8-H8A	108.7
C7-C8-H8A	108.7	C9-C8-H8B	108.7
C7-C8-H8B	108.7	H8A-C8-H8B	107.6
N1-C9-C8	179.5(11)	C11-C10-P1	106.2(4)
C11-C10-H10A	110.5	P1-C10-H10A	110.5
C11-C10-H10B	110.5	P1-C10-H10B	110.5
H10A-C10-H10B	108.7	C10-C11-P2	106.5(4)
C10-C11-H11A	110.4	P2-C11-H11A	110.4
C10-C11-H11B	110.4	P2-C11-H11B	110.4
H11A-C11-H11B	108.6	C13-C12-C17	120.0
C13-C12-P2	119.3(5)	C17-C12-P2	120.5(5)
C14-C13-C12	120.0	C14-C13-H13	120.0
C12-C13-H13	120.0	C15-C14-C13	120.0
C15-C14-H14	120.0	C13-C14-H14	120.0
C16-C15-C14	120.0	C16-C15-H15	120.0
C14-C15-H15	120.0	C15-C16-C17	120.0
C15-C16-H16	120.0	C17-C16-H16	120.0
C16-C17-C12	120.0	C16-C17-H17	120.0
C12-C17-H17	120.0	C19-C18-P2	110.6(5)
C19-C18-H18A	109.5	P2-C18-H18A	109.5
C19-C18-H18B	109.5	P2-C18-H18B	109.5
H18A-C18-H18B	108.1	C20-C19-C18	113.3(7)
C20-C19-H19A	108.9	C18-C19-H19A	108.9
C20-C19-H19B	108.9	C18-C19-H19B	108.9
H19A-C19-H19B	107.7	N2-C20-C19	178.9(12)
C1-P1-C10	104.0(3)	C1-P1-C7	104.9(3)
C10-P1-C7	108.8(3)	C1-P1-Pd1	114.0(2)
C10-P1-Pd1	107.8(2)	C7-P1-Pd1	116.5(3)
C12-P2-C11	107.1(4)	C12-P2-C18	106.7(4)
C11-P2-C18	107.5(3)	C11-P2-C12A	101.3(5)
C18-P2-C12A	108.0(5)	C12-P2-Pd1	111.7(3)
C11-P2-Pd1	108.5(2)	C18-P2-Pd1	114.9(2)
C12A-P2-Pd1	115.4(4)	P1-Pd1-P2	85.17(6)
P1-Pd1-Cl1	89.01(7)	P2-Pd1-Cl1	174.17(6)
P1-Pd1-Cl2	173.57(7)	P2-Pd1-Cl2	88.45(6)
Cl1-Pd1-Cl2	97.37(6)	C22-C21-C26	120.0
C22-C21-P3	118.3(6)	C26-C21-P3	121.7(6)
C23-C22-C21	120.0	C23-C22-H22	120.0
C21-C22-H22	120.0	C22-C23-C24	120.0
C22-C23-H23	120.0	C24-C23-H23	120.0

C25-C24-C23	120.0	C25-C24-H24	120.0
C23-C24-H24	120.0	C26-C25-C24	120.0
C26-C25-H25	120.0	C24-C25-H25	120.0
C25-C26-C21	120.0	C25-C26-H26	120.0
C21-C26-H26	120.0	C28-C27-P3	116.9(9)
C28-C27-H27A	108.1	P3-C27-H27A	108.1
C28-C27-H27B	108.1	P3-C27-H27B	108.1
H27A-C27-H27B	107.3	C29-C28-C27	112.7(12)
C29-C28-H28A	109.1	C27-C28-H28A	109.1
C29-C28-H28B	109.1	C27-C28-H28B	109.1
H28A-C28-H28B	107.8	N3-C29-C28	178.(2)
C31-C30-P3	106.2(8)	C31-C30-H30A	110.5
P3-C30-H30A	110.5	C31-C30-H30B	110.5
P3-C30-H30B	110.5	H30A-C30-H30B	108.7
C30-C31-P4	104.9(7)	C30-C31-H31A	110.8
P4-C31-H31A	110.8	C30-C31-H31B	110.8
P4-C31-H31B	110.8	H31A-C31-H31B	108.8
C33-C32-C37	120.0	C33-C32-P4	118.0(5)
C37-C32-P4	122.0(5)	C34-C33-C32	120.0
C34-C33-H33	120.0	C32-C33-H33	120.0
C33-C34-C35	120.0	C33-C34-H34	120.0
C35-C34-H34	120.0	C36-C35-C34	120.0
C36-C35-H35	120.0	C34-C35-H35	120.0
C35-C36-C37	120.0	C35-C36-H36	120.0
C37-C36-H36	120.0	C36-C37-C32	120.0
C36-C37-H37	120.0	C32-C37-H37	120.0
C39-C38-P4	116.7(11)	C39-C38-H38A	108.1
P4-C38-H38A	108.1	C39-C38-H38B	108.1
P4-C38-H38B	108.1	H38A-C38-H38B	107.3
C40-C39-C38	112.6(12)	C40-C39-H39A	109.1
C38-C39-H39A	109.1	C40-C39-H39B	109.1
C38-C39-H39B	109.1	H39A-C39-H39B	107.8
N4-C40-C39	178.(2)	C21-P3-C30	108.8(6)
C21-P3-C27	103.7(6)	C30-P3-C27	108.1(7)
C21-P3-Pd2	113.6(5)	C30-P3-Pd2	109.5(5)
C27-P3-Pd2	112.9(5)	C32-P4-C38	106.7(6)
C32-P4-C31	104.4(6)	C38-P4-C31	108.5(6)
C32-P4-Pd2	113.8(4)	C38-P4-Pd2	114.0(5)
C31-P4-Pd2	108.8(4)	P4-Pd2-P3	84.3(2)
P4-Pd2-Cl3	175.21(19)	P3-Pd2-Cl3	91.3(2)
P4-Pd2-Cl4	91.74(17)	P3-Pd2-Cl4	174.2(2)

Cl3-Pd2-Cl4	92.74(17)	C26A-C21A-C22A	117.4(11)
C26A-C21A-P3A	122.9(10)	C22A-C21A-P3A	119.2(10)
C23A-C22A-C21A	120.8(12)	C23A-C22A-H22A	119.6
C21A-C22A-H22A	119.6	C22A-C23A-C24A	120.3(13)
C22A-C23A-H23A	119.8	C24A-C23A-H23A	119.8
C23A-C24A-C25A	120.0(13)	C23A-C24A-H24A	120.0
C25A-C24A-H24A	120.0	C26A-C25A-C24A	117.7(12)
C26A-C25A-H25A	121.1	C24A-C25A-H25A	121.1
C21A-C26A-C25A	123.6(12)	C21A-C26A-H26A	118.2
C25A-C26A-H26A	118.2	C28A-C27A-P3A	117.0(11)
C28A-C27A-H27C	108.1	P3A-C27A-H27C	108.1
C28A-C27A-H27D	108.1	P3A-C27A-H27D	108.1
H27C-C27A-H27D	107.3	C29A-C28A-C27A	111.8(14)
C29A-C28A-H28C	109.2	C27A-C28A-H28C	109.2
C29A-C28A-H28D	109.2	C27A-C28A-H28D	109.2
H28C-C28A-H28D	107.9	N3A-C29A-C28A	176.(3)
C31A-C30A-P3A	113.6(9)	C31A-C30A-H30C	108.9
P3A-C30A-H30C	108.9	C31A-C30A-H30D	108.9
P3A-C30A-H30D	108.9	H30C-C30A-H30D	107.7
C30A-C31A-P4A	112.3(9)	C30A-C31A-H31C	109.1
P4A-C31A-H31C	109.1	C30A-C31A-H31D	109.1
P4A-C31A-H31D	109.1	H31C-C31A-H31D	107.9
C33A-C32A-C37A	119.0(9)	C33A-C32A-P4A	120.8(9)
C37A-C32A-P4A	120.1(9)	C32A-C33A-C34A	120.8(11)
C32A-C33A-H33A	119.6	C34A-C33A-H33A	119.6
C35A-C34A-C33A	120.2(12)	C35A-C34A-H34A	119.9
C33A-C34A-H34A	119.9	C36A-C35A-C34A	119.6(11)
C36A-C35A-H35A	120.2	C34A-C35A-H35A	120.2
C35A-C36A-C37A	120.0(12)	C35A-C36A-H36A	120.0
C37A-C36A-H36A	120.0	C36A-C37A-C32A	120.0(11)
C36A-C37A-H37A	120.0	C32A-C37A-H37A	120.0
C39A-C38A-P4A	113.6(11)	C39A-C38A-H38C	108.9
P4A-C38A-H38C	108.9	C39A-C38A-H38D	108.9
P4A-C38A-H38D	108.9	H38C-C38A-H38D	107.7
C40A-C39A-C38A	113.1(13)	C40A-C39A-H39C	109.0
C38A-C39A-H39C	109.0	C40A-C39A-H39D	109.0
C38A-C39A-H39D	109.0	H39C-C39A-H39D	107.8
N4A-C40A-C39A	177.(3)	C30A-P3A-C21A	110.6(8)
C30A-P3A-C27A	112.3(9)	C21A-P3A-C27A	102.0(8)
C30A-P3A-Pd2A	107.4(6)	C21A-P3A-Pd2A	115.7(8)
C27A-P3A-Pd2A	108.8(7)	C32A-P4A-C31A	104.4(8)

C32A-P4A-C38A	103.7(7)	C31A-P4A-C38A	108.1(8)
C32A-P4A-Pd2A	116.1(5)	C31A-P4A-Pd2A	109.4(5)
C38A-P4A-Pd2A	114.4(6)	P3A-Pd2A-P4A	87.2(3)
P3A-Pd2A-Cl3A	88.4(3)	P4A-Pd2A-Cl3A	175.5(3)
P3A-Pd2A-Cl4A	177.5(3)	P4A-Pd2A-Cl4A	90.5(2)
Cl3A-Pd2A-Cl4A	93.9(3)	C13A-C12A-C17A	120.0
C13A-C12A-P2	119.8(7)	C17A-C12A-P2	120.1(7)
C12A-C13A-C14A	120.0	C12A-C13A-H13A	120.0
C14A-C13A-H13A	120.0	C15A-C14A-C13A	120.0
C15A-C14A-H14A	120.0	C13A-C14A-H14A	120.0
C14A-C15A-C16A	120.0	C14A-C15A-H15A	120.0
C16A-C15A-H15A	120.0	C17A-C16A-C15A	120.0
C17A-C16A-H16A	120.0	C15A-C16A-H16A	120.0
C16A-C17A-C12A	120.0	C16A-C17A-H17A	120.0
C12A-C17A-H17A	120.0		

Crystallographic data for compound meso-13'aa

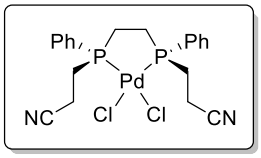

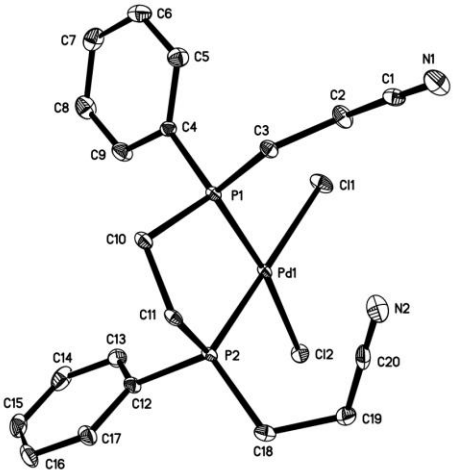

Identification code	leung1075m
Chemical formula	$C_{20}H_{22}Cl_2N_2P_2Pd$
Formula weight	529.63 g/mol
Temperature	100(2) K
Wavelength	0.71073 Å
Crystal size	0.080 x 0.200 x 0.220 mm
Crystal habit	colorless plate
Crystal system	monoclinic
Space group	P 1 21/c 1
Unit cell dimensions	a = 15.9062(6) Å α = 90°
	b = 11.5702(5) Å β = 112.5172(12)°
	c = 12.4964(5) Å γ = 90°
Volume	2124.48(15) $Å^3$
Z	4
Density (calculated)	1.656 g/cm^3
Absorption coefficient	1.284 mm^{-1}
F(000)	1064

Theta range for data collection	2.24 to 29.99°
Index ranges	-22<=h<=22, -16<=k<=16, -17<=l<=17
Reflections collected	28094
Independent reflections	6186 [R(int) = 0.0787]
Coverage of independent reflections	99.8%
Absorption correction	Multi-Scan

Max. and min. transmission	0.9040 and 0.7650	
Structure solution technique	direct methods	
Structure solution program	XT, VERSION 2014/5	
Refinement method	Full-matrix least-squares on F^2	
Refinement program	SHELXL-2016/6 (Sheldrick, 2016)	
Function minimized	$\Sigma\ w(F_o^2 - F_c^2)^2$	
Data / restraints / parameters	6186 / 0 / 244	
Goodness-of-fit on F^2	1.043	
Δ/σ_{max}	0.001	
Final R indices	4841 data; $I>2\sigma(I)$	R1 = 0.0433, wR2 = 0.0774
	all data	R1 = 0.0623, wR2 = 0.0856
Weighting scheme	$w=1/[\sigma^2(F_o^2)+(0.0209P)^2+1.8959P]$ where $P=(F_o^2+2F_c^2)/3$	
Largest diff. peak and hole	1.341 and -1.182 eÅ^{-3}	
R.M.S. deviation from mean	0.154 eÅ^{-3}	

Bond lengths (Å) of compound meso-13'aa

C1-N1	1.138(4)	C1-C2	1.466(4)
C2-C3	1.533(4)	C2-H2A	0.99
C2-H2B	0.99	C3-P1	1.821(3)
C3-H3A	0.99	C3-H3B	0.99
C4-C5	1.386(4)	C4-C9	1.393(4)
C4-P1	1.798(3)	C5-C6	1.379(5)
C5-H5	0.95	C6-C7	1.387(5)
C6-H6	0.95	C7-C8	1.386(5)
C7-H7	0.95	C8-C9	1.382(5)
C8-H8	0.95	C9-H9	0.95
C10-C11	1.531(4)	C10-P1	1.828(3)
C10-H10A	0.99	C10-H10B	0.99
C11-P2	1.825(3)	C11-H11A	0.99
C11-H11B	0.99	C12-C13	1.391(4)
C12-C17	1.392(4)	C12-P2	1.810(3)
C13-C14	1.385(5)	C13-H13	0.95

C14-C15	1.381(5)	C14-H14	0.95
C15-C16	1.384(5)	C15-H15	0.95
C16-C17	1.386(5)	C16-H16	0.95
C17-H17	0.95	C18-C19	1.536(4)
C18-P2	1.824(3)	C18-H18A	0.99
C18-H18B	0.99	C19-C20	1.472(5)
C19-H19A	0.99	C19-H19B	0.99
C20-N2	1.138(4)	Cl1-Pd1	2.3556(8)
Cl2-Pd1	2.3669(8)	P1-Pd1	2.2234(8)
P2-Pd1	2.2141(8)		

Bond angles (°) of compound meso-13'aa

N1-C1-C2	178.2(4)	C1-C2-C3	109.7(3)
C1-C2-H2A	109.7	C3-C2-H2A	109.7
C1-C2-H2B	109.7	C3-C2-H2B	109.7
H2A-C2-H2B	108.2	C2-C3-P1	117.6(2)
C2-C3-H3A	107.9	P1-C3-H3A	107.9
C2-C3-H3B	107.9	P1-C3-H3B	107.9
H3A-C3-H3B	107.2	C5-C4-C9	119.2(3)
C5-C4-P1	122.7(2)	C9-C4-P1	118.0(2)
C6-C5-C4	120.1(3)	C6-C5-H5	119.9
C4-C5-H5	119.9	C5-C6-C7	120.7(3)
C5-C6-H6	119.7	C7-C6-H6	119.7
C8-C7-C6	119.4(3)	C8-C7-H7	120.3
C6-C7-H7	120.3	C9-C8-C7	120.1(3)
C9-C8-H8	120.0	C7-C8-H8	120.0
C8-C9-C4	120.5(3)	C8-C9-H9	119.8
C4-C9-H9	119.8	C11-C10-P1	108.5(2)
C11-C10-H10A	110.0	P1-C10-H10A	110.0
C11-C10-H10B	110.0	P1-C10-H10B	110.0
H10A-C10-H10B	108.4	C10-C11-P2	106.9(2)
C10-C11-H11A	110.3	P2-C11-H11A	110.3
C10-C11-H11B	110.3	P2-C11-H11B	110.3
H11A-C11-H11B	108.6	C13-C12-C17	119.7(3)
C13-C12-P2	120.5(2)	C17-C12-P2	119.7(3)
C14-C13-C12	120.1(3)	C14-C13-H13	120.0
C12-C13-H13	120.0	C15-C14-C13	119.9(3)
C15-C14-H14	120.1	C13-C14-H14	120.1
C14-C15-C16	120.5(3)	C14-C15-H15	119.8

C16-C15-H15	119.8	C15-C16-C17	119.9(3)
C15-C16-H16	120.1	C17-C16-H16	120.1
C16-C17-C12	119.9(3)	C16-C17-H17	120.0
C12-C17-H17	120.0	C19-C18-P2	114.0(2)
C19-C18-H18A	108.7	P2-C18-H18A	108.7
C19-C18-H18B	108.7	P2-C18-H18B	108.7
H18A-C18-H18B	107.6	C20-C19-C18	113.8(3)
C20-C19-H19A	108.8	C18-C19-H19A	108.8
C20-C19-H19B	108.8	C18-C19-H19B	108.8
H19A-C19-H19B	107.7	N2-C20-C19	179.2(4)
C4-P1-C3	109.45(15)	C4-P1-C10	105.98(15)
C3-P1-C10	100.98(14)	C4-P1-Pd1	113.10(10)
C3-P1-Pd1	117.74(11)	C10-P1-Pd1	108.25(11)
C12-P2-C18	107.29(15)	C12-P2-C11	103.12(15)
C18-P2-C11	108.00(15)	C12-P2-Pd1	115.02(11)
C18-P2-Pd1	114.01(11)	C11-P2-Pd1	108.66(10)
P2-Pd1-P1	85.92(3)	P2-Pd1-Cl1	174.12(3)
P1-Pd1-Cl1	89.64(3)	P2-Pd1-Cl2	88.51(3)
P1-Pd1-Cl2	172.06(3)	Cl1-Pd1-Cl2	96.27(3)

Crystallographic data for compound chiral-17a

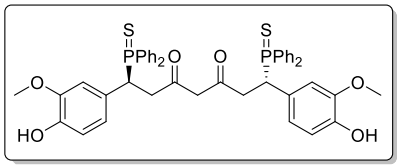

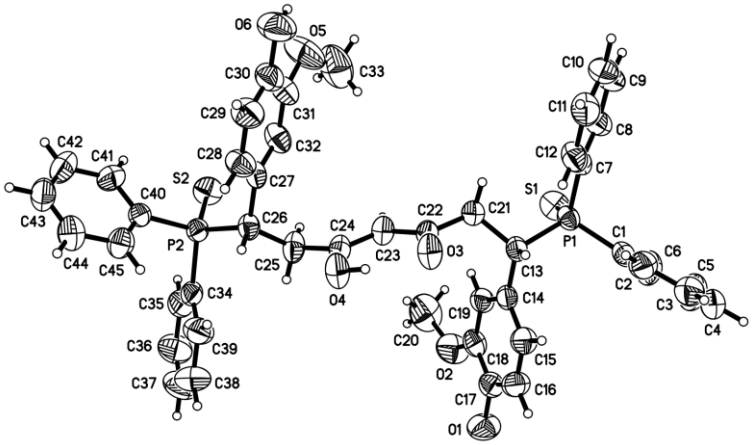

Identification code	leung1217s	
Chemical formula	$C_{45}H_{42}O_6P_2S_2$	
Formula weight	804.84 g/mol	
Temperature	296(2) K	
Wavelength	1.54178 Å	
Crystal size	0.020 x 0.200 x 0.280 mm	
Crystal habit	colorless needle	
Crystal system	monoclinic	
Space group	P 1 21 1	
Unit cell dimensions	a = 6.8741(4) Å	α = 90°
	b = 35.809(2) Å	β = 111.159(4)°
	c = 9.0649(5) Å	γ = 90°
Volume	2080.9(2) $Å^3$	
Z	2	
Density (calculated)	1.284 g/cm^3	
Absorption coefficient	2.268 mm^{-1}	
F(000)	844	

Theta range for data collection	2.47 to 67.90°
Index ranges	-8<=h<=8, -42<=k<=40, -10<=l<=10
Reflections collected	27001
Independent reflections	7293 [R(int) = 0.0550]
Coverage of independent reflections	99.0%
Absorption correction	Multi-Scan
Max. and min. transmission	0.9560 and 0.5690

Structure solution technique	direct methods	
Structure solution program	SHELXT 2014/5 (Sheldrick, 2014)	
Refinement method	Full-matrix least-squares on F^2	
Refinement program	SHELXL-2018/3 (Sheldrick, 2018)	
Function minimized	$\Sigma\ w(F_o^2 - F_c^2)^2$	
Data / restraints / parameters	7293 / 1 / 501	
Goodness-of-fit on F^2	1.033	
Δ/σ_{max}	0.001	
Final R indices	6742 data; $I>2\sigma(I)$	R1 = 0.0421, wR2 = 0.1024
	all data	R1 = 0.0462, wR2 = 0.1051
Weighting scheme	$w=1/[\sigma^2(F_o^2)+(0.0482P)^2+0.3982P]$ where $P=(F_o^2+2F_c^2)/3$	
Absolute structure parameter	0.030(10)	
Largest diff. peak and hole	0.405 and -0.203 eÅ^{-3}	
R.M.S. deviation from mean	0.039 eÅ^{-3}	

Bond lengths (Å) of compound chiral-17aa'

C1-C6	1.361(7)	C1-C2	1.371(7)
C1-P1	1.823(5)	C2-C3	1.401(8)
C3-C4	1.372(9)	C4-C5	1.341(10)
C5-C6	1.382(9)	C7-C12	1.384(6)
C7-C8	1.387(7)	C7-P1	1.824(4)
C8-C9	1.385(7)	C9-C10	1.370(9)
C10-C11	1.356(9)	C11-C12	1.403(7)
C13-C14	1.513(6)	C13-C21	1.541(6)
C13-P1	1.850(4)	C14-C15	1.378(6)
C14-C19	1.403(6)	C15-C16	1.375(7)
C16-C17	1.364(6)	C17-O1	1.375(6)
C17-C18	1.381(7)	C18-O2	1.376(5)
C18-C19	1.383(7)	C20-O2	1.413(8)
C21-C22	1.503(6)	C22-O3	1.272(6)
C22-C23	1.405(6)	C23-C24	1.389(6)
C24-O4	1.278(6)	C24-C25	1.500(6)

C25-C26	1.550(6)	C26-C27	1.520(6)
C26-P2	1.843(4)	C27-C28	1.371(6)
C27-C32	1.381(6)	C28-C29	1.404(7)
C29-C30	1.348(7)	C30-O6	1.387(6)
C30-C31	1.387(7)	C31-O5	1.360(6)
C31-C32	1.392(7)	C33-O5	1.411(9)
C34-C39	1.376(7)	C34-C35	1.378(7)
C34-P2	1.820(4)	C35-C36	1.385(8)
C36-C37	1.352(10)	C37-C38	1.375(10)
C38-C39	1.408(8)	C40-C45	1.370(7)
C40-C41	1.376(6)	C40-P2	1.820(4)
C41-C42	1.386(8)	C42-C43	1.372(9)
C43-C44	1.359(8)	C44-C45	1.397(7)
P1-S1	1.9488(15)	P2-S2	1.9535(15)

Bond angles (°) of compound chiral-17aa'

C6-C1-C2	119.1(5)	C6-C1-P1	120.3(4)
C2-C1-P1	120.4(3)	C1-C2-C3	119.9(5)
C4-C3-C2	119.4(6)	C5-C4-C3	120.3(6)
C4-C5-C6	120.4(6)	C1-C6-C5	120.9(6)
C12-C7-C8	119.8(4)	C12-C7-P1	123.1(3)
C8-C7-P1	117.2(4)	C9-C8-C7	119.9(5)
C10-C9-C8	120.1(5)	C11-C10-C9	120.7(5)
C10-C11-C12	120.3(5)	C7-C12-C11	119.2(5)
C14-C13-C21	114.8(3)	C14-C13-P1	111.3(3)
C21-C13-P1	106.9(3)	C15-C14-C19	117.4(4)
C15-C14-C13	120.6(4)	C19-C14-C13	122.0(4)
C16-C15-C14	121.8(4)	C17-C16-C15	120.6(5)
C16-C17-O1	119.1(4)	C16-C17-C18	119.3(4)
O1-C17-C18	121.6(4)	O2-C18-C17	114.1(4)
O2-C18-C19	125.5(4)	C17-C18-C19	120.3(4)
C18-C19-C14	120.6(4)	C22-C21-C13	112.4(4)
O3-C22-C23	121.6(4)	O3-C22-C21	118.2(4)
C23-C22-C21	120.1(4)	C24-C23-C22	120.1(4)
O4-C24-C23	122.3(4)	O4-C24-C25	116.8(4)
C23-C24-C25	120.8(4)	C24-C25-C26	112.3(3)
C27-C26-C25	114.5(3)	C27-C26-P2	112.4(3)
C25-C26-P2	106.9(3)	C28-C27-C32	118.4(4)
C28-C27-C26	119.2(4)	C32-C27-C26	122.4(4)

C27-C28-C29	120.9(4)	C30-C29-C28	120.3(5)
C29-C30-O6	119.3(5)	C29-C30-C31	120.0(5)
O6-C30-C31	120.7(5)	O5-C31-C30	114.9(5)
O5-C31-C32	125.6(5)	C30-C31-C32	119.5(4)
C27-C32-C31	121.0(4)	C39-C34-C35	120.2(5)
C39-C34-P2	122.4(4)	C35-C34-P2	117.4(4)
C34-C35-C36	120.8(6)	C37-C36-C35	118.9(6)
C36-C37-C38	121.9(6)	C37-C38-C39	119.3(6)
C34-C39-C38	118.8(6)	C45-C40-C41	118.4(4)
C45-C40-P2	121.6(3)	C41-C40-P2	119.8(4)
C40-C41-C42	121.1(5)	C43-C42-C41	119.7(5)
C44-C43-C42	120.2(5)	C43-C44-C45	119.8(5)
C40-C45-C44	120.8(5)	C18-O2-C20	117.5(5)
C31-O5-C33	116.9(6)	C1-P1-C7	103.57(19)
C1-P1-C13	108.72(19)	C7-P1-C13	106.05(19)
C1-P1-S1	112.74(15)	C7-P1-S1	112.92(16)
C13-P1-S1	112.26(15)	C34-P2-C40	104.21(19)
C34-P2-C26	104.8(2)	C40-P2-C26	108.88(18)
C34-P2-S2	113.30(16)	C40-P2-S2	112.17(15)
C26-P2-S2	112.86(15)		

Crystallographic data for compound mono-17aa

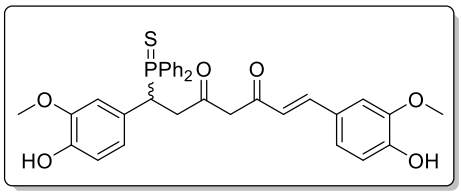

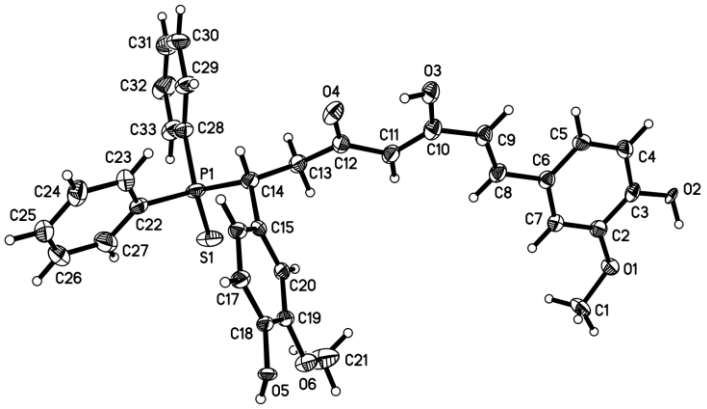

Identification code	leung1205s	
Chemical formula	$C_{34}H_{33}Cl_2O_6PS$	
Formula weight	671.53 g/mol	
Temperature	100(2) K	
Wavelength	1.54178 Å	
Crystal size	0.010 x 0.020 x 0.280 mm	
Crystal habit	colorless needle	
Crystal system	monoclinic	
Space group	P 1 21/c 1	
Unit cell dimensions	a = 12.7335(5) Å	α = 90°
	b = 8.8031(3) Å	β = 91.317(3)°
	c = 28.6775(9) Å	γ = 90°
Volume	3213.7(2) $Å^3$	
Z	4	
Density (calculated)	1.388 g/cm^3	
Absorption coefficient	3.265 mm^{-1}	
F(000)	1400	

Theta range for data collection	3.08 to 68.28°
Index ranges	-15<=h<=13, -10<=k<=10, -30<=l<=34
Reflections collected	23783
Independent reflections	5804 [R(int) = 0.0909]
Coverage of independent reflections	98.4%
Absorption correction	Multi-Scan
Max. and min. transmission	0.9680 and 0.4620

Structure solution technique	direct methods	
Structure solution program	XT, VERSION 2014/5	
Refinement method	Full-matrix least-squares on F^2	
Refinement program	SHELXL-2018/3 (Sheldrick, 2018)	
Function minimized	$\Sigma\ w(F_o^2 - F_c^2)^2$	
Data / restraints / parameters	5804 / 1739 / 625	
Goodness-of-fit on F^2	1.027	
Final R indices	4734 data; $I>2\sigma(I)$	R1 = 0.0884, wR2 = 0.2210
	all data	R1 = 0.1001, wR2 = 0.2353
Weighting scheme	$w=1/[\sigma^2(F_o^2)+(0.1627P)^2+2.3670P]$ where $P=(F_o^2+2F_c^2)/3$	
Largest diff. peak and hole	0.900 and -1.299 eÅ^{-3}	
R.M.S. deviation from mean	0.128 eÅ^{-3}	

Bond lengths (Å) of compound mono-17aa

C1-O1	1.432(7)	C1-H1A	0.98
C1-H1B	0.98	C1-H1C	0.98
C2-O1	1.365(5)	C2-C3	1.39
C2-C7	1.39	C3-O2	1.377(5)
C3-C4	1.39	C4-C5	1.39
C4-H4	0.95	C5-C6	1.39
C5-H5	0.95	C6-C7	1.39
C6-C8	1.482(6)	C7-H7	0.95
C8-C9	1.327(7)	C8-H8	0.95
C9-C10	1.461(8)	C9-H9	0.95
C10-O3	1.335(10)	C10-C11	1.352(11)
C11-C12	1.438(7)	C11-H11	0.95
C12-O4	1.258(8)	C12-C13	1.506(9)
C13-C14	1.543(7)	C13-H13A	0.99
C13-H13B	0.99	C14-C15	1.535(5)
C14-P1	1.864(6)	C14-H14	1.0
C15-C16	1.39	C15-C20	1.39
C16-C17	1.39	C16-H16	0.95
C17-C18	1.39	C17-H17	0.95

C18-O5	1.383(5)	C18-C19	1.39
C19-O6	1.367(5)	C19-C20	1.39
C20-H20	0.95	C21-O6	1.430(8)
C21-H21A	0.98	C21-H21B	0.98
C21-H21C	0.98	O5-H5A	0.84
O2-H2	0.84	O3-H3	0.84
C1A-O1A	1.429(9)	C1A-H1A1	0.98
C1A-H1A2	0.98	C1A-H1A3	0.98
C2A-O1A	1.368(7)	C2A-C3A	1.39
C2A-C7A	1.39	C3A-O2A	1.374(6)
C3A-C4A	1.39	C4A-C5A	1.39
C4A-H4A	0.95	C5A-C6A	1.39
C5A-H5A1	0.95	C6A-C7A	1.39
C6A-C8A	1.473(7)	C7A-H7A	0.95
C8A-C9A	1.327(8)	C8A-H8A	0.95
C9A-C10A	1.464(10)	C9A-H9A	0.95
C10A-O3A	1.319(11)	C10A-C11A	1.352(11)
C11A-C12A	1.430(9)	C11A-H11A	0.95
C12A-O4A	1.257(9)	C12A-C13A	1.508(9)
C13A-C14A	1.540(8)	C13A-H13C	0.99
C13A-H13D	0.99	C14A-C15A	1.528(7)
C14A-P1	1.851(7)	C14A-H14A	1.0
C15A-C16A	1.39	C15A-C20A	1.39
C16A-C17A	1.39	C16A-H16A	0.95
C17A-C18A	1.39	C17A-H17A	0.95
C18A-O5A	1.385(6)	C18A-C19A	1.39
C19A-O6A	1.366(6)	C19A-C20A	1.39
C20A-H20A	0.95	C21A-O6A	1.434(9)
C21A-H21D	0.98	C21A-H21E	0.98
C21A-H21F	0.98	O5A-H5A2	0.84
O2A-H2A	0.84	O3A-H3A	0.84
C22-C27	1.380(5)	C22-C23	1.381(5)
C22-P1	1.813(3)	C23-C24	1.398(5)
C23-H23	0.95	C24-C25	1.372(6)
C24-H24	0.95	C25-C26	1.360(7)
C25-H25	0.95	C26-C27	1.408(6)
C26-H26	0.95	C27-H27	0.95
C28-C33	1.381(6)	C28-C29	1.391(6)
C28-P1	1.822(3)	C29-C30	1.396(6)
C29-H29	0.95	C30-C31	1.374(8)
C30-H30	0.95	C31-C32	1.357(7)

C31-H31	0.95	C32-C33	1.392(6)
C32-H32	0.95	C33-H33	0.95
C34-Cl2	1.709(8)	C34-Cl1	1.716(9)
C34-H34A	0.99	C34-H34B	0.99
C34A-Cl2A	1.700(10)	C34A-Cl1A	1.703(11)
C34A-H34C	0.99	C34A-H34D	0.99
P1-S1	1.9558(13)		

Bond angles (°) of compound mono-17aa

O1-C1-H1A	109.5	O1-C1-H1B	109.5
H1A-C1-H1B	109.5	O1-C1-H1C	109.5
H1A-C1-H1C	109.5	H1B-C1-H1C	109.5
O1-C2-C3	113.5(4)	O1-C2-C7	126.5(4)
C3-C2-C7	120.0	O2-C3-C4	118.8(5)
O2-C3-C2	120.9(5)	C4-C3-C2	120.0
C5-C4-C3	120.0	C5-C4-H4	120.0
C3-C4-H4	120.0	C4-C5-C6	120.0
C4-C5-H5	120.0	C6-C5-H5	120.0
C5-C6-C7	120.0	C5-C6-C8	121.3(4)
C7-C6-C8	118.6(4)	C6-C7-C2	120.0
C6-C7-H7	120.0	C2-C7-H7	120.0
C9-C8-C6	126.8(6)	C9-C8-H8	116.6
C6-C8-H8	116.6	C8-C9-C10	124.4(6)
C8-C9-H9	117.8	C10-C9-H9	117.8
O3-C10-C11	122.1(7)	O3-C10-C9	111.4(7)
C11-C10-C9	126.5(8)	C10-C11-C12	121.3(7)
C10-C11-H11	119.4	C12-C11-H11	119.4
O4-C12-C11	121.4(8)	O4-C12-C13	121.0(7)
C11-C12-C13	116.9(7)	C12-C13-C14	114.6(6)
C12-C13-H13A	108.6	C14-C13-H13A	108.6
C12-C13-H13B	108.6	C14-C13-H13B	108.6
H13A-C13-H13B	107.6	C15-C14-C13	113.2(6)
C15-C14-P1	110.9(6)	C13-C14-P1	113.0(5)
C15-C14-H14	106.4	C13-C14-H14	106.4
P1-C14-H14	106.4	C16-C15-C20	120.0
C16-C15-C14	120.1(4)	C20-C15-C14	119.5(4)
C15-C16-C17	120.0	C15-C16-H16	120.0
C17-C16-H16	120.0	C18-C17-C16	120.0
C18-C17-H17	120.0	C16-C17-H17	120.0

O5-C18-C17	119.4(5)	O5-C18-C19	120.6(5)
C17-C18-C19	120.0	O6-C19-C18	114.7(4)
O6-C19-C20	125.3(4)	C18-C19-C20	120.0
C19-C20-C15	120.0	C19-C20-H20	120.0
C15-C20-H20	120.0	O6-C21-H21A	109.5
O6-C21-H21B	109.5	H21A-C21-H21B	109.5
O6-C21-H21C	109.5	H21A-C21-H21C	109.5
H21B-C21-H21C	109.5	C18-O5-H5A	109.5
C19-O6-C21	116.6(6)	C2-O1-C1	117.2(7)
C3-O2-H2	109.5	C10-O3-H3	109.5
O1A-C1A-H1A1	109.5	O1A-C1A-H1A2	109.5
H1A1-C1A-H1A2	109.5	O1A-C1A-H1A3	109.5
H1A1-C1A-H1A3	109.5	H1A2-C1A-H1A3	109.5
O1A-C2A-C3A	113.5(6)	O1A-C2A-C7A	126.4(6)
C3A-C2A-C7A	120.0	O2A-C3A-C2A	121.1(7)
O2A-C3A-C4A	118.8(7)	C2A-C3A-C4A	120.0
C5A-C4A-C3A	120.0	C5A-C4A-H4A	120.0
C3A-C4A-H4A	120.0	C4A-C5A-C6A	120.0
C4A-C5A-H5A1	120.0	C6A-C5A-H5A1	120.0
C5A-C6A-C7A	120.0	C5A-C6A-C8A	118.1(5)
C7A-C6A-C8A	121.9(5)	C6A-C7A-C2A	120.0
C6A-C7A-H7A	120.0	C2A-C7A-H7A	120.0
C9A-C8A-C6A	127.6(7)	C9A-C8A-H8A	116.2
C6A-C8A-H8A	116.2	C8A-C9A-C10A	122.5(7)
C8A-C9A-H9A	118.7	C10A-C9A-H9A	118.7
O3A-C10A-C11A	123.0(9)	O3A-C10A-C9A	115.3(8)
C11A-C10A-C9A	121.4(9)	C10A-C11A-C12A	121.8(10)
C10A-C11A-H11A	119.1	C12A-C11A-H11A	119.1
O4A-C12A-C11A	122.3(9)	O4A-C12A-C13A	120.9(8)
C11A-C12A-C13A	116.8(9)	C12A-C13A-C14A	111.6(8)
C12A-C13A-H13C	109.3	C14A-C13A-H13C	109.3
C12A-C13A-H13D	109.3	C14A-C13A-H13D	109.3
H13C-C13A-H13D	108.0	C15A-C14A-C13A	115.7(9)
C15A-C14A-P1	108.4(9)	C13A-C14A-P1	100.0(6)
C15A-C14A-H14A	110.7	C13A-C14A-H14A	110.7
P1-C14A-H14A	110.7	C16A-C15A-C20A	120.0
C16A-C15A-C14A	117.8(6)	C20A-C15A-C14A	122.2(6)
C17A-C16A-C15A	120.0	C17A-C16A-H16A	120.0
C15A-C16A-H16A	120.0	C16A-C17A-C18A	120.0
C16A-C17A-H17A	120.0	C18A-C17A-H17A	120.0
O5A-C18A-C19A	121.7(6)	O5A-C18A-C17A	118.3(7)

C19A-C18A-C17A	120.0	O6A-C19A-C18A	114.4(6)
O6A-C19A-C20A	125.6(6)	C18A-C19A-C20A	120.0
C19A-C20A-C15A	120.0	C19A-C20A-H20A	120.0
C15A-C20A-H20A	120.0	O6A-C21A-H21D	109.5
O6A-C21A-H21E	109.5	H21D-C21A-H21E	109.5
O6A-C21A-H21F	109.5	H21D-C21A-H21F	109.5
H21E-C21A-H21F	109.5	C18A-O5A-H5A2	109.5
C19A-O6A-C21A	115.5(8)	C2A-O1A-C1A	118.7(9)
C3A-O2A-H2A	109.5	C10A-O3A-H3A	109.5
C27-C22-C23	119.4(3)	C27-C22-P1	119.0(3)
C23-C22-P1	121.5(3)	C22-C23-C24	120.3(3)
C22-C23-H23	119.8	C24-C23-H23	119.8
C25-C24-C23	119.9(4)	C25-C24-H24	120.1
C23-C24-H24	120.1	C26-C25-C24	120.3(4)
C26-C25-H25	119.8	C24-C25-H25	119.8
C25-C26-C27	120.3(4)	C25-C26-H26	119.8
C27-C26-H26	119.8	C22-C27-C26	119.8(4)
C22-C27-H27	120.1	C26-C27-H27	120.1
C33-C28-C29	119.7(3)	C33-C28-P1	117.1(3)
C29-C28-P1	123.2(3)	C28-C29-C30	119.3(4)
C28-C29-H29	120.4	C30-C29-H29	120.4
C31-C30-C29	120.1(4)	C31-C30-H30	120.0
C29-C30-H30	120.0	C32-C31-C30	120.7(4)
C32-C31-H31	119.7	C30-C31-H31	119.7
C31-C32-C33	120.3(4)	C31-C32-H32	119.9
C33-C32-H32	119.9	C28-C33-C32	119.9(4)
C28-C33-H33	120.0	C32-C33-H33	120.0
Cl2-C34-Cl1	113.3(6)	Cl2-C34-H34A	108.9
Cl1-C34-H34A	108.9	Cl2-C34-H34B	108.9
Cl1-C34-H34B	108.9	H34A-C34-H34B	107.7
Cl2A-C34A-Cl1A	114.6(9)	Cl2A-C34A-H34C	108.6
Cl1A-C34A-H34C	108.6	Cl2A-C34A-H34D	108.6
Cl1A-C34A-H34D	108.6	H34C-C34A-H34D	107.6
C22-P1-C28	105.67(15)	C22-P1-C14A	104.0(4)
C28-P1-C14A	107.8(4)	C22-P1-C14	108.0(3)
C28-P1-C14	104.7(3)	C22-P1-S1	113.01(12)
C28-P1-S1	111.60(13)	C14A-P1-S1	114.1(5)
C14-P1-S1	113.3(4)		

Crystallographic data for compound rac-18aa

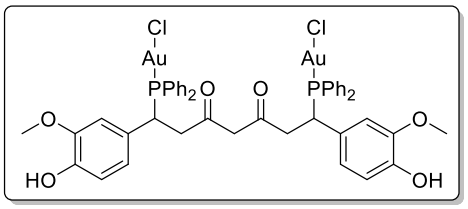

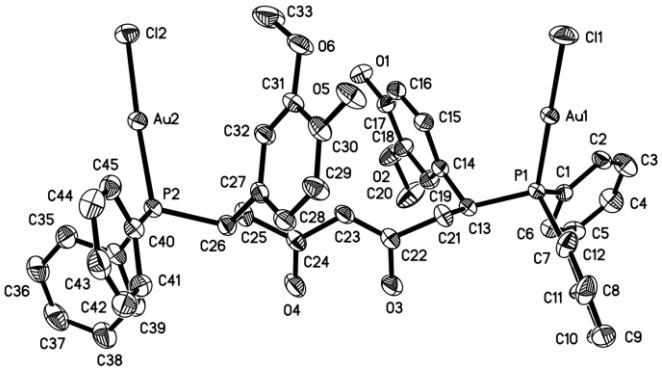

Identification code	leung1167m
Chemical formula	$C_{47.94}H_{48.66}Au_2Cl_{3.22}O_6P_2$
Formula weight	1290.95 g/mol
Temperature	100(2) K
Wavelength	0.71073 Å
Crystal size	0.020 x 0.140 x 0.200 mm
Crystal habit	colorless plate
Crystal system	monoclinic
Space group	P 1 21/c 1
Unit cell dimensions	a = 9.4719(2) Å α = 90°
	b = 29.6113(5) Å β = 101.1373(8)°
	c = 20.1946(3) Å γ = 90°
Volume	5557.41(17) $Å^3$
Z	4
Density (calculated)	1.543 g/cm^3
Absorption coefficient	5.526 mm^{-1}
F(000)	2508

Theta range for data collection	2.30 to 34.34°
Index ranges	-15<=h<=15, -43<=k<=47, -32<=l<=29
Reflections collected	78104
Independent reflections	23148 [R(int) = 0.0518]
Coverage of independent reflections	99.5%
Absorption correction	Multi-Scan
Max. and min. transmission	0.8980 and 0.4040
Structure solution technique	direct methods

Structure solution program	XT, VERSION 2014/5	
Refinement method	Full-matrix least-squares on F^2	
Refinement program	SHELXL-2018/3 (Sheldrick, 2018)	
Function minimized	$\Sigma\, w(F_o^2 - F_c^2)^2$	
Data / restraints / parameters	23148 / 430 / 660	
Goodness-of-fit on F^2	1.047	
Δ/σ_{max}	0.003	
Final R indices	15723 data; $I>2\sigma(I)$	R1 = 0.0498, wR2 = 0.1088
	all data	R1 = 0.0889, wR2 = 0.1240
Weighting scheme	$w=1/[\sigma^2(F_o^2)+(0.0375P)^2+22.2845P]$ where $P=(F_o^2+2F_c^2)/3$	
Largest diff. peak and hole	2.550 and -2.173 eÅ^{-3}	
R.M.S. deviation from mean	0.181 eÅ^{-3}	

Bond lengths (Å) of compound rac-18aa

Au1-P1	2.2283(12)	Au1-Cl1	2.2794(14)
Au2-P2	2.2328(12)	Au2-Cl2	2.2800(12)
C1-C2	1.390(6)	C1-C6	1.405(7)
C1-P1	1.814(5)	C2-C3	1.378(7)
C2-H2	0.95	C3-C4	1.384(8)
C3-H3	0.95	C4-C5	1.385(8)
C4-H4	0.95	C5-C6	1.360(7)
C5-H5	0.95	C6-H6	0.95
C7-C8	1.39	C7-C12	1.39
C7-P1	1.830(4)	C8-C9	1.39
C8-H8	0.95	C9-C10	1.39
C9-H9	0.95	C10-C11	1.39
C10-H10	0.95	C11-C12	1.39
C11-H11	0.95	C12-H12	0.95
C7A-C8A	1.39	C7A-C12A	1.39
C7A-P1	1.815(6)	C8A-C9A	1.39
C8A-H8A	0.95	C9A-C10A	1.39
C9A-H9A	0.95	C10A-C11A	1.39
C10A-H10A	0.95	C11A-C12A	1.39
C11A-H11A	0.95	C12A-H12A	0.95

C13-C14	1.520(6)	C13-C21	1.528(7)
C13-P1	1.849(5)	C13-H13	1.0
C14-C15	1.392(7)	C14-C19	1.401(7)
C15-C16	1.380(7)	C15-H15	0.95
C16-C17	1.398(7)	C16-H16	0.95
C17-O1	1.358(6)	C17-C18	1.391(7)
C18-O2	1.373(6)	C18-C19	1.391(7)
C19-H19	0.95	C20-O2	1.429(7)
C20-H20A	0.98	C20-H20B	0.98
C20-H20C	0.98	C21-C22	1.487(7)
C21-H21A	0.99	C21-H21B	0.99
C22-O3	1.314(6)	C22-C23	1.359(7)
C23-C24	1.421(6)	C23-H23	0.95
C24-O4	1.243(6)	C24-C25	1.516(7)
C25-C26	1.541(7)	C25-H25A	0.99
C25-H25B	0.99	C26-C27	1.518(7)
C26-P2	1.851(5)	C26-H26	1.0
C27-C28	1.393(7)	C27-C32	1.405(6)
C28-C29	1.395(7)	C28-H28	0.95
C29-C30	1.370(7)	C29-H29	0.95
C30-O5	1.362(6)	C30-C31	1.391(7)
C31-O6	1.376(6)	C31-C32	1.382(7)
C32-H32	0.95	C33-O6	1.428(7)
C33-H33A	0.98	C33-H33B	0.98
C33-H33C	0.98	C34-C39	1.387(7)
C34-C35	1.395(7)	C34-P2	1.814(5)
C35-C36	1.378(8)	C35-H35	0.95
C36-C37	1.364(9)	C36-H36	0.95
C37-C38	1.404(9)	C37-H37	0.95
C38-C39	1.388(8)	C38-H38	0.95
C39-H39	0.95	C40-C41	1.391(7)
C40-C45	1.393(7)	C40-P2	1.808(5)
C41-C42	1.384(8)	C41-H41	0.95
C42-C43	1.376(9)	C42-H42	0.95
C43-C44	1.386(8)	C43-H43	0.95
C44-C45	1.403(7)	C44-H44	0.95
C45-H45	0.95	O1-H1	0.84
O3-H3A	0.84	O5-H5A	0.84
C50-Cl4	1.720(12)	C50-Cl3	1.735(13)
C50-H50A	0.99	C50-H50B	0.99
C50A-Cl4A	1.718(13)	C50A-Cl3A	1.733(14)

C50A-H50C	0.99	C50A-H50D	0.99
C51-C52	1.621(18)	C51-H51A	0.98
C51-H51B	0.98	C51-H51C	0.98
C52-C53	1.528(17)	C52-H52A	0.99
C52-H52B	0.99	C53-C54	1.508(17)
C53-H53A	0.99	C53-H53B	0.99
C54-C55	1.498(17)	C54-H54A	0.99
C54-H54B	0.99	C55-C56	1.482(17)
C55-H55A	0.99	C55-H55B	0.99
C56-H56A	0.98	C56-H56B	0.98
C56-H56C	0.98		

Bond angles (°) of compound rac-18aa

P1-Au1-Cl1	179.10(6)	P2-Au2-Cl2	176.85(5)
C2-C1-C6	119.0(4)	C2-C1-P1	118.8(4)
C6-C1-P1	122.0(4)	C3-C2-C1	120.0(5)
C3-C2-H2	120.0	C1-C2-H2	120.0
C2-C3-C4	120.5(5)	C2-C3-H3	119.8
C4-C3-H3	119.8	C3-C4-C5	119.5(5)
C3-C4-H4	120.3	C5-C4-H4	120.3
C6-C5-C4	120.7(5)	C6-C5-H5	119.6
C4-C5-H5	119.6	C5-C6-C1	120.2(5)
C5-C6-H6	119.9	C1-C6-H6	119.9
C8-C7-C12	120.0	C8-C7-P1	122.8(4)
C12-C7-P1	117.1(4)	C9-C8-C7	120.0
C9-C8-H8	120.0	C7-C8-H8	120.0
C8-C9-C10	120.0	C8-C9-H9	120.0
C10-C9-H9	120.0	C11-C10-C9	120.0
C11-C10-H10	120.0	C9-C10-H10	120.0
C10-C11-C12	120.0	C10-C11-H11	120.0
C12-C11-H11	120.0	C11-C12-C7	120.0
C11-C12-H12	120.0	C7-C12-H12	120.0
C8A-C7A-C12A	120.0	C8A-C7A-P1	120.5(6)
C12A-C7A-P1	119.4(6)	C7A-C8A-C9A	120.0
C7A-C8A-H8A	120.0	C9A-C8A-H8A	120.0
C8A-C9A-C10A	120.0	C8A-C9A-H9A	120.0
C10A-C9A-H9A	120.0	C11A-C10A-C9A	120.0
C11A-C10A-H10A	120.0	C9A-C10A-H10A	120.0
C10A-C11A-C12A	120.0	C10A-C11A-H11A	120.0

C12A-C11A-H11A	120.0	C11A-C12A-C7A	120.0
C11A-C12A-H12A	120.0	C7A-C12A-H12A	120.0
C14-C13-C21	112.5(4)	C14-C13-P1	112.4(3)
C21-C13-P1	108.5(3)	C14-C13-H13	107.7
C21-C13-H13	107.7	P1-C13-H13	107.7
C15-C14-C19	118.8(4)	C15-C14-C13	122.0(4)
C19-C14-C13	119.1(4)	C16-C15-C14	121.1(5)
C16-C15-H15	119.5	C14-C15-H15	119.5
C15-C16-C17	120.4(5)	C15-C16-H16	119.8
C17-C16-H16	119.8	O1-C17-C18	122.0(4)
O1-C17-C16	119.3(4)	C18-C17-C16	118.7(4)
O2-C18-C17	113.7(4)	O2-C18-C19	125.2(4)
C17-C18-C19	121.0(5)	C18-C19-C14	119.9(4)
C18-C19-H19	120.1	C14-C19-H19	120.1
O2-C20-H20A	109.5	O2-C20-H20B	109.5
H20A-C20-H20B	109.5	O2-C20-H20C	109.5
H20A-C20-H20C	109.5	H20B-C20-H20C	109.5
C22-C21-C13	111.6(4)	C22-C21-H21A	109.3
C13-C21-H21A	109.3	C22-C21-H21B	109.3
C13-C21-H21B	109.3	H21A-C21-H21B	108.0
O3-C22-C23	122.8(4)	O3-C22-C21	112.2(4)
C23-C22-C21	125.0(5)	C22-C23-C24	120.2(4)
C22-C23-H23	119.9	C24-C23-H23	119.9
O4-C24-C23	121.5(5)	O4-C24-C25	117.9(4)
C23-C24-C25	120.6(4)	C24-C25-C26	109.6(4)
C24-C25-H25A	109.8	C26-C25-H25A	109.8
C24-C25-H25B	109.8	C26-C25-H25B	109.8
H25A-C25-H25B	108.2	C27-C26-C25	114.3(4)
C27-C26-P2	107.7(3)	C25-C26-P2	109.6(3)
C27-C26-H26	108.4	C25-C26-H26	108.4
P2-C26-H26	108.4	C28-C27-C32	118.7(4)
C28-C27-C26	119.9(4)	C32-C27-C26	121.4(4)
C27-C28-C29	120.2(5)	C27-C28-H28	119.9
C29-C28-H28	119.9	C30-C29-C28	120.8(5)
C30-C29-H29	119.6	C28-C29-H29	119.6
O5-C30-C29	120.0(5)	O5-C30-C31	120.5(5)
C29-C30-C31	119.5(5)	O6-C31-C32	124.7(4)
O6-C31-C30	114.7(4)	C32-C31-C30	120.6(4)
C31-C32-C27	120.2(4)	C31-C32-H32	119.9
C27-C32-H32	119.9	O6-C33-H33A	109.5
O6-C33-H33B	109.5	H33A-C33-H33B	109.5

O6-C33-H33C	109.5	H33A-C33-H33C	109.5
H33B-C33-H33C	109.5	C39-C34-C35	119.4(5)
C39-C34-P2	123.7(4)	C35-C34-P2	116.8(4)
C36-C35-C34	119.9(5)	C36-C35-H35	120.1
C34-C35-H35	120.1	C37-C36-C35	121.5(6)
C37-C36-H36	119.2	C35-C36-H36	119.2
C36-C37-C38	118.9(5)	C36-C37-H37	120.5
C38-C37-H37	120.5	C39-C38-C37	120.2(6)
C39-C38-H38	119.9	C37-C38-H38	119.9
C34-C39-C38	120.0(5)	C34-C39-H39	120.0
C38-C39-H39	120.0	C41-C40-C45	119.1(5)
C41-C40-P2	121.0(4)	C45-C40-P2	119.9(4)
C42-C41-C40	120.5(5)	C42-C41-H41	119.7
C40-C41-H41	119.7	C43-C42-C41	120.8(5)
C43-C42-H42	119.6	C41-C42-H42	119.6
C42-C43-C44	119.5(5)	C42-C43-H43	120.2
C44-C43-H43	120.2	C43-C44-C45	120.3(5)
C43-C44-H44	119.8	C45-C44-H44	119.8
C40-C45-C44	119.8(5)	C40-C45-H45	120.1
C44-C45-H45	120.1	C17-O1-H1	109.5
C18-O2-C20	117.1(4)	C22-O3-H3A	109.5
C30-O5-H5A	109.5	C31-O6-C33	117.1(4)
Cl4-C50-Cl3	110.4(10)	Cl4-C50-H50A	109.6
Cl3-C50-H50A	109.6	Cl4-C50-H50B	109.6
Cl3-C50-H50B	109.6	H50A-C50-H50B	108.1
Cl4A-C50A-Cl3A	107.5(10)	Cl4A-C50A-H50C	110.2
Cl3A-C50A-H50C	110.2	Cl4A-C50A-H50D	110.2
Cl3A-C50A-H50D	110.2	H50C-C50A-H50D	108.5
C52-C51-H51A	109.5	C52-C51-H51B	109.5
H51A-C51-H51B	109.5	C52-C51-H51C	109.5
H51A-C51-H51C	109.5	H51B-C51-H51C	109.5
C53-C52-C51	103.7(15)	C53-C52-H52A	111.0
C51-C52-H52A	111.0	C53-C52-H52B	111.0
C51-C52-H52B	111.0	H52A-C52-H52B	109.0
C54-C53-C52	119.0(17)	C54-C53-H53A	107.6
C52-C53-H53A	107.6	C54-C53-H53B	107.6
C52-C53-H53B	107.6	H53A-C53-H53B	107.0
C55-C54-C53	119.2(18)	C55-C54-H54A	107.5
C53-C54-H54A	107.5	C55-C54-H54B	107.5
C53-C54-H54B	107.5	H54A-C54-H54B	107.0
C56-C55-C54	121.5(19)	C56-C55-H55A	107.0

C54-C55-H55A	107.0	C56-C55-H55B	107.0
C54-C55-H55B	107.0	H55A-C55-H55B	106.7
C55-C56-H56A	109.5	C55-C56-H56B	109.5
H56A-C56-H56B	109.5	C55-C56-H56C	109.5
H56A-C56-H56C	109.5	H56B-C56-H56C	109.5
C1-P1-C7A	108.2(3)	C1-P1-C7	105.7(3)
C1-P1-C13	108.1(2)	C7A-P1-C13	98.2(3)
C7-P1-C13	104.5(2)	C1-P1-Au1	114.46(15)
C7A-P1-Au1	114.0(4)	C7-P1-Au1	110.9(2)
C13-P1-Au1	112.54(16)	C40-P2-C34	105.3(2)
C40-P2-C26	103.9(2)	C34-P2-C26	107.7(2)
C40-P2-Au2	114.77(16)	C34-P2-Au2	112.77(17)
C26-P2-Au2	111.71(16)		

Crystallographic data for compound meso-18aa'

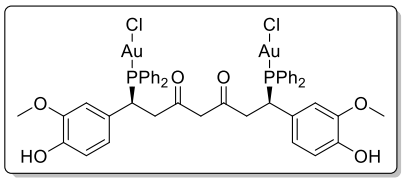

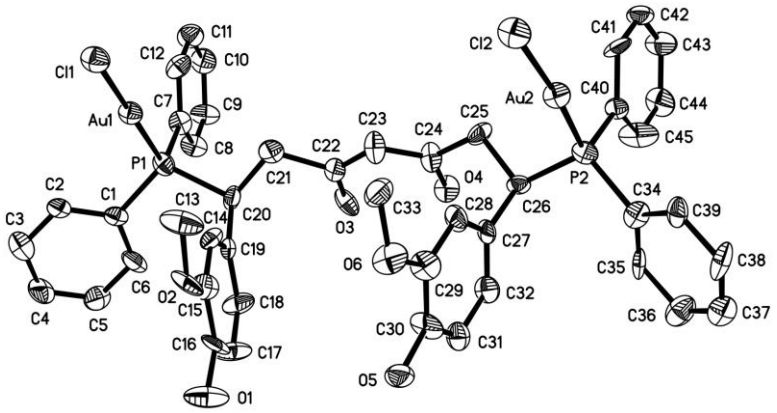

Identification code	leung1175m_sq	
Chemical formula	$C_{45.50}H_{42}Au_2Cl_3O_6P_2$	
Formula weight	1247.01 g/mol	
Temperature	100(2) K	
Wavelength	0.71073 Å	
Crystal size	0.010 x 0.020 x 0.200 mm	
Crystal habit	colorless needle	
Crystal system	orthorhombic	
Space group	P 21 21 2	
Unit cell dimensions	a = 27.9225(15) Å	α = 90°
	b = 44.567(2) Å	β = 90°
	c = 8.9967(6) Å	γ = 90°
Volume	11195.7(11) $Å^3$	
Z	8	
Density (calculated)	1.480 g/cm^3	
Absorption coefficient	5.473 mm^{-1}	
F(000)	4816	

Theta range for data collection	2.23 to 26.39°
Index ranges	-34<=h<=33, -51<=k<=55, -11<=l<=11
Reflections collected	71061
Independent reflections	22707 [R(int) = 0.1506]
Coverage of independent reflections	99.4%
Absorption correction	Multi-Scan
Max. and min. transmission	0.9470 and 0.4070

Structure solution technique	direct methods	
Structure solution program	XT, VERSION 2014/5	
Refinement method	Full-matrix least-squares on F^2	
Refinement program	SHELXL-2018/3 (Sheldrick, 2018)	
Function minimized	$\Sigma\ w(F_o^2 - F_c^2)^2$	
Data / restraints / parameters	22707 / 869 / 911	
Goodness-of-fit on F^2	0.953	
Δ/σ_{max}	0.001	
Final R indices	13380 data; $I>2\sigma(I)$	R1 = 0.0619, wR2 = 0.1084
	all data	R1 = 0.1312, wR2 = 0.1322
Weighting scheme	$w=1/[\sigma^2(F_o^2)+(0.0280P)^2]$ where $P=(F_o^2+2F_c^2)/3$	
Largest diff. peak and hole	1.108 and -1.097 eÅ^{-3}	
R.M.S. deviation from mean	0.178 eÅ^{-3}	

Bond lengths (Å) of compound meso-18aa'

Au1-P1	2.238(5)	Au1-Cl1	2.291(5)
Au2-P2	2.243(5)	Au2-Cl2	2.288(5)
Au3-P3	2.240(6)	Au3-Cl3	2.285(6)
Au4-P4	2.224(6)	Au4-Cl4	2.289(5)
C1-C2	1.39	C1-C6	1.39
C1-P1	1.812(10)	C2-C3	1.39
C2-H2	0.95	C3-C4	1.39
C3-H3	0.95	C4-C5	1.39
C4-H4	0.95	C5-C6	1.39
C5-H5	0.95	C6-H6	0.95
C7-C8	1.39	C7-C12	1.39
C7-P1	1.831(11)	C8-C9	1.39
C8-H8	0.95	C9-C10	1.39
C9-H9	0.95	C10-C11	1.39
C10-H10	0.95	C11-C12	1.39
C11-H11	0.95	C12-H12	0.95
C13-O2	1.444(19)	C13-H13A	0.98
C13-H13B	0.98	C13-H13C	0.98

C14-C15	1.39	C14-C19	1.39
C14-H14	0.95	C15-O2	1.347(16)
C15-C16	1.39	C16-O1	1.385(16)
C16-C17	1.39	C17-C18	1.39
C17-H17	0.95	C18-C19	1.39
C18-H18	0.95	C19-C20	1.58(2)
C20-C21	1.51(2)	C20-P1	1.847(18)
C20-H20	1.0	C21-C22	1.58(3)
C21-H21A	0.99	C21-H21B	0.99
C22-O3	1.26(2)	C22-C23	1.37(2)
C23-C24	1.36(2)	C23-H23	0.95
C24-O4	1.32(2)	C24-C25	1.48(2)
C25-C26	1.55(2)	C25-H25A	0.99
C25-H25B	0.99	C26-C27	1.51(2)
C26-P2	1.847(18)	C26-H26	1.0
C27-C28	1.39	C27-C32	1.39
C28-C29	1.39	C28-H28	0.95
C29-C30	1.39	C29-O6	1.423(15)
C30-C31	1.39	C30-O5	1.400(16)
C31-C32	1.39	C31-H31	0.95
C32-H32	0.95	C33-O6	1.43(2)
C33-H33A	0.98	C33-H33B	0.98
C33-H33C	0.98	C34-C35	1.39
C34-C39	1.39	C34-P2	1.806(10)
C35-C36	1.39	C35-H35	0.95
C36-C37	1.39	C36-H36	0.95
C37-C38	1.39	C37-H37	0.95
C38-C39	1.39	C38-H38	0.95
C39-H39	0.95	C40-C41	1.39
C40-C45	1.39	C40-P2	1.815(11)
C41-C42	1.39	C41-H41	0.95
C42-C43	1.39	C42-H42	0.95
C43-C44	1.39	C43-H43	0.95
C44-C45	1.39	C44-H44	0.95
C45-H45	0.95	C46-C47	1.39
C46-C51	1.39	C46-P3	1.815(10)
C47-C48	1.39	C47-H47	0.95
C48-C49	1.39	C48-H48	0.95
C49-C50	1.39	C49-H49	0.95
C50-C51	1.39	C50-H50	0.95
C51-H51	0.95	C52-C53	1.39

C52-C57	1.39	C52-P3	1.827(10)
C53-C54	1.39	C53-H53	0.95
C54-C55	1.39	C54-H54	0.95
C55-C56	1.39	C55-H55	0.95
C56-C57	1.39	C56-H56	0.95
C57-H57	0.95	C58-O8	1.40(2)
C58-H58A	0.98	C58-H58B	0.98
C58-H58C	0.98	C59-C60	1.39
C59-C64	1.39	C59-H59	0.95
C60-O8	1.342(16)	C60-C61	1.39
C61-O7	1.351(15)	C61-C62	1.39
C62-C63	1.39	C62-H62	0.95
C63-C64	1.39	C63-H63	0.95
C64-C65	1.53(2)	C65-C66	1.59(2)
C65-P3	1.851(19)	C65-H65	1.0
C66-C67	1.46(3)	C66-H66A	0.99
C66-H66B	0.99	C67-O9	1.35(3)
C67-C68	1.38(3)	C68-C69	1.41(3)
C68-H68	0.95	C69-O10	1.23(2)
C69-C70	1.52(3)	C70-C71	1.54(2)
C70-H70A	0.99	C70-H70B	0.99
C71-C72	1.52(2)	C71-P4	1.82(2)
C71-H71	1.0	C72-C73	1.39
C72-C77	1.39	C73-C74	1.39
C73-H73	0.95	C74-O12	1.342(16)
C74-C75	1.39	C75-O11	1.387(15)
C75-C76	1.39	C76-C77	1.39
C76-H76	0.95	C77-H77	0.95
C78-O12	1.47(3)	C78-H78A	0.98
C78-H78B	0.98	C78-H78C	0.98
C79-C80	1.39	C79-C84	1.39
C79-P4	1.811(10)	C80-C81	1.39
C80-H80	0.95	C81-C82	1.39
C81-H81	0.95	C82-C83	1.39
C82-H82	0.95	C83-C84	1.39
C83-H83	0.95	C84-H84	0.95
C85-C86	1.39	C85-C90	1.39
C85-P4	1.834(10)	C86-C87	1.39
C86-H86	0.95	C87-C88	1.39
C87-H87	0.95	C88-C89	1.39
C88-H88	0.95	C89-C90	1.39

C89-H89	0.95	C90-H90	0.95
C91-Cl6	1.72(2)	C91-Cl5	1.72(3)
C91-H91A	0.99	C91-H91B	0.99
O1-H1	0.84	O5-H5A	0.84
O7-H7	0.84	O11-H11A	0.84

Bond angles (°) of compound meso-18aa'

P1-Au1-Cl1	177.1(2)	P2-Au2-Cl2	174.1(2)
P3-Au3-Cl3	177.9(2)	P4-Au4-Cl4	177.6(2)
C2-C1-C6	120.0	C2-C1-P1	117.8(7)
C6-C1-P1	122.2(7)	C1-C2-C3	120.0
C1-C2-H2	120.0	C3-C2-H2	120.0
C4-C3-C2	120.0	C4-C3-H3	120.0
C2-C3-H3	120.0	C3-C4-C5	120.0
C3-C4-H4	120.0	C5-C4-H4	120.0
C4-C5-C6	120.0	C4-C5-H5	120.0
C6-C5-H5	120.0	C5-C6-C1	120.0
C5-C6-H6	120.0	C1-C6-H6	120.0
C8-C7-C12	120.0	C8-C7-P1	122.4(7)
C12-C7-P1	117.6(7)	C9-C8-C7	120.0
C9-C8-H8	120.0	C7-C8-H8	120.0
C8-C9-C10	120.0	C8-C9-H9	120.0
C10-C9-H9	120.0	C9-C10-C11	120.0
C9-C10-H10	120.0	C11-C10-H10	120.0
C10-C11-C12	120.0	C10-C11-H11	120.0
C12-C11-H11	120.0	C11-C12-C7	120.0
C11-C12-H12	120.0	C7-C12-H12	120.0
O2-C13-H13A	109.5	O2-C13-H13B	109.5
H13A-C13-H13B	109.5	O2-C13-H13C	109.5
H13A-C13-H13C	109.5	H13B-C13-H13C	109.5
C15-C14-C19	120.0	C15-C14-H14	120.0
C19-C14-H14	120.0	O2-C15-C16	115.1(11)
O2-C15-C14	124.9(11)	C16-C15-C14	120.0
O1-C16-C15	121.7(11)	O1-C16-C17	118.2(11)
C15-C16-C17	120.0	C16-C17-C18	120.0
C16-C17-H17	120.0	C18-C17-H17	120.0
C19-C18-C17	120.0	C19-C18-H18	120.0
C17-C18-H18	120.0	C18-C19-C14	120.0
C18-C19-C20	120.2(11)	C14-C19-C20	119.7(11)

C21-C20-C19	112.5(15)	C21-C20-P1	105.8(12)
C19-C20-P1	112.2(12)	C21-C20-H20	108.7
C19-C20-H20	108.7	P1-C20-H20	108.7
C20-C21-C22	111.9(15)	C20-C21-H21A	109.2
C22-C21-H21A	109.2	C20-C21-H21B	109.2
C22-C21-H21B	109.2	H21A-C21-H21B	107.9
O3-C22-C23	123.2(18)	O3-C22-C21	118.4(17)
C23-C22-C21	118.3(17)	C24-C23-C22	119.6(17)
C24-C23-H23	120.2	C22-C23-H23	120.2
O4-C24-C23	122.5(18)	O4-C24-C25	114.5(17)
C23-C24-C25	123.0(17)	C24-C25-C26	110.1(15)
C24-C25-H25A	109.6	C26-C25-H25A	109.6
C24-C25-H25B	109.6	C26-C25-H25B	109.6
H25A-C25-H25B	108.2	C27-C26-C25	115.1(15)
C27-C26-P2	112.4(13)	C25-C26-P2	108.4(11)
C27-C26-H26	106.8	C25-C26-H26	106.8
P2-C26-H26	106.8	C28-C27-C32	120.0
C28-C27-C26	121.6(11)	C32-C27-C26	118.3(11)
C27-C28-C29	120.0	C27-C28-H28	120.0
C29-C28-H28	120.0	C30-C29-C28	120.0
C30-C29-O6	114.6(10)	C28-C29-O6	125.4(10)
C29-C30-C31	120.0	C29-C30-O5	118.7(11)
C31-C30-O5	121.0(11)	C32-C31-C30	120.0
C32-C31-H31	120.0	C30-C31-H31	120.0
C31-C32-C27	120.0	C31-C32-H32	120.0
C27-C32-H32	120.0	O6-C33-H33A	109.5
O6-C33-H33B	109.5	H33A-C33-H33B	109.5
O6-C33-H33C	109.5	H33A-C33-H33C	109.5
H33B-C33-H33C	109.5	C35-C34-C39	120.0
C35-C34-P2	121.0(7)	C39-C34-P2	119.0(7)
C36-C35-C34	120.0	C36-C35-H35	120.0
C34-C35-H35	120.0	C37-C36-C35	120.0
C37-C36-H36	120.0	C35-C36-H36	120.0
C36-C37-C38	120.0	C36-C37-H37	120.0
C38-C37-H37	120.0	C39-C38-C37	120.0
C39-C38-H38	120.0	C37-C38-H38	120.0
C38-C39-C34	120.0	C38-C39-H39	120.0
C34-C39-H39	120.0	C41-C40-C45	120.0
C41-C40-P2	118.9(7)	C45-C40-P2	121.1(7)
C42-C41-C40	120.0	C42-C41-H41	120.0
C40-C41-H41	120.0	C41-C42-C43	120.0

C41-C42-H42	120.0	C43-C42-H42	120.0
C44-C43-C42	120.0	C44-C43-H43	120.0
C42-C43-H43	120.0	C43-C44-C45	120.0
C43-C44-H44	120.0	C45-C44-H44	120.0
C44-C45-C40	120.0	C44-C45-H45	120.0
C40-C45-H45	120.0	C47-C46-C51	120.0
C47-C46-P3	116.9(7)	C51-C46-P3	123.0(7)
C46-C47-C48	120.0	C46-C47-H47	120.0
C48-C47-H47	120.0	C49-C48-C47	120.0
C49-C48-H48	120.0	C47-C48-H48	120.0
C48-C49-C50	120.0	C48-C49-H49	120.0
C50-C49-H49	120.0	C49-C50-C51	120.0
C49-C50-H50	120.0	C51-C50-H50	120.0
C50-C51-C46	120.0	C50-C51-H51	120.0
C46-C51-H51	120.0	C53-C52-C57	120.0
C53-C52-P3	121.8(7)	C57-C52-P3	118.2(8)
C52-C53-C54	120.0	C52-C53-H53	120.0
C54-C53-H53	120.0	C55-C54-C53	120.0
C55-C54-H54	120.0	C53-C54-H54	120.0
C56-C55-C54	120.0	C56-C55-H55	120.0
C54-C55-H55	120.0	C57-C56-C55	120.0
C57-C56-H56	120.0	C55-C56-H56	120.0
C56-C57-C52	120.0	C56-C57-H57	120.0
C52-C57-H57	120.0	O8-C58-H58A	109.5
O8-C58-H58B	109.5	H58A-C58-H58B	109.5
O8-C58-H58C	109.5	H58A-C58-H58C	109.5
H58B-C58-H58C	109.5	C60-C59-C64	120.0
C60-C59-H59	120.0	C64-C59-H59	120.0
O8-C60-C59	123.3(12)	O8-C60-C61	116.7(12)
C59-C60-C61	120.0	O7-C61-C62	119.1(11)
O7-C61-C60	120.9(11)	C62-C61-C60	120.0
C61-C62-C63	120.0	C61-C62-H62	120.0
C63-C62-H62	120.0	C64-C63-C62	120.0
C64-C63-H63	120.0	C62-C63-H63	120.0
C63-C64-C59	120.0	C63-C64-C65	121.8(12)
C59-C64-C65	118.1(12)	C64-C65-C66	110.9(15)
C64-C65-P3	108.3(11)	C66-C65-P3	112.6(14)
C64-C65-H65	108.3	C66-C65-H65	108.3
P3-C65-H65	108.3	C67-C66-C65	113.7(17)
C67-C66-H66A	108.8	C65-C66-H66A	108.8
C67-C66-H66B	108.8	C65-C66-H66B	108.8

H66A-C66-H66B	107.7	O9-C67-C68	121.(2)
O9-C67-C66	115.4(19)	C68-C67-C66	124.(2)
C67-C68-C69	120.(2)	C67-C68-H68	119.9
C69-C68-H68	119.9	O10-C69-C68	122.9(19)
O10-C69-C70	117.0(19)	C68-C69-C70	120.(2)
C69-C70-C71	111.7(16)	C69-C70-H70A	109.3
C71-C70-H70A	109.3	C69-C70-H70B	109.3
C71-C70-H70B	109.3	H70A-C70-H70B	107.9
C72-C71-C70	114.7(16)	C72-C71-P4	110.6(11)
C70-C71-P4	110.7(13)	C72-C71-H71	106.8
C70-C71-H71	106.8	P4-C71-H71	106.8
C73-C72-C77	120.0	C73-C72-C71	117.7(10)
C77-C72-C71	122.3(11)	C74-C73-C72	120.0
C74-C73-H73	120.0	C72-C73-H73	120.0
O12-C74-C73	126.1(11)	O12-C74-C75	113.8(11)
C73-C74-C75	120.0	O11-C75-C74	123.1(11)
O11-C75-C76	116.9(11)	C74-C75-C76	120.0
C77-C76-C75	120.0	C77-C76-H76	120.0
C75-C76-H76	120.0	C76-C77-C72	120.0
C76-C77-H77	120.0	C72-C77-H77	120.0
O12-C78-H78A	109.5	O12-C78-H78B	109.5
H78A-C78-H78B	109.5	O12-C78-H78C	109.5
H78A-C78-H78C	109.5	H78B-C78-H78C	109.5
C80-C79-C84	120.0	C80-C79-P4	120.9(8)
C84-C79-P4	119.0(8)	C81-C80-C79	120.0
C81-C80-H80	120.0	C79-C80-H80	120.0
C80-C81-C82	120.0	C80-C81-H81	120.0
C82-C81-H81	120.0	C81-C82-C83	120.0
C81-C82-H82	120.0	C83-C82-H82	120.0
C84-C83-C82	120.0	C84-C83-H83	120.0
C82-C83-H83	120.0	C83-C84-C79	120.0
C83-C84-H84	120.0	C79-C84-H84	120.0
C86-C85-C90	120.0	C86-C85-P4	123.1(7)
C90-C85-P4	116.4(7)	C85-C86-C87	120.0
C85-C86-H86	120.0	C87-C86-H86	120.0
C88-C87-C86	120.0	C88-C87-H87	120.0
C86-C87-H87	120.0	C89-C88-C87	120.0
C89-C88-H88	120.0	C87-C88-H88	120.0
C88-C89-C90	120.0	C88-C89-H89	120.0
C90-C89-H89	120.0	C89-C90-C85	120.0
C89-C90-H90	120.0	C85-C90-H90	120.0

Cl6-C91-Cl5	116.4(14)	Cl6-C91-H91A	108.2
Cl5-C91-H91A	108.2	Cl6-C91-H91B	108.2
Cl5-C91-H91B	108.2	H91A-C91-H91B	107.3
C16-O1-H1	108.9	C15-O2-C13	121.4(15)
C30-O5-H5A	109.5	C29-O6-C33	114.9(15)
C61-O7-H7	109.5	C60-O8-C58	118.4(16)
C75-O11-H11A	109.1	C74-O12-C78	113.6(15)
C1-P1-C7	105.9(6)	C1-P1-C20	108.5(7)
C7-P1-C20	101.4(8)	C1-P1-Au1	113.8(5)
C7-P1-Au1	114.1(5)	C20-P1-Au1	112.2(7)
C34-P2-C40	108.9(6)	C34-P2-C26	107.5(7)
C40-P2-C26	102.3(8)	C34-P2-Au2	113.9(5)
C40-P2-Au2	113.1(5)	C26-P2-Au2	110.4(7)
C46-P3-C52	109.5(6)	C46-P3-C65	104.7(8)
C52-P3-C65	106.1(7)	C46-P3-Au3	112.0(5)
C52-P3-Au3	112.7(5)	C65-P3-Au3	111.3(7)
C79-P4-C71	105.2(7)	C79-P4-C85	107.9(6)
C71-P4-C85	105.7(8)	C79-P4-Au4	113.8(5)
C71-P4-Au4	112.4(7)	C85-P4-Au4	111.3(5)

Crystallographic data for compound 26

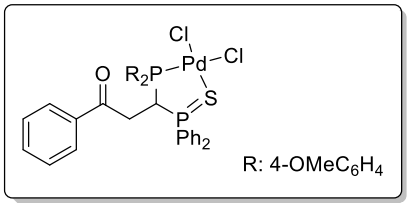

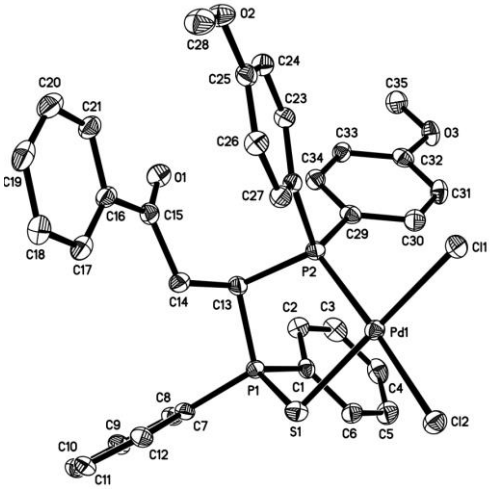

Identification code	leung1208
Chemical formula	$C_{36}H_{34}Cl_4O_3P_2PdS$
Formula weight	856.83 g/mol
Temperature	100(2) K
Wavelength	0.71073 Å
Crystal size	0.020 x 0.200 x 0.240 mm
Crystal habit	yellow plate
Crystal system	monoclinic
Space group	P 1 21/c 1
Unit cell dimensions	a = 11.663(3) Å α = 90°
	b = 18.114(5) Å β = 103.162(10)°
	c = 16.851(6) Å γ = 90°
Volume	3466.5(18) $Å^3$
Z	4
Density (calculated)	1.642 g/cm^3
Absorption coefficient	1.034 mm^{-1}
F(000)	1736

Theta range for data collection	1.68 to 32.34°
Index ranges	-10<=h<=17, -27<=k<=21, -25<=l<=24
Reflections collected	36982
Independent reflections	12166 [R(int) = 0.0867]
Coverage of independent reflections	98.2%
Absorption correction	Multi-Scan

Max. and min. transmission	0.9800 and 0.7900	
Structure solution technique	direct methods	
Structure solution program	XT, VERSION 2018/2	
Refinement method	Full-matrix least-squares on F^2	
Refinement program	SHELXL-2018/3 (Sheldrick, 2018)	
Function minimized	$\Sigma\ w(F_o^2 - F_c^2)^2$	
Data / restraints / parameters	12166 / 0 / 426	
Goodness-of-fit on F^2	1.057	
Δ/σ_{max}	0.001	
Final R indices	8111 data; $I>2\sigma(I)$	R1 = 0.0565, wR2 = 0.1118
	all data	R1 = 0.0951, wR2 = 0.1323
Weighting scheme	$w=1/[\sigma^2(F_o^2)+(0.0268P)^2+2.7517P]$ where $P=(F_o^2+2F_c^2)/3$	
Largest diff. peak and hole	1.050 and -1.591 eÅ^{-3}	
R.M.S. deviation from mean	0.158 eÅ^{-3}	

Bond lengths (Å) of compound 26

C1-C2	1.368(5)	C1-C6	1.384(4)
C1-P1	1.783(4)	C2-C3	1.382(5)
C3-C4	1.364(5)	C4-C5	1.368(6)
C5-C6	1.383(5)	C7-C8	1.384(5)
C7-C12	1.393(5)	C7-P1	1.788(4)
C8-C9	1.380(5)	C9-C10	1.375(5)
C10-C11	1.379(5)	C11-C12	1.379(5)
C13-C14	1.514(5)	C13-P1	1.810(3)
C13-P2	1.872(3)	C14-C15	1.510(4)
C15-O1	1.205(4)	C15-C16	1.478(5)
C16-C17	1.378(5)	C16-C21	1.386(4)
C17-C18	1.386(5)	C18-C19	1.381(5)
C19-C20	1.369(6)	C20-C21	1.367(5)
C22-C27	1.379(5)	C22-C23	1.394(5)
C22-P2	1.798(3)	C23-C24	1.370(5)
C24-C25	1.388(5)	C25-O2	1.342(4)

C25-C26	1.381(5)	C26-C27	1.381(5)
C28-O2	1.423(5)	C29-C34	1.380(5)
C29-C30	1.385(5)	C29-P2	1.795(4)
C30-C31	1.368(5)	C31-C32	1.378(5)
C32-O3	1.346(4)	C32-C33	1.387(5)
C33-C34	1.375(5)	C35-O3	1.420(5)
C36-Cl3	1.742(4)	C36-Cl4	1.752(4)
Cl1-Pd1	2.3176(10)	Cl2-Pd1	2.3427(10)
P1-S1	1.9872(13)	P2-Pd1	2.2155(10)
Pd1-S1	2.2800(10)		

Bond angles (°) of compound 26

C2-C1-C6	120.4(3)	C2-C1-P1	121.5(3)
C6-C1-P1	118.1(3)	C1-C2-C3	120.1(3)
C4-C3-C2	119.6(4)	C3-C4-C5	120.6(4)
C4-C5-C6	120.4(3)	C5-C6-C1	118.8(4)
C8-C7-C12	120.3(3)	C8-C7-P1	119.5(3)
C12-C7-P1	120.1(3)	C9-C8-C7	119.2(3)
C10-C9-C8	120.5(4)	C9-C10-C11	120.4(3)
C10-C11-C12	119.9(4)	C11-C12-C7	119.6(3)
C14-C13-P1	108.7(2)	C14-C13-P2	112.7(2)
P1-C13-P2	105.40(16)	C15-C14-C13	113.5(3)
O1-C15-C16	122.9(3)	O1-C15-C14	120.8(3)
C16-C15-C14	116.3(3)	C17-C16-C21	119.1(3)
C17-C16-C15	122.5(3)	C21-C16-C15	118.4(3)
C16-C17-C18	120.8(3)	C19-C18-C17	119.2(4)
C20-C19-C18	119.9(4)	C21-C20-C19	121.0(3)
C20-C21-C16	119.9(4)	C27-C22-C23	118.8(3)
C27-C22-P2	119.0(2)	C23-C22-P2	122.2(3)
C24-C23-C22	119.7(4)	C23-C24-C25	120.9(3)
O2-C25-C26	124.4(3)	O2-C25-C24	115.7(3)
C26-C25-C24	119.9(3)	C27-C26-C25	118.7(3)
C22-C27-C26	121.9(3)	C34-C29-C30	117.9(3)
C34-C29-P2	121.7(3)	C30-C29-P2	120.4(3)
C31-C30-C29	120.9(3)	C30-C31-C32	121.0(3)
O3-C32-C31	116.4(3)	O3-C32-C33	124.8(3)
C31-C32-C33	118.8(4)	C34-C33-C32	119.8(3)
C33-C34-C29	121.7(3)	Cl3-C36-Cl4	112.1(2)
C25-O2-C28	117.6(3)	C32-O3-C35	118.1(3)

C1-P1-C7	108.67(16)	C1-P1-C13	107.65(16)
C7-P1-C13	111.21(15)	C1-P1-S1	112.71(12)
C7-P1-S1	109.62(12)	C13-P1-S1	106.99(12)
C29-P2-C22	107.43(16)	C29-P2-C13	104.28(17)
C22-P2-C13	106.53(15)	C29-P2-Pd1	117.93(11)
C22-P2-Pd1	110.22(12)	C13-P2-Pd1	109.77(11)
P2-Pd1-S1	94.07(4)	P2-Pd1-Cl1	88.08(4)
S1-Pd1-Cl1	176.19(4)	P2-Pd1-Cl2	176.10(4)
S1-Pd1-Cl2	83.26(4)	Cl1-Pd1-Cl2	94.44(4)
P1-S1-Pd1	99.89(5)		

Crystallographic data for compound 27

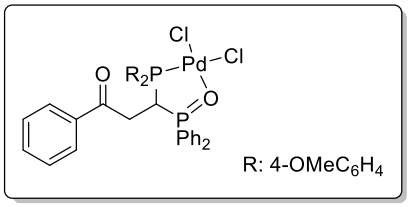

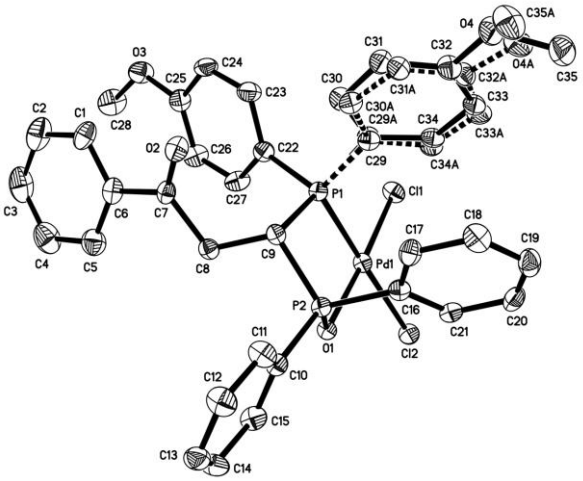

Identification code	leung1209m_0m_5
Chemical formula	$C_{35}H_{32}Cl_2O_4P_2Pd$
Formula weight	755.84 g/mol
Temperature	100(2) K
Wavelength	0.71073 Å
Crystal size	0.080 x 0.100 x 0.120 mm
Crystal habit	orange block
Crystal system	triclinic
Space group	P -1
Unit cell dimensions	a = 11.9486(16) Å α = 112.003(3)°
	b = 12.2159(14) Å β = 101.349(3)°
	c = 12.2479(15) Å γ = 95.636(3)°
Volume	1595.8(3) $Å^3$
Z	2
Density (calculated)	1.573 g/cm^3
Absorption coefficient	0.888 mm^{-1}
F(000)	768

Theta range for data collection	2.01 to 29.60°
Reflections collected	9052
Independent reflections	9052 [R(int) = 0.0975]
Coverage of independent reflections	99.3%
Absorption correction	Multi-Scan
Max. and min. transmission	0.9320 and 0.9010

Structure solution technique	direct methods	
Structure solution program	XT, VERSION 2018/2	
Refinement method	Full-matrix least-squares on F^2	
Refinement program	SHELXL-2018/3 (Sheldrick, 2018)	
Function minimized	$\Sigma\ w(F_o^2 - F_c^2)^2$	
Data / restraints / parameters	9052 / 360 / 463	
Goodness-of-fit on F^2	1.029	
Δ/σ_{max}	0.001	
Final R indices	6373 data; $I>2\sigma(I)$	R1 = 0.0621, wR2 = 0.1325
	all data	R1 = 0.1042, wR2 = 0.1571
Weighting scheme	$w=1/[\sigma^2(F_o^2)+(0.0498P)^2+3.5185P]$ where $P=(F_o^2+2F_c^2)/3$	
Largest diff. peak and hole	1.347 and -1.528 eÅ^{-3}	
R.M.S. deviation from mean	0.170 eÅ^{-3}	

Bond lengths (Å) of compound 27

C1-C6	1.387(7)	C1-C2	1.395(7)
C2-C3	1.371(9)	C3-C4	1.377(9)
C4-C5	1.396(8)	C5-C6	1.397(8)
C6-C7	1.489(6)	C7-O2	1.211(6)
C7-C8	1.521(6)	C8-C9	1.529(6)
C9-P2	1.815(5)	C9-P1	1.884(4)
C10-C15	1.378(7)	C10-C11	1.407(6)
C10-P2	1.794(5)	C11-C12	1.370(7)
C12-C13	1.393(7)	C13-C14	1.372(7)
C14-C15	1.399(7)	C16-C17	1.394(7)
C16-C21	1.402(6)	C16-P2	1.796(5)
C17-C18	1.388(7)	C18-C19	1.394(7)
C19-C20	1.381(7)	C20-C21	1.376(7)
C22-C23	1.393(7)	C22-C27	1.394(7)
C22-P1	1.798(5)	C23-C24	1.378(7)
C24-C25	1.396(7)	C25-O3	1.366(6)
C25-C26	1.378(7)	C26-C27	1.385(7)
C28-O3	1.431(6)	C29-C34	1.390(8)

C29-C30	1.395(8)	C29-P1	1.802(7)
C30-C31	1.384(8)	C31-C32	1.391(8)
C32-O4	1.371(8)	C32-C33	1.385(8)
C33-C34	1.388(8)	C35-O4	1.421(10)
C29A-C30A	1.39	C29A-C34A	1.39
C29A-P1	1.824(5)	C30A-C31A	1.39
C31A-C32A	1.39	C32A-O4A	1.382(7)
C32A-C33A	1.39	C33A-C34A	1.39
C35A-O4A	1.430(10)	Cl1-Pd1	2.2616(12)
Cl2-Pd1	2.3476(12)	O1-P2	1.519(3)
O1-Pd1	2.090(3)	P1-Pd1	2.2290(13)
P2-Pd1	2.9513(13)		

Bond angles (°) of compound 27

C6-C1-C2	119.6(6)	C3-C2-C1	120.5(6)
C2-C3-C4	120.6(5)	C3-C4-C5	119.6(6)
C4-C5-C6	120.0(6)	C1-C6-C5	119.6(5)
C1-C6-C7	118.5(5)	C5-C6-C7	121.9(5)
O2-C7-C6	121.8(4)	O2-C7-C8	120.7(4)
C6-C7-C8	117.6(4)	C7-C8-C9	111.7(4)
C8-C9-P2	110.1(3)	C8-C9-P1	112.6(3)
P2-C9-P1	102.5(2)	C15-C10-C11	120.2(4)
C15-C10-P2	119.3(4)	C11-C10-P2	120.5(4)
C12-C11-C10	119.5(5)	C11-C12-C13	120.4(5)
C14-C13-C12	120.3(5)	C13-C14-C15	120.1(5)
C10-C15-C14	119.6(5)	C17-C16-C21	120.4(4)
C17-C16-P2	122.6(4)	C21-C16-P2	117.0(4)
C18-C17-C16	119.5(5)	C17-C18-C19	120.0(5)
C20-C19-C18	120.1(5)	C21-C20-C19	120.8(5)
C20-C21-C16	119.3(5)	C23-C22-C27	119.0(5)
C23-C22-P1	122.6(4)	C27-C22-P1	118.4(4)
C24-C23-C22	120.0(5)	C23-C24-C25	120.0(5)
O3-C25-C26	124.7(5)	O3-C25-C24	114.7(5)
C26-C25-C24	120.6(5)	C25-C26-C27	119.0(5)
C26-C27-C22	121.2(5)	C34-C29-C30	119.8(7)
C34-C29-P1	122.9(10)	C30-C29-P1	116.5(10)
C31-C30-C29	120.0(8)	C30-C31-C32	119.3(7)
O4-C32-C33	121.5(8)	O4-C32-C31	117.3(7)
C33-C32-C31	121.2(7)	C32-C33-C34	118.9(7)

C33-C34-C29	120.5(7)	C32-O4-C35	117.6(8)
C30A-C29A-C34A	120.0	C30A-C29A-P1	125.0(9)
C34A-C29A-P1	114.5(9)	C29A-C30A-C31A	120.0
C32A-C31A-C30A	120.0	O4A-C32A-C31A	121.6(6)
O4A-C32A-C33A	118.2(6)	C31A-C32A-C33A	120.0
C34A-C33A-C32A	120.0	C33A-C34A-C29A	120.0
C32A-O4A-C35A	117.9(8)	P2-O1-Pd1	108.67(17)
C25-O3-C28	119.0(4)	C22-P1-C29	110.0(8)
C22-P1-C29A	113.2(8)	C22-P1-C9	107.6(2)
C29-P1-C9	103.6(7)	C29A-P1-C9	99.7(7)
C22-P1-Pd1	114.09(17)	C29-P1-Pd1	116.7(6)
C29A-P1-Pd1	116.4(6)	C9-P1-Pd1	103.79(15)
O1-P2-C10	110.1(2)	O1-P2-C16	111.5(2)
C10-P2-C16	111.3(2)	O1-P2-C9	107.9(2)
C10-P2-C9	107.4(2)	C16-P2-C9	108.5(2)
O1-P2-Pd1	42.14(12)	C10-P2-Pd1	151.47(16)
C16-P2-Pd1	89.93(15)	C9-P2-Pd1	82.05(14)
O1-Pd1-P1	90.27(9)	O1-Pd1-Cl1	176.75(9)
P1-Pd1-Cl1	87.23(5)	O1-Pd1-Cl2	88.75(9)
P1-Pd1-Cl2	177.42(5)	Cl1-Pd1-Cl2	93.83(5)
O1-Pd1-P2	29.19(9)	P1-Pd1-P2	65.98(4)
Cl1-Pd1-P2	149.68(4)	Cl2-Pd1-P2	112.38(4)

Crystallographic data for compound 28

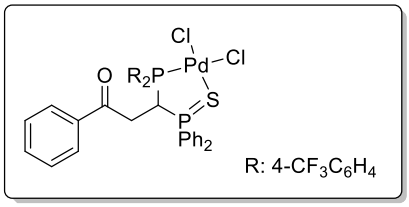

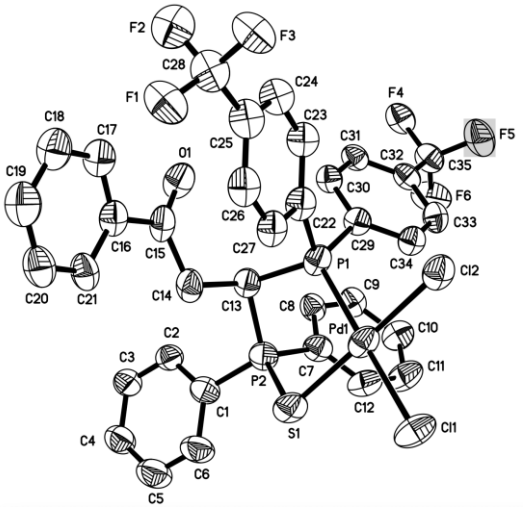

Identification code	leung1216m
Chemical formula	$C_{36}H_{28}Cl_4F_6OP_2PdS$
Formula weight	932.78 g/mol
Temperature	100(2) K
Wavelength	0.71073 Å
Crystal size	0.020 x 0.060 x 0.200 mm
Crystal habit	orange needle
Crystal system	monoclinic
Space group	P 1 21/n 1
Unit cell dimensions	a = 22.5677(9) Å α = 90°
	b = 15.2023(8) Å β = 98.9804(12)°
	c = 35.2410(16) Å γ = 90°
Volume	11942.3(10) $Å^3$
Z	12
Density (calculated)	1.556 g/cm^3
Absorption coefficient	0.924 mm^{-1}
F(000)	5592

Theta range for data collection	1.85 to 28.72°
Index ranges	-26<=h<=30, -20<=k<=20, -47<=l<=47
Reflections collected	282358
Independent reflections	30868 [R(int) = 0.1269]
Coverage of independent reflections	99.8%
Absorption correction	Multi-Scan

Max. and min. transmission	0.9820 and 0.8370	
Refinement method	Full-matrix least-squares on F^2	
Refinement program	SHELXL-2018/3 (Sheldrick, 2018)	
Function minimized	$\Sigma\, w(F_o^2 - F_c^2)^2$	
Data / restraints / parameters	30868 / 4395 / 1851	
Goodness-of-fit on F^2	1.028	
Δ/σ_{max}	0.002	
Final R indices	18415 data; $I>2\sigma(I)$	R1 = 0.0686, wR2 = 0.1695
	all data	R1 = 0.1318, wR2 = 0.2157
Weighting scheme	$w=1/[\sigma^2(F_o^2)+(0.0854P)^2+58.1752P]$ where $P=(F_o^2+2F_c^2)/3$	
Largest diff. peak and hole	1.988 and -1.716 eÅ^{-3}	
R.M.S. deviation from mean	0.137 eÅ^{-3}	

Bond lengths (Å) of compound 28

C1-C2	1.39	C1-C6	1.39
C1-P2	1.809(6)	C2-C3	1.39
C3-C4	1.39	C4-C5	1.39
C5-C6	1.39	C1A-C2A	1.39
C1A-C6A	1.39	C1A-P2	1.778(10)
C2A-C3A	1.39	C3A-C4A	1.39
C4A-C5A	1.39	C5A-C6A	1.39
C7-C8	1.39	C7-C12	1.39
C7-P2	1.795(4)	C8-C9	1.39
C9-C10	1.39	C10-C11	1.39
C11-C12	1.39	C13-C14	1.551(9)
C13-P2	1.818(7)	C13-P1	1.887(7)
C14-C15	1.517(10)	C15-O1	1.224(8)
C15-C16	1.490(7)	C16-C17	1.39
C16-C21	1.39	C17-C18	1.39
C18-C19	1.39	C19-C20	1.39
C20-C21	1.39	C22-C23	1.39
C22-C27	1.39	C22-P1	1.838(10)
C23-C24	1.39	C24-C25	1.39
C25-C26	1.39	C25-C28	1.480(10)

C26-C27	1.39	C28-F2	1.336(12)
C28-F1	1.343(11)	C28-F3	1.355(12)
C22A-C23A	1.39	C22A-C27A	1.39
C22A-P1	1.787(8)	C23A-C24A	1.39
C24A-C25A	1.39	C25A-C26A	1.39
C25A-C28A	1.476(10)	C26A-C27A	1.39
C28A-F2A	1.334(12)	C28A-F1A	1.339(11)
C28A-F3A	1.353(11)	C29-C30	1.39
C29-C34	1.39	C29-P1	1.816(3)
C30-C31	1.39	C31-C32	1.39
C32-C33	1.39	C32-C35	1.494(7)
C33-C34	1.39	C35-F6A	1.322(14)
C35-F6	1.324(8)	C35-F5A	1.335(14)
C35-F5	1.337(8)	C35-F4	1.341(8)
C35-F4A	1.359(14)	C36-C37	1.39
C36-C41	1.39	C36-P4	1.780(3)
C37-C38	1.39	C38-C39	1.39
C39-C40	1.39	C40-C41	1.39
C42-C43	1.39	C42-C47	1.39
C42-P4	1.797(11)	C43-C44	1.39
C44-C45	1.39	C45-C46	1.39
C46-C47	1.39	C42A-C43A	1.39
C42A-C47A	1.39	C42A-P4	1.803(8)
C43A-C44A	1.39	C44A-C45A	1.39
C45A-C46A	1.39	C46A-C47A	1.39
C48-C49	1.540(8)	C48-C49A	1.541(11)
C48-P4	1.829(6)	C48-P3	1.864(6)
C49-C50	1.524(9)	C50-O2	1.212(9)
C50-C51	1.492(8)	C51-C52	1.39
C51-C56	1.39	C52-C53	1.39
C53-C54	1.39	C54-C55	1.39
C55-C56	1.39	C49A-C50A	1.524(12)
C50A-O2A	1.213(12)	C50A-C51A	1.492(11)
C51A-C56A	1.391(9)	C51A-C52A	1.393(9)
C52A-C53A	1.392(9)	C53A-C54A	1.390(10)
C54A-C55A	1.391(9)	C55A-C56A	1.391(9)
C57-C58	1.39	C57-C62	1.39
C57-P3	1.822(3)	C58-C59	1.39
C59-C60	1.39	C60-C61	1.39
C60-C63	1.494(7)	C61-C62	1.39
C63-F9	1.305(8)	C63-F8	1.336(9)

C63-F7	1.344(10)	C64-C65	1.39
C64-C69	1.39	C64-P3	1.814(3)
C65-C66	1.39	C66-C67	1.39
C67-C68	1.39	C67-C70A	1.494(7)
C67-C70	1.499(9)	C68-C69	1.39
C70-F12	1.328(11)	C70-F11	1.341(12)
C70-F10	1.347(12)	C70A-F12A	1.326(9)
C70A-F11A	1.337(10)	C70A-F10A	1.345(10)
C71-C72	1.39	C71-C76	1.39
C71-P6	1.793(3)	C72-C73	1.39
C73-C74	1.39	C74-C75	1.39
C75-C76	1.39	C77-C78	1.39
C77-C82	1.39	C77-P6	1.807(5)
C78-C79	1.39	C79-C80	1.39
C80-C81	1.39	C81-C82	1.39
C77A-C78A	1.39	C77A-C82A	1.39
C77A-P6	1.808(14)	C78A-C79A	1.39
C79A-C80A	1.39	C80A-C81A	1.39
C81A-C82A	1.39	C83-C84	1.530(11)
C83-C84A	1.531(10)	C83-P6	1.841(6)
C83-P5	1.876(7)	C84-C85	1.520(11)
C85-O3	1.219(10)	C85-C86	1.505(11)
C86-C87	1.39	C86-C91	1.39
C87-C88	1.39	C88-C89	1.39
C89-C90	1.39	C90-C91	1.39
C84A-C85A	1.519(11)	C85A-O3A	1.220(10)
C85A-C86A	1.506(10)	C86A-C87A	1.39
C86A-C91A	1.39	C87A-C88A	1.39
C88A-C89A	1.39	C89A-C90A	1.39
C90A-C91A	1.39	C92-C93	1.39
C92-C97	1.39	C92-P5	1.815(3)
C93-C94	1.39	C94-C95	1.39
C95-C96	1.39	C95-C98A	1.500(9)
C95-C98	1.502(7)	C96-C97	1.39
C98-F15	1.321(9)	C98-F13	1.326(10)
C98-F14	1.341(10)	C98A-F15A	1.322(12)
C98A-F13A	1.327(13)	C98A-F14A	1.342(13)
C99-C100	1.39	C99-C104	1.39
C99-P5	1.772(13)	C100-C101	1.39
C101-C102	1.39	C102-C103	1.39
C102-C105	1.474(11)	C103-C104	1.39

C105-F16	1.234(16)	C105-F17	1.348(16)
C105-F18	1.411(17)	C99A-C10A	1.39
C99A-C14A	1.39	C99A-P5	1.844(7)
C10A-C11A	1.39	C11A-C12A	1.39
C12A-C13A	1.39	C12A-C15A	1.471(9)
C13A-C14A	1.39	C15A-F16A	1.238(15)
C15A-F17A	1.342(14)	C15A-F18A	1.400(16)
C108-Cl12	1.748(8)	C108-Cl11	1.754(8)
C106-Cl7	1.744(11)	C106-Cl8	1.750(11)
C111-Cl17	1.739(11)	C111-Cl18	1.742(12)
C112-Cl20	1.742(11)	C112-Cl19	1.745(11)
Cl20-Cl16	1.59(3)	C107-Cl9	1.729(10)
C107-Cl10	1.738(10)	C109-Cl13	1.734(11)
C109-Cl14	1.734(11)	C110-Cl15	1.738(11)
C110-Cl16	1.746(12)	Cl1-Pd1	2.3308(18)
Cl2-Pd1	2.323(2)	Cl3-Pd2	2.2893(16)
Cl4-Pd2	2.3387(16)	Cl5-Pd3	2.3078(16)
Cl6-Pd3	2.3484(16)	P1-Pd1	2.2205(17)
P2-S1	2.007(2)	P3-Pd2	2.2403(16)
P4-S2	2.005(2)	P5-Pd3	2.2264(16)
P6-S3	2.008(2)	Pd1-S1	2.309(2)
Pd2-S2	2.2974(15)	Pd3-S3	2.2852(16)

Bond angles (°) of compound 28

C2-C1-C6	120.0	C2-C1-P2	119.7(5)
C6-C1-P2	120.3(5)	C1-C2-C3	120.0
C2-C3-C4	120.0	C5-C4-C3	120.0
C6-C5-C4	120.0	C5-C6-C1	120.0
C2A-C1A-C6A	120.0	C2A-C1A-P2	121.4(9)
C6A-C1A-P2	118.4(9)	C3A-C2A-C1A	120.0
C4A-C3A-C2A	120.0	C3A-C4A-C5A	120.0
C6A-C5A-C4A	120.0	C5A-C6A-C1A	120.0
C8-C7-C12	120.0	C8-C7-P2	120.8(2)
C12-C7-P2	119.2(2)	C7-C8-C9	120.0
C10-C9-C8	120.0	C11-C10-C9	120.0
C10-C11-C12	120.0	C11-C12-C7	120.0
C14-C13-P2	108.5(5)	C14-C13-P1	113.9(5)
P2-C13-P1	103.3(3)	C15-C14-C13	113.7(6)
O1-C15-C16	122.7(7)	O1-C15-C14	120.2(6)

C16-C15-C14	117.1(6)	C17-C16-C21	120.0
C17-C16-C15	118.1(4)	C21-C16-C15	121.6(4)
C18-C17-C16	120.0	C17-C18-C19	120.0
C18-C19-C20	120.0	C21-C20-C19	120.0
C20-C21-C16	120.0	C23-C22-C27	120.0
C23-C22-P1	124.(2)	C27-C22-P1	115.(2)
C24-C23-C22	120.0	C23-C24-C25	120.0
C24-C25-C26	120.0	C24-C25-C28	120.5(8)
C26-C25-C28	119.3(8)	C25-C26-C27	120.0
C26-C27-C22	120.0	F2-C28-F1	105.6(12)
F2-C28-F3	106.1(11)	F1-C28-F3	106.2(10)
F2-C28-C25	114.3(10)	F1-C28-C25	112.7(11)
F3-C28-C25	111.4(11)	C23A-C22A-C27A	120.0
C23A-C22A-P1	123.7(16)	C27A-C22A-P1	116.3(16)
C22A-C23A-C24A	120.0	C25A-C24A-C23A	120.0
C26A-C25A-C24A	120.0	C26A-C25A-C28A	120.3(7)
C24A-C25A-C28A	119.7(7)	C25A-C26A-C27A	120.0
C26A-C27A-C22A	120.0	F2A-C28A-F1A	106.2(10)
F2A-C28A-F3A	106.6(10)	F1A-C28A-F3A	106.8(9)
F2A-C28A-C25A	113.1(8)	F1A-C28A-C25A	113.6(10)
F3A-C28A-C25A	110.1(9)	C30-C29-C34	120.0
C30-C29-P1	119.4(2)	C34-C29-P1	120.0(2)
C31-C30-C29	120.0	C30-C31-C32	120.0
C31-C32-C33	120.0	C31-C32-C35	120.2(4)
C33-C32-C35	119.6(4)	C34-C33-C32	120.0
C33-C34-C29	120.0	F6A-C35-F5A	107.8(14)
F6-C35-F5	107.8(6)	F6-C35-F4	107.7(6)
F5-C35-F4	105.0(6)	F6A-C35-F4A	105.1(14)
F5A-C35-F4A	104.9(13)	F6A-C35-C32	119.8(19)
F6-C35-C32	113.1(6)	F5A-C35-C32	112.9(17)
F5-C35-C32	111.0(6)	F4-C35-C32	111.9(6)
F4A-C35-C32	105.0(15)	C37-C36-C41	120.0
C37-C36-P4	117.95(19)	C41-C36-P4	121.9(2)
C36-C37-C38	120.0	C39-C38-C37	120.0
C38-C39-C40	120.0	C41-C40-C39	120.0
C40-C41-C36	120.0	C43-C42-C47	120.0
C43-C42-P4	120.6(18)	C47-C42-P4	119.0(18)
C42-C43-C44	120.0	C45-C44-C43	120.0
C44-C45-C46	120.0	C47-C46-C45	120.0
C46-C47-C42	120.0	C43A-C42A-C47A	120.0
C43A-C42A-P4	119.8(12)	C47A-C42A-P4	120.0(12)

C42A-C43A-C44A	120.0	C45A-C44A-C43A	120.0
C44A-C45A-C46A	120.0	C45A-C46A-C47A	120.0
C46A-C47A-C42A	120.0	C49-C48-P4	114.5(6)
C49A-C48-P4	116.(2)	C49-C48-P3	115.6(8)
C49A-C48-P3	111.(4)	P4-C48-P3	103.6(3)
C50-C49-C48	108.7(6)	O2-C50-C51	120.2(6)
O2-C50-C49	119.4(7)	C51-C50-C49	120.2(6)
C52-C51-C56	120.0	C52-C51-C50	117.2(4)
C56-C51-C50	122.7(4)	C51-C52-C53	120.0
C52-C53-C54	120.0	C53-C54-C55	120.0
C54-C55-C56	120.0	C55-C56-C51	120.0
C50A-C49A-C48	113.1(14)	O2A-C50A-C51A	120.2(14)
O2A-C50A-C49A	118.9(13)	C51A-C50A-C49A	120.6(13)
C56A-C51A-C52A	120.1(11)	C56A-C51A-C50A	122.8(12)
C52A-C51A-C50A	117.0(12)	C53A-C52A-C51A	119.2(12)
C54A-C53A-C52A	119.1(13)	C53A-C54A-C55A	120.6(12)
C54A-C55A-C56A	118.8(13)	C51A-C56A-C55A	119.5(12)
C58-C57-C62	120.0	C58-C57-P3	122.9(2)
C62-C57-P3	117.1(2)	C57-C58-C59	120.0
C60-C59-C58	120.0	C59-C60-C61	120.0
C59-C60-C63	120.8(4)	C61-C60-C63	119.1(4)
C62-C61-C60	120.0	C61-C62-C57	120.0
F9-C63-F8	107.5(6)	F9-C63-F7	108.1(7)
F8-C63-F7	104.3(6)	F9-C63-C60	113.2(6)
F8-C63-C60	111.2(6)	F7-C63-C60	112.1(6)
C65-C64-C69	120.0	C65-C64-P3	120.3(2)
C69-C64-P3	119.5(2)	C64-C65-C66	120.0
C67-C66-C65	120.0	C66-C67-C68	120.0
C66-C67-C70A	119.9(5)	C68-C67-C70A	120.1(5)
C66-C67-C70	124.4(8)	C68-C67-C70	115.4(8)
C69-C68-C67	120.0	C68-C69-C64	120.0
F12-C70-F11	107.2(13)	F12-C70-F10	106.6(13)
F11-C70-F10	105.5(12)	F12-C70-C67	111.(2)
F11-C70-C67	115.0(17)	F10-C70-C67	111.1(16)
F12A-C70A-F11A	108.0(8)	F12A-C70A-F10A	106.4(8)
F11A-C70A-F10A	106.0(8)	F12A-C70A-C67	111.7(11)
F11A-C70A-C67	110.8(9)	F10A-C70A-C67	113.5(8)
C72-C71-C76	120.0	C72-C71-P6	118.9(3)
C76-C71-P6	121.0(3)	C73-C72-C71	120.0
C72-C73-C74	120.0	C73-C74-C75	120.0
C76-C75-C74	120.0	C75-C76-C71	120.0

C78-C77-C82	120.0	C78-C77-P6	117.6(6)
C82-C77-P6	122.2(6)	C77-C78-C79	120.0
C80-C79-C78	120.0	C79-C80-C81	120.0
C82-C81-C80	120.0	C81-C82-C77	120.0
C78A-C77A-C82A	120.0	C78A-C77A-P6	131.(3)
C82A-C77A-P6	109.(3)	C77A-C78A-C79A	120.0
C80A-C79A-C78A	120.0	C79A-C80A-C81A	120.0
C82A-C81A-C80A	120.0	C81A-C82A-C77A	120.0
C84-C83-P6	109.5(9)	C84A-C83-P6	115.1(8)
C84-C83-P5	120.6(14)	C84A-C83-P5	113.3(11)
P6-C83-P5	103.8(3)	C85-C84-C83	106.2(12)
O3-C85-C86	121.1(13)	O3-C85-C84	120.2(12)
C86-C85-C84	117.2(9)	C87-C86-C91	120.0
C87-C86-C85	118.0(7)	C91-C86-C85	121.9(7)
C88-C87-C86	120.0	C89-C88-C87	120.0
C88-C89-C90	120.0	C89-C90-C91	120.0
C90-C91-C86	120.0	C85A-C84A-C83	116.3(11)
O3A-C85A-C86A	120.6(9)	O3A-C85A-C84A	120.4(9)
C86A-C85A-C84A	117.9(9)	C87A-C86A-C91A	120.0
C87A-C86A-C85A	117.3(6)	C91A-C86A-C85A	122.6(6)
C86A-C87A-C88A	120.0	C89A-C88A-C87A	120.0
C88A-C89A-C90A	120.0	C89A-C90A-C91A	120.0
C90A-C91A-C86A	120.0	C93-C92-C97	120.0
C93-C92-P5	122.0(2)	C97-C92-P5	118.0(2)
C94-C93-C92	120.0	C93-C94-C95	120.0
C96-C95-C94	120.0	C96-C95-C98A	118.7(12)
C94-C95-C98A	121.3(12)	C96-C95-C98	118.7(5)
C94-C95-C98	121.3(5)	C95-C96-C97	120.0
C96-C97-C92	120.0	F15-C98-F13	107.2(8)
F15-C98-F14	106.8(7)	F13-C98-F14	105.8(7)
F15-C98-C95	112.3(6)	F13-C98-C95	112.0(7)
F14-C98-C95	112.2(7)	F15A-C98A-F13A	106.2(15)
F15A-C98A-F14A	107.2(15)	F13A-C98A-F14A	105.2(15)
F15A-C98A-C95	114.(2)	F13A-C98A-C95	114.(2)
F14A-C98A-C95	110.(2)	C100-C99-C104	120.0
C100-C99-P5	119.4(19)	C104-C99-P5	120.5(19)
C101-C100-C99	120.0	C102-C101-C100	120.0
C101-C102-C103	120.0	C101-C102-C105	119.4(9)
C103-C102-C105	120.6(9)	C104-C103-C102	120.0
C103-C104-C99	120.0	F16-C105-F17	120.1(15)
F16-C105-F18	96.2(13)	F17-C105-F18	98.1(15)

F16-C105-C102	118.2(14)	F17-C105-C102	111.3(12)
F18-C105-C102	108.6(14)	C10A-C99A-C14A	120.0
C10A-C99A-P5	120.2(10)	C14A-C99A-P5	119.8(10)
C11A-C10A-C99A	120.0	C10A-C11A-C12A	120.0
C13A-C12A-C11A	120.0	C13A-C12A-C15A	117.7(6)
C11A-C12A-C15A	122.3(6)	C12A-C13A-C14A	120.0
C13A-C14A-C99A	120.0	F16A-C15A-F17A	116.8(11)
F16A-C15A-F18A	95.5(11)	F17A-C15A-F18A	99.6(11)
F16A-C15A-C12A	117.8(12)	F17A-C15A-C12A	112.1(10)
F18A-C15A-C12A	111.9(9)	Cl12-C108-Cl11	112.3(4)
Cl7-C106-Cl8	111.7(8)	Cl17-C111-Cl18	113.8(11)
Cl20-C112-Cl19	114.2(10)	Cl16-Cl20-C112	139.1(15)
Cl9-C107-Cl10	113.0(6)	Cl13-C109-Cl14	113.2(10)
Cl15-C110-Cl16	115.8(12)	Cl20-Cl16-C110	162.(3)
C22A-P1-C29	108.8(12)	C29-P1-C22	107.1(15)
C22A-P1-C13	105.0(5)	C29-P1-C13	103.5(2)
C22-P1-C13	110.4(8)	C22A-P1-Pd1	111.3(9)
C29-P1-Pd1	116.86(15)	C22-P1-Pd1	108.3(12)
C13-P1-Pd1	110.4(2)	C1A-P2-C7	117.3(6)
C7-P2-C1	105.3(3)	C1A-P2-C13	100.4(6)
C7-P2-C13	107.2(3)	C1-P2-C13	114.6(4)
C1A-P2-S1	110.7(5)	C7-P2-S1	112.40(18)
C1-P2-S1	109.8(3)	C13-P2-S1	107.6(2)
C64-P3-C57	107.61(19)	C64-P3-C48	102.3(2)
C57-P3-C48	105.9(2)	C64-P3-Pd2	118.69(14)
C57-P3-Pd2	110.44(14)	C48-P3-Pd2	110.93(19)
C36-P4-C42	112.0(14)	C36-P4-C42A	111.3(10)
C36-P4-C48	110.1(2)	C42-P4-C48	105.6(14)
C42A-P4-C48	101.6(10)	C36-P4-S2	110.20(14)
C42-P4-S2	110.2(12)	C42A-P4-S2	114.6(9)
C48-P4-S2	108.57(19)	C99-P5-C92	104.3(11)
C92-P5-C99A	107.3(6)	C99-P5-C83	101.5(5)
C92-P5-C83	108.9(3)	C99A-P5-C83	102.3(3)
C99-P5-Pd3	115.5(14)	C92-P5-Pd3	113.07(15)
C99A-P5-Pd3	111.9(7)	C83-P5-Pd3	112.7(2)
C71-P6-C77	110.9(6)	C71-P6-C77A	110.(3)
C71-P6-C83	113.9(3)	C77-P6-C83	103.5(5)
C77A-P6-C83	107.(2)	C71-P6-S3	106.75(17)
C77-P6-S3	113.6(4)	C77A-P6-S3	111.(2)
C83-P6-S3	108.4(2)	P1-Pd1-S1	94.04(7)
P1-Pd1-Cl2	86.02(7)	S1-Pd1-Cl2	177.30(7)

P1-Pd1-Cl1	178.46(8)	S1-Pd1-Cl1	86.90(8)
Cl2-Pd1-Cl1	92.99(8)	P3-Pd2-Cl3	88.21(6)
P3-Pd2-S2	93.96(6)	Cl3-Pd2-S2	175.70(6)
P3-Pd2-Cl4	178.24(6)	Cl3-Pd2-Cl4	91.28(6)
S2-Pd2-Cl4	86.44(6)	P5-Pd3-S3	93.14(6)
P5-Pd3-Cl5	87.61(6)	S3-Pd3-Cl5	175.35(7)
P5-Pd3-Cl6	174.28(6)	S3-Pd3-Cl6	87.51(6)
Cl5-Pd3-Cl6	92.21(6)	P2-S1-Pd1	97.93(10)
P4-S2-Pd2	98.42(7)	P6-S3-Pd3	100.80(8)

Crystallographic data for compound 29

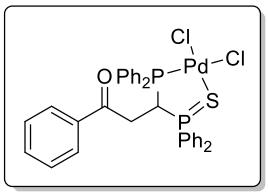

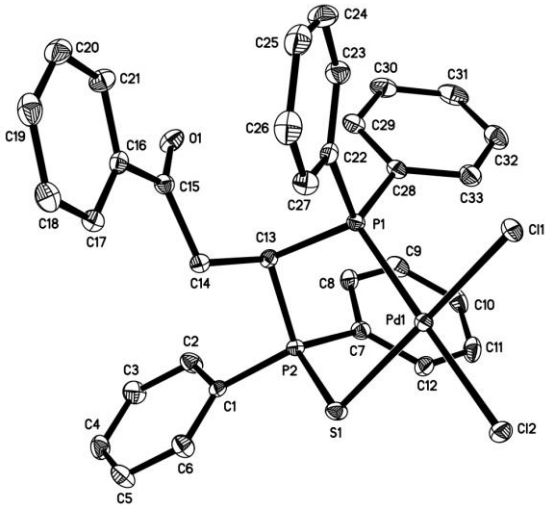

Identification code	leung1224m
Chemical formula	$C_{35}H_{32}Cl_6OP_2PdS$
Formula weight	881.70 g/mol
Temperature	100(2) K
Wavelength	0.71073 Å
Crystal size	0.100 x 0.120 x 0.180 mm
Crystal habit	yellow block
Crystal system	triclinic
Space group	P -1
Unit cell dimensions	a = 12.0462(6) Å α = 117.9699(16)°
	b = 13.6016(6) Å β = 110.1228(17)°
	c = 13.8617(7) Å γ = 94.362(2)°
Volume	1804.64(15) $Å^3$
Z	2
Density (calculated)	1.623 g/cm^3
Absorption coefficient	1.134 mm^{-1}
F(000)	888

Theta range for data collection	1.99 to 31.64°
Index ranges	-17<=h<=15, -20<=k<=20, -16<=l<=20
Reflections collected	29905
Independent reflections	12080 [R(int) = 0.0512]
Coverage of independent reflections	99.4%
Absorption correction	Multi-Scan

Max. and min. transmission	0.8950 and 0.8220	
Refinement method	Full-matrix least-squares on F^2	
Refinement program	SHELXL-2018/3 (Sheldrick, 2018)	
Function minimized	$\Sigma\, w(F_o^2 - F_c^2)^2$	
Data / restraints / parameters	12080 / 0 / 415	
Goodness-of-fit on F^2	1.019	
Δ/σ_{max}	0.001	
Final R indices	8663 data; $I>2\sigma(I)$	R1 = 0.0435, wR2 = 0.0793
	all data	R1 = 0.0759, wR2 = 0.0925
Weighting scheme	$w=1/[\sigma^2(F_o^2)+(0.0218P)^2+1.5421P]$ where $P=(F_o^2+2F_c^2)/3$	
Largest diff. peak and hole	1.533 and -0.943 eÅ^{-3}	
R.M.S. deviation from mean	0.140 eÅ^{-3}	

Bond lengths (Å) of compound 29

Pd1-P1	2.2418(7)	Pd1-Cl1	2.2998(6)
Pd1-S1	2.3083(6)	Pd1-Cl2	2.3595(6)
C1-C6	1.386(3)	C1-C2	1.400(4)
C1-P2	1.805(2)	C2-C3	1.386(4)
C3-C4	1.383(4)	C4-C5	1.384(4)
C5-C6	1.393(4)	C7-C8	1.395(4)
C7-C12	1.396(4)	C7-P2	1.804(3)
C8-C9	1.385(4)	C9-C10	1.392(4)
C10-C11	1.382(4)	C11-C12	1.387(4)
C13-C14	1.531(3)	C13-P2	1.824(2)
C13-P1	1.879(2)	C14-C15	1.529(3)
C15-O1	1.221(3)	C15-C16	1.483(3)
C16-C17	1.397(4)	C16-C21	1.400(3)
C17-C18	1.388(4)	C18-C19	1.384(4)
C19-C20	1.388(4)	C20-C21	1.385(4)
C22-C27	1.395(4)	C22-C23	1.397(4)
C22-P1	1.816(2)	C23-C24	1.385(4)
C24-C25	1.377(4)	C25-C26	1.389(4)
C26-C27	1.387(4)	C28-C33	1.395(4)
C28-C29	1.403(4)	C28-P1	1.812(3)

C29-C30	1.391(4)	C30-C31	1.391(4)
C31-C32	1.380(4)	C32-C33	1.388(4)
C34-Cl4	1.738(3)	C34-Cl3	1.752(3)
C35-Cl5	1.751(3)	C35-Cl6	1.780(3)
P2-S1	1.9990(9)		

Bond angles (°) of compound 29

P1-Pd1-Cl1	86.29(2)	P1-Pd1-S1	94.65(2)
Cl1-Pd1-S1	175.62(3)	P1-Pd1-Cl2	178.57(2)
Cl1-Pd1-Cl2	92.42(2)	S1-Pd1-Cl2	86.59(2)
C6-C1-C2	119.7(2)	C6-C1-P2	119.27(19)
C2-C1-P2	121.00(19)	C3-C2-C1	119.4(2)
C4-C3-C2	120.8(3)	C3-C4-C5	120.1(2)
C4-C5-C6	119.6(3)	C1-C6-C5	120.5(2)
C8-C7-C12	119.8(2)	C8-C7-P2	120.52(19)
C12-C7-P2	119.4(2)	C9-C8-C7	119.9(2)
C8-C9-C10	119.8(3)	C11-C10-C9	120.5(3)
C10-C11-C12	119.9(3)	C11-C12-C7	119.9(3)
C14-C13-P2	111.76(16)	C14-C13-P1	112.65(17)
P2-C13-P1	103.96(12)	C15-C14-C13	110.6(2)
O1-C15-C16	122.1(2)	O1-C15-C14	118.7(2)
C16-C15-C14	119.2(2)	C17-C16-C21	119.3(2)
C17-C16-C15	122.2(2)	C21-C16-C15	118.4(2)
C18-C17-C16	120.1(2)	C19-C18-C17	120.1(3)
C18-C19-C20	120.3(3)	C21-C20-C19	120.0(2)
C20-C21-C16	120.2(3)	C27-C22-C23	118.9(2)
C27-C22-P1	118.56(19)	C23-C22-P1	122.2(2)
C24-C23-C22	119.8(3)	C25-C24-C23	120.9(3)
C24-C25-C26	120.1(3)	C27-C26-C25	119.3(3)
C26-C27-C22	121.0(2)	C33-C28-C29	119.6(2)
C33-C28-P1	120.7(2)	C29-C28-P1	119.71(19)
C30-C29-C28	120.0(3)	C31-C30-C29	119.7(3)
C32-C31-C30	120.3(3)	C31-C32-C33	120.6(3)
C32-C33-C28	119.8(3)	Cl4-C34-Cl3	113.14(18)
Cl5-C35-Cl6	111.98(16)	C28-P1-C22	107.07(12)
C28-P1-C13	103.56(11)	C22-P1-C13	108.51(11)
C28-P1-Pd1	118.18(9)	C22-P1-Pd1	110.01(9)
C13-P1-Pd1	109.03(8)	C7-P2-C1	112.05(12)
C7-P2-C13	106.86(11)	C1-P2-C13	108.29(11)

C7-P2-S1	111.70(9)	C1-P2-S1	110.11(9)
C13-P2-S1	107.62(8)	P2-S1-Pd1	97.49(3)

Crystallographic data for compound 30

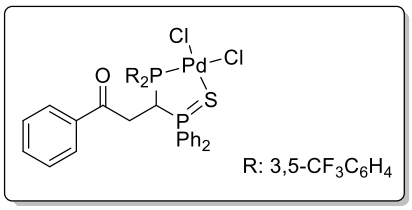

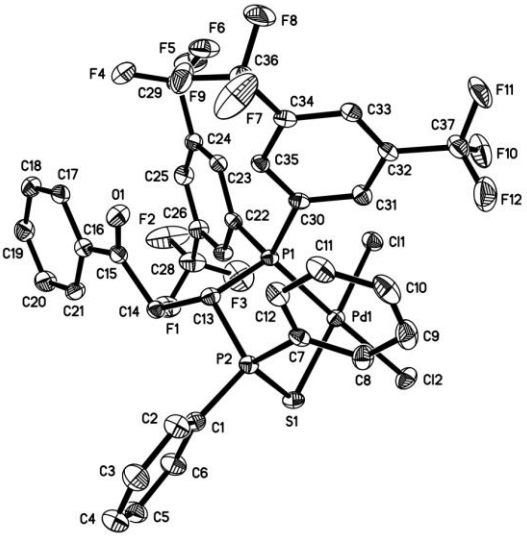

Identification code	leung1219m	
Chemical formula	$C_{39}H_{28}Cl_6F_{12}OP_2PdS$	
Formula weight	1153.71 g/mol	
Temperature	100(2) K	
Wavelength	0.71073 Å	
Crystal size	0.040 x 0.080 x 0.100 mm	
Crystal habit	orange block	
Crystal system	monoclinic	
Space group	P 1 21/n 1	
Unit cell dimensions	a = 13.6763(7) Å	α = 90°
	b = 15.5279(9) Å	β = 93.844(2)°
	c = 20.5854(11) Å	γ = 90°
Volume	4361.8(4) $Å^3$	
Z	4	
Density (calculated)	1.757 g/cm^3	
Absorption coefficient	0.999 mm^{-1}	
F(000)	2288	

Theta range for data collection	2.27 to 29.15°
Index ranges	-18<=h<=18, -21<=k<=20, -28<=l<=28
Reflections collected	89412
Independent reflections	11724 [R(int) = 0.1304]
Coverage of independent reflections	99.7%
Absorption correction	Multi-Scan

Max. and min. transmission	0.9610 and 0.9070	
Structure solution technique	direct methods	
Structure solution program	XT, VERSION 2018/2	
Refinement method	Full-matrix least-squares on F^2	
Refinement program	SHELXL-2018/3 (Sheldrick, 2018)	
Function minimized	$\Sigma\ w(F_o^2 - F_c^2)^2$	
Data / restraints / parameters	11724 / 57 / 587	
Goodness-of-fit on F^2	1.026	
Δ/σ_{max}	0.004	
Final R indices	7869 data; $I>2\sigma(I)$	R1 = 0.0507, wR2 = 0.1163
	all data	R1 = 0.0952, wR2 = 0.1372
Weighting scheme	$w=1/[\sigma^2(F_o^2)+(0.0543P)^2+9.9065P]$ where $P=(F_o^2+2F_c^2)/3$	
Largest diff. peak and hole	0.844 and -0.936 eÅ^{-3}	
R.M.S. deviation from mean	0.137 eÅ^{-3}	

Bond lengths (Å) of compound 30

Pd1-P1	2.2219(10)	Pd1-S1	2.2931(11)
Pd1-Cl1	2.3187(11)	Pd1-Cl2	2.3333(10)
C1-C2	1.400(6)	C1-C6	1.404(6)
C1-P2	1.789(4)	C2-C3	1.389(6)
C3-C4	1.390(7)	C4-C5	1.382(7)
C5-C6	1.382(6)	C7-C12	1.395(6)
C7-C8	1.400(6)	C7-P2	1.808(4)
C8-C9	1.395(6)	C9-C10	1.390(7)
C10-C11	1.375(7)	C11-C12	1.385(6)
C13-C14	1.534(5)	C13-P2	1.836(4)
C13-P1	1.872(4)	C14-C15	1.525(5)
C15-O1	1.226(5)	C15-C16	1.485(6)
C16-C21	1.393(6)	C16-C17	1.401(6)
C17-C18	1.377(6)	C18-C19	1.387(6)
C19-C20	1.382(6)	C20-C21	1.394(6)
C22-C27	1.396(5)	C22-C23	1.398(5)

C22-P1	1.818(4)	C23-C24	1.387(6)
C24-C25	1.393(6)	C24-C29	1.505(6)
C25-C26	1.388(6)	C26-C27	1.385(6)
C26-C28	1.502(6)	C28-F2	1.320(5)
C28-F1	1.331(6)	C28-F3	1.340(6)
C29-F6	1.331(5)	C29-F5	1.337(5)
C29-F4	1.338(5)	C30-C31	1.397(5)
C30-C35	1.403(5)	C30-P1	1.816(4)
C31-C32	1.388(5)	C32-C33	1.383(5)
C32-C37	1.506(6)	C33-C34	1.400(5)
C34-C35	1.391(5)	C34-C36	1.508(6)
C36-F8	1.310(5)	C36-F7	1.327(5)
C36-F9	1.328(5)	C37-F11	1.323(5)
C37-F12	1.337(5)	C37-F10	1.342(5)
C38-Cl3	1.761(6)	C38-Cl4	1.775(6)
C39-Cl5	1.761(6)	C39-Cl6	1.770(6)
C39A-Cl5A	1.753(11)	C39A-Cl6A	1.766(12)
P2-S1	2.0072(14)		

Bond angles (°) of compound 30

P1-Pd1-S1	93.29(4)	P1-Pd1-Cl1	87.28(4)
S1-Pd1-Cl1	175.13(4)	P1-Pd1-Cl2	176.77(4)
S1-Pd1-Cl2	87.17(4)	Cl1-Pd1-Cl2	92.53(4)
C2-C1-C6	120.0(4)	C2-C1-P2	121.4(3)
C6-C1-P2	118.5(3)	C3-C2-C1	119.4(4)
C2-C3-C4	120.4(4)	C5-C4-C3	120.1(4)
C6-C5-C4	120.6(4)	C5-C6-C1	119.6(4)
C12-C7-C8	120.0(4)	C12-C7-P2	120.8(3)
C8-C7-P2	119.1(3)	C9-C8-C7	119.0(4)
C10-C9-C8	120.4(4)	C11-C10-C9	120.2(4)
C10-C11-C12	120.4(4)	C11-C12-C7	119.9(4)
C14-C13-P2	114.6(3)	C14-C13-P1	113.2(3)
P2-C13-P1	103.80(19)	C15-C14-C13	109.8(3)
O1-C15-C16	121.0(4)	O1-C15-C14	119.4(4)
C16-C15-C14	119.6(3)	C21-C16-C17	119.0(4)
C21-C16-C15	122.9(4)	C17-C16-C15	118.1(4)
C18-C17-C16	120.7(4)	C17-C18-C19	119.9(4)
C20-C19-C18	120.2(4)	C19-C20-C21	120.2(4)
C16-C21-C20	120.0(4)	C27-C22-C23	119.2(4)

C27-C22-P1	116.5(3)	C23-C22-P1	124.3(3)
C24-C23-C22	119.9(4)	C23-C24-C25	120.9(4)
C23-C24-C29	120.7(4)	C25-C24-C29	118.4(4)
C26-C25-C24	118.9(4)	C27-C26-C25	120.8(4)
C27-C26-C28	118.6(4)	C25-C26-C28	120.5(4)
C26-C27-C22	120.3(4)	F2-C28-F1	107.1(4)
F2-C28-F3	107.4(4)	F1-C28-F3	105.5(4)
F2-C28-C26	112.7(4)	F1-C28-C26	112.4(4)
F3-C28-C26	111.3(4)	F6-C29-F5	107.0(4)
F6-C29-F4	106.5(4)	F5-C29-F4	106.1(4)
F6-C29-C24	112.6(4)	F5-C29-C24	112.2(4)
F4-C29-C24	112.1(4)	C31-C30-C35	119.4(4)
C31-C30-P1	119.2(3)	C35-C30-P1	121.3(3)
C32-C31-C30	119.8(4)	C33-C32-C31	121.6(4)
C33-C32-C37	120.4(4)	C31-C32-C37	118.0(4)
C32-C33-C34	118.6(4)	C35-C34-C33	120.8(4)
C35-C34-C36	119.6(4)	C33-C34-C36	119.5(4)
C34-C35-C30	119.8(4)	F8-C36-F7	107.3(4)
F8-C36-F9	107.4(4)	F7-C36-F9	105.4(4)
F8-C36-C34	112.7(4)	F7-C36-C34	111.3(4)
F9-C36-C34	112.3(4)	F11-C37-F12	107.8(4)
F11-C37-F10	106.9(4)	F12-C37-F10	106.2(4)
F11-C37-C32	112.8(4)	F12-C37-C32	111.4(4)
F10-C37-C32	111.4(4)	Cl3-C38-Cl4	111.0(3)
Cl5-C39-Cl6	110.9(3)	Cl5A-C39A-Cl6A	108.4(12)
C30-P1-C22	107.75(18)	C30-P1-C13	103.52(18)
C22-P1-C13	106.73(17)	C30-P1-Pd1	114.12(13)
C22-P1-Pd1	111.63(13)	C13-P1-Pd1	112.49(13)
C1-P2-C7	109.87(19)	C1-P2-C13	112.32(18)
C7-P2-C13	104.57(18)	C1-P2-S1	108.60(14)
C7-P2-S1	113.01(14)	C13-P2-S1	108.49(13)
P2-S1-Pd1	100.02(5)		

Crystallographic data for compound 31

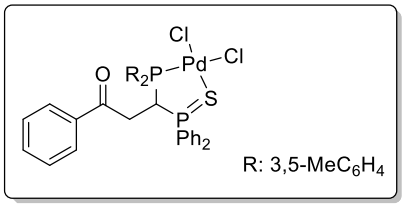

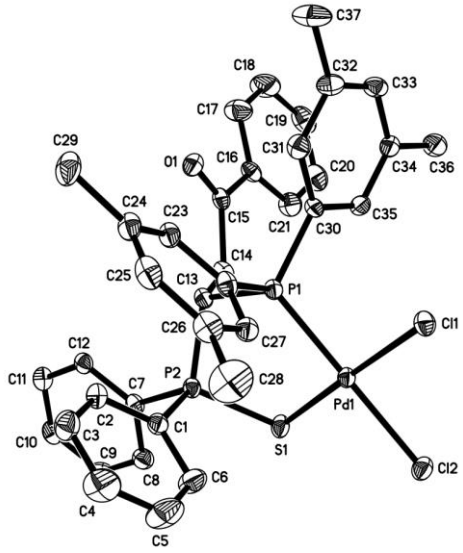

Identification code	leung1215m	
Chemical formula	$C_{38.25}H_{38.50}Cl_{4.50}OP_2PdS$	
Formula weight	874.11 g/mol	
Temperature	100(2) K	
Wavelength	0.71073 Å	
Crystal size	0.040 x 0.120 x 0.240 mm	
Crystal habit	yellow plate	
Crystal system	tetragonal	
Space group	P -4 21 c	
Unit cell dimensions	a = 21.8814(4) Å	α = 90°
	b = 21.8814(4) Å	β = 90°
	c = 16.3351(3) Å	γ = 90°
Volume	7821.2(3) $Å^3$	
Z	8	
Density (calculated)	1.485 g/cm^3	
Absorption coefficient	0.947 mm^{-1}	
F(000)	3556	

Theta range for data collection	2.24 to 31.02°
Index ranges	-31<=h<=29, -31<=k<=29, -17<=l<=23
Reflections collected	78778
Independent reflections	12485 [R(int) = 0.1018]
Coverage of independent reflections	99.9%
Absorption correction	Multi-Scan

Max. and min. transmission	0.9630 and 0.8050	
Structure solution technique	direct methods	
Structure solution program	XT, VERSION 2018/2	
Refinement method	Full-matrix least-squares on F^2	
Refinement program	SHELXL-2018/3 (Sheldrick, 2018)	
Function minimized	$\Sigma\ w(F_o^2 - F_c^2)^2$	
Data / restraints / parameters	12485 / 101 / 478	
Goodness-of-fit on F^2	1.012	
Δ/σ_{max}	0.006	
Final R indices	9833 data; $I>2\sigma(I)$	R1 = 0.0445, wR2 = 0.0820
	all data	R1 = 0.0721, wR2 = 0.0934
Weighting scheme	$w=1/[\sigma^2(F_o^2)+(0.0313P)^2+6.1225P]$ where $P=(F_o^2+2F_c^2)/3$	
Absolute structure parameter	-0.028(15)	
Largest diff. peak and hole	1.025 and -0.534 eÅ^{-3}	
R.M.S. deviation from mean	0.104 eÅ^{-3}	

Bond lengths (Å) of compound 31

C1-C2	1.388(7)	C1-C6	1.395(7)
C1-P2	1.806(5)	C2-C3	1.397(7)
C3-C4	1.391(8)	C4-C5	1.367(9)
C5-C6	1.398(8)	C7-C8	1.389(7)
C7-C12	1.398(6)	C7-P2	1.801(5)
C8-C9	1.375(7)	C9-C10	1.387(7)
C10-C11	1.392(7)	C11-C12	1.383(6)
C13-C14	1.545(6)	C13-P2	1.823(5)
C13-P1	1.878(5)	C14-C15	1.519(7)
C15-O1	1.218(6)	C15-C16	1.493(7)
C16-C21	1.383(7)	C16-C17	1.388(7)
C17-C18	1.390(8)	C18-C19	1.391(9)
C19-C20	1.370(8)	C20-C21	1.392(7)
C22-C27	1.381(7)	C22-C23	1.398(7)

C22-P1	1.815(5)	C23-C24	1.395(7)
C24-C25	1.384(8)	C24-C29	1.496(7)
C25-C26	1.401(8)	C26-C27	1.394(7)
C26-C28	1.502(8)	C30-C31	1.390(7)
C30-C35	1.403(6)	C30-P1	1.812(5)
C31-C32	1.395(7)	C32-C33	1.380(7)
C32-C37	1.507(7)	C33-C34	1.400(7)
C34-C35	1.389(7)	C34-C36	1.505(7)
Cl1-Pd1	2.3189(12)	Cl2-Pd1	2.3543(12)
P1-Pd1	2.2434(12)	P2-S1	2.0128(16)
Pd1-S1	2.3059(12)	C38-Cl4	1.77(2)
C38-Cl3	1.765(11)	C38A-Cl4A	1.76(2)
C38A-Cl3A	1.762(14)	C39-Cl6	1.76(2)
C39-Cl5	1.756(15)		

Bond angles (°) of compound 31

C2-C1-C6	121.0(5)	C2-C1-P2	119.8(4)
C6-C1-P2	119.1(4)	C1-C2-C3	119.2(5)
C4-C3-C2	119.4(5)	C5-C4-C3	121.2(5)
C4-C5-C6	120.1(6)	C1-C6-C5	118.9(5)
C8-C7-C12	120.0(4)	C8-C7-P2	119.0(4)
C12-C7-P2	121.0(4)	C9-C8-C7	120.1(5)
C8-C9-C10	120.4(5)	C9-C10-C11	119.9(4)
C12-C11-C10	120.0(5)	C11-C12-C7	119.7(5)
C14-C13-P2	109.4(3)	C14-C13-P1	112.9(3)
P2-C13-P1	103.1(2)	C15-C14-C13	113.1(4)
O1-C15-C16	121.7(5)	O1-C15-C14	121.1(4)
C16-C15-C14	117.2(4)	C21-C16-C17	118.6(5)
C21-C16-C15	123.1(5)	C17-C16-C15	118.2(5)
C16-C17-C18	120.5(6)	C17-C18-C19	119.9(6)
C20-C19-C18	120.0(5)	C19-C20-C21	119.7(5)
C16-C21-C20	121.2(5)	C27-C22-C23	120.4(4)
C27-C22-P1	119.8(4)	C23-C22-P1	119.9(4)
C24-C23-C22	120.4(5)	C25-C24-C23	118.1(4)
C25-C24-C29	121.5(5)	C23-C24-C29	120.4(5)
C24-C25-C26	122.6(5)	C27-C26-C25	118.0(5)
C27-C26-C28	120.7(5)	C25-C26-C28	121.3(5)
C22-C27-C26	120.5(4)	C31-C30-C35	119.3(4)
C31-C30-P1	122.5(4)	C35-C30-P1	118.2(4)

C30-C31-C32	120.6(5)	C33-C32-C31	118.9(5)
C33-C32-C37	121.5(5)	C31-C32-C37	119.5(5)
C32-C33-C34	122.0(5)	C35-C34-C33	118.3(4)
C35-C34-C36	121.2(5)	C33-C34-C36	120.5(5)
C34-C35-C30	120.8(4)	C30-P1-C22	107.7(2)
C30-P1-C13	107.5(2)	C22-P1-C13	103.4(2)
C30-P1-Pd1	112.33(15)	C22-P1-Pd1	116.22(17)
C13-P1-Pd1	109.04(15)	C7-P2-C1	108.2(2)
C7-P2-C13	110.6(2)	C1-P2-C13	109.2(2)
C7-P2-S1	109.98(16)	C1-P2-S1	111.65(16)
C13-P2-S1	107.16(15)	P1-Pd1-S1	94.56(4)
P1-Pd1-Cl1	87.33(4)	S1-Pd1-Cl1	176.22(5)
P1-Pd1-Cl2	179.14(5)	S1-Pd1-Cl2	84.98(4)
Cl1-Pd1-Cl2	93.09(4)	P2-S1-Pd1	97.66(6)
Cl4-C38-Cl3	108.7(8)	Cl4A-C38A-Cl3A	110.9(11)
Cl6-C39-Cl5	111.2(9)		

Crystallographic data for compound 33

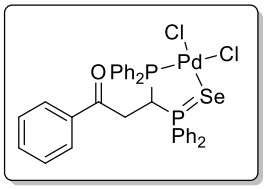

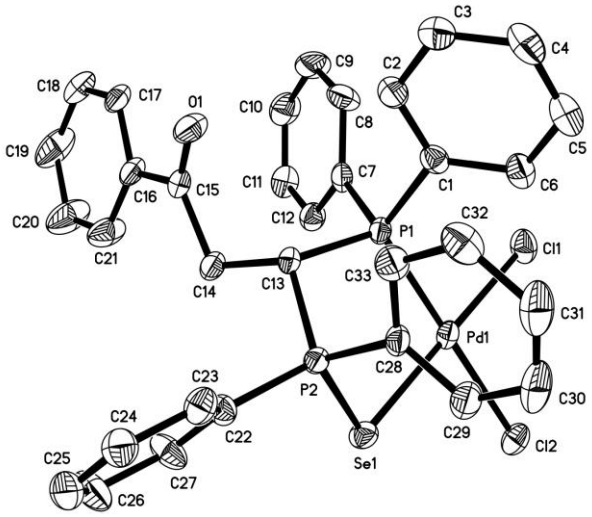

Identification code	leung1222m
Chemical formula	$C_{35.65}H_{33.77}Cl_{4.54}OP_2PdSe$
Formula weight	886.44 g/mol
Temperature	100(2) K
Wavelength	0.71073 Å
Crystal size	0.120 x 0.200 x 0.220 mm
Crystal habit	yellow block
Crystal system	orthorhombic
Space group	A b a 2
Unit cell dimensions	a = 24.1786(10) Å α = 90°
	b = 18.5809(6) Å β = 90°
	c = 16.6442(6) Å γ = 90°
Volume	7477.6(5) $Å^3$
Z	8
Density (calculated)	1.575 g/cm^3
Absorption coefficient	1.908 mm^{-1}
F(000)	3543

Theta range for data collection	2.35 to 31.56°
Index ranges	-28<=h<=35, -27<=k<=27, -19<=l<=24
Reflections collected	55129
Independent reflections	11338 [R(int) = 0.0977]
Coverage of independent reflections	99.8%
Absorption correction	Multi-Scan

Max. and min. transmission	0.8030 and 0.6790	
Structure solution technique	direct methods	
Structure solution program	XT, VERSION 2018/2	
Refinement method	Full-matrix least-squares on F^2	
Refinement program	SHELXL-2018/3 (Sheldrick, 2018)	
Function minimized	$\Sigma\, w(F_o^2 - F_c^2)^2$	
Data / restraints / parameters	11338 / 160 / 472	
Goodness-of-fit on F^2	1.038	
Δ/σ_{max}	0.001	
Final R indices	8702 data; $I>2\sigma(I)$	R1 = 0.0513, wR2 = 0.1062
	all data	R1 = 0.0794, wR2 = 0.1157
Weighting scheme	$w=1/[\sigma^2(F_o^2)+(0.0471P)^2+0.7259P]$ where $P=(F_o^2+2F_c^2)/3$	
Absolute structure parameter	0.025(13)	
Largest diff. peak and hole	0.970 and -0.915 eÅ^{-3}	
R.M.S. deviation from mean	0.122 eÅ^{-3}	

Bond lengths (Å) of compound 33

C1-C2	1.389(10)	C1-C6	1.399(8)
C1-P1	1.821(7)	C2-C3	1.380(10)
C2-H2	0.95	C3-C4	1.383(10)
C3-H3	0.95	C4-C5	1.381(11)
C4-H4	0.95	C5-C6	1.368(9)
C5-H5	0.95	C6-H6	0.95
C7-C12	1.383(9)	C7-C8	1.405(9)
C7-P1	1.807(7)	C8-C9	1.386(10)
C8-H8	0.95	C9-C10	1.398(11)
C9-H9	0.95	C10-C11	1.360(11)
C10-H10	0.95	C11-C12	1.378(10)
C11-H11	0.95	C12-H12	0.95
C13-C14	1.539(7)	C13-P2	1.821(7)
C13-P1	1.875(6)	C13-H13	1.0

C14-C15	1.518(9)	C14-H14A	0.99
C14-H14B	0.99	C15-O1	1.207(8)
C15-C16	1.497(9)	C16-C17	1.381(9)
C16-C21	1.399(10)	C17-C18	1.383(10)
C17-H17	0.95	C18-C19	1.393(12)
C18-H18	0.95	C19-C20	1.378(13)
C19-H19	0.95	C20-C21	1.366(11)
C20-H20	0.95	C21-H21	0.95
C22-C27	1.388(9)	C22-C23	1.393(9)
C22-P2	1.792(6)	C23-C24	1.380(9)
C23-H23	0.95	C24-C25	1.353(10)
C24-H24	0.95	C25-C26	1.393(11)
C25-H25	0.95	C26-C27	1.392(10)
C26-H26	0.95	C27-H27	0.95
C28-C29	1.365(9)	C28-C33	1.395(9)
C28-P2	1.823(6)	C29-C30	1.391(10)
C29-H29	0.95	C30-C31	1.365(12)
C30-H30	0.95	C31-C32	1.387(11)
C31-H31	0.95	C32-C33	1.393(9)
C32-H32	0.95	C33-H33	0.95
C34-Cl4	1.717(8)	C34-Cl3	1.763(11)
C34-H34A	0.99	C34-H34B	0.99
C35-Cl5	1.54(3)	C35-Cl6	1.54(3)
C35-H35A	0.99	C35-H35B	0.99
C36-C37	1.54(3)	C36-H36A	0.98
C36-H36B	0.98	C36-H36C	0.98
C37-C38	1.51(3)	C37-H37A	0.99
C37-H37B	0.99	C38-C39	1.54(3)
C38-H38A	0.99	C38-H38B	0.99
C39-C40	1.49(3)	C39-H39A	0.99
C39-H39B	0.99	C40-C41	1.55(3)
C40-H40A	0.99	C40-H40B	0.99
C41-H41A	0.98	C41-H41B	0.98
C41-H41C	0.98	Cl1-Pd1	2.3175(17)
Cl2-Pd1	2.3627(16)	P1-Pd1	2.2393(16)
P2-Se1	2.1596(16)	Pd1-Se1	2.3928(8)

Bond angles (°) of compound 33

C2-C1-C6	119.1(6)	C2-C1-P1	120.9(5)

C6-C1-P1	119.9(5)	C3-C2-C1	120.2(6)
C3-C2-H2	119.9	C1-C2-H2	119.9
C2-C3-C4	120.7(7)	C2-C3-H3	119.6
C4-C3-H3	119.6	C5-C4-C3	118.6(7)
C5-C4-H4	120.7	C3-C4-H4	120.7
C6-C5-C4	121.9(7)	C6-C5-H5	119.1
C4-C5-H5	119.1	C5-C6-C1	119.5(7)
C5-C6-H6	120.3	C1-C6-H6	120.3
C12-C7-C8	118.2(6)	C12-C7-P1	119.3(5)
C8-C7-P1	122.6(5)	C9-C8-C7	120.0(7)
C9-C8-H8	120.0	C7-C8-H8	120.0
C8-C9-C10	120.0(7)	C8-C9-H9	120.0
C10-C9-H9	120.0	C11-C10-C9	120.0(7)
C11-C10-H10	120.0	C9-C10-H10	120.0
C10-C11-C12	120.2(7)	C10-C11-H11	119.9
C12-C11-H11	119.9	C11-C12-C7	121.6(7)
C11-C12-H12	119.2	C7-C12-H12	119.2
C14-C13-P2	112.6(5)	C14-C13-P1	114.2(4)
P2-C13-P1	105.5(3)	C14-C13-H13	108.1
P2-C13-H13	108.1	P1-C13-H13	108.1
C15-C14-C13	110.3(5)	C15-C14-H14A	109.6
C13-C14-H14A	109.6	C15-C14-H14B	109.6
C13-C14-H14B	109.6	H14A-C14-H14B	108.1
O1-C15-C16	120.5(6)	O1-C15-C14	118.9(6)
C16-C15-C14	120.5(5)	C17-C16-C21	119.9(6)
C17-C16-C15	118.8(6)	C21-C16-C15	121.4(6)
C16-C17-C18	120.9(7)	C16-C17-H17	119.5
C18-C17-H17	119.5	C17-C18-C19	118.8(7)
C17-C18-H18	120.6	C19-C18-H18	120.6
C20-C19-C18	119.8(7)	C20-C19-H19	120.1
C18-C19-H19	120.1	C21-C20-C19	121.8(9)
C21-C20-H20	119.1	C19-C20-H20	119.1
C20-C21-C16	118.8(8)	C20-C21-H21	120.6
C16-C21-H21	120.6	C27-C22-C23	119.5(6)
C27-C22-P2	119.4(5)	C23-C22-P2	121.2(5)
C24-C23-C22	120.1(6)	C24-C23-H23	119.9
C22-C23-H23	119.9	C25-C24-C23	120.4(7)
C25-C24-H24	119.8	C23-C24-H24	119.8
C24-C25-C26	121.0(7)	C24-C25-H25	119.5
C26-C25-H25	119.5	C27-C26-C25	119.1(7)
C27-C26-H26	120.5	C25-C26-H26	120.5

C22-C27-C26	119.9(6)	C22-C27-H27	120.0
C26-C27-H27	120.0	C29-C28-C33	120.9(6)
C29-C28-P2	118.9(5)	C33-C28-P2	120.3(5)
C28-C29-C30	119.2(7)	C28-C29-H29	120.4
C30-C29-H29	120.4	C31-C30-C29	120.7(7)
C31-C30-H30	119.6	C29-C30-H30	119.6
C30-C31-C32	120.6(7)	C30-C31-H31	119.7
C32-C31-H31	119.7	C31-C32-C33	119.1(7)
C31-C32-H32	120.4	C33-C32-H32	120.4
C32-C33-C28	119.4(6)	C32-C33-H33	120.3
C28-C33-H33	120.3	Cl4-C34-Cl3	112.2(5)
Cl4-C34-H34A	109.2	Cl3-C34-H34A	109.2
Cl4-C34-H34B	109.2	Cl3-C34-H34B	109.2
H34A-C34-H34B	107.9	Cl5-C35-Cl6	138.(6)
Cl5-C35-H35A	102.5	Cl6-C35-H35A	102.5
Cl5-C35-H35B	102.5	Cl6-C35-H35B	102.5
H35A-C35-H35B	104.9	C37-C36-H36A	109.5
C37-C36-H36B	109.5	H36A-C36-H36B	109.5
C37-C36-H36C	109.5	H36A-C36-H36C	109.5
H36B-C36-H36C	109.5	C38-C37-C36	116.(3)
C38-C37-H37A	108.4	C36-C37-H37A	108.4
C38-C37-H37B	108.4	C36-C37-H37B	108.4
H37A-C37-H37B	107.5	C37-C38-C39	114.(3)
C37-C38-H38A	108.6	C39-C38-H38A	108.6
C37-C38-H38B	108.6	C39-C38-H38B	108.6
H38A-C38-H38B	107.6	C40-C39-C38	117.(3)
C40-C39-H39A	108.0	C38-C39-H39A	108.0
C40-C39-H39B	108.0	C38-C39-H39B	108.0
H39A-C39-H39B	107.3	C39-C40-C41	116.(3)
C39-C40-H40A	108.3	C41-C40-H40A	108.3
C39-C40-H40B	108.3	C41-C40-H40B	108.3
H40A-C40-H40B	107.4	C40-C41-H41A	109.5
C40-C41-H41B	109.5	H41A-C41-H41B	109.5
C40-C41-H41C	109.5	H41A-C41-H41C	109.5
H41B-C41-H41C	109.5	C7-P1-C1	108.7(3)
C7-P1-C13	105.9(3)	C1-P1-C13	101.5(3)
C7-P1-Pd1	111.2(2)	C1-P1-Pd1	116.5(2)
C13-P1-Pd1	112.2(2)	C22-P2-C13	110.0(3)
C22-P2-C28	108.5(3)	C13-P2-C28	107.1(3)
C22-P2-Se1	110.4(2)	C13-P2-Se1	108.21(19)
C28-P2-Se1	112.50(18)	P1-Pd1-Cl1	86.45(6)

P1-Pd1-Cl2	179.07(7)	Cl1-Pd1-Cl2	93.04(6)
P1-Pd1-Se1	95.20(5)	Cl1-Pd1-Se1	177.38(5)
Cl2-Pd1-Se1	85.27(5)	P2-Se1-Pd1	95.11(5)

Crystallographic data for compound 34

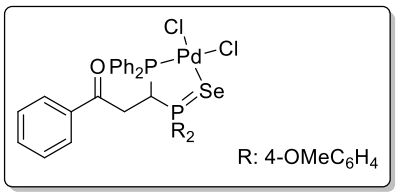

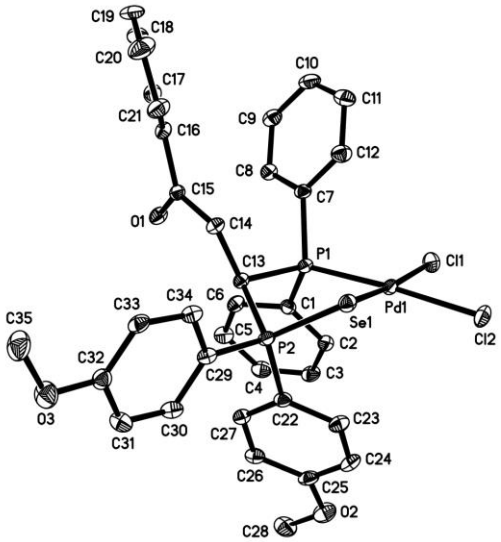

Identification code	leung1210m
Chemical formula	$C_{35}H_{32}Cl_2O_3P_2PdSe$
Formula weight	818.80 g/mol
Temperature	100(2) K
Wavelength	0.71073 Å
Crystal size	0.010 x 0.220 x 0.240 mm
Crystal habit	orange plate
Crystal system	monoclinic
Space group	P 1 21/n 1
Unit cell dimensions	a = 13.2411(7) Å α = 90°
	b = 16.1259(6) Å β = 105.776(2)°
	c = 15.6837(7) Å γ = 90°
Volume	3222.7(3) $Å^3$
Z	4
Density (calculated)	1.688 g/cm^3
Absorption coefficient	2.007 mm^{-1}
F(000)	1640

Theta range for data collection	2.04 to 34.37°
Index ranges	-21<=h<=21, -25<=k<=18, -24<=l<=24
Reflections collected	64021
Independent reflections	13503 [R(int) = 0.1117]
Coverage of independent reflections	99.9%

Absorption correction	Multi-Scan	
Max. and min. transmission	0.9800 and 0.6450	
Structure solution technique	direct methods	
Structure solution program	XT, VERSION 2018/2	
Refinement method	Full-matrix least-squares on F^2	
Refinement program	SHELXL-2018/3 (Sheldrick, 2018)	
Function minimized	$\Sigma\ w(F_o^2 - F_c^2)^2$	
Data / restraints / parameters	13503 / 0 / 399	
Goodness-of-fit on F^2	1.021	
Δ/σ_{max}	0.002	
Final R indices	8323 data; $I>2\sigma(I)$	R1 = 0.0516, wR2 = 0.0989
	all data	R1 = 0.1117, wR2 = 0.1190
Weighting scheme	$w=1/[\sigma^2(F_o^2)+(0.0442P)^2]$ where $P=(F_o^2+2F_c^2)/3$	
Largest diff. peak and hole	0.983 and -2.098 eÅ^{-3}	
R.M.S. deviation from mean	0.175 eÅ^{-3}	

Bond lengths (Å) of compound 34

C1-C2	1.390(4)	C1-C6	1.407(4)
C1-P1	1.816(3)	C2-C3	1.392(4)
C3-C4	1.375(4)	C4-C5	1.393(5)
C5-C6	1.384(4)	C7-C8	1.386(4)
C7-C12	1.396(4)	C7-P1	1.827(3)
C8-C9	1.382(4)	C9-C10	1.373(5)
C10-C11	1.393(5)	C11-C12	1.383(4)
C13-C14	1.523(4)	C13-P2	1.837(3)
C13-P1	1.879(3)	C14-C15	1.510(4)
C15-O1	1.215(4)	C15-C16	1.482(4)
C16-C21	1.394(5)	C16-C17	1.394(4)
C17-C18	1.379(5)	C18-C19	1.384(6)
C19-C20	1.375(5)	C20-C21	1.378(5)
C22-C27	1.389(4)	C22-C23	1.403(4)
C22-P2	1.798(3)	C23-C24	1.378(5)
C24-C25	1.392(5)	C25-O2	1.352(4)
C25-C26	1.389(4)	C26-C27	1.378(4)

C28-O2	1.441(4)	C29-C34	1.395(4)
C29-C30	1.401(4)	C29-P2	1.791(3)
C30-C31	1.373(4)	C31-C32	1.384(5)
C32-O3	1.352(4)	C32-C33	1.394(4)
C33-C34	1.377(4)	C35-O3	1.436(4)
Cl1-Pd1	2.3243(8)	Cl2-Pd1	2.3494(8)
P1-Pd1	2.2479(8)	P2-Se1	2.1546(8)
Pd1-Se1	2.4198(4)		

Bond angles (°) of compound 34

C2-C1-C6	119.1(3)	C2-C1-P1	120.7(2)
C6-C1-P1	120.0(2)	C1-C2-C3	120.0(3)
C4-C3-C2	120.7(3)	C3-C4-C5	119.9(3)
C6-C5-C4	120.0(3)	C5-C6-C1	120.3(3)
C8-C7-C12	118.9(3)	C8-C7-P1	123.8(2)
C12-C7-P1	117.2(2)	C9-C8-C7	120.2(3)
C10-C9-C8	120.8(3)	C9-C10-C11	119.9(3)
C12-C11-C10	119.4(3)	C11-C12-C7	120.8(3)
C14-C13-P2	113.7(2)	C14-C13-P1	114.2(2)
P2-C13-P1	104.30(14)	C15-C14-C13	112.3(3)
O1-C15-C16	121.4(3)	O1-C15-C14	121.3(3)
C16-C15-C14	117.3(3)	C21-C16-C17	119.2(3)
C21-C16-C15	121.1(3)	C17-C16-C15	119.6(3)
C18-C17-C16	120.3(3)	C17-C18-C19	119.6(3)
C20-C19-C18	120.6(3)	C19-C20-C21	120.2(4)
C20-C21-C16	120.1(3)	C27-C22-C23	119.0(3)
C27-C22-P2	119.3(2)	C23-C22-P2	121.2(2)
C24-C23-C22	119.5(3)	C23-C24-C25	121.1(3)
O2-C25-C26	124.5(3)	O2-C25-C24	116.3(3)
C26-C25-C24	119.2(3)	C27-C26-C25	119.9(3)
C26-C27-C22	121.2(3)	C34-C29-C30	118.8(3)
C34-C29-P2	120.1(2)	C30-C29-P2	121.1(2)
C31-C30-C29	119.8(3)	C30-C31-C32	120.9(3)
O3-C32-C31	116.1(3)	O3-C32-C33	123.9(3)
C31-C32-C33	120.0(3)	C34-C33-C32	119.1(3)
C33-C34-C29	121.3(3)	C25-O2-C28	118.3(3)
C32-O3-C35	117.4(3)	C1-P1-C7	108.60(14)
C1-P1-C13	101.59(13)	C7-P1-C13	107.51(13)
C1-P1-Pd1	116.27(10)	C7-P1-Pd1	110.42(10)

C13-P1-Pd1	111.84(10)	C29-P2-C22	112.17(14)
C29-P2-C13	109.59(13)	C22-P2-C13	105.09(14)
C29-P2-Se1	111.88(10)	C22-P2-Se1	111.68(10)
C13-P2-Se1	105.99(9)	P1-Pd1-Cl1	87.79(3)
P1-Pd1-Cl2	176.46(3)	Cl1-Pd1-Cl2	92.42(3)
P1-Pd1-Se1	93.72(2)	Cl1-Pd1-Se1	173.11(2)
Cl2-Pd1-Se1	86.48(2)	P2-Se1-Pd1	91.91(3)